

**Characterization of the Cellular Functions of
the Nucleoporins Nup153 and Nup88**

Inauguraldissertation

zur

Erlangung der Würde eines Doktors der Philosophie

vorgelegt der

Philosophisch-Naturwissenschaftlichen Fakultät

der Universität Basel

von

Yvonne Christine Lussi

aus Stans, Schweiz

Basel, 2010

Genehmigt von der Philosophisch-Naturwissenschaftlichen Fakultät
auf Antrag von

Prof. Dr. Ueli Aebi

Prof. Dr. Birthe Fahrenkrog

Prof. Dr. Roland Foisner

Basel, den 30. März 2010

Prof. Dr. Eberhard Parlow

Dekan

Abstract

Nuclear pore complexes (NPCs) and nuclear lamins are major constituents of the nuclear envelope (NE) in metazoan cells. NPCs are embedded in the NE and they mediate all nucleocytoplasmic transport events. NPCs are built of around 30 nucleoporins, which, besides being involved in nuclear transport, have been shown to be engaged in a number of other cellular processes, such as transcriptional regulation, kinetochore organization and cell division. Here, we provide an analysis of Nup153 function in mitosis in Chapter 2. We show that overexpression and deletion of Nup153 leads to mitotic defects due to a misregulation of the spindle assembly checkpoint protein Mad1. In Chapter 3, we identify Nup88 as novel lamin A-binding protein. Using interaction assays and immunofluorescence microscopy, we characterize the direct interaction of Nup88 with lamin A. We show that the interaction of lamin A with Nup88 is mediated by the lamin A Ig-fold, and that the interaction between the two proteins is abrogated in the presence of laminopathy-associated mutations lying in the Ig-fold domain of lamin A. Finally, in Chapter 4, we show that Nup88 is implicated in cell cycle regulation due to an interaction with the lamin A-LAP2 α complex.

Our results presented in this thesis contribute to broaden the current knowledge of cellular functions of the nucleoporins Nup153 and Nup88, as well as to increased understanding of the interaction of nucleoporins with the nuclear lamina and the impact of laminopathy-associated mutations on the interaction of lamin A with Nup88. The finding that Nup88 is involved in gene regulation and proliferation is a key step in understanding Nup88's implication in cancer development.

Contents

List of Figures	vi
List of Tables	viii
List of Abbreviations	ix
1 General Introduction	12
1.1 Nuclear pore complex architecture	13
1.2 Nucleoporins at the atomic level	14
1.3 NPC subcomplexes	19
1.4 Vertebrate nucleoporins	23
1.4.1 Nup153	23
1.4.2 Nup88	24
1.4.3 Nup214	28
1.4.4 Nup98	29
1.5 FG-nucleoporins in nucleocytoplasmic transport	30
1.6 Nucleoporins in transcription	31
1.7 Nucleoporins in mitosis	33
1.7.1 The spindle assembly checkpoint	34
1.7.2 Mad1 and Mad2	34
1.7.3 Nup153	35
1.7.4 The Nup107-160 complex	36
1.7.5 Nup358	36
1.7.6 Nup98	37
1.8 NPCs and diseases	37
1.8.1 Triple A syndrome	37
1.8.2 Nucleoporins in cancer	38
1.8.3 Nucleoporins in autoimmune disease	41
1.9 The nuclear lamina	42
1.9.1 Nuclear lamins	43
1.9.2 Nucleoplasmic lamin A and the lamina-associated polypeptide 2 α (LAP2 α)	44
1.10 The lamin A- LAP2α complex and the retinoblastoma protein (pRb)	46
1.11 Laminopathies	47
2 The nucleoporin Nup153 affects spindle checkpoint activity due to an association with Mad1	49
2.1 Abstract	50
2.2 Introduction	51
2.3 Results	53

2.3.1	Enhanced levels of Nup153 lead to multinucleation and multilobulation of cells	53
2.3.2	Enhanced levels of Nup153 lead to multinucleation in live cells	55
2.3.3	Expression of Nup153 induces multipolar spindles	57
2.3.4	Nup153 levels affect the spindle assembly checkpoint	59
2.3.5	Nup153 and Mad1 are directly interacting	61
2.3.6	Nup153 affects the spindle checkpoint	62
2.3.7	Nup153 levels affect Mad1 localization	64
2.3.8	Depletion of Nup153 causes cytokinetic abnormalities	67
2.4	Discussion	69
2.4.1	Altered Nup153 levels are associated with abnormal mitosis	69
2.4.2	Nup153 function in mitosis is related to the mitotic checkpoint	70
2.4.3	Nup153 levels regulate SAC activity	71
2.5	Materials and Methods	73
2.5.1	Cell culture and transfections	73
2.5.2	Constructs and antibodies	73
2.5.3	Immunofluorescence	74
2.5.4	RNA interference	74
2.5.5	Quantitative real-time PCR	74
2.5.6	Quantitative immunoblotting and gel electrophoresis	75
2.5.7	Flow cytometry	75
2.5.8	Live cell imaging	76
2.5.9	Immunoprecipitation	76
2.5.10	Solution binding assays	76
2.5.11	Immuno-EM	77
2.6	Acknowledgements	78
3	Direct association of the nucleoporin Nup88 with lamin A	79
3.1	Abstract	80
3.2	Introduction	81
3.3	Results	84
3.3.1	Lamin A is an interaction partner of Nup88	84
3.3.2	Nup88 is interacting with lamin A in vivo and in vitro	85
3.3.3	Nup88 is localizing partially to the nuclear face of the NPC	87
3.3.4	The apparent depletion of Nup88 in human embryonic kidney cells overexpressing GFP-lamin A is due to epitope masking	91
3.3.5	Nup88 interaction with lamin A is lost in presence of the EDMD-associated R453W mutant and the FPLD-associated R482W mutant lamin A	95
3.4	Discussion	99
3.4.1	Lamin A is a novel interaction partner of Nup88	99
3.4.2	Nup88 is localizing to both sides of the NPC	100
3.4.3	Nup88 interaction is lost with disease-associated lamin A Ig-fold mutants	102
3.4.4	Overexpression of GFP-lamin A is masking the Nup88 antibody epitope	102
3.5	Materials and Methods	104
3.5.1	Preparation of nuclei from HeLa cell suspension cultures by osmotic swelling	104
3.5.2	Cell culture and transfections	104

3.5.3	Constructs	104
3.5.4	Antibodies	105
3.5.5	Immunofluorescence	105
3.5.6	Gel electrophoresis and immunoblotting	106
3.5.7	Colloidal blue staining	106
3.5.8	Immunoprecipitation	106
3.5.9	In vitro transcription and translation	107
3.5.10	Expression of recombinant Nup88 and lamin A	107
3.5.11	In vitro binding assays	107
3.5.12	Expression and purification of lamin A and vimentin	108
3.5.13	Blot-overlay assay	108
3.5.14	Immuno-EM	108
4	The nucleoporin Nup88 is a regulator of the lamin A-LAP2α complex	109
4.1	Abstract	110
4.2	Introduction	111
4.3	Results	114
4.3.1	Nup88 associates with lamin A and LAP2 α	114
4.3.2	Nup88 overexpression disrupts the lamin A-LAP2 α complex and accelerates G1 to S transition	115
4.3.3	Depletion of Nup88 slows down S-phase, leaving the lamin A-LAP2 α complex intact	118
4.4	Discussion	120
4.4.1	Nup88 associates with the lamin A- LAP2 α complex	120
4.4.2	Overexpression of Nup88 is associated with the disruption of the lamin A-LAP2 α complex and impaired G1 cell cycle arrest	121
4.4.3	Depletion of Nup88 slows down G1-S transition	121
4.5	Materials and Methods	124
4.5.1	Cell culture and transfections	124
4.5.2	Constructs and Antibodies	124
4.5.3	Immunofluorescence microscopy	124
4.5.4	RNA interference	125
4.5.5	Quantitative immunoblotting and gel electrophoresis	125
4.5.6	Flow cytometry	126
4.5.7	Immunoprecipitation	126
5	Conclusions and Perspectives	127
5.1	Nup153 as a novel regulator of the spindle assembly checkpoint protein Mad1	127
5.2	Nup88 interacts with the lamin A Ig-fold: implications in laminopathies?	131
5.3	Implications of Nup88 in nuclear assembly?	132
5.4	Nup88 localizes on both the cytoplasmic and nuclear side of the NPC	134
5.5	Nup88 in proliferation	134
5.6	Implications of nucleoporins in gene regulation	136
6	References	139
7	Appendix	160
7.1	Supplementary Figures	161

7.2	Curriculum Vitae	172
7.3	List of Publications	175
7.4	Acknowledgements	176

List of Figures

Figure 1.1: Schematic representation of the nuclear pore complex architecture.	14
Figure 1.2: Subcomplex organization of the NPC.	22
Figure 1.3: Domain organization of the nucleoporins Nup153 and Nup88	25
Figure 1.4: The nuclear lamina.	43
Figure 1.5: Structural model of a lamin A dimer based on structural data and structure predictions.	44
Figure 2.1: Overexpression of human Nup153 causes changes in nuclear shape and aberrant mitosis.	54
Figure 2.2: High levels of Nup153 expression interfere with cytokinesis and induce aneuploidy.	56
Figure 2.3: Overexpression of the nuclear pore complex assembly region (NPAR) of Nup153 induces mitotic abnormalities.	58
Figure 2.4: Nup153 interacts with the spindle checkpoint protein Mad1.	60
Figure 2.5: Enhanced levels of Nup153 affect spindle checkpoint activity.	64
Figure 2.6: Localization of the spindle assembly checkpoint protein Mad1 is dependent on Nup153.	66
Figure 2.7: Depletion of Nup153 inhibits cytokinesis.	68
Figure 2.8: Schematic model of Nup153 function in SAC activity.	72
Figure 3.1: Lamin A is a novel interaction partner of Nup88.	85
Figure 3.2: Nup88 is interacting with lamin A in vivo and in vitro.	87
Figure 3.3: Domain topology of endogenous and ectopically expressed Nup88 within the NPC.	90
Figure 3.4: Overexpression of GFP-lamin A is masking an antibody epitope within the N-terminus of Nup88.	94
Figure 3.5: EDMD-associated lamin A(R453W) and FPLD-associated lamin A(R482W) mutants do not interact with Nup88.	97
Figure 4.1: Nup88 associates with lamin A and Lap2 α .	114
Figure 4.2: Overexpression of Nup88 disrupts the lamin A-LAP2 α complex and accelerates cell cycle progression.	117

Figure 4.3: Depletion of Nup88 slows down S-phase, leaving the lamin A- LAP2 α complex intact.	119
Figure 4.4: Model depicting the potential function of Nup88 in the regulation of the lamin A-LAP2 α complex in pRb-mediated cell cycle progression	123
Figure 5.1: Schematic model depicting the effect of Nup153 overexpression and depletion on Mad1, the SAC and mitosis.	130
Figure 5.2: Excess Nup88 leads to aberrant nuclear morphology.	133
Figure 5.3: Immunoprecipitation assays with HEK cells transfected with GFP-Nup98, GFP-Nup98/HoxA and GFP-Nup98/HHEX fusion proteins using monoclonal GFP-antibodies.	137
Figure S7.1: Electron micrographs of GFP-Nup153 overexpressing cells.	161
Figure S7.2: Over-expression of Nup153 induces cellular multinucleation.	162
Figure S7.3: HeLa cells expressing truncations of the N-terminal domain of human Nup153 cause nuclear lobulations and multinucleation.	163
Figure S7.4: Mad2 localization and co-precipitation with Mad1	164
Figure S7.5: Enhanced levels of Nup153 do not cause G1 or G2 arrest.	165
Figure S7.6: Mad1 does not precipitate with protein G agarose beads.	165
Figure S7.7: HeLa cells expressing histone H2B-GFP were transfected either with Nup153 siRNA or siRNA directed against cyclophilin B as a control.	166
Figure S7.8: Flow cytometric analysis of siRNA treated HeLa cells expressing histone H2B-GFP.	167
Figure S7.9: Nup88-lamin A complex is not associated with transport.	168
Figure S7.10: Localization of endogenous lamin A and Nup88 in HEK cells.	168
Figure S7.11: Expression of GFP-lamin A in Nup88-myc overexpressing HEK cells.	169
Figure S7.12: Masking can be circumvented by the use of a different antibody epitope or a different fixation method.	170
Figure S7.13: Nup88 protein levels are dependent on lamin A.	171
Figure S7.14: Immunoblot analysis of BJ1 fibroblasts transfected with GFP-Nup88 or GFP, respectively.	171

List of Tables

Table 1.1: Secondary structures found in nucleoporins.

18

List of Abbreviations

ABL1	Abelson murine leukemia viral oncogene homolog 1
ACTH	adrenocorticotropin hormone
ALADIN	alacrima-alachasia-adrenal insufficiency neurological disorder
ALD	autoimmune liver disease
ALK	anaplastic lymphoma kinase
APC	adenomatous polyposis coli
APC/C	anaphase promoting complex/cyclosome
APS	phospholipid syndrome
BAF	barrier-to-autointegration protein
CAAX	C=cysteine, A=aliphatic, X=any amino acid
CCD	charge-coupled device
CENP-F	centromere protein F
CET	cryo-electron tomography
COPI	coatamer protein I
CRM1	chromosome region maintenance 1 protein
CTE	C-terminal extended
DCE	dilated cardiomyopathy
DME	Dulbecco's modified Eagle's medium
DNA	deoxyribonucleic acid
EDMD	Emery-Dreifuss muscular dystrophy
EM	electron microscopy
FBS	fetal bovine serum
FEISEM	field emission in-lens scanning electron microscopy
FG	phenylalanine-glycine

FPLD	Dunnigan-type familial partial lipodystrophy
GFP	green fluorescent protein
GST	glutathione S-transferase
HBV-pol	Hepatitis B virus DNA polymerase
HEK	human embryonic kidney
HGPS	Hutchinson-Gilford progeria syndrome
HP1	heterochromatin protein 1
HOX	homeobox
IF	intermediate filament
Ig	immunoglobulin
IMT	inflammatory myofibroblastic tumor
INM	inner nuclear membrane
IPT:	isopropyl- β -D-thiogalactopyranoside
kDa	kilo Dalton
LAP	lamin-associated protein
LEM	LAP2, Emerin, MAN1
LGMD1B	limb-girdle muscular dystrophy 1B
MAD	mandibuloacral dysplasia
mbo	members only
MDa	Mega Dalton
Cdc20	cell-division cycle protein 20
NE	nuclear envelope
NEBD	nuclear envelope breakdown
NES	nuclear export signal
NETC	nuclear envelope targeting cassette
NF- κ B	nuclear factor kappa-light-chain-enhancer of activated B cells
NLS	nuclear localization signal
NPAR	NPC assembly region
NPC	nuclear pore complex
Nup	nucleoporin
PBC	primary biliary cirrhosis
PCR	polymerase chain reaction
Plk1	Polo-like kinase 1
pSTY	phosphorylated serine/threonine/or tyrosine

qRT-PCR	quantitative real-time PCR
PVDF	polyvinylidene difluoride
R	arginine
Rb	retinoblastoma protein
RNA	ribonucleic acid
RNase	ribonuclease
RNAi	ribonucleic acid interference
RPR1	RNase P RNA
SAC	spindle assembly checkpoint
SDS-PAGE	sodium dodecyl sulfate polyacrylamide gel electrophoresis
siRNA	small interfering RNA
SjS	Sjogren's syndrome
SLE	systemic lupus erythematosus
SREB	sterol regulatory element-binding protein
SSc	systemic sclerosis
SUMO	small ubiquitin-like modifier
Tpr	translocated promotor region
TRK	tropomyosin-receptor-kinase
W	tryptophan
WD	tryptophan-aspartic acid

1

General Introduction

Yvonne Lussi and Birthe Fahrenkrog[†]

M.E Müller Institute for Structural Biology, Biozentrum, University of Basel,
Klingelbergstrasse 70, 4056 Basel, Switzerland

Key words: Nuclear pore complex; nuclear envelope; nucleoporin; transcription; cancer;
autoimmune disease; nuclear lamina; lamin A; LAP2 α ; pRb; laminopathy

1.1 Nuclear pore complex architecture

The structure of the NPC has been studied since almost 40 years, and distinct electron microscopy (EM) and cryo-electron tomography (CET) have nowadays provided high-resolution images of this fascinating and most distinctive structure of the NE. Three substructures of the NPC are easily distinguishable: a cylindrical core known as central framework or spoke complex, eight cytoplasmic filaments and a nuclear basket (Figure 1.1). Early EM studies used negatively stained and frozen-hydrated NPCs from *Xenopus laevis* oocyte NEs (Akey and Radermacher, 1993; Hinshaw et al., 1992) or frozen-hydrated yeast nuclei (Yang et al., 1998) to reconstruct the central framework of the NPC. Accordingly, the central framework is composed of eight multi-domain spokes and found embedded between the inner and outer nuclear membranes (Figure 1.1) (Akey, 1989). Each of the spokes consists of an inner domain, a central domain and a luminal domain (Akey, 1989). Only recently it became evident that, at least in yeast, each spoke can be divided into two parallel columns, suggesting that the NPC is made of a 16-fold repetition of columns, each with a similar architecture (Alber et al., 2007b). A cytoplasmic and a nucleoplasmic ring are integrated moieties of the central framework and associated with the outer and inner nuclear membrane, respectively. Recent 3-D reconstruction of NPCs from *Xenopus laevis* or *Dictyostelium discoideum* nuclei increased the resolution of the central framework to now 5-6 nm and revealed the first reconstruction of the peripheral and flexible cytoplasmic filaments and the nuclear basket (Beck et al., 2004; Beck et al., 2007; Stoffer et al., 2003). In *Dictyostelium discoideum*, the NPC has an outer diameter of 125 nm and a total length of ~150 nm, whereof the cytoplasmic filaments are ~35 nm in length, the nuclear basket about 60 nm and the central framework ~50 nm (Beck et al., 2004; Beck et al., 2007). This overall 3D architecture appears evolutionary conserved, while the linear dimensions of the NPC can vary among different species (Fahrenkrog et al., 1998; Kiseleva et al., 2004; Yang et al., 1998).

Embraced by the central framework is the central pore of the NPC, which mediates all trafficking between the cytoplasm and the nucleoplasm (Feldherr et al., 2002). The central pore is hourglass shaped with a diameter of 60-70 nm at its cytoplasmic and nuclear periphery and ~45 nm at its narrowest point at the midplane of

the NE (Beck et al., 2004; Beck et al., 2007; Pante and Kann, 2002; Stoffler et al., 2003). Small molecules and ions with a diameter of up to 9 nm can pass the NPC by passive diffusion (Kiseleva et al., 1998), while larger molecules depend on a translocation signal, which is recognized by nuclear transport receptors of the importin β /karyopherin β family. Receptor-facilitated transport allows passage of macromolecules with diameters up to 39 nm (Pante and Kann, 2002).

Peripheral channels, about 8 nm in diameter, are formed at the interface between the nuclear membrane and the central framework and their function is still controversially discussed (for review see: (Fahrenkrog and Aebi, 2003)).

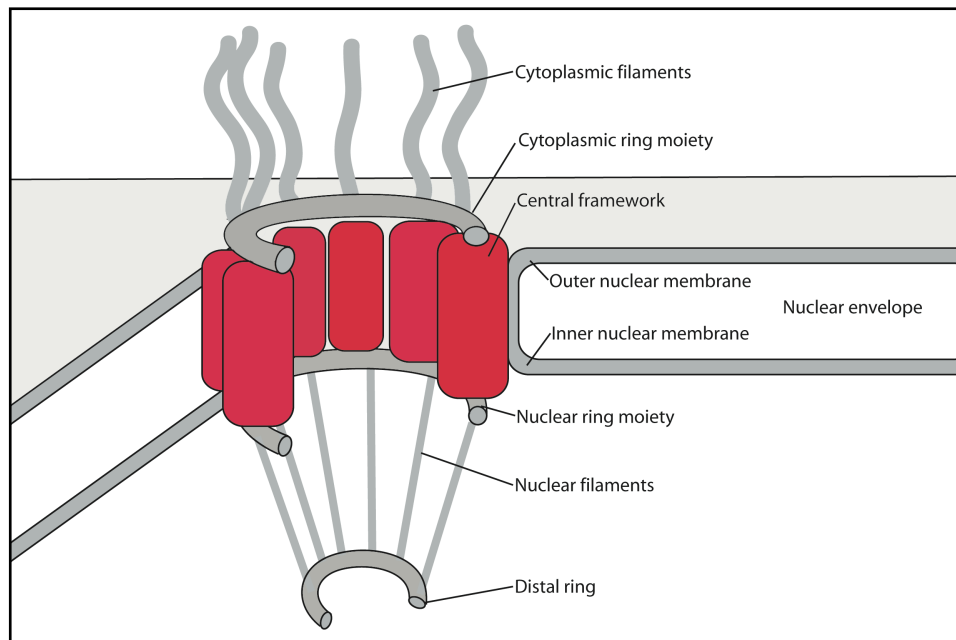


Figure 1.1: Schematic representation of the nuclear pore complex architecture.

The main structural components of the nuclear pore complex include the central framework (or spoke complex) embedded in the nuclear envelope, the cytoplasmic filaments and the nuclear basket.

1.2 Nucleoporins at the atomic level

At the molecular level, the NPC assembles from a set of ~30 different proteins, called nucleoporins or Nups (Cronshaw et al., 2002; Rout et al., 2000). A minimum of eight copies of each nucleoporin is present per NPC (or multiples of eight) and only recently it has been shown that each NPC, at least in yeast, is made up of ~456 individual

nucleoporins (Rout et al., 2000). Structural knowledge of nucleoporins at the atomic level thus far was limited, but computational analysis has indicated that most nucleoporins consist of a small number of protein folds, such as α -helical solenoids, β -propeller, coiled-coil and unstructured, natively unfolded phenylalanine-glycine (FG)-repeat domains (Table 1.1) (Devos et al., 2004; Devos et al., 2006; Schwartz, 2005). Less frequent structural motifs found in nucleoporins are transmembrane helices as in the integral membrane protein POM152 and gp210 (Wozniak and Blobel, 1992; Wozniak et al., 1994), zinc-finger domains as in Nup153 and Nup358/RanBP2 (Higa et al., 2007) or an RNA recognition motif in Nup35 (Handa et al., 2006) (Table 1.1).

Besides these predictions, a growing number of crystal structures of nucleoporin domains are available and the crystal structure is not always consistent with the previous prediction. The first crystal structure of an α -helical nucleoporin domain was solved for Nic96p, the *S. cerevisiae* homologue of vertebrate Nup93 (Jeudy and Schwartz, 2007; Schrader et al., 2008). Nic96p is located at the cytoplasmic and nuclear side of the NPC (Figure 1.2) and is composed of two structural predicted domains: an N-terminal coiled-coil domain of about 150 residues and a C-terminal helical domain of about 600 residues. Crystallization of this C-terminal domain revealed that it folds into an elongated mostly α -helical structure with strong deviation from the predicted α -solenoid fold (Jeudy and Schwartz, 2007; Schrader et al., 2008).

About one third of the nucleoporins contain a predicted β -propeller or α -solenoid domain or a combination of both. Seven-bladed β -propeller domains have been determined by X-ray crystallography for the N-terminal domains of the human nucleoporins Nup133 and Nup214 and Nup214's yeast homologue Nup159p (Berke et al., 2004; Napetschnig et al., 2007; Weirich et al., 2004). β -propellers have the ability to interact with several partners, making this fold ideal to organize dynamic multiprotein complexes. The β -propeller found in Nup214 differs from the β -propeller of its yeast homologue Nup159p or the one found in Nup133 by an additional peptide segment attached to the N-terminal β -propeller. The crystal structure analysis revealed that the N-terminal seven-bladed β -propeller of Nup214 is followed by a 30-residue C-terminal extended unique peptide segment (CTE) that binds to the bottom face of the β -propeller

and has been proposed to play an autoinhibitory role in NPC assembly (Napetschnig et al., 2007).

The autoproteolytic, NPC targeting domain of Nup98 was the first crystal structure obtained for a nucleoporin (Hodel et al., 2002). This domain contains a six-stranded β -sheet sandwiched against a two-stranded β -sheet, flanked on both sides by α -helical stretches, similar to the structure of its yeast homologues Nup116p (Hodel et al., 2002; Robinson et al., 2005). This domain adopts multiple conformations and is stabilized only when bound to a ligand, i.e. to Nup96 and Nup145-C, respectively (Robinson et al., 2005). Conformational diversity might allow Nup98 and Nup116p to bind to multiple binding partners within the NPC or to associate and dissociate from the NPC to increase the mobility of the two nucleoporins, as it was described for Nup98, which shuttles in transcription-dependent manner (Griffis et al., 2002; Griffis et al., 2004). More recently, a high-resolution crystal structure of this autoproteolytic fragment of Nup98 revealed that autoproteolysis of Nup98 might occur due to an energetically unfavorable, so-called N-O acyl-shift (Sun and Guo, 2008). Nup98 may therefore utilize autoprocesing to control its biogenesis pathway and intracellular translocation.

The crystal structure of protein complexes for two nucleoporins have been solved for human Sec13 and yeast Nup145Cp as well as human Nup107 and Nup133 (Boehmer et al., 2008; Hsia et al., 2007), all members of the Nup84p subcomplex of the NPC, and its vertebrate homologue the Nup107-160 complex (see below). Sec13p and Nup145Cp form heterodimers and four of these heterodimers assemble to build a heterooctamer (Hsia et al., 2007). The heterooctamer forms a slightly curved, rigid structure of sufficient length to span the entire height of the central framework (Hsia et al., 2007). In contrast to that, the C-terminal domains Nup107 and Nup133 each form elongated α -helical structures and also the complex of both exhibits a largely extended overall structure (Boehmer et al., 2008). It remains to be seen how these four nucleoporins assemble with their other complex partners to form the central framework, or part of it.

The attempt to crystallize the Nup62 complex, i.e. Nup62, Nup58 and Nup54, yielded the α -helical core structure of rat Nup58/45, whereas Nup62 and Nup54 did not crystallize (Melcak et al., 2007). Nup58/45 forms tetramers, each consisting of two antiparallel hairpin dimers, in which two α -helices are connected by a short loop. The

dimerization interphase is hydrophobic, whereas the dimer interaction occurs through hydrophilic residues. These residues are laterally displaced in various tetramer conformations, which suggests an intermolecular sliding mechanism (Melcak et al., 2007). Recent immunogold localization studies of different domains of the Nup62 complex showed that it is anchored to the cytoplasmic side of the NPC, probably through the coiled-coil structures of Nup62 and Nup54 (Schwarz-Herion et al., 2007), so that intermolecular sliding of Nup58/45 could contribute to a flexible pore diameter (Melcak et al., 2007).

Yeast	Folding Domain	Vertebrate	Folding Domain
Pom34p	transmembrane helices	Nup358/RanBP2*	α -helical repeat
Ndc1p			β -barrel
Pom152p	transmembrane helices cadherin domain		Zinc-finger Ran-binding motif FG-repeat Leucine zipper
Sec13p*	β -propeller		
Seh1p		Tpr	coiled-coil
Nup145Cp*	α -helical repeat	Nup214/CAN*	β -propeller coiled-coil FG-repeat
Nup84p			
Nup85p		Nup205	α -helical repeat
Nup188p		Nup188	
Nup192p		Nup107*	
Nic96p*	elongated α -helical structure coiled-coil	Nup96	
Nup120p	α -solenoid domain	Nup75	
Nup133p	β -propeller	Nup153*	Zinc-finger FG-repeat
Nup157p		Nup155	β -propeller
Nup170p		Nup160	α -helical repeat
Nup82p	coiled-coil β -propeller	Nup133*	
Nup159p*	coiled-coil β -propeller FG-repeats	Nup98	FG-repeat autoproteolytic domain
Nup49p	FG-repeats	Nup93	coiled-coil α -helical repeat
Nup57p	coiled-coil	Nup88	β -propeller coiled-coil
Nsp1p		Nup58/45	FG-repeat
Nup145Np	FG-repeats	Nup62	coiled-coil
Nup100p	β -sandwich like fold	Nup54	
Nup116p*		Nup50	FG-repeat Ran-binding domain
Nup53p	FG-repeats	pom121	transmembrane helices FG-repeat
Nup59p	RNA recognition motif(/RRM)	gp210	transmembrane helices
Nup42p	FG-repeats	Seh1	β -propeller
Nup60p		Sec13	
Nup1p		Nup43	
Nup2p	FG-repeats Ran-binding domain	Nup37	
Mlp1	coiled-coil	ALADIN	
Mlp2		Rae1/Gle2	
		Sec13	
		Nup35/53*	RNA recognition motif(/RRM) FG-repeats
		Ndc1	transmembrane helices FG-repeats

Table 1.1: Secondary structures found in nucleoporins.

Based on secondary structure predictions, nucleoporins can be grouped into three classes (Devos et al., 2006). The transmembrane group contains transmembrane helices. A transmembrane helix is a hydrophobic helical segment spanning the membrane. The second group of nucleoporins contains β -propellers and α -helical repeats. β -propellers have seven blades arranged around a central axis, each blade consisting of four-stranded antiparallel β -sheets, α -helical repeats consist of antiparallel α -helices and can fold into a solenoid or similar structures. The third class of nucleoporins harbors conserved sequence motif of phenylalanine-glycine (FG)-repeats. Those FG-repeats adapt no secondary structure, but are natively unfolded. Another frequent structure observed in nucleoporins is a coiled-coil fold, which is formed by α -helices twisting together. Other less frequently observed secondary structures are the cadherin domain, which is a seven-

stranded β -sandwich structure; the autoproteolytic domain exhibiting a β -sandwich structure with helices capping the two ends; RRM is a two layer α/β sandwich involved in RNA binding; a zinc-finger DNA-binding motif consisting of two antiparallel β -strands and a α -helix and the Ran-binding domain folds in a β -barrel topology with pleckstrin-homology (PH-like domain).

* indicates proteins with folding domains which have been crystallized: Nup116p: β -sandwich like fold (Robinson et al., 2005); Nup145Cp: α -solenoid domain (Hsia et al., 2007); Sec13p: β -propeller (Hsia et al., 2007); Nic96p: α -helical structure (Jeudy and Schwartz, 2007); Nup159p: β -propeller (Weirich et al., 2004); RanBP2/Nup358: Ran-binding motif (Vetter et al., 1999); Nup214/CAN: β -propeller (Napetschnig et al., 2007); Nup107: α -helical repeat (Boehmer et al., 2008); Nup133: α -helical repeat (Boehmer et al., 2008); Nup153: Zinc-finger (Schrader et al., 2008); Nup98: autoproteolytic domain (Sun and Guo, 2008); Nup58/45: coiled-coil (Melcak et al., 2007); Sec13: β -propeller (Stagg et al., 2008); Nup35/53: RNA recognition motif (/RRM) (Handa et al., 2006).

1.3 NPC subcomplexes

Nucleoporins are typically organized into distinct biochemically defined subcomplexes, which consequently build up the NPC (Figure 1.2) (Alber et al., 2007a; Schwartz, 2005). A well-studied and conserved subcomplex is the vertebrate Nup107-160 complex, which consists of nine nucleoporins (i.e. Nup107, Nup160, Nup133, Nup96, Nup85, Sec13, Nup43, Nup37 and Seh1) (Belgareh et al., 2001; Harel et al., 2003; Loiodice et al., 2004; Vasu et al., 2001). The Nup107-Nup160 complex localizes to both sides of the NPC's central framework (Belgareh et al., 2001; Krull et al., 2004) and its conserved homologue is the Nup84p complex in *S. cerevisiae* (Allen et al., 2002; Lutzmann et al., 2002; Siniosoglou et al., 1996). Depletion of any nucleoporin of the Nup107-160 complex in nuclear reconstitution assays from *X. laevis* egg extracts or by RNA interference (RNAi) in HeLa cells results in NE devoid of NPCs or nuclei with severe deficiencies in NPC formation, indicating that the complex is needed for NPC assembly at least in situ (Boehmer et al., 2003; Harel et al., 2003; Walther et al., 2003). In mice, however, NPCs assemble into the NE in the absence of Nup133 (Lupu et al., 2008). Besides its central role for NPC assembly, the Nup107-160 complex is essential for anchoring the nuclear basket protein Nup153 to the nuclear side of the NPC, which, in turn seems to anchor the nucleoporin Tpr to the nuclear basket (Hase and Cordes, 2003; Krull et al., 2004; Vasu et al., 2001). In mitosis, the Nup107-160 complex is recruited to kinetochores (Belgareh et al., 2001; Loiodice et al., 2004) and its depletion from HeLa cells by RNAi leads to failure in establishing a proper microtubule attachment to the

kinetochores, which in turn causes a checkpoint-dependent mitotic delay in the G2 phase of the cell cycle (Loiodice et al., 2004; Orjalo et al., 2006; Zuccolo et al., 2007).

The Nup93 complex is assembled by the nucleoporins Nup205, Nup155, Nup35/53 and most likely Nup188 (Grandi et al., 1997; Hawryluk-Gara et al., 2005; Miller et al., 2000). The yeast homologue of this complex consists of Nic96p as well as Nup188p, Nup192p, Nup157p and Nup170p (see Figure 1.2)(Aitchison et al., 1995; Grandi et al., 1995; Kosova et al., 1999; Nehrbass et al., 1996; Zabel et al., 1996). Immunodepletion of the Nup93 complex from *Xenopus* egg extracts showed that assembled nuclei are lacking proper NPCs, indicating that the Nup93 subcomplex is required for NPC assembly (Grandi et al., 1997). Biochemical data showed that the Nup93 complex is anchored in the NE through the binding of Nup35 to the integral membrane protein Ndc1 (Mansfeld et al., 2006). Ndc1 (Chial et al., 1998) is an important player in NPC assembly (Lau et al., 2004; Madrid et al., 2006; Mansfeld et al., 2006; Marelli et al., 2001; Stavru et al., 2006a), since depletion of Ndc1 from mammalian cells by RNAi caused a severe reduction in NPC staining, indicating defects in NPC assembly and/or stability (Mansfeld et al., 2006). The loss of Ndc1 function in *C. elegans* also causes, besides severe NPC defects, high larval and embryonic mortality (Stavru et al., 2006a).

Another important integral membrane protein is POM121, which interacts with the Nup107-160 complex (Antonin et al., 2005). POM121 is restricted to vertebrates and its depletion from *Xenopus* egg extracts leads to early block in NE assembly (Antonin et al., 2005). Nonetheless, when POM121 was depleted from human cells, functional NPCs and intact NEs were observed (Stavru et al., 2006b). The third metazoan transmembrane protein gp210 seems to be redundant in function with Ndc1 as well (Eriksson et al., 2004; Mansfeld et al., 2006; Stavru et al., 2006b). Similarly, in yeast, Ndc1 was found to be partially redundant with POM152p (Madrid et al., 2006). These observations suggest redundancies in protein-protein interactions within NPCs, ensuring that NPC formation is a robust process (Kitano, 2004; Stavru et al., 2006a).

The Nup214/Nup88 subcomplex is localized to the cytoplasmic face of the NPC (Bastos et al., 1997; Fornerod et al., 1997b). Interaction between Nup214 and Nup88 is likely mediated by their coiled-coil domains (Bastos et al., 1997; Fornerod et al., 1997b).

Interdependence of Nup88 and Nup214 for the localization at the NPC has been consistently observed in all species analyzed so far. Nup88 is undetectable in cells derived from Nup214-deficient mouse embryos (Fornerod et al., 1997b) and RNAi inhibition of each of the genes in human tissue culture results in reduced protein levels for the other (Bernad et al., 2004). Yeast cells with a temperature-sensitive mutation of the Nup88 homologue Nup82p show a reduction of Nup159p, the yeast homologue of Nup214, from the nuclear rim (Belgareh et al., 1998). The molecular mechanisms underlying this interplay remain unknown.

The major structural component of the cytoplasmic filaments is Nup358/RanBP2 (Delphin et al., 1997; Walther et al., 2002). Based on knockdown analysis in cultured human cells, Nup88 and Nup214 were proposed to play a key role in recruiting Nup358 to create the cytoplasmic filaments of the NPC (Bernad et al., 2004). Conversely, Hutten and Kehlenbach found that depletion of Nup214 resulted in codepletion of Nup88, but not of Nup358 (Hutten and Kehlenbach, 2006). Consistently, cytoplasmic filaments are intact in *nup214 Drosophila* larvae (Xylourgidis et al., 2006) and depletion of Nup214 from *Xenopus* egg extracts did not affect Nup358 localization at the NE (Walther et al., 2002). Furthermore, high-resolution FEISEM images of the cytoplasmic face of Nup214 deficient NPCs showed that cytoplasmic filaments were present (Walther et al., 2002). Together these data indicate that the Nup214/Nup88 complex does not play a major role in maintaining Nup358 on the cytoplasmic filaments.

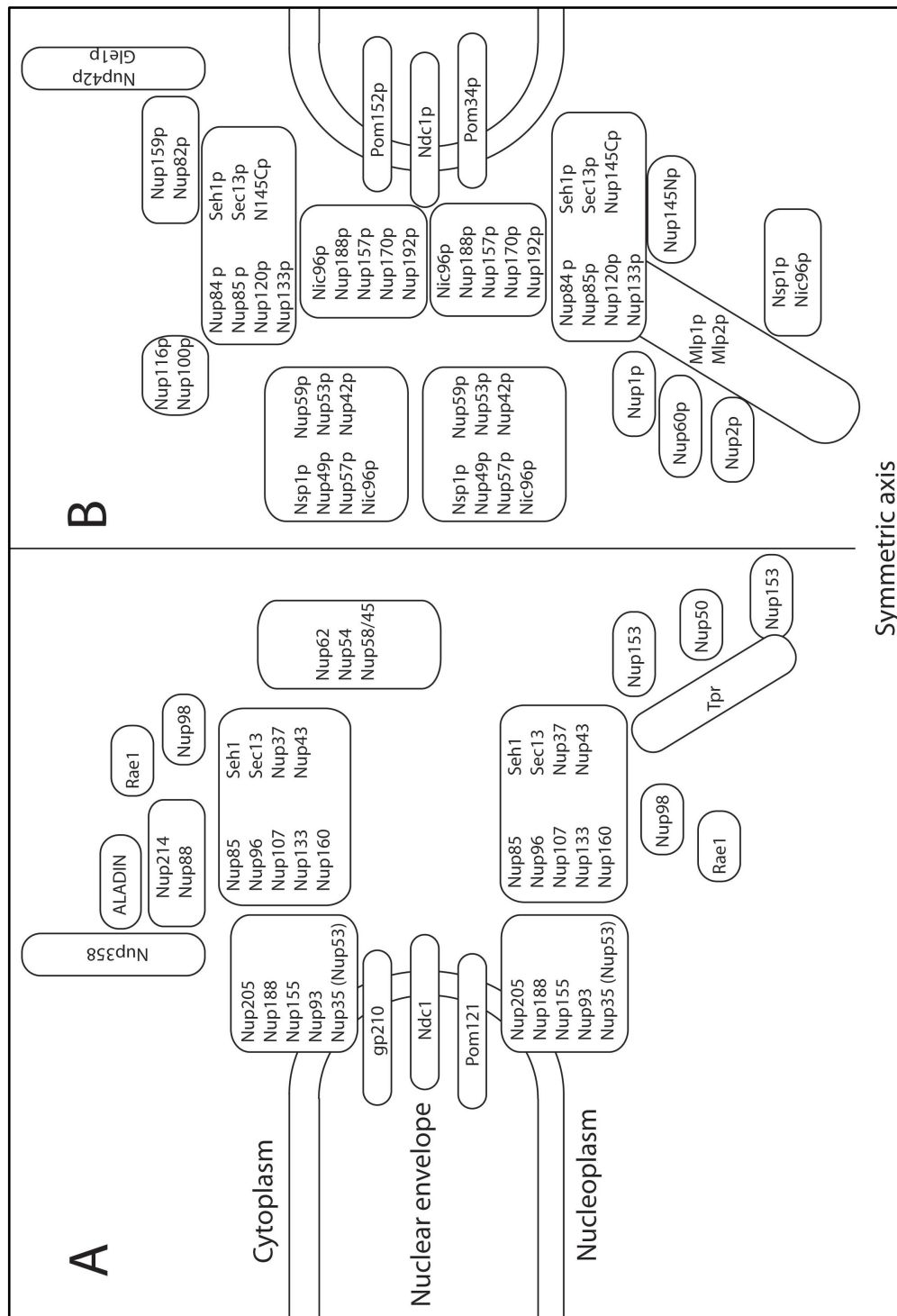


Figure 1.2: Subcomplex organization of the NPC.

Schematic overview on subcomplex organization in the NPC. **(A)** Subcomplex organization in metazoan NPC. **(B)** Subcomplex organization in yeast NPC. Adapted from (Schwartz, 2005).

1.4 Vertebrate nucleoporins

1.4.1 Nup153

The nucleoporin Nup153 is asymmetrically located on the nuclear side of the NPC and it consists of three distinct domains (Figure 1.3A). The N-terminal domain contains a nuclear envelope targeting cassette (NETC; 2-144), a RNA binding domain (RBD; 250-400) and the NPC assembly region (NPAR; 39-339), which directs Nup153 incorporation into the NPC and includes a M9-like nuclear localization signal (NLS; 247-290) (Bastos et al., 1996; Enarson et al., 1998; Nakielny et al., 1999). In the central domain, four zinc fingers of the C₂-C₂ type can be found that interact with DNA, RanGDP and the COPI complex (Liu et al., 2003; Nakielny et al., 1999; Sukegawa and Blobel, 1993). The C-terminus consists of natively unfolded FG-repeats, is highly mobile and mediates interactions with the soluble transport receptors importin- β and CRM1 (Denning et al., 2003; Nakielny et al., 1999; Shah et al., 1998; Sukegawa and Blobel, 1993). Immuno-electron microscopy revealed that the N-terminus of Nup153 is anchored at the nuclear ring moiety of the NPC, whereas the central zinc-finger domains are located at the distal ring (Fahrenkrog et al., 2002). The localization of the C-terminal domain is highly variable and can be detected at the nuclear basket and at the cytoplasmic ring of the NPC, depending on the nucleocytoplasmic transport state of the NPC (Fahrenkrog et al., 2002; Paulillo et al., 2005).

Nup153 is an essential protein as RNA interference (RNAi) studies showed that its depletion affects both the viability of *C. elegans* embryos and growth of tissue culture cells (Galy et al., 2003; Harborth et al., 2001). Furthermore, depletion of Nup153 by RNAi revealed that Nup153 is required for maintaining the structural integrity of the nuclear basket and incorporation of Nup153 itself depends on the Nup107-160 complex, which has an essential role in overall pore formation (Boehmer et al., 2003; Krull et al., 2004; Walther et al., 2003). Moreover, Nup153 provides an important link between the NPC and the nuclear lamina and it is critical for pore anchoring, as Nup153 deficient NPCs become mobile within the NE (Smythe et al., 2000; Walther et al., 2001). Nup153 also plays a role in NE breakdown (NEBD) in *Xenopus* nuclei through the recruitment of

the COPI coatomer complex (Liu et al., 2003; Prunuske et al., 2006). The COPI complex plays a major role in membrane remodeling at the Golgi apparatus and has been implicated in the process of NEBD, involving the dispersal of the nuclear membrane as well as disassembling of the NPCs (Bonifacino and Glick, 2004; Prunuske et al., 2006). Three members of the COPI coatomer complex (α , β and β') were reported to specifically interact with the zinc finger domains of Nup153 and Nup358 (Liu et al., 2003). These nucleoporins appear to be involved in the recruitment of COPI to the vicinity of the NE during mitosis, however, many questions remain about how the recruitment of COPI is regulated (Prunuske et al., 2006).

Recently, chromosomal rearrangements of *NUP153* have been identified that are associated with Nup153's increased expression in urothelial and retinoblastoma cancer (Heidenblad et al., 2008; Orlic et al., 2006). Furthermore, Nup153 is a positive regulator of Hedgehog signaling, which is crucial for developmental processes in many organisms (Nybakken et al., 2005). Moreover, Nup153 directly associates with adenomatous polyposis coli (APC) protein, a tumor suppressor, which promotes the association of microtubules with the nuclear membrane in neurons and this interaction is required for centrosome reorientation during cell migration (Collin et al., 2008). Taken together, these results suggest that Nup153 is involved in differentiation and tissue development and deficiencies in Nup153 function are related to human disease. Recently, Nup153 was implicated in both early mitotic defects and in a delay of late stages of mitosis in a dose-dependent manner (Mackay et al., 2009). Furthermore, the finding that Nup153 affects spindle checkpoint due to Mad1 hypophosphorylation suggests that Nup153 is an important regulator of mitotic events, which might be related to Nup153's role in development and cancer (Lussi et al., 2010).

1.4.2 Nup88

Nup88 was found to be localized on the cytoplasmic side of the NPC in a complex with Nup214, NUP358 and the protein export factor CRM1 (Bastos et al., 1997; Fornerod et al., 1997b). However, recent evidence suggests that a pool of Nup88 localizes to the nucleoplasmic side as well (Lussi et al., submitted, see Chapter 3). Based on its amino acid sequence, Nup88 is organized into two distinct domains: an N-terminal

domain, which is predicted to fold as a β -propeller, and a C-terminal domain that contains predicted coiled-coil segments (Fornerod et al., 1997b; Schwartz, 2005) (Figure 1.3 B). Interaction between Nup88 and Nup214 is likely mediated by their coiled-coil domains, and it seems that Nup88 and Nup214 are interdependent on each other for NPC localization, as one partner is unstable in the absence of the other (Bernad et al., 2004). However, Nup88 can be overexpressed relative to Nup214 and under these conditions it accumulates in the cytoplasm of both cultured human cells and *Drosophila melanogaster* larvae (Bernad et al., 2004; Xylourgidis et al., 2006).

Nup88 seems to play an important role in recruiting the FG nucleoporin Nup358/RanBP2, the major component of the cytoplasmic filaments of the NPC and the binding site for the Ran GTPase activating enzyme RanGAP (Bernad et al., 2004; Delphin et al., 1997; Walther et al., 2002). However, the amount of Nup358 in the cells appears not to be linked to the protein levels of Nup88, indicating that only the recruitment, but not the stability of Nup358 depends on Nup88 (Bernad et al., 2004).

Another interaction partner of Nup88 is Nup98, a nucleoporin localizing to both sides of the NPC (Griffis et al., 2003). Nup98 interacts via its C-terminal NPC-targeting domain with the β -propeller domain of Nup88 (Griffis et al., 2003). Nup98 seems to play a role in the assembly of Nup88 and other cytoplasmic nucleoporins into the NPC, as Nup88 relocates from the NE to annulate lamellae in Nup98 deficient mouse cells (Wu et al., 2001).

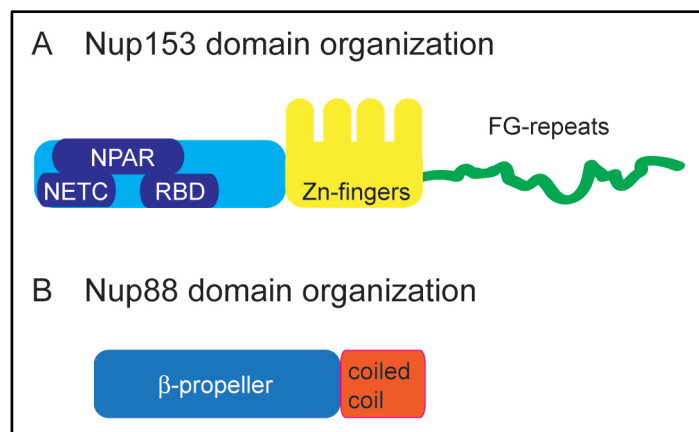


Figure 1.3: Domain organization of the nucleoporins Nup153 and Nup88

(A) Nup153 domain organization. The domain architecture of Nup153 is depicted. The N-terminal region of Nup153 contains the nuclear envelope targeting cassette (NETC; 2-144), which is required for targeting to the inner nuclear envelope, the nuclear pore assembly region (NPAR; 39-339), which is needed for the incorporation into the nuclear pore complex and an RNA binding domain (RBD; 250-400). The central zinc finger region (650-880) is comprised of four C₂-C₂ type zinc fingers. The C-terminal region (881-1475) contains FG-rich motifs that are thought to be natively unfolded. Adapted from (Ball and Ullman, 2005). (B) Nup88 domain organization. The domain architecture of Nup88 is shown. The N-terminal region of Nup88 folds into a predicted β -propeller, and the C-terminal domain contains predicted coiled-coil segments (Fornerod et al., 1997b; Schwartz, 2005).

1.4.2.1 Nup88 in nucleocytoplasmic transport

Nup88, together with Nup214, has been implicated in CRM1-mediated nuclear export. The FG-repeat domain of Nup214 and the N-terminal β -propeller of Nup88 directly interact with CRM1/exportin, the export factor for many nuclear export signal (NES)-containing proteins from the nucleus (Roth et al., 2003; Takahashi et al., 2008). However, the contribution of the Nup214/Nup88 complex in export of NES-containing cargo varies between systems. In *Drosophila* larvae, it was found that members only (*mbo*), the *Drosophila* Nup88 homologue, regulates the nuclear accumulation of Dorsal and Dif, members of the Rel/NF- κ B family of transcription factors (Roth et al., 2003; Uv et al., 2000). Therefore, it is assumed that, in *Drosophila*, the Nup214/Nup88-complex controls the recruitment of CRM1 to the NPC and the export of CRM1-dependent proteins, such as Dorsal and Dif, in a concentration-dependent manner (Xylourgidis et al., 2006) and Nup88 is hence assumed as nuclear export attenuator for NES-dependent export. Similarly, selective depletion of Nup88 by small interfering RNA (siRNA) inhibited the nuclear translocation of NF- κ B and NF- κ B-dependent reporter gene activation in human cells (Takahashi et al., 2008), suggesting that Nup88 is regulating the activity of NF- κ B at the level of nucleocytoplasmic transport. This notion is confirmed by the finding that nuclear accumulation and constitutive activation of NF- κ B in metastatic melanoma cells overexpressing Nup88 can be reduced by Nup88 depletion (Takahashi et al., 2008). Thus, overexpression of Nup88 in tumor cells might be involved in constitutive NF- κ B activation and in NF- κ B mediated malignancy.

In mammalian cell culture, the Nup214/Nup88 subcomplex was furthermore shown to be required for CRM1-mediated nuclear export of the 60 S pre-ribosomal subunits (Bernad et al., 2006). Further, depletion of the Nup214/Nup88 complex in HeLa

cells leads to greatly diminished export of the nuclear transcription factor NFAT, a transcription factor containing two classical NLS and one NES (Klemm et al., 1997).

Interestingly, a study in *Drosophila* S2 cells implicated Nup88 in nuclear import (Takano and Gusella, 2002). In this study, Nup88 was shown to be involved in the regulation of the transport of the huntingtin protein, the major determinant protein of Huntington's neurodegenerative disorder (Takano and Gusella, 2002). The NF- κ B/Rel family of transcription factors associates with huntingtin to form complexes for its nuclear import, which seems to be Nup88-dependent (Takano and Gusella, 2002). However, Nup88 has not been involved in import of any other cargoes than huntingtin so far.

1.4.2.2 Nup88 in disease

Nup88 was found to be overexpressed in a wide variety of human tumors (Emterling et al., 2003; Gould et al., 2000; Gould et al., 2002; Martinez et al., 1999; Schneider et al., 2004). In 75% of ovarian tumors, Nup88 is overexpressed in malignant tissue compared to adjacent healthy tissue (Martinez et al., 1999). In an analysis with an extended variety of tumor types, Nup88 was found to be overexpressed in a broad spectrum of neoplasias. Immunohistochemistry revealed overexpression of Nup88 especially evident in carcinomas, but was also observed in sarcomas, lymphomas and mesotheliomas (Gould et al., 2000; Gould et al., 2002). Overexpression of Nup88 was not associated with overexpression of other nucleoporins, i.e. Nup214 and Nup153, suggesting that overexpression in tumor tissues seems to be specific for Nup88 (Gould et al., 2002).

Nup88 can be found in the cytoplasm of tumor cells, what correlates with studies in cultured cells, where Nup88 accumulates in the cytoplasm when overexpressed (Bastos et al., 1997). Nup88 protein levels correlate to tumor development, aggressiveness and differentiation in breast, colorectal and hepatocellular carcinomas, melanoma, ovarian tumors and other neoplastic disease (Agudo et al., 2004; Emterling et al., 2003; Gould et al., 2000; Gould et al., 2002; Knoess et al., 2006; Martinez et al., 1999; Zhang et al., 2002; Zhang et al., 2007). Benign tumors and mild hyperplasia showed no overexpression, whereas Nup88 overexpression increased in more advanced tumors. In

colorectal cancer, highest expression was detected in invasive margins of tumors and in metastasis, suggesting a putative function in invasion (Emterling et al., 2003). Nup88 overexpression seems to increase with the progression of tumors and is associated with poorly differentiated tumors. Therefore, Nup88 was suggested as tumor marker and potential indicator for tumor prognosis.

How Nup88 overexpression is involved in tumorigenesis is not clear yet, but the notion that Nup88 is also overexpressed in fetal tissue supports the idea that Nup88 might play a role in proliferation (Gould et al., 2000; Schneider et al., 2004). A possible mechanism of how Nup88 influences proliferation might be through transport of transcription factors and its impact on signal transduction pathways, since it is known that Nup88 is involved, both in *Drosophila* and human cells, in the nuclear export of NF- κ B transcription factors (Takahashi et al., 2008; Uv et al., 2000). In *Drosophila*, active NF- κ B accumulates in the cytoplasm due to increased nuclear export in the absence of Nup88 (Uv et al., 2000). Conversely, Nup88 overexpression in cancer cells might lead to a decreased export of transcription factors, leading to an accumulation in the nucleus. Indeed, in breast, pancreas and colon carcinomas, NF- κ B is predominantly found in the nucleus where it could contribute to constitutive upregulation of target genes (Kau et al., 2004). Alternatively, Nup88 overexpression might be a cellular stress response, as its overexpression can be induced by UVA light in melanoma cells or by hypertonic stress in mice and human kidney cells (Andres-Hernando et al., 2008; Zhang and Rosdahl, 2003).

1.4.3 Nup214

The Nup214-Nup88 subcomplex is localized to the cytoplasmic face of the NPC (Bastos et al., 1997; Kraemer et al., 1994). Nup214 is dispensable for in vitro NPC assembly and protein import, but it is essential in vertebrate cells, and its depletion causes a strong mRNA export defect (van Deursen et al., 1996; Walther et al., 2002). Nup214 is organized in three distinct domains: an N-terminal domain, which is predicted to fold into a β -propeller (Weirich et al., 2004), a central domain with a leucine zipper motif and two predicted coiled-coil segments known to interact with Nup88 (Bastos et al., 1997; Fornerod et al., 1997a), and a long C-terminal FG-repeat that interacts strongly with the transport factor CRM1 in vitro in a RanGTP- and cargo-stimulated fashion (Askjaer et

al., 1999; Fornerod et al., 1995; Fornerod et al., 1997a; Kehlenbach et al., 1999). These data suggest that Nup214 plays an essential role in CRM1-mediated nuclear export. Interestingly, recent studies showed that the FG-rich domain of the asymmetric nuclear Nup153 and cytoplasmic Nup214 can cross the NPC to bind transport receptors and escorting transport complexes through the NPC (Fahrenkrog and Aebi, 2003; Fahrenkrog et al., 2002; Paulillo et al., 2005). However, it remains to be elucidated as to whether and how NPC asymmetry influences transport processes that are initiated on the opposite side of the NPC.

1.4.4 Nup98

Nup98 is located on both the nuclear and cytoplasmic side of the NPC, where it associates with the structural Nup107-160 complex or with Nup88, respectively, as the two interactions seem to be mutually exclusive (Griffis et al., 2003; Hodel et al., 2002; Vasu et al., 2001). Nup98 is expressed in two forms as a result of alternative splicing. The first splice variant encodes the 920 amino acid protein Nup98, which is posttranslationally cleaved into the 90 kDa N-terminal Nup98 and an 8 kDa C-terminal fragment. The second variant encodes a Nup98-Nup96 polyprotein that is also posttranslationally cleaved to form the N-terminal Nup98 and the C-terminal Nup96 (Fontoura et al., 1999).

The N-terminal domain of Nup98 contains FG and GLFG repeat motifs that are intersected by a small coiled-coil domain. Interestingly, Nup98 is the only vertebrate nucleoporin with GLFG-type repeats (Powers et al., 1995; Radu et al., 1995). The C-terminus is a domain with a unique β -sandwich structure with autoproteolytic activity, and it is important for directing Nup98 to the NPC and mediates the binding to the Nup107-160 complex and to Nup88 (Fontoura et al., 1999; Griffis et al., 2003; Hodel et al., 2002; Vasu and Forbes, 2001).

Nup98 interacts with the β -propeller nucleoporin Rae1/Gle2 through its coiled-coil domain (Pritchard et al., 1999). Rae1 is implicated in mRNA export, functions in cell cycle regulation and has a role in mitotic spindle function (Babu et al., 2003; Blower et al., 2005; Jeganathan et al., 2006; Pritchard et al., 1999). Both Nup98 and Rae1 are dynamic components of the NPC, that is, they can move on and off the NPC. Nup98 can

also be found within the nucleoplasm, where it is associated with intranuclear bodies termed GLFG bodies, as this domain is required for association with these structures. The mobility of Nup98 in the nucleoplasm can be blocked by inhibitors of transcription, suggesting a role for Nup98 in transcription and/or RNA shuttling to the NPC (Griffis et al., 2002).

1.5 FG-nucleoporins in nucleocytoplasmic transport

About one third of the nucleoporins contain FG-repeat domains, which mediate the interaction between transport receptor-cargo complexes and the NPC. These FG-repeat domains also likely contribute to the selective barrier that limits diffusion through the NPC. Crystal structures of importin- β or the mRNA export factor TAP in complex with FG-repeat peptides showed that the interaction interface involves primarily the phenylalanine rings of the FG-repeat domain and hydrophobic residues on the surface of the transport receptor (Bayliss et al., 2000; Fribourg et al., 2001). The length and composition of hydrophilic linker between individual FG-motifs seem to influence the affinity of the binding and allow simultaneous binding of several FG-repeats to the transport receptor (Liu and Stewart, 2005). Biochemical and biophysical measurements demonstrated that the FG-repeats are natively unfolded, i.e. they do not adopt any secondary structure (Denning et al., 2003; Denning et al., 2002). This notion was confirmed by the use of atomic force microscopy on single molecules, which revealed that the FG-repeat domain of Nup153 resembles a 180nm long unfolded polypeptide chain if spread on a surface (Lim et al., 2006). Along this line, immuno-EM studies on two FG-repeat nucleoporins Nup153 and Nup214 furthermore showed that FG-repeat domains adopt highly variable locations within the NPC (Fahrenkrog et al., 2002; Paulillo et al., 2005). Interestingly, systematic deletion of FG-repeat regions in yeast nucleoporins revealed a high level of functional redundancy, since yeast NPCs are able to compensate the loss of 50% of their FG-repeats with only little effect on nucleocytoplasmic transport (Strawn et al., 2004; Zeitler and Weis, 2004).

While the main function of the NPC and its constituents is to control nucleocytoplasmic transport of macromolecules in and out of the nucleus, it became

evident in the past few years that individual nucleoporins play important roles in other cellular processes, such as chromatin organization, gene expression and kinetochore organization during mitosis. We will concentrate here on novel functions of nucleoporins in transcription and mitosis, which will be discussed in sections 1.6 and 1.7, respectively.

1.6 Nucleoporins in transcription

The nuclear periphery and the NPCs were generally considered as region of gene repression, despite Blobel's gene gating hypothesis that proposed NPCs as anchoring sites for active genes (Blobel, 1985). Heterochromatin and gene poor sequences were found enriched at the periphery of the nucleus (Brown and Silver, 2007) and in yeast the two nucleoporins Nup60p and Nup145Cp are involved in repression of the silent mating type loci HML and HMR and in silencing telomeres (Brown and Silver, 2007; Feuerbach et al., 2002; Galy et al., 2000). Evidence for Blobel's theory came from studies on the nucleoporin Nup2p, which, together with several proteins of the nuclear transport machinery, exhibits boundary activity and can recruit actively transcribed genes to the NPC (Cabal et al., 2006; Casolari et al., 2005; Ishii et al., 2002; Luthra et al., 2007; Menon et al., 2005; Schmid et al., 2006).

NPC association of transcribed genes might increase the efficiency of mRNA processing and export through, for example, recruitment of the SAGA and TREX complex (Cabal et al., 2006; Taddei et al., 2006). Accordingly, Sus1p, a member of the SAGA chromatin-remodeling complex in yeast that is also present in the mRNA export complex TREX, interacts with Nup1p (Fischer et al., 2002; Rodriguez-Navarro et al., 2004). Similarly, Nup153, the vertebrate homologue of Nup1p, and Nup98 are thought to be involved in the link between transcription and mRNA export (Griffis et al., 2004). Moreover, the yeast myosin-like proteins Mlp1p and Mlp2p, both homologous to human Tpr (Cordes et al., 1997), appear to link these two processes (Vinciguerra et al., 2005). Loss of Mlp1p/Mlp2p is rescuing lacZ reporter mRNA levels and enhances their export to the cytoplasm in a yeast strain defective for mRNA export (Vinciguerra et al., 2005). Microarray analysis further showed that Mlp2p reduces a subset of cellular transcripts, such as RNase P RNA (RPR1) or proteins involved in fatty acid biosynthesis, in the mRNA export mutant strain (Vinciguerra et al., 2005), indicating that loss of Mlp

proteins negatively affects transcription of several genes when mRNA export is disturbed.

Nup2p and the Nup84p complex can exhibit repressive and activating behavior in gene expression (Dilworth et al., 2005; Ishii et al., 2002; Menon et al., 2005; Schmid et al., 2006; Therizols et al., 2006), although it is not understood how this switch is regulated. Nup2p is furthermore involved in epigenetic regulation of transcription (Brickner et al., 2007). Nup2p interacts with the histone variant H2A.Z (Dilworth et al., 2005) and tethers genes to it (Brickner et al., 2007). H2A.Z in turn is inserted at inducible promoters after activation (Brickner et al., 2007), which leads to a heritable memory of transcriptional activation through epigenetic information, i.e. the localization at the nuclear periphery.

Nucleoporins are also involved in transcription regulation in higher eukaryotes, e.g. in dosage compensation in the fruit fly *Drosophila melanogaster* (Lucchesi et al., 2005; Mendjan and Akhtar, 2007; Mendjan et al., 2006). Dosage compensation ensures the equalization of X-linked gene expression, which in mammals is achieved by an inactivation of one X chromosome in female cells (reviewed in (Royce-Tolland and Panning, 2008), whereas in *D. melanogaster* X-linked genes in males are 2-fold upregulated (Mendjan and Akhtar, 2007). In *Drosophila* Nup153 and Mtor, the homologue of the human Tpr, are essential for the correct localization of dosage compensation complex proteins on the X chromosome and dosage compensation is abolished in male cells when Nup153 or Mtor are depleted (Mendjan et al., 2006). Similarly, knockdown of Tpr, but not Nup153, lead to impaired dosage compensation in human cells (Tullio-Pelet et al., 2000).

Human Nup93 was shown to directly associate with chromosomes 5, 7, and 16 at the nuclear periphery (Brown et al., 2008). Nup93 interacts with regions of transcriptional repression and enriched heterochromatin in HeLa cells. Upon global histone acetylation mediated by the histone deacetylase inhibitor trichostatin A, Nup93 binding sites are highly enriched in several factors including the histone variant H2A.Z and active histone methylation marks (Brown et al., 2008), corresponding to an exchange of silent for active chromatin at the NPC. The presence of H2A.Z at sites of NPC-chromatin interaction

indicates a similar form of transcriptional memory in human nuclei, as found in yeast due to Nup2p and H2A.Z binding.

Taken together, these studies indicate that gene targeting to the NPC is evolutionary conserved from yeast to human. Targeting of genes to the NPC can lead to their silencing or activation and NPCs are also acting as epigenetic mark, underlying the decisive role of NPCs in the control of gene expression.

1.7 Nucleoporins in mitosis

A hallmark of eukaryotic cells is the compartmentalization of the genetic material inside the nucleus. By restricting the accessibility of cytoplasmic proteins to DNA with the physical barrier of the NE, eukaryotic cells have achieved a complexity in transcriptional regulation not found in prokaryotes. Higher eukaryotes undergo an open mitosis during which the NE and NPCs disassemble into soluble subcomplexes that disperse throughout the mitotic cytoplasm (Burke and Ellenberg, 2002; Suntharalingam and Wentz, 2003; Vasu and Forbes, 2001). After the chromosomes are segregated, the nuclei are reassembled and cytokinesis is completed by abscission of the two daughter cells. The whole scenario is tightly controlled by several checkpoints, including the spindle assembly checkpoint (SAC). The SAC prevents chromosome mis-segregation and aneuploidy by delaying the metaphase-anaphase transition until all chromosomes are properly attached to the mitotic spindle and aligned at the metaphase plate (Musacchio and Salmon, 2007).

Nucleoporins were originally thought to be stored inertly once released from the NPC at the entry of mitosis and incorporated into NPCs during late mitosis. However, recent evidence suggests that certain nucleoporins perform important mitotic functions independently of their roles during interphase. For example, the Nup107-160 as well as Nup358 localize in part to kinetochores after their release from the NPC, where they exert functions in chromosome segregation (Dawlaty et al., 2008; Joseph et al., 2004; Salina et al., 2003; Zuccolo et al., 2007). On the other hand, important regulators of the spindle assembly checkpoint, namely Mad1 and Mad2, localize to the NPC in interphase cells (Campbell et al., 2001; Iouk et al., 2002). The function of the SAC proteins at the NPC

has remained largely elusive although it has been suggested that the NPC may play a role in the duration of the SAC (Kastenmayer et al., 2005; Scott et al., 2005).

1.7.1 The spindle assembly checkpoint

The spindle assembly checkpoint (SAC), alternatively referred to as the mitotic checkpoint, is a molecular system that ensures accurate segregation of mitotic chromosomes by delaying anaphase onset until each kinetochore has properly attached to the mitotic spindle and aligned at the metaphase plate (Kops et al., 2005; Musacchio and Salmon, 2007; Rieder et al., 1995; Rieder et al., 1994). Kinetochores that are not yet attached to mitotic microtubules and chromosome pairs that lack tension across sister chromatids generated by the spindle poles activate the SAC (Rieder and Maiato, 2004; Yu, 2002). Various mitotic checkpoint proteins, including Mad1, Mad2, Bub1, BubR1 and Bub3, bind to kinetochores that lack attachment or tension to signal that not all chromosomes are properly attached and to stop progression of the mitotic program (Kops et al., 2005; Shah and Cleveland, 2000; Sharp-Baker and Chen, 2001; Taylor et al., 2001; Yu, 2002). The SAC inhibits the anaphase promoting complex/cyclosome (APC/C), a multisubunit E3 ubiquitin ligase that marks target proteins for degradation by the proteasome (Hwang et al., 1998; Kim et al., 1998). Specifically, the SAC negatively regulates the ability of the cell-division cycle protein Cdc20 to activate the APC/C-mediated polyubiquitylation of two key substrates, cyclin B and securin, thereby preventing their degradation. When the last chromosome is captured by the spindle microtubules, the inhibitory SAC proteins are released from the APC/C, which allows progression into anaphase.

1.7.2 Mad1 and Mad2

Mad2 appears to have the most direct role in inhibiting the activity of the APC/C-activating protein Cdc20. Mad2 binds directly to Cdc20 when the SAC is active, and this binding is sufficient to block ubiquitylation of securin or cyclin B by the APC/C in vitro (Fang et al., 1998; Li et al., 1997). Protein levels of Mad2 do not change much during mitosis, and it is thought that Mad2 in its monomeric form is inactive and not capable to stably bind Cdc20. However, oligomerized Mad2 inhibits activation of APC/C and blocks

cell cycle progression (Fang et al., 1998). Therefore, a change in Mad2 structure, which facilitates oligomerization, might play a role in transducing the checkpoint signal. However, it is suggested that Mad2's activity is stimulated by kinetochores that are unoccupied by microtubules and that the association with other checkpoint proteins, including Bub3 and the kinase BubR1, enhances the ability of Mad2 to inhibit the APC/C (Sudakin et al., 2001). How the kinetochores of chromosomes that have not yet bioriented can trigger Mad2 to adopt a form capable of inhibiting Cdc20 is not exactly clear.

Mad2 directly interacts with Mad1, which is crucial for the recruitment of Mad2 to kinetochores (Chen et al., 1998). The recruitment of Mad1 to the kinetochores is one of the first events in activating the SAC and depends on its phosphorylation by the Polo-like kinase 1 (Plk1) (Chi et al., 2008). Attenuation of Mad1 phosphorylation by depleting Plk1 using siRNAs inhibits Mad1's kinetochore association and cells with reduced Mad1 phosphorylation levels due to overexpression of Nup153 show defective SAC function (Chi et al., 2008)(Lussi et al., 2010).

1.7.3 Nup153

Nup153 is phosphorylated throughout the cell cycle and hyperphosphorylated during mitosis (Favreau et al., 1996). Studies performed in *Xenopus* egg extract, a system to reconstitute cell division and nuclear assembly in vitro, have implicated Nup153 in NE breakdown (Liu et al., 2003; Prunuske et al., 2006), indicating that Nup153 plays a role in mitosis. Increased expression of Nup153 in urothelial and retinoblastoma cancer and its requirement for centrosome reorientation through interaction with the adenomatous polyposis coli (APC) protein during cell migration in neurons suggests a role for Nup153 in tissue development and differentiation, probably by regulation of the cell cycle (Collin et al., 2008; Heidenblad et al., 2008; Orlic et al., 2006). Interestingly, a study showed that reduction of Nup153 causes a delay in cytokinesis in a dose-dependent manner without affecting global nucleocytoplasmic transport (Mackay et al., 2009), indicating a role for Nup153 in mitotic events. However, the exact mechanism of how Nup153 functions in mitosis remained largely elusive. A possible link between Nup153 and mitosis constitutes the SAC protein Mad1, since Nup153 is required for the localization of Mad1 to NPCs in interphase cells (Hawryluk-Gara et al., 2005). The exact role of Mad1 at the NPC during

interphase is not clear, but it is suggested that the tethering of SAC proteins to the NPC in interphase plays a role in the timing of the SAC (Kastenmayer et al., 2005; Scott et al., 2005). However, it was shown recently that overexpression and deletion of Nup153 exhibits strong mitotic defects due to a misregulation of Mad1 phosphorylation (Lussi et al., 2010, see Chapter 2).

1.7.4 The Nup107-160 complex

A fraction of the Nup107-160 complex has been shown to localize dynamically to kinetochores from prophase to late anaphase (Belgareh et al., 2001; Loiodice et al., 2004) and to reconstituted spindles from *Xenopus laevis* egg extracts (Orjalo et al., 2006). The recruitment of the human Nup107-160 complex to kinetochores is dependent on the NDC80 complex and the centromere protein F (CENP-F), which is also involved in microtubule-kinetochore interaction (Zuccolo et al., 2007). At the kinetochores, the Nup107-160 complex is required for chromosome congression, maintenance of tension between sister kinetochores and the attachment of microtubules to the kinetochores (Zuccolo et al., 2007). In human cells, depletion of the Nup107-160 complex by RNAi from kinetochores affects proper microtubule attachment and is leading to a mitotic delay (Zuccolo et al., 2007).

Only recently, the transcription factor ELYS/Mel-28 has been identified as a new binding partner of the Nup107-160 complex at both the NPC and the kinetochores (Rasala et al., 2006). ELYS/Mel-28 and Nup107-160 complex also act together in NPC assembly in *C. elegans* and human cells (Fernandez and Piano, 2006; Galy et al., 2006; Rasala et al., 2006). Therefore, both ELYS/Mel-28 and Nup107-160 complex are required for NPC assembly and proper cell division.

1.7.5 Nup358

Nup358, together with RanGAP and the protein export factor CRM1, is recruited by the Nup107-160 complex to the kinetochores (Zuccolo et al., 2007). RanGAP1 is a substrate of the ubiquitin-like protein SUMO-1 (Matunis et al., 1996) and sumoylation is needed for its association with kinetochores (Joseph et al., 2002). Nup358 and RanGAP1 are involved in chromosome congression and segregation, stable kinetochore-microtubule

association and kinetochore assembly (Askjaer et al., 2002; Joseph et al., 2004; Salina et al., 2003) and it is CRM1 that provides an anchoring site for the Nup358/RanGAP1 complex at the kinetochores (Arnaoutov et al., 2005).

1.7.6 Nup98

Nup98 and the nucleocytoplasmic transport factor Rae1 function in anaphase onset via regulation of the anaphase promoting complex/cyclosome (APC/C) (Jeganathan et al., 2005). APC/C drives the cells into anaphase by inducing degradation of cyclin B and the anaphase inhibitor securin, an inhibitor of the separase enzyme. To prevent chromosome missegregation, APC/C activity directed against these mitotic regulators must be inhibited until all chromosomes are properly attached to the mitotic spindle. Rae1 and Nup98 act together to regulate the timely destruction of securin by APC/C (Jeganathan et al., 2005). The functional significance of the interaction between Nup98/Rae1 and the APC/C is highlighted by the notion that knockdown of Nup98 and Rae1 leads to premature separation of sister chromatids and severe aneuploidy in mice splenocytes (Jeganathan et al., 2006).

1.8 NPCs and diseases

The main function of NPCs is to mediate the passage of molecules between the nucleus and the cytoplasm. Alterations in NPC components and/or nucleocytoplasmic transport have a strong impact on cell growth and survival. Therefore, it is not surprising that nucleoporins are implicated in many diseases, such as Triple A syndrome, cancer and autoimmune diseases.

1.8.1 Triple A syndrome

Triple A syndrome (also called Allgrove syndrome) is a rare, autosomal, recessive disorder characterized by alacrima, neurological abnormalities, achalasia and adrenocorticotrophic hormone (ACTH) resistant adrenal failure (Allgrove et al., 1978; Clark and Weber, 1998; Gazarian et al., 1995; Khelif et al., 2003; Kimber et al., 2003; Moore et al., 1991; Prpic et al., 2003; Tsao et al., 1994). These four major syndromes are often highly variable in severity and age of onset and usually are progressive. Triple A

syndrome is caused by mutations in the *AAAS* gene, which encodes a protein known as ALADIN (alacrima-alachasia-adrenal insufficiency neurologic disorder) or adracalin (Handschug et al., 2001; Tullio-Pelet et al., 2000). ALADIN is thought to localize to the cytoplasmic side of the NPC and contains four WD (tryptophan-aspartic acid) repeats (Cronshaw et al., 2002; Cronshaw and Matunis, 2003; Handschug et al., 2001; Tullio-Pelet et al., 2000). Most of the mutations causing triple A syndrome are truncations of the C-terminus of ALADIN, which delete a domain essential for NPC targeting, leading to mislocalization of ALADIN to the cytoplasm (Cronshaw and Matunis, 2003). In addition, four point mutations have been identified in patients, three of which are within the WD-repeat domain, whereas the fourth is close to the N-terminus of ALADIN (Goizet et al., 2002; Handschug et al., 2001; Houlden et al., 2002; Persic et al., 2001; Sandrini et al., 2001; Schmittmann-Ohters et al., 2001; Tullio-Pelet et al., 2000).

Characterization of a mutant ALADIN cell line indicates that the absence of functional ALADIN does not result in morphological abnormalities in nuclei, NPCs or NE, indicating that the effect is functional rather than structural (Cronshaw and Matunis, 2003). As a member of the WD-repeat family of proteins, which are thought to be involved in assembly of macromolecular complexes (Smith et al., 1999), ALADIN could be involved in mediating the assembly of subdomains of the NPC or the formation of transport complexes through its WD-domain (Cronshaw and Matunis, 2003). The tissue-specific expression of the *AAAS* gene in both neuroendocrine and cerebral structures points to a role for ALADIN in the normal development of the peripheral and central nervous systems (Tullio-Pelet et al., 2000). Together this suggests that ALADIN might play a cell type-specific role in regulating nucleocytoplasmic transport and this might be essential for the proper maintenance and/or development of certain tissues.

1.8.2 Nucleoporins in cancer

Nucleoporins are involved in several cases of acute myeloid leukemia and a few other hematological malignancies as well as rare cases of other tumors (Cronshaw and Matunis, 2004). For Nup88, its overexpression is associated with malignant tumors (Agudo et al., 2004; Emterling et al., 2003; Gould et al., 2000), whereas in most other

cases the involvement of nucleoporins originates from chromosomal rearrangements that result in oncogenic fusion proteins.

Several nucleoporin genes, such as Nup98 and Nup214, are involved in chromosomal translocations that lead to oncogenic fusion proteins. Nup98 was found fused to more than 20 different partners and these fusion proteins are associated with leukemic transformations giving rise to myeloid and lymphoid malignancies (Lam and Aplan, 2001; Panagopoulos et al., 2003; Rosati et al., 2002; Suzuki et al., 2002; Taketani et al., 2002a; Taketani et al., 2002b; Taketani et al., 2002c). Nup98 fusion partners include nine members of the homeobox (HOX) family of transcription factors, which are fused to the FG-repeat-domain of Nup98 (Panagopoulos et al., 2003; Suzuki et al., 2002; Taketani et al., 2002a; Taketani et al., 2002b; Taketani et al., 2002c). Homeobox transcription factors are involved in early embryonic development and regulate hematopoiesis and the fusion of the FG-repeat domain of Nup98 to the DNA binding domains of these transcription factors appears to enhance their transcriptional activity (Ghannam et al., 2004; Kasper et al., 1999). However, more recently it became evident that Nup98 containing fusion proteins exhibit repressive function on transcription (Bagley et al., 2000). Whether Nup98 is exhibiting transcriptional regulation activity only in oncogenic fusion or it is related to a role of endogenous Nup98 is not known so far. However, it is known that human Nup98 is able to stimulate transcription of reporter genes at the nuclear periphery in yeast suggesting that transcription activation by Nup98 also occurs in a normal context of the NPC (Menon et al., 2005).

The nucleoporin Nup214 (earlier named CAN) was for the first time discovered as DEK-CAN fusion protein in acute myeloid leukemia (Fornerod et al., 1995). Since then, the *NUP214* gene was found in two other chromosomal translocations that fuse it to genes encoding SET (von Lindern et al., 1992) and ABL1 (Graux et al., 2004; Li et al., 1996). Fusions to DEK and SET contain the FG-repeat domain of Nup214 and are thought to act as transcriptional activator (Kasper et al., 1999). Fusions of Nup214 to ABL contain the N-terminal domain of Nup214 and are thought to increase the kinase activity of ABL (Allen et al., 1996; Graux et al., 2004).

A rare chromosomal translocation fuses the N-terminus of Nup358 to the protein kinase domain of ALK, which was identified in three reported cases in inflammatory

myofibroblastic tumors (IMTs) (Ma et al., 2003; Patel et al., 2007). It is speculated that the N-terminal domain of Nup358 promotes oligomerization and constitutive activation of the ALK protein kinase domain. Interestingly, Nup358 was found to be required for sumoylation of topoisomerase II α through its SUMO E3 ligase activity in mitosis (Dawlaty et al., 2008). Mice with low amounts of Nup358 develop severe aneuploidy in the absence of obvious transport defects and are highly sensitive to tumor formation. Therefore, Nup358 seems to play an important role in tumor suppression. Accordingly, reduced Nup358 transcription levels were found in human non-small cell lung cancers (Beer et al., 2002; Garber et al., 2001).

Tpr (translocated promoter region) was originally identified in a chromosomal rearrangement found in a human sarcoma cell line (Park et al., 1986). Subsequently, chromosomal translocations which fuse the N-terminal coiled-coil domain of Tpr to the protein kinase domains of the *MET* (Park et al., 1986), *RAF* (King et al., 1988) and *TRK* (Greco et al., 1992) protooncogenes were identified, which are involved in osteosarcoma, adenocarcinoma or fibroblastoma and papillary thyroid carcinoma, respectively. Biochemical studies indicate that the N-terminal coiled-coil domain of Tpr can activate the protein kinase domain of MET by mediating protein oligomerization (Hays and Watowich, 2003; Rodrigues and Park, 1993). The resulting constitutive protein kinase activity is believed to be involved in cellular transformation. Whether specific defects in NPC function are also involved is currently unknown.

The *NUP153* gene, among other proteins, was found to be amplified in chromosomal translocations leading to 6p22 genomic gain in retinoblastoma and urothelial carcinomas (Heidenblad et al., 2008; Orlic et al., 2006). Interestingly, chromosomal translocation leads to an amplification of the *NUP153* gene and subsequent overexpression of the Nup153 mRNA transcript (Heidenblad et al., 2008; Orlic et al., 2006). However, protein levels of Nup153 were not altered relative to normal adult human retina (Orlic et al., 2006).

Additionally to oncogenic chromosomal translocations, Nup88 was found to be overexpressed in a wide variety of human tumors (Emterling et al., 2003; Gould et al., 2002; Martinez et al., 1999). In normal cells, Nup88 is found on the cytoplasmic side of the NPC in a subcomplex with Nup214 and is involved in CRM1 mediated nuclear export

(Bernad et al., 2006; Bernad et al., 2004; Fornerod et al., 1997b; Roth et al., 2003). When Nup88 is overexpressed in tumor cells, it accumulates in the cytoplasm. The functional significance of this mislocalization is not known yet, but overexpression of Nup88 is clearly associated with tumor development and aggressiveness (Agudo et al., 2004; Emterling et al., 2003; Gould et al., 2000; Gould et al., 2002; Martinez et al., 1999; Zhang et al., 2002; Zhang et al., 2007). The exact mechanism as of how Nup88 is involved in tumorigenesis is still obscure, but it is suggested that Nup88 might play a role in proliferation as it is not only overexpressed during tumorigenesis but also during development in the earliest stages of embryological differentiation in chicken embryos (Schneider et al., 2004). Alternatively, Nup88 might be involved in DNA repair mechanism and stress response as its expression can be induced by UVA light in melanoma cells (Zhang and Rosdahl, 2003). Furthermore, Nup88 is involved in the nuclear export of NF- κ B transcription factors, both in *Drosophila* and human cells (Takahashi et al., 2008; Uv et al., 2000), indicating that its involvement in tumorigenesis might be related to specific signal transduction pathways.

1.8.3 Nucleoporins in autoimmune disease

The NPC is one of many intracellular targets in patients with autoimmune disease. Autoantigen targets include gp210, proteins of the Nup62 complex, Tpr and Nup153.

Primary biliary cirrhosis (PBC) is a poorly understood autoimmune disease that slowly destroys the bile ducts and can lead to cirrhosis of the liver (Worman and Courvalin, 2003). Autoantibodies against gp210 and Nup62 are found in \square 25% of individuals with PBC and appear to be associated with a poor outcome of PBC (Invernizzi et al., 2001; Itoh et al., 1998). Tpr antibodies were found in a variety of autoimmune disease, e.g. autoimmune liver disease (ALD), systemic lupus erythematosus (SLE), motor and/or sensory neuropathy, anti-phospholipid syndrome (APS), systemic sclerosis (SSc), Sjogren's syndrome (SjS), and others with a variety of diagnoses. This indicates that Tpr is a common target of human autoantibodies (Ou et al., 2004). Two other nucleoporins have been identified as targets for human autoantibodies. Antibodies from a patient with an overlap connective tissue disorder bound to Nup358 (Wilken et al.,

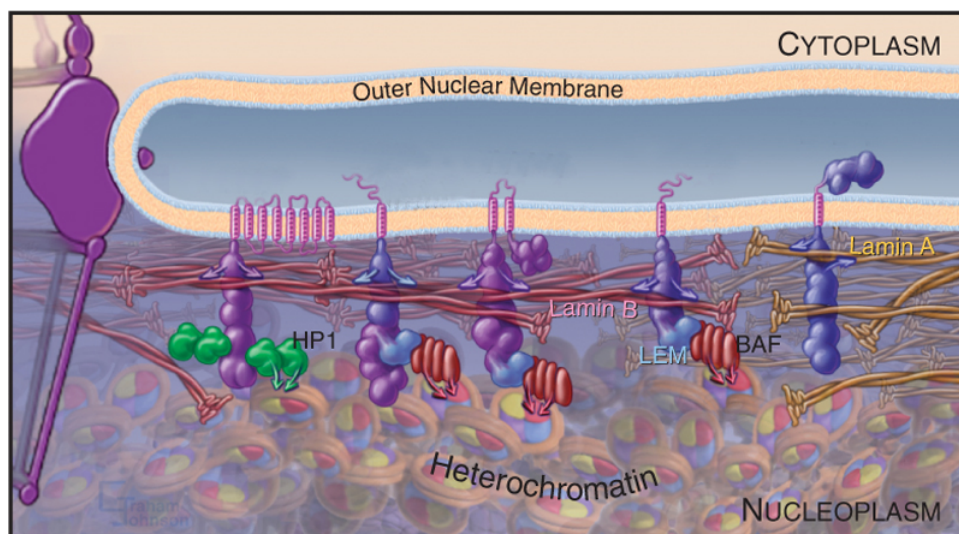
1993) and Nup153 has been identified as autoantigen in chronic hepatitis B and C viral infection, in Wilson's disease and other autoimmune diseases (Gregorio et al., 1999).

Although the list of antigens is growing, little is known about the mechanism of activation of autoimmune response. A possible mechanism might be molecular mimicry, where similarities between proteins from a pathogen and self-protein are sufficient enough to result in the cross-activation of autoreactive T or B cells and trigger autoimmune-response. Nup153, for example, displays sequence similarity to the Hepatitis B virus DNA polymerase (HBV-pol), and could therefore trigger the autoimmune response after HBV infection (Gregorio et al., 1999). Another evidence for molecular mimicry comes from studies with gp210 (Greber et al., 1990), where it was shown that the transmembrane domain of gp210 had significant sequence similarities to the topology of the envelope glycoproteins of different animal viruses. Therefore, molecular mimicry might be the mechanism leading to a loss of tolerance to nucleoporins and the subsequent production of autoantibodies.

1.9 The nuclear lamina

The nuclear lamina is a filamentous meshwork at the inner NE and supports stabilization of the nuclear architecture and is involved in the anchoring and spacing of NPCs (Aaronson and Blobel, 1975; Akey, 1989; Liu et al., 2000; Maeshima et al., 2006). The major components of the nuclear lamina are lamins, nuclear specific type V intermediate filament (IF) proteins, and various lamin-binding proteins (Burke and Stewart, 2002; Herrmann and Aebi, 2004; Stuurman et al., 1998) (Figure 1.4). Lamins bind to integral membrane proteins, such as LAP2, emerin and MAN1, proteins containing the so-called LEM-domain, through which they interact with the barrier-to-autointegration protein (BAF) and DNA. Those integral membrane proteins associate the nuclear lamina with the INM, thereby providing mechanical stability for the nuclear envelope. Lamins can interact directly with DNA and with chromatin proteins, e.g. the heterochromatin protein HP1, and organizing the chromatin structure at the nuclear periphery (Schirmer and Foisner, 2007). Several nucleoporins have been identified to interact with lamins, mainly Nup153, which is interacting with both A- and B-type lamins (Al-Haboubi et al., submitted)(Smythe et al., 2000). Lamin B has been shown to interact

with Nup53, and more recently, Nup88 has been identified as novel lamin A binding partner (Hawryluk-Gara et al., 2005) (Lussi et al., submitted). Moreover, lamins interfere with the assembly and distribution of NPCs and clustering of NPCs is associated with lamin mutations (Schirmer et al., 2001; Smythe et al., 2000). In recent years, however, it became more and more evident that lamins are involved in cellular processes like DNA replication, transcription, cell survival and cell cycle regulation (Broers et al., 2006; Dechat et al., 2009; Dechat et al., 2008).



© Elsevier, Pollard et al.: Cell Biology 2e - www.studentconsult.com

Figure 1.4: The nuclear lamina.

The nuclear lamina is engaged in the organization of chromatin and nuclear architecture and in anchoring and spacing of NPCs. The main components of the nuclear lamina are A- and B-type lamins. Different proteins bind to the lamins, anchor the lamina to the nuclear membrane and interact with chromatin. HP1: heterochromatin protein 1; LEM: LAP2, emerin, MAN1; BAF: barrier-to-auto-integration factor. Figure from Elsevier, Pollard et al.: Cell Biology 2e.

1.9.1 Nuclear lamins

According to their sequence homology and their biochemical behaviour, lamins can be classified in A- and B-type lamins. A-type lamins, mainly lamin A and lamin C, are encoded by the *LMNA* gene, arise through alternative splicing and are only expressed in differentiated cells. B-type lamins are encoded by two different genes, *LMB1* and *LMB2*, giving rise to two major isoforms lamin B1 and lamin B2 and they are ubiquitously expressed and essential for cell viability and development (Harborth et al., 2001; Lenz-Bohme et al., 1997; Liu et al., 2000; Osouda et al., 2005; Vergnes et al.,

2004). Lamins are organized in three distinct domains: a N-terminal head domain, a central α -helical coiled-coil rod domain and a C-terminal tail domain (Figure 1.5). The rod domain can be divided into four coiled-coil segments 1A, 1B, 2A and 2B, which are separated by linker segments. The C-terminal domain contains a NLS and an immunoglobulin-like (Ig)-fold domain (Dhe-Paganon et al., 2002; Krimm et al., 2002). Furthermore, B-type lamins carry a motif in their C-terminus, referred to as the CAAX box (C = cysteine, A = aliphatic, X = any amino acid), which is posttranslationally modified through farnesylation, tethering the protein to the inner nuclear membrane (Prufert et al., 2004; Ralle et al., 2004). A-type lamins, except for lamin C, also contain a CAAX-motif and are farnesylated post-translationally, which is later on removed to produce the mature lamin A. The removal of the farnesylation renders the A-type lamins more soluble and they can therefore also be found distributed throughout the nucleoplasm (Bridger et al., 1993; Hozak et al., 1995; Moir et al., 2000b).

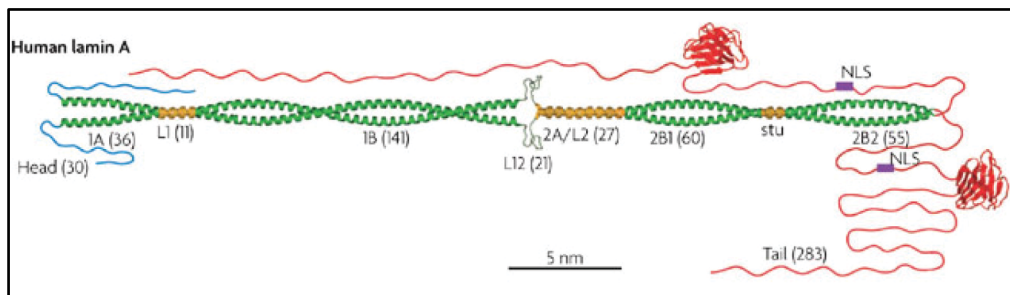


Figure 1.5: Structural model of a lamin A dimer based on structural data and structure predictions.

The central α -helical rod domain is subdivided into the coil segments 1A, 1B, 2A, 2B1 and 2B2. Linker segments that connect the individual α -helical segments are indicated: L1, L12 and L2. Left-handed coiled-coil segments are shown in green. Regions that are predicted to form nearly parallel α -helical bundles are represented in yellow. Non- α -helical linkers are shown in grey. The non- α -helical N- (head) and C-terminal (tail) domains are colored in blue and red, respectively. Adapted from (Herrmann et al., 2007).

1.9.2 Nucleoplasmic lamin A and the lamina-associated polypeptide 2 α (LAP2 α)

In the nucleoplasm, A-type lamins appear in tight foci or in general nucleoplasmic distribution (Broers et al., 1999; Moir et al., 2000b). The distribution of lamin A seems to be cell cycle dependent, as the most nucleoplasmic lamin A accumulates in G1 phase (Bridger et al., 1993; Dechat et al., 2004; Moir et al., 2000b).

How the pool of nucleoplasmic lamin A is recruited to the nucleoplasm was not clear until recently. Several possibilities were discussed, one is that lamins are only transiently localizing to the nucleoplasm during their posttranslational modification before they assemble into the more peripheral filamentous lamina (Barrowman et al., 2008; Pendas et al., 2002). However, different observations speak for the existence of mature lamin A in the nucleoplasm (Barrowman et al., 2008; Dechat et al., 2000a). Another possibility is that lamin A might be posttranslationally modified to be targeted to the nucleoplasm, but the relevance of known lamin A modifications, such as phosphorylation and ubiquitination, regarding nucleoplasmic targeting has not been elucidated yet (Gruenbaum et al., 2003; Zhang and Sarge, 2008).

Several studies addressed the question of how lamin A is targeted to the nucleoplasm and found the lamina-associated polypeptide 2 α (LAP2 α) to be involved in lamin A nucleoplasmic targeting (Berger et al., 1996; Dechat et al., 2000a; Dechat et al., 2000b). LAP2 α is a splice variant of the *LAP2* gene. Up to six isoforms exist in humans (α , β , χ , δ , ϵ and ζ), generated by alternative splicing from a single gene (Berger et al., 1996; Foisner and Gerace, 1993; Harris et al., 1994). Most LAP2 isoforms have a closely related N-terminal nucleoplasmic domain of variable length with a NLS sequence, a single-membrane spanning region, and a short luminal domain at their C-terminus. At their N-terminus, LAP2 proteins share a LEM (LAP2, emerin, MAN1) domain, which binds the DNA binding protein BAF (Furukawa, 1999; Lin et al., 2000; Shumaker et al., 2001), and a LEM-like domain, which binds to DNA and chromosomes (Cai et al., 2001). Five of the LAP2 isoforms are integral proteins of the inner nuclear membrane and predominantly bind B-type lamins at the nuclear periphery. LAP2 α is structurally and functionally unique. It shares the N-terminal 187 residues with all other LAPs but contains a unique C-terminal domain of 506 residues, which lacks a membrane-spanning domain. As a result, LAP2 α is distributed diffusely throughout the interphase nucleus except for nucleoli (Dechat et al., 1998), where it interacts with lamin A and chromatin in a cell cycle dependent manner (Dechat et al., 2004; Dechat et al., 2000a). LAP2 α - deficient mouse fibroblasts have greatly reduced nucleoplasmic A-type lamins in G1 phase (Naetar et al., 2008), suggesting that LAP2 α is targeting or stabilizing nucleoplasmic lamin A in G1 phase of the cell cycle. In S phase, however, there is an

unknown LAP2 α -independent pathway that leads to recruitment of nucleoplasmic lamins A and C to the nuclear periphery.

1.10 The lamin A- LAP2 α complex and the retinoblastoma protein (pRb)

Several observations have implicated the lamin A-LAP2 α complex in cell cycle regulation. During myoblast differentiation *in vitro*, nucleoplasmic lamins A/C and LAP2 α expression is lost when cells stop to proliferate and fuse to myotubes (Markiewicz et al., 2005). Similarly, cells going from a proliferating to a permanently arrested, senescent state, lose nucleoplasmic lamin A and downregulate the expression of LAP2 α (Pekovic et al., 2007). Both lamin A and LAP2 α have been shown to interact with the tumor suppressor retinoblastoma protein (pRb), a major cell cycle regulator, which provides a potential mechanism as to how the lamin A-LAP2 α complex can affect cell cycle progression (Dechat et al., 2000a; Mancini et al., 1994; Markiewicz et al., 2002; Ozaki et al., 1994).

pRb is involved, besides many other functions, in the control of E2F transcription factors and is itself regulated by cyclin-dependent kinase (Cdk)-mediated phosphorylation (Kitagawa et al., 1994; Suzuki-Takahashi et al., 1995). In early G1, hypophosphorylated Rb is tethered in the nucleus and is capable of binding transcription factor E2F-1, which prevents the transcriptional activation of S phase-specific genes and cell cycle progression to S phase. By binding to the transcription factor, pRb blocks the transactivation domain of E2F-1, inhibits recruitment of preinitiation complexes and represses genes directly by recruiting chromatin-modifying proteins, including histone deacetylase HDAC1 (Brehm, 1998), methyl transferase Suv39h, and heterochromatin protein HP1 (Nielsen, 2001; Ait-Si-Ali, 2004). Hyperphosphorylation of pRb during late G1 phase by cyclin D and E-dependent kinases (Mittnacht 1998) releases it from E2F-1, causing its activation as a transcription factor, which leads to expression of cell cycle genes and to passage through S phase. LAP2 α was found to localize to E2F-dependent promoter sequences and to maintain E2F in a repressed state (Dorner et al., 2006). In human cells, depletion of LAP2 α accelerates G1-S transition, leads to impaired cell cycle arrest and upregulation of E2F target genes, whereas overexpression of C-terminal pRb-

binding domain of LAP2 α causes a cell cycle arrest in interphase, and overexpressed LAP2 α inhibits E2F/pRb-dependent reporter gene activity and leads to cell cycle exit and initiates differentiation (Dorner et al., 2006; Naetar et al., 2008; Vlcek et al., 2002). Similarly, lamin A-deficient murine fibroblast cells proliferate faster and have an impaired cell cycle arrest upon DNA damage (Nitta et al., 2006; Van Berlo et al., 2005). One study in mouse fibroblast cells showed that cells lacking lamin A have decreased pRb levels and that the remaining pRb is mislocalized, which might explain the disturbed proliferation control (Johnson et al., 2004). However, a different study suggests an altered pRb phosphorylation that underlies the observed proliferation defects. Altogether, lamin A-LAP2 α complexes have a role in regulating pRb activity during the cell cycle, and whether the lamin A-LAP2 α complex regulates stability or phosphorylation of pRb or both, needs to be further elucidated.

1.11 Laminopathies

Mutations in *LMNA* have been discovered in a variety of human disease syndromes including forms of muscular dystrophy, lipodystrophy and premature aging, so called laminopathies (Burke and Stewart, 2002; Hutchison and Worman, 2004; Mounkes and Stewart, 2004; Worman and Bonne, 2007). These laminopathies can be broadly divided into two groups: first, neuromuscular disorders affecting directly the skeletal muscle, cardiac muscle and peripheral nervous system, e.g. Emery-Dreifuss muscular dystrophy (EDMD), dilated cardiomyopathy (DCM) or limb-girdle muscular dystrophy 1B (LGMD1B), characterized by skeletal muscle wasting and striated and smooth muscle defects and subsequent heart failure (Bonne et al., 1999); second, partial lipodystrophy syndromes with or without developmental abnormalities and premature aging, such as mandibuloacral dysplasia (MAD) and Dunnigan-type familial partial lipodystrophy (FPLD) characterized by aberrant adipose tissue distribution (Boguslavsky et al., 2006) and Hutchinson-Gilford progeria Syndrome (HGPS) as well as atypical Werner's syndrome, which are characterized by loss of subcutaneous fat, decreased bone density, osteoporosis and growth retardation. How lamin A mutations lead to these tissue-specific syndromes is not exactly clear, and it is an ongoing discussion on how lamin A contributes to healthy tissue differentiation. It is known that lamin A interacts with the

sterol regulatory element-binding protein (SREB), a transcription factor, which is involved in adipogenesis (Lloyd et al., 2002), raising the possibility that lamin-associated lipodystrophies might be caused by altered interaction between SREB and lamin A. Given that lamin A, together with LAP2 α , controls stability and function of pRb, which is required for the differentiation of muscle and adipose tissue (Haigis et al., 2006; Hansen et al., 2004; Huh et al., 2004; Korenjak and Brehm, 2005; Lipinski and Jacks, 1999; Ruiz et al., 2004; Smith et al., 2005), it is possible that dystrophic syndromes arising from *LMNA* mutations may result, as least in part, from deregulation of pRb function. Indeed, analysis of biopsies from laminopathy-type muscular dystrophy patients revealed an impairment of the Rb/MyoD pathway, which is required for muscle generation (Bakay et al., 2006). Whether pRb misregulation plays a role in other laminopathic disease needs to be further elucidated.

2

The nucleoporin Nup153 affects spindle checkpoint activity due to an association with Mad1

Yvonne Lussi¹¶, Dale K. Shumaker^{2,3}¶, Takeshi Shimi³, and Birthe Fahrenkrog^{1,*}

¹M.E. Müller Institute for Structural Biology, Biozentrum, University of Basel, Klingelbergstrasse 70, 4056 Basel, Switzerland,

²Department of Urology, Feinberg School of Medicine, Northwestern University, 303 East Chicago Avenue, Chicago, IL 60611,

³Department of Cell and Molecular Biology, Feinberg School of Medicine, Northwestern University, 303 East Chicago Avenue, Chicago, IL 60611

¶: these authors contributed equally

Running title: Nup153 in spindle checkpoint regulation.

Keyword: Nup153; nuclear pore complex; Mad1; spindle assembly checkpoint

2.1 Abstract

The nucleoporin Nup153 is known to play pivotal roles in nuclear import and export in interphase cells and as the cell transitions into mitosis, Nup153 is involved in nuclear envelope breakdown. In this study, we demonstrate that the interaction of Nup153 with the spindle assembly checkpoint protein Mad1 is important in the regulation of the spindle checkpoint. Overexpression of human Nup153 in HeLa cells leads to the appearance of multinucleated cells and induces the formation of multipolar spindles. Importantly, it causes inactivation of the spindle checkpoint due to hypophosphorylation of Mad1. Depletion of Nup153 using RNA interference results in the decline of Mad1 at nuclear pores during interphase and more significantly causes a delayed dissociation of Mad1 from kinetochores in metaphase and an increase in the number of unresolved midbodies. In the absence of Nup153 the spindle checkpoint remains active. In vitro studies indicate direct binding of Mad1 to the N-terminal domain of Nup153. Importantly, Nup153 binding to Mad1 affects Mad1's phosphorylation status, but not its ability to interact with Mad2. Our data suggest that Nup153 levels regulate the localization of Mad1 during the metaphase/anaphase transition thereby affecting its phosphorylation status and in turn spindle checkpoint activity and mitotic exit.

2.2 Introduction

Nuclear pore complexes (NPCs) are macromolecular assemblies that bridge the double membrane of the nuclear envelope (NE) and control nucleocytoplasmic transport in interphase cells (D'Angelo and Hetzer, 2008; Lim et al., 2008; Lim and Fahrenkrog, 2006; Tran and Wentz, 2006). The vertebrate NPC is composed of ~30 different proteins, called nucleoporins (Nups), which include Nup153. Nup153 resides on the nuclear side of the NPC and immuno-electron microscopy (EM) analysis revealed that the N-terminal and central zinc-finger domains of Nup153 are anchored to different sites within the NPC's nuclear basket (Fahrenkrog et al., 2002). The localization of the Nup153 C-terminal domain, which mediates interactions with soluble nuclear transport receptors, is variable and dependent on the nucleocytoplasmic transport state (Fahrenkrog et al., 2002; Paulillo et al., 2005). Through its interactions with various nuclear transport receptors, Nup153 is known to be critical for both nuclear import and export (Bastos et al., 1996; Nakielny et al., 1999; Shah et al., 1998; Ullman et al., 1999; Walther et al., 2001).

Further support for the importance of Nup153 has resulted from RNA interference (RNAi) studies showing that it is required for maintaining the structural integrity of the nuclear basket and the survival of both tissue culture cells and *C. elegans* (Galy et al., 2003; Harborth et al., 2001; Walther et al., 2001). Nup153 also plays a role in NE breakdown in *Xenopus* nuclei (Liu et al., 2003; Prunuske et al., 2006) and in dosage compensation in *Drosophila* (Mendjan et al., 2006). In addition, chromosomal rearrangements of *NUP153* are associated with its increased expression in urothelial and retinoblastoma cancer (Heidenblad et al., 2008; Orlic et al., 2006). Furthermore, Nup153 is a positive regulator of Hedgehog signaling (Nybakken et al., 2005) and it is required for centrosome reorientation during cell migration in neurons (Collin et al., 2008). These results suggest that Nup153 is involved in differentiation and tissue development and that altering either the amount of Nup153 or its function is related to human disease. The mechanistic basis for Nup153 function in these different cellular processes has remained largely elusive. Many of these functions, however, point to a role in cell cycle regulation. A putative role for Nup153 in cell cycle regulation is further supported by the notion that Nup153 appears to be required for the localization of the spindle assembly checkpoint (SAC) protein Mad1 to NPCs in interphase cells (Hawryluk-Gara et al., 2005).

The SAC acts to prevent chromosome mis-segregation and aneuploidy by delaying the metaphase-anaphase transition until all chromosomes are properly attached to the mitotic spindle and aligned at the metaphase plate (Musacchio and Salmon, 2007). Two SAC proteins, Mad1 and Mad2, are located at NPCs in interphase cells (Campbell et al., 2001; Iouk et al., 2002). Mad2 is thought to play a key role for mitotic checkpoint because of its inhibitory effect on the anaphase promoting complex/cyclosome (APC/C) (Musacchio and Salmon, 2007; To-Ho et al., 2008). The binding of Mad2 to Mad1 and Cdc20, a co-factor of APC/C, is thought to be crucial for Mad2 function. Loss of the interaction between these proteins results in an impaired SAC, aneuploidy and failed cytokinesis (Musacchio and Salmon, 2007; To-Ho et al., 2008). The role of Mad1 during metaphase/anaphase transition on the other hand appears regulatory as the depletion of Mad1 results in SAC deficiency without significantly altering the duration of mitosis (Musacchio and Salmon, 2007).

The function of the SAC proteins at the NPC has remained largely elusive, although it has been suggested that the NPC may play a role in the duration of the SAC (Kastenmayer et al., 2005; Scott et al., 2005). Here, we have examined the effect of altering Nup153 expression in HeLa cells and found that Nup153 levels affect spindle checkpoint activity due to binding of Nup153 to the SAC protein Mad1.

2.3 Results

2.3.1 Enhanced levels of Nup153 lead to multinucleation and multilobulation of cells

To gain further insights into Nup153 function, we analyzed the effects of altering Nup153 levels in HeLa cells. Following transfection with GFP-human Nup153 (GFP-Nup153), cells with low to moderate expression levels displayed typical nucleoporin staining patterns at the NE (Figure 2.1a), while higher expression levels resulted in dramatic alterations in nuclear architecture. These alterations include misshapen nuclei and the accumulation of GFP-Nup153 in intranuclear foci that are frequently associated with the NE (Figure 2.1b and c) as has been previously described (Bastos et al., 1996). Moreover, enhanced levels of GFP-Nup153 cause highly lobulated nuclei (Figure 2.1, d-f) with some similarities to so-called flower cells (Jin et al., 1998). Most strikingly, the accumulation of GFP-Nup153 induces the formation of multinucleated cells (Figure 2.1, f-m). The NEs of nuclei in multinucleated cells have an abnormal nuclear shape and are more invaginated than NE's in cells containing a single nucleus. In addition, nuclei in multinucleated cells frequently appear to be closely apposed to each other, lending to the impression that their envelopes are fused in certain regions (Figure 2.1, g and k, arrows). These fusions are also detectable on electron microscopy levels (Figure S7.1). Further work will be needed to elucidate the actual nature of these fusions.

Overexpression effects of Nup153 were not restricted to HeLa cells as the same phenotypes were obtained in HEK293 and *Xenopus* A6 cells following transfection with GFP-Nup153 (Figure S7.2, a and b), while expression of other nucleoporins, i.e. Nup358/RanBP2, Nup62, Nup88 (not shown) and Tpr (Figure S7.2, d-f), or GFP alone (Figure S7.2c) did not result in nuclear foci, nuclear lobulation or multinucleation. These experiments indicate that overexpression of GFP-Nup153 can cause rearrangements in the nuclear envelope indicated by lobulation of the nuclei and multinucleation, which implies abnormal mitosis.

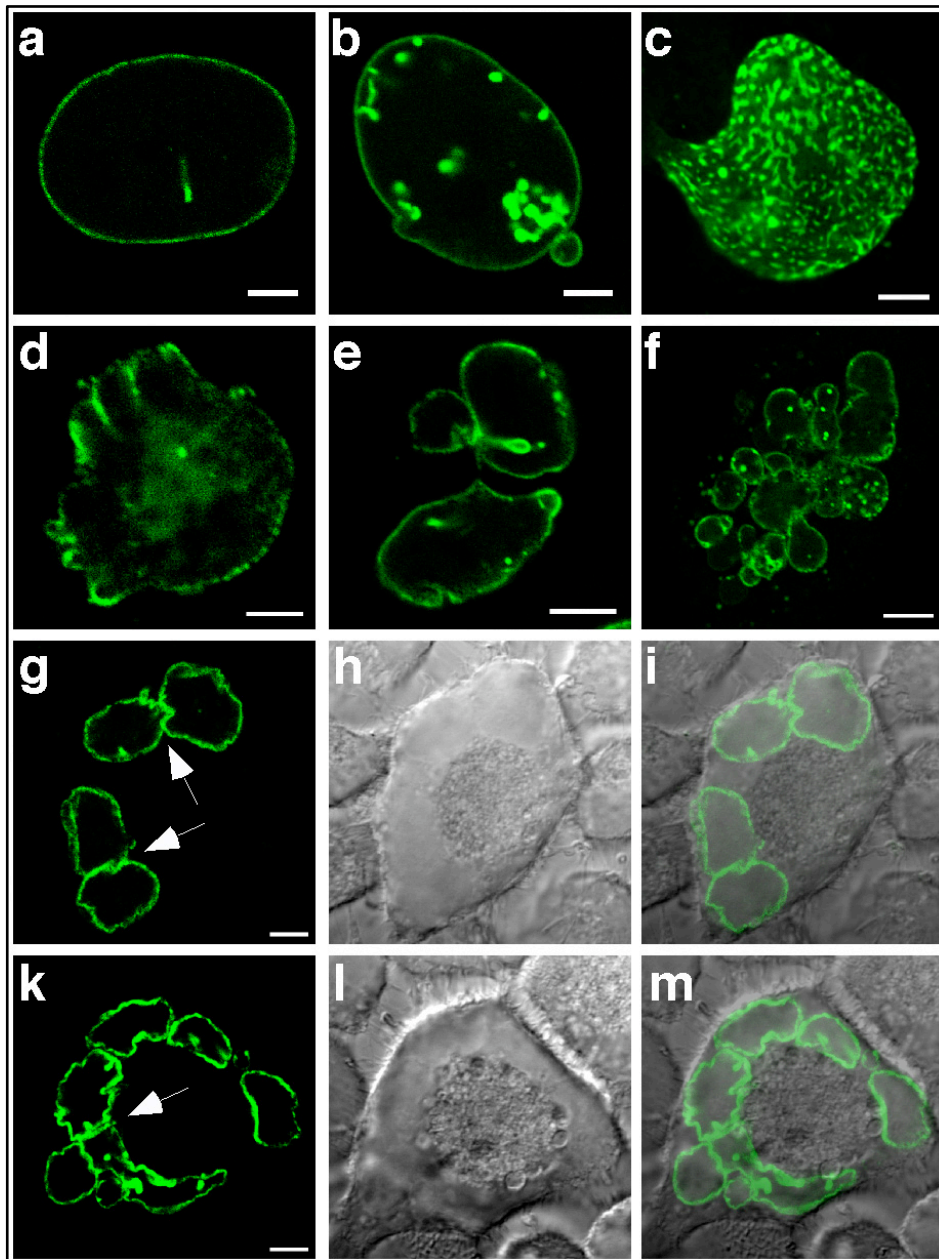


Figure 2.1: Overexpression of human Nup153 causes changes in nuclear shape and aberrant mitosis.

HeLa cells were transfected with GFP-Nup153 and visualized by direct fluorescence microscopy 48 hours post transfection. (a) At lower expression levels GFP-Nup153 localizes to nuclear pore complexes as indicated by a typical rim staining, whereas at higher levels (b- e) GFP-Nup153 accumulates in the nucleus close to the nuclear envelope and causes strong lobulation of nuclei. (e- i) Enhanced levels of GFP-Nup153 lead to the appearance of multinucleated cells and in some cases micronuclei (e). Arrows in g and k mark nuclei of multinucleated cells, which appear to be closely apposed to each other or fused in certain regions. Shown are confocal fluorescence

micrographs (**a-f**, **g**, **k**), differential-interference-contrast (**h**, **l**) and coincident fluorescence/differential-interference-contrast images (**i**, **m**). Scale bars, 5 μm (**a-e**), 10 μm (**f-m**).

2.3.2 Enhanced levels of Nup153 lead to multinucleation in live cells

Multinucleation of cells can be a consequence of various alterations in cell division, such as altered chromosome separation or failures of the spindle checkpoint and cytokinesis (King, 2008). To determine how cells become multinucleated, we studied the effect of GFP-Nup153 overexpression in HeLa cells by live cell imaging. A representative series of time-lapse images shows a normal cell division (Figure 2.2a) compared with an abnormal mitotic progression without cytokinesis in a cell containing an apparent tri-polar spindle culminating in a cell with at least two nuclei (Figure 2.2b). Even more striking, progression through mitosis without cytokinesis of a cell with an apparent multipolar spindle resulted in a multinucleated cell with more than 10 nuclei (Figure 2.2c; see also Figure 2.1f). Multinucleation was not observed in 23 untransfected HeLa cells that were followed through mitosis by live cell imaging (data not shown). Together these data indicate that multinucleation in the presence of increased GFP-Nup153 levels in the cells is a consequence of failed cytokinesis rather than abnormal chromosome separation.

To further support this notion, we performed cell sorting and flow cytometric analysis to determine the DNA content of nuclei isolated from cells expressing GFP-Nup153 (nuclei, not the intact cells) as compared to nuclei from untransfected control cells. Our analysis revealed changes in ploidy in nuclei expressing GFP-Nup153 compared to nuclei from untransfected cells (Figure 2.2, d and e). GFP-Nup153 nuclei show a strong increase in aneuploidy indicated by both low N nuclei (Figure 2.2e, arrow) as well as a substantial increase in high N nuclei (Figure 2.2e, inset) compared to control nuclei ($15.2 \pm 5.1\%$ versus $1.2 \pm 0.2\%$ aneuploid cells). In both populations, the percentage of nuclei in G1, S and G2 phase of the cell cycle, respectively, and the overall G1:G2 ratio were similar (Figure 2.2, d-f), indicating that despite a failure in cytokinesis, DNA synthesis and chromosome segregation appear to be unaffected.

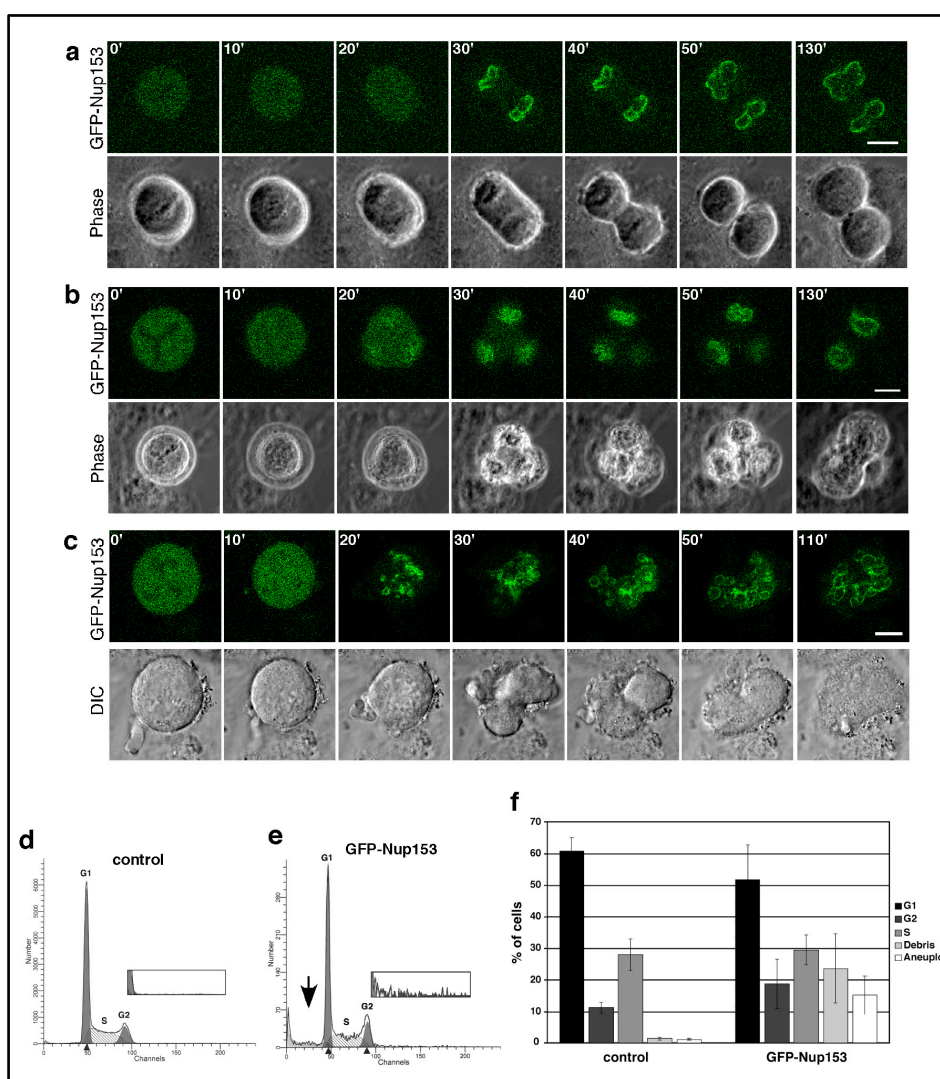


Figure 2.2: High levels of Nup153 expression interfere with cytokinesis and induce aneuploidy.

GFP-Nup153 (green) and phase contrast time-lapse images of HeLa cells 48 hours post transfection and their progression through mitosis are presented. (a) Normal cell division and (b, c) nuclear division without cell separation can be observed. Scale bars, 10 μm (a), 5 μm (b, c). HeLa cells expressing GFP-Nup153 48 h post transfection were prepared for flow cytometry by staining DNA with propidium iodide and control cells not expressing GFP (d) were compared with GFP-positive cells (e). Whereas no significant effect on cell cycle progression as demonstrated by the G1:G2 ratio was detectable, there was a significant increase in the number of aneuploid nuclei in GFP-Nup153 expressing cells. Insets are 6x enlarged in the vertical axis showing a substantial increase in high N nuclei in cells expressing GFP-Nup153. (f) Quantification of the cell cycle profiles from six independent experiments.

2.3.3 Expression of Nup153 induces multipolar spindles

Our data suggest a possible link between Nup153, mitotic spindle function and completion of cytokinesis. To better understand the effect of Nup153 on these processes, HeLa cells stably expressing histone H2B-GFP were transfected to express GFP-Nup153 and immunostained for actin and microtubules, two key players in cell division (Eggert et al., 2006). Whereas these cells displayed a normal actin cytoskeleton in interphase and at the cleavage furrows in mitosis (not shown), we observed alterations in the microtubule networks (Figure 2.3, a-c). Cells expressing GFP-Nup153 displayed a substantial increase in the number of aberrant mitoses, shown by multipolar spindles (Figure 2.3, a and b) and lagging chromosomes (Figure 2.3c). In controls, 6% ($5.8 \pm 1.8\%$) of the mitotic cells displayed multipolar spindles, while $\sim 26\%$ ($26.2 \pm 3.7\%$; $p < 0.005$) of GFP-Nup153 expressing cells exhibited multipolar spindles (Figure 2.3g).

Nup153 is a multi-domain protein and we next aimed to determine which domain of Nup153 was responsible for the aberrant mitosis phenotype. To do so, various truncations of Nup153 were prepared. The N-terminal domain of Nup153 harbors the NPC assembly region (NPAR), residues 39 to 339 (Enarson et al., 1998). The NPAR is sufficient to target Nup153 to the NPC, but lacks residues that are required to target soluble proteins, such as nuclear transport receptors, to the inner nuclear membrane (Ball and Ullman, 2005; Enarson et al., 1998). When fused to GFP and transfected into HeLa cells, GFP-Nup153-39-339 associates with NPCs and the nucleoplasm (Figure S7.3a), aggregates in intranuclear foci, induces nuclear deformation (Figure S7.3b), and multinucleation (Figure S7.3, c and d). Moreover, GFP-Nup153-39-339 causes multipolar spindle formation in $\sim 25\%$ of the mitotic cells ($24.7 \pm 2.5\%$; $p < 0.005$) as revealed by staining with an antibody against β -tubulin (Figure 2.3d). Further truncating the NPAR into two fragments, residues 39-144 and 145-339, revealed that residues 145-339 induced multipolar spindles in $\sim 20\%$ of the mitotic cells (Figure 2.3, e and i; $19.2 \pm 5.5\%$; $p < 0.005$) and are targeted to the nucleus (Figure S7.3e-h). GFP-Nup153-39-144 is found in the cytoplasm and nucleus (Figure S7.3i-m) and the number of cells with multipolar spindles is not significantly increased ($12.1 \pm 2.2\%$; Figure 2.3i). Together these data show that the NPAR of Nup153 and in particular residues 145-339 interfere with normal mitoses.

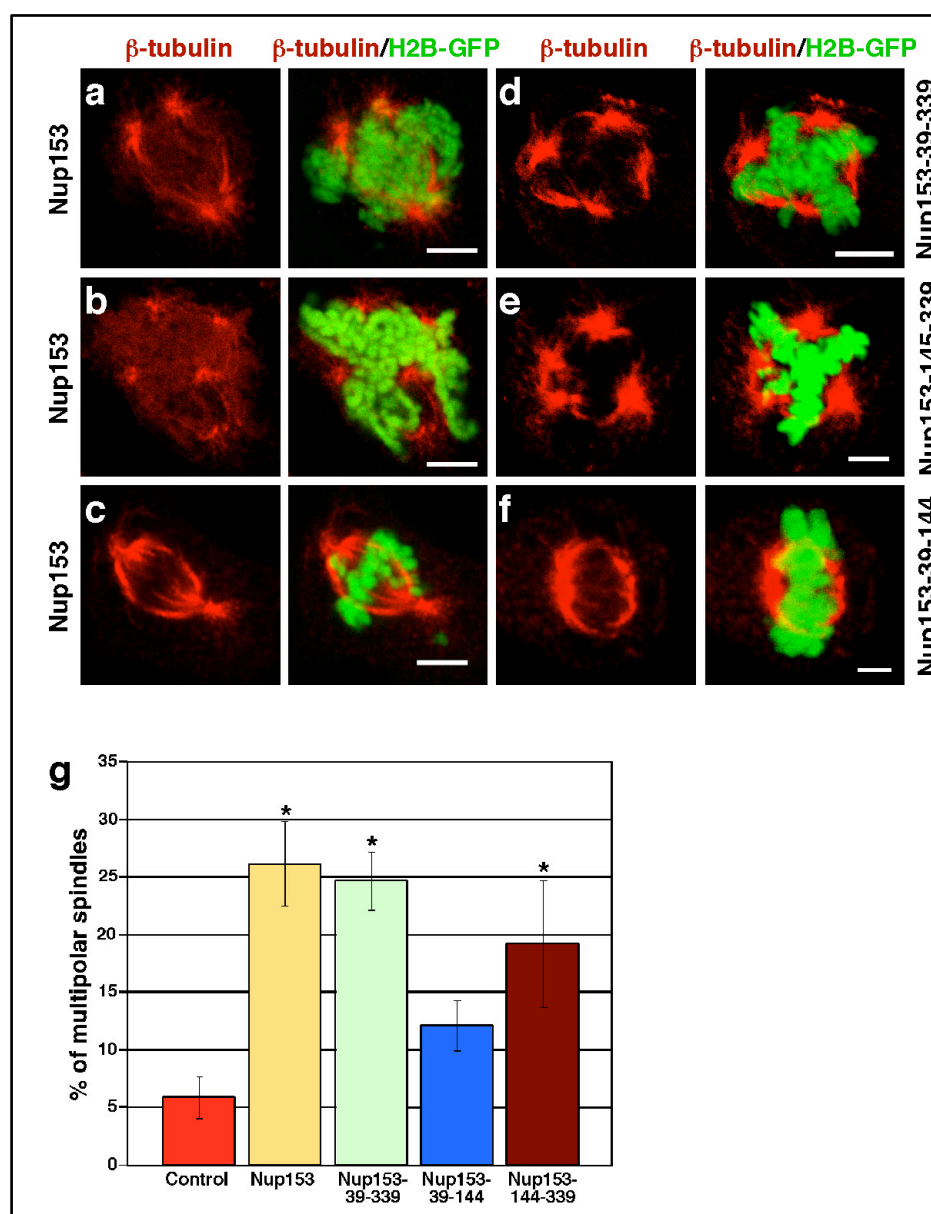


Figure 2.3: Overexpression of the nuclear pore complex assembly region (NPAR) of Nup153 induces mitotic abnormalities.

HeLa cells expressing histone H2B-GFP were transfected with GFP-Nup153 (a-c), GFP-Nup153-39-339 (d; i.e. the NPAR of Nup153), GFP-Nup153-39-144 (e) or GFP-Nup153-144-339 (f) and prepared for immunofluorescence 48 hours post transfection using monoclonal antibodies directed against β - (e-f). Cells expressing either GFP-Nup153, GFP-Nup153-39-339, or GFP-Nup153-144-339 showed poor spindle morphology and a strong increase in the frequency of multipolar spindles (a, b, d and e) and lagging chromosomes (c). Cells expressing the N-terminal portion of the NPAR, GFP-Nup153-39-144, show predominantly normal bipolar spindles (f). Scale bars, 5 μ m. (g) Quantification of the number of multipolar spindles among mitotic cells. Cells were significantly more likely to have multipolar mitotic spindles when expressing Nup153 (26.2 ± 3.7 %), Nup153-39-339 (24.7 ± 2.5 %), or Nup153-144-339 (19.2 ± 5.5 %) than control cells or cells

expressing Nup153-39-144. Spindles were counted from 3-4 independent experiments with typically 100-200 spindles per experiment.

2.3.4 Nup153 levels affect the spindle assembly checkpoint

Abnormal mitoses with lagging chromosomes and multipolar spindles indicated a weakened SAC and two SAC factors, Mad1 and Mad2, are known to localize to NPCs in interphase cells. In turn, the Mad1- and Mad2-binding nucleoporins may have some activity during mitosis. Several nucleoporins appear to mediate the association of the Mad1-Mad2 complex to the NPC (Iouk et al., 2002; Lee et al., 2008; Scott et al., 2005) and Nup153 has been suggested to be required for Mad1 localization (Hawryluk-Gara et al., 2005; Scott et al., 2005). To test if Nup153 function in mitosis is related to the spindle checkpoint, we examined the potential interaction between Nup153 and Mad1 by indirect immunofluorescence and found that Mad1 in fact colocalizes with NPCs as indicated by a punctated nuclear rim staining, typical for nucleoporins (Figure 2.4a, top panels) and consistent with previously published data (Campbell et al., 2001).

To more precisely determine the position of Mad1 within the NPC, we next performed immuno-EM using *Xenopus* oocyte nuclei. Nuclei were isolated manually and incubated with an anti-Mad1 antibody directly conjugated to 8-nm colloidal gold and processed for thin-sectioning EM. As illustrated in Figure 2.4b, the Mad1 antibody recognizes distinct epitopes on the nuclear side of the NPC. Quantification of the gold particle distribution with respect to the central plane of the NE revealed the major epitope, with about 50% of the gold particles, at distances of -10 to -50 nm from the central plane with a peak at -28.8 nm (\pm 8.5 nm). Together with corresponding radial distances of 0 to 30 nm (peak at 19.1 nm \pm 14.2 nm) this corresponds to an epitope at the nuclear ring moiety of the NPC.

We have previously mapped the N-terminal domain of Nup153 to the nuclear ring moiety of the NPC (Fahrenkrog et al., 2002) and compared the localization of Nup153 with the Mad1 epitope at the nuclear ring. As shown in Figure 2.4b (right panel), both antibody epitopes are overlapping, indicating that in fact about 50% of Mad1 colocalizes with Nup153's N-terminal domain. The remaining 50% of Mad1 epitopes are found within the nuclear basket of the NPC (Figure 2.4b), consistent with Mad1 having multiple binding partners at the NPC (see (Hawryluk-Gara et al., 2005; Lee et al., 2008)).

In contrast to Mad1, Mad2 was not found in close proximity to Nup153. Antibodies against Mad2 conjugated to 8-nm colloidal gold recognized distinct epitopes in the centre as well as on the cytoplasmic face of the NPC (Figure S7.4a).

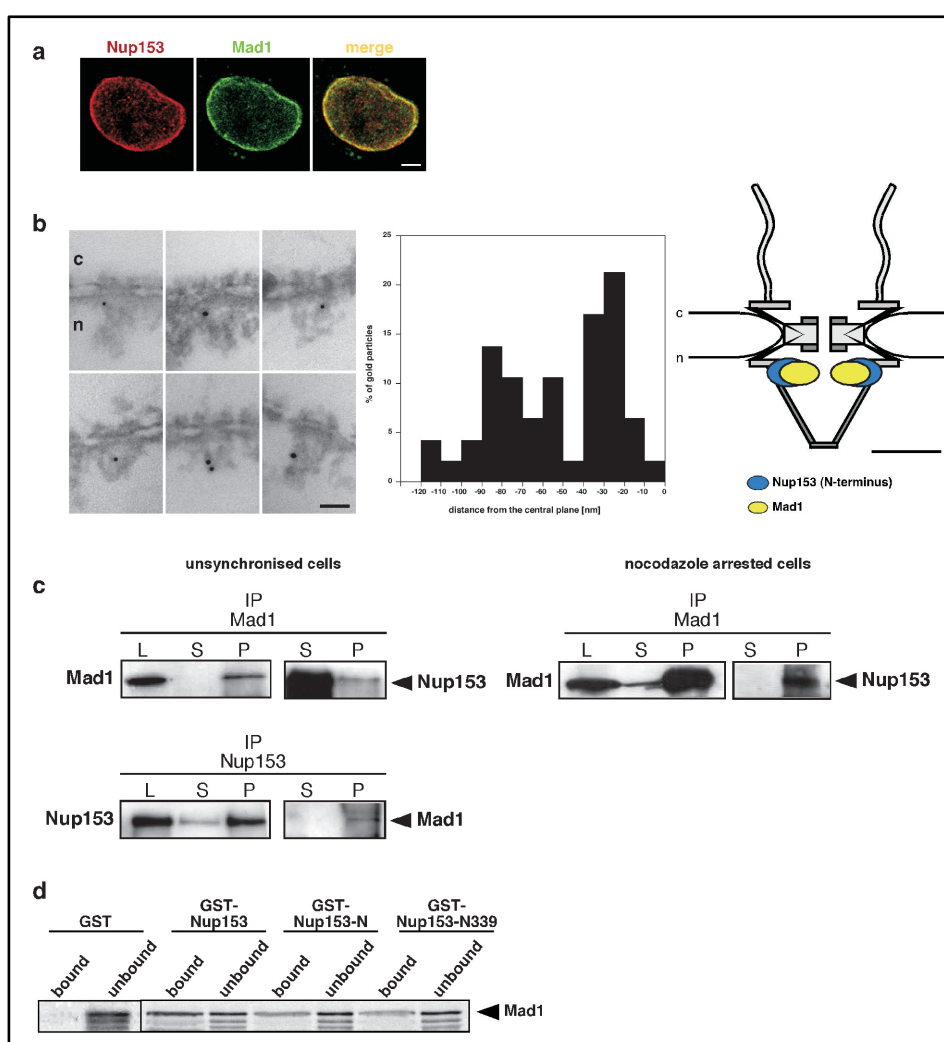


Figure 2.4: Nup153 interacts with the spindle checkpoint protein Mad1.

(a) Mad1 localizes to nuclear pore complexes (NPCs) in interphase cells. HeLa cells were double immunostained with a polyclonal antibody against Nup153 and a monoclonal antibody against Mad1. Scale bars, 5 μ m. (b) Immuno-electron microscopy localization of Mad1 in *Xenopus* oocyte nuclei. Nuclei were isolated manually and labeled with a monoclonal Mad1 antibody directly conjugated to 8nm colloidal gold. Mad1 localizes to the nuclear side of the NPC with several epitopes at the nuclear basket (left). Quantification of the gold particle distribution revealed that about 50% of the gold particles were associated with the nuclear ring moiety of the NPC (middle). The epitope at the nuclear ring moiety that is recognized by the Mad1 antibody overlaps with the epitope that is recognized by an antibody against the N-terminal domain of Nup153 (Fahrenkrog et al., 2002; Walther et al., 2001) as shown schematically by elliptical location clouds (right). Scale

bar, 100 nm. (c) Total HeLa extracts from unsynchronized or nocodazole arrested cells were immunoprecipitated using either anti-Mad1 or anti-Nup153 antibody. Equivalent amounts of HeLa extracts (L), immune supernatants (S) and immune precipitate (P) were separated by SDS-PAGE and analyzed by immunoblotting using Mad1 and Nup153 antibodies. Immunoprecipitations brought down the corresponding protein. (d) Bacterially expressed GST-Nup153, GST-Nup153-N, GST-Nup153-N339 and GST were bound to glutathione beads then incubated with in vitro synthesized ³⁵S-labeled Mad1. Expressed and purified GST was unable to bind ³⁵S-Mad1 while all truncations of GST-Nup153 containing the NPAR region bound ³⁵S-Mad1. Unbound and bound fractions were analyzed by SDS-PAGE and autoradiography.

2.3.5 Nup153 and Mad1 are directly interacting

To further confirm that Nup153 interacts with Mad1 at NPCs, lysates from HeLa cells were immunoprecipitated both with antibodies directed against Mad1 (Figure 2.4c, top left panel) and Nup153 (Figure 2.4c, bottom left panel). The HeLa extracts, supernatant, and pellet proteins were separated by SDS-PAGE, transferred to a PVDF membrane and probed with antibodies to Nup153 and Mad1. This set of experiments demonstrated that Nup153 associates with Mad1 in HeLa cells. To elucidate if the interaction between Nup153 and Mad1 is maintained during mitosis, we prepared lysates from HeLa cells that had been arrested in mitosis after treatment with nocodazole. Mitotic lysates that were immunoprecipitated with antibodies against Mad1 co-precipitated Nup153 (Figure 2.4c, top right panel), indicating that Nup153 and Mad1 interact throughout the cell cycle. Under the same conditions, Mad2 was found to co-precipitate with Mad1 antibodies (Figure S7.4b), but not with Nup153 (Figure S7.4c), indicating that Nup153 specifically interacts with Mad1.

To determine which domain of Nup153 interacts with Mad1, we next performed solution-binding assays. Purified recombinant Nup153 domains fused to GST were attached to glutathione sepharose beads and incubated with in vitro transcribed and translated ³⁵S-labeled Mad1. Mad1 interacts with GST-Nup153, with the N-terminal domain of Nup153 (GST-Nup153-N, i.e. residues 2 to 610) and a truncation of the N-terminal domain comprising the first 339 residues of Nup153 (GST-Nup153-N339), but not with GST alone (Figure 2.4d). Together, these data indicate that the interaction of Nup153 with Mad1 is mediated by Nup153's NPAR.

2.3.6 Nup153 affects the spindle checkpoint

We next explored the functional significance of the Nup153-Mad1 interaction on the spindle checkpoint. To do so, we treated control, Nup153-depleted (see below), Mad1-depleted (80% reduction of Mad1 mRNA as determined by qRT-PCR; data not shown) and GFP-Nup153 expressing HeLa cells, respectively, with nocodazole to activate the spindle checkpoint and analyzed their ability to arrest in mitosis by light microscopy. As shown in Figure 2.5a, HeLa cells as well as HeLa cells transfected with control siRNA rounded up and became arrested in mitosis upon nocodazole treatment for 20 hours. Similarly, Nup153 depleted cells were able to arrest in mitosis. In contrast, cells overexpressing GFP-Nup153 or depleted for Mad1 failed to arrest in mitosis. Although unlikely, a lack of mitotic cells after nocodazole treatment could also be due to a G1 and a G2 arrest upon overexpression of Nup153. To exclude this possibility, HeLa cells transfected with GFP-Nup153 were subjected to a double thymidine block to study their ability to progress into mitosis after release. Cells overexpressing GFP-Nup153 were able to enter mitosis, similarly to various control cells (Figure S7.5).

Together our data therefore indicate that enhanced Nup153 levels disable a functional checkpoint. To test if Nup153 in fact directly affects the SAC via Mad1, we co-expressed GFP-Nup153 together with GFP-Mad1. GFP-Mad1 was found to localize to NPCs in interphase cells and to kinetochores in prometaphase (data not shown), indicating that it is functional. HeLa cells that were co-transfected with GFP-Nup153 and GFP-Mad1 were found to arrest in mitosis when treated with nocodazole (Figure 2.5a), suggesting that Nup153 directly acts on the SAC via Mad1.

To further examine whether cells were in mitosis following nocodazole treatment, cells were immunostained with antibodies directed against histone H3 phosphorylated on Ser10. Cells expressing GFP-Nup153 were substantially decreased in their mitotic index (20%) as compared to control cells (60%). Similarly Mad1-depleted cells exhibited a low mitotic index (6%), while Nup153-depleted cells and cells co-expressing GFP-Nup153 and GFP-Mad1 were more similar to controls (50%; Figure 2.5b). Together these data indicate that enhanced levels of Nup153 abrogate SAC function, while the SAC remains intact in the absence of Nup153.

A functional SAC requires the interaction between Mad1 and Mad2. Mad1 is a phosphoprotein and hyperphosphorylated when bound to Mad2 in mitosis and phosphorylation of Mad1 is critical for SAC function (Chen et al., 1999). To determine if Nup153 affects Mad1 phosphorylation, we conducted co-immunoprecipitation experiments of cells after nocodazole treatment. We immunoprecipitated Mad1 from lysates of nocodazole arrested HeLa cells that were either transfected with GFP-Nup153 or Nup153 siRNAs using a monoclonal Mad1 antibody. Mad1 phosphorylation was assessed by Western blotting using an antibody that recognizes a phosphorylated serine/threonine/or tyrosine residue (α -pSTY). Indeed, the α -pSTY antibody detected phosphorylated Mad1 in control cells, whereas the levels of phosphorylated Mad1 were largely reduced in GFP-Nup153 transfected cells (Figure 2.5c, left panels), but not in Nup153-depleted cells (Figure 2.5c, right panels). Neither the Mad1 nor the pSTY antibody was found to bind to the protein G-agarose beads alone (Figure S7.6). Quantification of the band intensity revealed that about 28% of the precipitated Mad1 was phosphorylated in control cells, but only 17.8% in the GFP-Nup153 transfected cells. The amount of Mad2 that co-precipitated with Mad1 was not affected in cells expressing GFP-Nup153 (Figure 2.5c, left) or Nup153-depleted cells (Figure 2.1c, right). Together these data suggest that increased levels of Nup153 abrogate SAC function by diminishing Mad1 phosphorylation without affecting its association with Mad2. Reduced levels of Nup153 on the contrary do not impair Mad1's phosphorylation status, leaving the SAC functional.

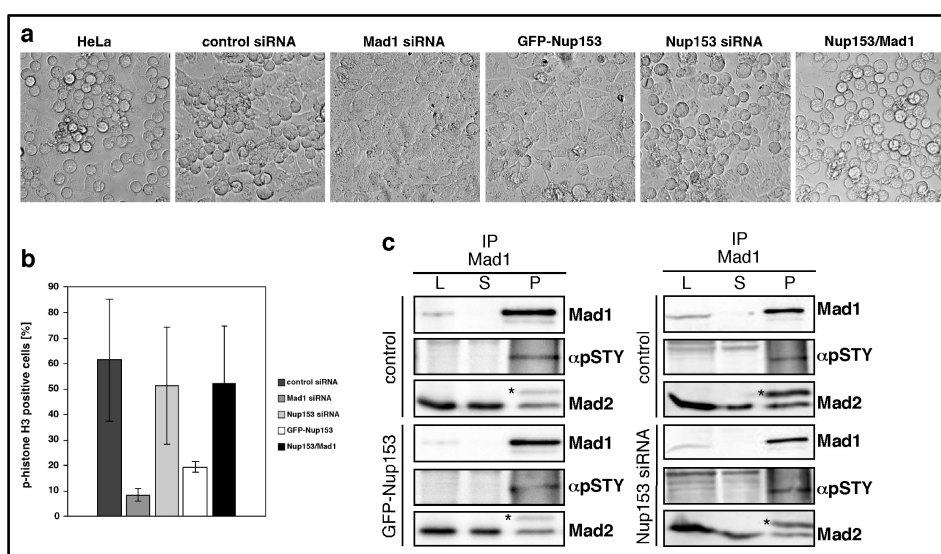


Figure 2.5: Enhanced levels of Nup153 affect spindle checkpoint activity.

(a) Phase contrast images of untransfected HeLa cells or cells that were transfected with control siRNA, Mad1 siRNA, Nup153 siRNA, GFP-Nup153 or GFP-Nup153 and GFP-Mad1, respectively, and treated with nocodazole for 20 hours to activate the spindle checkpoint. Whereas untransfected or GFP-Nup153/GFP-Mad1 transfected HeLa cells or cells treated with control and Nup153 siRNAs rounded up and arrested in mitosis, cells treated with Mad1 siRNA or expressing GFP-Nup153 did not. (b) HeLa cells were transfected with siRNAs or GFP-Nup153, respectively, and treated with nocodazole for 20 hours. After nocodazole treatment, cells were stained with a phospho-histone H3 antibody and immunofluorescence microscopy was performed. Quantification of the mitotic index by counting the population of cells positive for phospho-histone H3 staining ($n > 300$). (c) Total HeLa extracts from GFP-Nup153 transfected and untransfected nocodazole arrested cells were immunoprecipitated using anti-Mad1 antibody. Equivalent amounts of HeLa extracts (L), immune supernatants (S) and immune precipitate (P) were separated by SDS-PAGE and analyzed by immunoblotting using an anti-pSTY antibody (α pSTY) that specifically recognizes a phosphorylated serine/threonine/tyrosine residue and an anti-Mad2 antibody. Asterisks mark the antibody light chain. Immunoblotting using anti-Mad1 verified the immunoprecipitation of Mad1.

2.3.7 Nup153 levels affect Mad1 localization

To explore how Nup153 might affect Mad1 phosphorylation, we tested whether Nup153 is important for regulating the localization of Mad1 in interphase and/or mitosis. To do so, Nup153 was depleted from HeLa cells using RNA interference. Transfection of HeLa cells expressing histone H2B-GFP with short interfering (si) RNAs resulted in an 80% reduction in Nup153 both at the mRNA and protein levels as determined by quantitative real-time PCR (qRT-PCR) and immunoblotting, respectively (Figure S7.7, a and b). Under these conditions the HeLa cells remain viable, whereas a more complete knock down causes growth arrest of the cells (Harborth et al., 2001). The siRNAs

specifically depleted Nup153 from NPCs without co-depleting other nucleoporins, such as Nup62 or Tpr as analyzed by Western blotting (Figure S7.7b) and immunofluorescence (Figure S7.7d). Additionally, qRT-PCR demonstrated that Tpr mRNA was also not reduced (Figure S7.7c). These results are at variance with a recent study, where a near complete loss of Nup153 resulted in a Tpr mislocalization and a reduction in its protein level (Hase and Cordes, 2003). These discrepancies likely result from the different levels of Nup153 depletion (~80% versus ~100%).

Having determined that our siRNA treatment specifically affected Nup153, we studied the effect of Nup153 depletion on Mad1 localization throughout the cell cycle.

This resulted in a reduced localization of Mad1 at the NPC in interphase (Figure 2.6a), indicating that Nup153 is in part required for Mad1 binding to the NPC. As cells progress through mitosis, Mad1 localization at kinetochores in prometaphase remains unchanged in the presence or absence of Nup153 (Figure 2.6a). However, in metaphase, Mad1 dissociates from kinetochores and is found dispersed in control cells, whereas it remains associated with kinetochores in Nup153-depleted cells. Moreover, in telophase, the recruitment of Mad1 to the newly formed NE is inefficient in the absence of Nup153 (Figure 2.6a).

We next performed co-localization experiments of GFP-Nup153 with Mad1 and determined that by indirect immunofluorescence Mad1 and GFP-Nup153 colocalize at the NE and in the intranuclear GFP-Nup153 foci of interphase cells (Figure 2.6b). We have not observed colocalization with GFP-Nup153 foci for Tpr (Figure S7.7), other FG-repeat nucleoporins recognized by the mAb414 antibody or the nuclear lamina protein lamin A and only partially with lamin B2 (not shown), indicating that Nup153 overexpression specifically perturbs Mad1 localization. Nup153 overexpression most likely also affects Mad1 localization during mitosis, however, our attempts to colocalize GFP-Nup153 and Mad1 in mitotic cells were inconclusive likely due to a temporary interaction between Mad1 and Nup153.

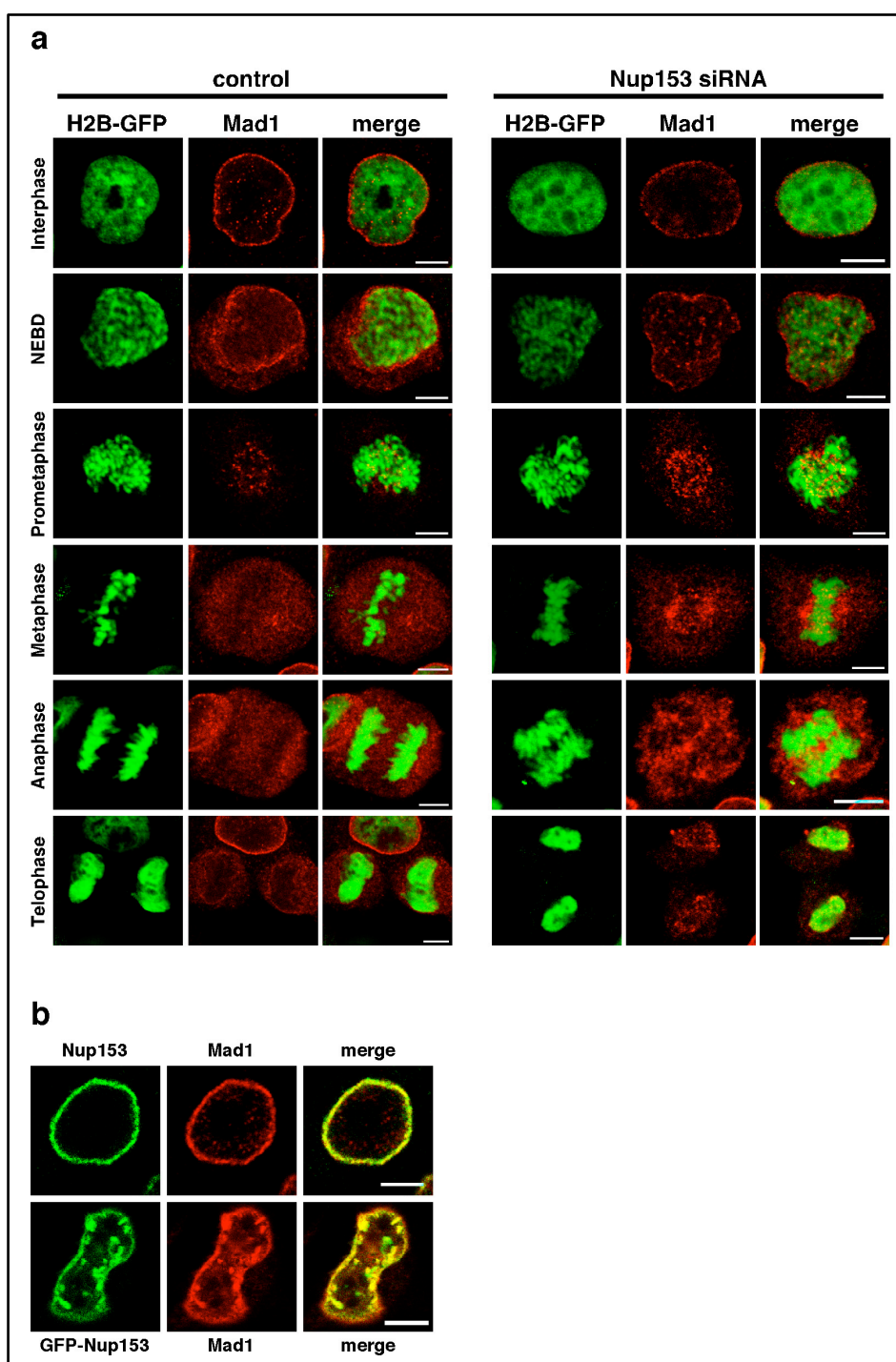


Figure 2.6: Localization of the spindle assembly checkpoint protein Mad1 is dependent on Nup153.

(a) HeLa cells expressing histone H2B-GFP were transfected with control or Nup153 siRNAs, fixed and stained with anti-Mad1 antibodies. Control nuclei displayed a significant localization of Mad1 at the nuclear rim, while cells depleted for Nup153 lost Mad1 from the nuclear rim. Mad1

localizes to kinetochores in prometaphase cells and dissociates from the kinetochores in mitosis, before it is recruited back to the NE in telophase (left panels). In the absence of Nup153, Mad1 is present at kinetochores in prometaphase, where a significant pool remains during mitosis. Mad1 recruitment to the reforming NE in telophase is impaired in cells lacking Nup153 (right panels). **(b)** Overexpression of GFP-Nup153 perturbs Mad1 localization in HeLa cells. HeLa cells were transiently transfected with GFP-Nup153 and immuno-stained with a Mad1 antibody. Mad1 colocalizes with GFP-Nup153 foci in the nucleus (bottom), while both proteins reside at NPCs in control cells stained with antibodies against Mad1 and Nup153, respectively. Scale bars, 5 μ m.

2.3.8 Depletion of Nup153 causes cytokinetic abnormalities

To further examine the role of Nup153 in mitosis, we studied the effect of Nup153 depletion on cell division. Cells transfected with control siRNA underwent normal cytokinesis (Figure 2.7a). In contrast, Nup153-depleted cells co-immunostained with an anti- β -tubulin antibody frequently showed abnormal midbodies and peripheral midbody remnants (Figure 2.7, b and c), prolonged persistence of midbodies in interphase cells (Figure 2.7d) and unresolved midbodies between multiple cells (Figure 2.7e). These effects are consistent with delayed and abortive cytokinesis (Bruzzone-Giovanelli et al., 1999; Li, 2007; Plans et al., 2008). Overall, the number of midbodies in Nup153-depleted cells was twice that of control cells (Figure 2.7f). Failed cytokinesis upon Nup153 depletion does not affect the ploidy of the nuclei or cell cycle progression as monitored by flow cytometry of isolated nuclei from Nup153-depleted cells as compared to nuclei isolated from cells treated with control siRNA (Figure S7.8). Together, these data indicate that Nup153 depletion results in delayed and/or aborted cytokinesis.

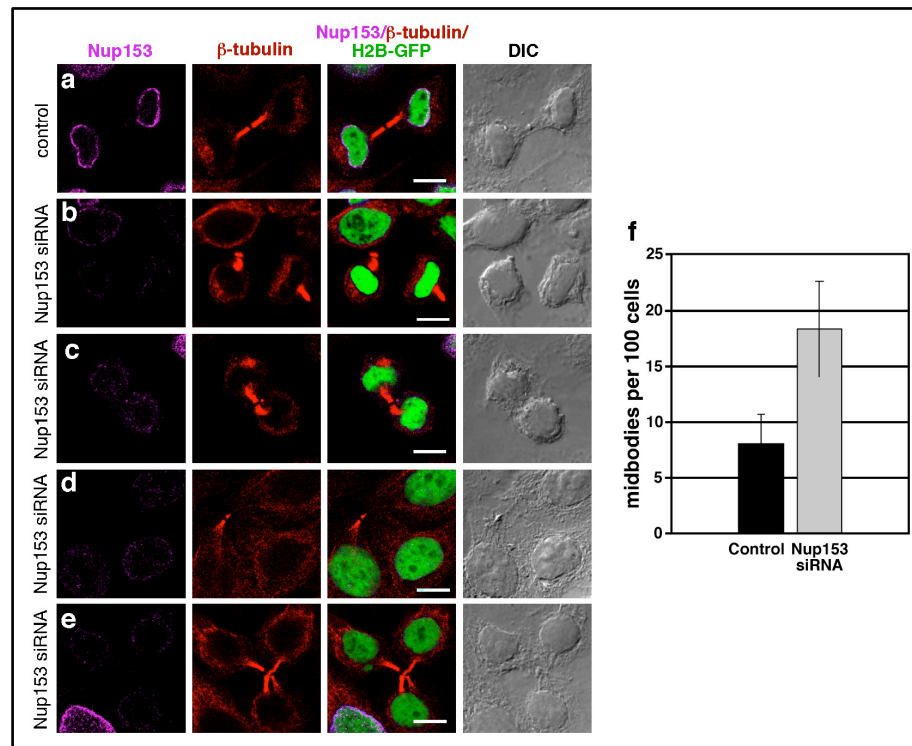


Figure 2.7: Depletion of Nup153 inhibits cytokinesis.

HeLa cells expressing histone H2B-GFP treated with cyclophilin B siRNA and then stained with anti- β -tubulin antibodies (a) show a normal mitotic spindle interrupted at the midbody following cytokinesis. Knocking down Nup153 gave a variety of phenotypes: peripheral residual midbodies (b and d), poorly defined midbody spindles (c), and multipolar midbody spindles (e). (f) Quantification of the number of midbodies on random areas of a coverslip. 500-1000 cells per coverslip from four independent experiments were analyzed. Scale bars, 10 μ m.

2.4 Discussion

NPCs control the trafficking of macromolecules between the nucleus and the cytoplasm of interphase cells and the nucleoporin Nup153 is a critical player in both nuclear import as well as export. Besides their function in interphase, it has become evident that many nucleoporins have important roles in mitosis, such as the nucleoporins of the Nup107-160 complex or Nup358 (Chakraborty et al., 2008; Loiodice et al., 2004; Salina et al., 2003; Zuccolo et al., 2007). The mitotic function of nucleoporins is often associated with their localization to kinetochores in mitosis, while on the other hand kinetochore proteins, such as the SAC proteins Mad1 and Mad2 are found at NPCs during interphase (Campbell et al., 2001). In this study we show that Nup153 binds directly to Mad1 and that Nup153 expression levels regulate Mad1 phosphorylation, which in turn modulates checkpoint activity.

2.4.1 Altered Nup153 levels are associated with abnormal mitosis

To gain further insight into the cellular function(s) of Nup153 we have altered its expression levels in HeLa cells and found that enhanced levels of Nup153 coincide with a number of nuclear abnormalities, such as intranuclear Nup153 foci, nuclear lobulation and multinucleation (Figure 2.1 and Figure 2.2), coinciding with multipolar spindles (Figure 2.3). Depletion of Nup153 from HeLa cells by RNAi results in an increase in cells with unresolved midbodies, indicative of delayed or aborted cytokinesis (Figure 2.7). Therefore, both up- and down-regulation of Nup153 causes abnormal mitoses, indicating that Nup153 levels need to be tightly controlled to achieve normal cell division. Most importantly, the role of Nup153 in mitosis appears independent of its ability to recruit soluble nuclear transport receptors to the inner nuclear membrane, since overexpression of its NPAR, i.e. residues 39-399 of human Nup153, is sufficient to induce the aberrant mitotic phenotype. This region of Nup153 is required for its incorporation into NPCs, but an interaction of this domain with nuclear transport receptor is unknown (Bastos et al., 1996; Enarson et al., 1998). Based on our data presented here it is therefore conceivable to conclude that the role of Nup153 in mitosis is independent from its transport role, at least from "conventional" nucleocytoplasmic transport pathways, since the role of Nup153 in nucleocytoplasmic transport is due to interactions

of Nup153's C-terminal FG-repeat domain with soluble nuclear transport receptors (Ball and Ullman, 2005). While this manuscript was in preparation, a study was published that supported this notion (Mackay et al., 2009). In this study, the authors showed that reduction of Nup153 causes a delay in cytokinesis without affecting global nucleocytoplasmic transport.

2.4.2 Nup153 function in mitosis is related to the mitotic checkpoint

Multinucleation can originate from several malfunctions, such as errors in chromosome segregation, incorrect microtubule-kinetochore attachments, failure of the spindle checkpoint or cytokinesis (King, 2008). In this context, multinucleated cells have been described as a phenotype that is consistent with the loss of Mad1 function (Jin et al., 1998) or due to mutations in Mad2 (Michel et al., 2001). Impaired Mad1 function does not affect cell cycle progression and duration of mitosis (Musacchio and Salmon, 2007). Consistent with loss of Mad1 function, overexpression of Nup153 results in multinucleation of cells without affecting cell cycle progression (Figure 2.2 and Figure 2.3). While the ratio of nuclei having G1, S and G2 phase DNA content were similar in cells expressing GFP-Nup153 as compared to untransfected control cells, GFP-Nup153 nuclei exhibited a significant increase in aneuploid cells (Figure 2.2, d-f), corresponding to cells undergoing abnormal mitoses.

The given similarities in the phenotypes that result from Mad1 inactivation and enhancing Nup153 levels, respectively, and the known localization of Mad1 to NPCs in interphase, prompted us to explore a direct interaction between Nup153 and Mad1. We found in fact that both proteins bind to each other in unsynchronised as well as in cells arrested in mitosis (Figure 2.4c), indicating that the interaction between Nup153 and Mad1 is maintained throughout the cell cycle. Moreover, we could show that Nup153's NPAR mediates binding to Mad1, consistent with the observation that expression of this domain causes abnormal mitoses (see above). By immuno-EM, we furthermore found Mad1 to colocalize with the N-terminal domain of Nup153 on the nuclear face of the NPC (Figure 2.4b). Our findings therefore strongly suggest that an interaction between the NPAR of Nup153 and Mad1 contributes to the regulation of the Mad1 and spindle checkpoint activity.

During the course of our study, a recent report has implicated Tpr, another component of the NPC and a known interacting partner of Nup153 (Hase and Cordes, 2003), in proper spindle checkpoint activation due to direct binding of Tpr to Mad1 and Mad2 (Lee et al., 2008). The function of Nup153 and Tpr in SAC regulation appear independent from each other, as we found that the loss of Nup153 neither affect mRNA nor protein levels of Tpr (Figure S7.7, b-d). Moreover, Nup153 and Tpr appear to have opposing effects in SAC regulation, as increased levels of Nup153, but reduction of Tpr cause multinucleation and impaired checkpoint activity. Evidently both components of the NPC's nuclear basket are critically engaged in SAC regulation and further investigations are required to more systematically dissect the underlying regulatory mechanisms.

2.4.3 Nup153 levels regulate SAC activity

Challenging HeLa cells that either express GFP-Nup153 or are depleted for Mad1 with nocodazole lead to a lowered mitotic index as compared to control cells, in contrast to Nup153-depleted cells (Figure 2.5b). This data indicated that Nup153 overexpression abrogates the mitotic checkpoint to a comparable extend to depletion of Mad1, whereas the SAC remains functional in the absence of Nup153. Importantly, co-expression of Nup153 and Mad1 rescue cells from Nup153-induced SAC impairment, indicating that the Nup153-Mad1 ratio is important for proper SAC function. Consistent with an impaired SAC, we found phosphorylation of Mad1 to be reduced in the presence of enhanced Nup153 levels (Figure 2.5c).

Decreased concentrations of Nup153, on the other hand, leave the SAC intact and may lead to persistent checkpoint activity. A hyperactive spindle checkpoint alters the sequence of mitotic events and cells display marked difficulties in completing cytokinesis (Brito and Rieder, 2006; Hernando et al., 2004). Consistent with this model, reduction of Nup153 causes abnormal cytokinesis (Figure 2.7) and persistent association of Mad1 to kinetochores beyond prometaphase (Figure 2.6), but neither Mad1 phosphorylation nor the association of Mad2 is compromised. Further studies are required to analyze the underlying molecular mechanism as to how varying Nup153 levels affect Mad1 phosphorylation and SAC activity.

In summary, we have shown that the nucleoporin Nup153 is involved in spindle checkpoint regulation due to an interaction with the checkpoint protein Mad1. Both, up- and down-regulation of Nup153 gives rise to abnormalities in mitosis and cytokinesis. Furthermore, our data indicate that Mad1 interacts with the NPAR region of Nup153 and that this interaction is likely responsible for localizing Mad1 at the NPCs and its translocation to kinetochores in mitosis. Interestingly, Nup153 itself was not found at kinetochores (data not shown; see also (Mackay et al., 2009)), indicating that Nup153 acts to keep Mad1 away from kinetochores and that this regulates SAC activity. Interestingly, this role for Nup153 in controlling the mitotic checkpoint appears evolutionarily conserved, since its yeast homologue, Nup1p, is also required for the association of Mad1p with the NPC (Kastenmayer et al., 2005). Moreover, mutations in *nup1* result in altered spindle organization with an increase in multinucleate and anucleate daughter cells as well as failure to exit from mitosis (Bogerd et al., 1994; Harper et al., 2008). Given a role for Nup153 in development and cancer (Heidenblad et al., 2008; Nybakken et al., 2005; Orlic et al., 2006) it will be interesting to determine how this is related to Nup153's novel function in cell division.

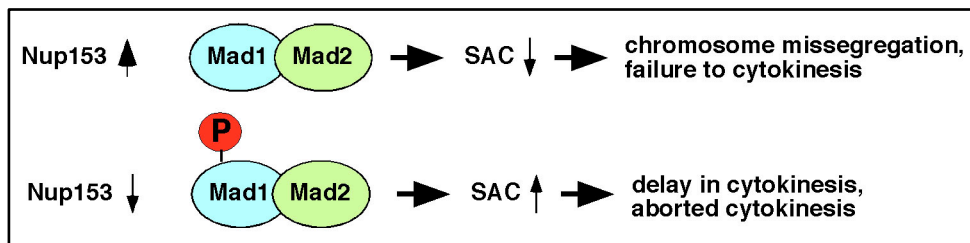


Figure 2.8: Schematic model of Nup153 function in SAC activity.

Overexpression of Nup153 causes hypophosphorylation of Mad1, which leads to an impaired SAC and consequently chromosome missegregation and failures of cytokinesis. Depletion of Nup153 does not affect Mad1 phosphorylation (P) leaving the SAC intact, which may cause a persistently activated SAC consistent with delayed and/or aborted cytokinesis. Mad1 binding to Mad2 is neither affected by enhanced nor by reduced Nup153 levels.

2.5 Materials and Methods

2.5.1 Cell culture and transfections

HeLa cells were grown in Dulbecco's modified Eagle's medium (DMEM) supplemented with 10% fetal bovine serum (FBS) plus penicillin and streptomycin. HeLa cells stably expressing H2B-GFP cells were cultivated in DMEM supplemented with 10% FBS plus penicillin, streptomycin and blasticidin.

Cells were transfected using Lipofectamine 2000 (Invitrogen, Paisley, UK) following the instructions of the manufacturer.

2.5.2 Constructs and antibodies

N-terminally tagged GFP-Nup153 was produced as described previously (Fahrenkrog et al., 2002). N-terminally tagged GFP-Nup153-39-339 was subcloned from Nup153-39-339 with a N-terminal HA-tag and a C-terminal 6 His-tag from pGEX-4T-3 (Amersham-Pharmacia, Little Chalfont, England) into BamHI cut pEGFP-C1 (Clontech, Palo Alto, CA). The correct orientation of the insert was confirmed by enzymatic digestion. pEGFP-Nup153-39-144 and pEGFP-Nup153-144-339 were subcloned following the same strategy.

The polyclonal antibody against the zinc-finger of human Nup153 (anti-Nup153-Z: 1:1000 for immunofluorescence) was kindly provided by Katie Ullman (University of Utah). The monoclonal antibodies SA1 (1:2 for immunofluorescence) and QE5 against the C-terminal FG-repeat domain of Nup153 were obtained from Brian Burke (University of Florida). Further primary antibodies were the monoclonal antibodies mAB414 (1:2000; Covance, Berkely, CA), anti-Mad1 (1:50; Santa-Cruz, Santa Cruz, CA), anti-Tpr (1:400, Abnova, Taipei, Taiwan), anti- β tubulin (1:2000; Chemicon, Billerica, MA), anti-phospho-Ser/Thr/Tyr (1:1000, Abcam) as well as polyclonal anti-phospho-histone H3 (1:50; Santa Cruz). Secondary antibodies include anti-mouse IgG-Alexa 568, anti-mouse Alexa 647, anti-rabbit IgG Alexa 488, anti-rabbit IgG-Alexa 568, anti-rabbit Alexa 647 and anti-human Cy5 are from Molecular Probes (Paisley, UK) and used 1:400 (Alexa 488), 1:1000 (Alexa 568), 1:350 (Alexa 647), and 1:200 (Cy5).

2.5.3 Immunofluorescence

Cells were grown on coverslips and fixed either in 2% formaldehyde for 15 min or -20°C methanol for 5 min, washed three times for 5-10 min with PBS, and permeabilized with PBS containing 2% bovine serum albumin (BSA) and 0.2% Triton X-100 for 10 min. Next the cells were washed three times for 5-10 min in PBS containing 2% BSA and incubated with the appropriate primary antibodies for 1 hour, washed three times in PBS containing 2% BSA and incubated with the appropriate secondary antibodies for 1 hour, washed 5x with PBS then mounted with Mowiol and stored at 4°C until viewed. Cells were prepared for triple label immunofluorescence as described previously (Joseph et al., 2002) and mounted in 50% glycerol in 20 mM Tris (pH 9.0) containing 2 mg/ml p-phenylenediamine (PPD). Cells were viewed using a confocal laser scanning microscope (Leica TCS NT/SP1 or SP5, Leica, Vienna, Austria). Images were recorded using the microscope system software and processed using Adobe Photoshop (Adobe Systems, Mountain View, CA, USA).

2.5.4 RNA interference

HeLa cells were depleted of Nup153 using On-target smart pool duplex siRNA to human Nup153 (Dharmacon, Lafayette, CO). Cells were grown on 12 mm diameter coverslips and exposed to the Nup153 siRNA in the presence of Lipofectamine RNAiMax (Invitrogen, Paisley, UK) following the instructions of the manufacturer. As a control cells were exposed to Lipofectamine RNAiMax alone or to siRNA against cyclophilin B (Dharmacon, Lafayette, CO). Knock down efficiency was determined by qRT-PCR and immunoblotting 48 h post transfection. For indirect immunofluorescence, cells were prepared as described above.

2.5.5 Quantitative real-time PCR

Cells were lysed using QIAshreddersTM (Qiagen, Hilden Germany) and total RNA was extracted using the RNeasy[®] Mini Kit (Qiagen, Hilden Germany) according to manufacturer's recommendations. Messenger RNA (mRNA) was purified using the GenEluteTM-mRNA Miniprep Kit (Sigma, St. Louis, MO). Reverse transcription was

performed using the first-strand cDNA and SuperscriptTMIII reverse transcriptase (Invitrogen, Carlsbad, CA) according to the manufacturer's instructions.

Probes were designed with the Real-Time PCR Primer Design program (www.genscript.com). Nup153 probes were 5'-ATT TGG AAC TGG ACC CTC AG and 5'-TGG GAA ATA ATG CTG TGG AA and β -Actin probes were 5'-AGC ACG GCA TCG TCA CCA ACT and 5'-TGG CTG GGG TGT TGA AGG TCT. These probes generated 256 and 180 bp replicons, respectively (W. Dietmeier, Rapid cycle real-time PCR, Springer).

2.5.6 Quantitative immunoblotting and gel electrophoresis

Cells were resuspended in lysis buffer containing 50 mM Tris-HCl pH 7.8, 150 mM NaCl, 1% Nonidet P-40, and protease inhibitor cocktail tablets (Roche, Basel, Switzerland). Sample aliquots were resolved by sodium dodecyl sulfate-polyacrylamide (10%) gel electrophoresis (SDS-PAGE). The proteins were transferred onto a PVDF membrane and the membrane was incubated in I-Block solution (Tropix, Bedford, MA) containing 0.1% Tween-20 (blocking solution) over night at 4°C, then incubated in blocking solution containing a primary antibody directed against either SA1 (1:100), QE5 (1:3) or anti- β -tubulin (1:1000) for 1 hour followed by washing 3x with PBS containing 0.1% Tween-20. The membrane was then incubated in the dark with anti-mouse IRDye 800 (1:10000; LI-COR, Biosciences, NE, USA) in blocking solution. Images were recorded using the Odyssey infrared imaging system and analyzed by the systems software program (LI-COR, Biosciences, NE, USA).

2.5.7 Flow cytometry

Cells were fixed in ice-cold 70% ethanol for 30 minutes, washed 2x in PBS by vortexing and pelleting at 1000 g for 5 minutes, and suspended at 1×10^6 cells/ml, pelleted again and stained with PI stain (50 μ g/ml propidium iodide, 180 units/ml RNase A, 0.1% Triton-X 100, 4 mM citrate buffer, 0.03g/ml polyethylene glycol 6000) for 20 minutes at 37°C. An additional PI salt solution (50 μ g/ml propidium iodide, 0.1% Triton-X 100, 0.4 M NaCl, 0.03g/ml polyethylene glycol 6000) was added and the cell preparation was stored at 4°C in the dark until flow cytometric acquisition and analysis.

2.5.8 Live cell imaging

For live cell imaging, HeLa cells were transfected with GFP-Nup153 by electroporation, seeded onto Lab-Tek chamber (Nunc, Roskilde, Denmark) and maintained at 37°C in DMEM. 48 hours after transfection, cells were equilibrated to Leibowitz medium complemented with 10% FCS and time-lapse sequences were recorded every 60 sec for a maximum of 300 cycles using a 63x N.A. 1.4 objective on a Zeiss LSM 510 META confocal microscope (Zeiss, Thornwood, NY) with a heated stage.

2.5.9 Immunoprecipitation

Subconfluent HeLa cells (3×10^6) were trypsinized, washed with PBS and resuspended in 160 μ l lysis buffer (50 mM Tris-HCl, pH 7.4, 250 mM NaCl, 0.1 % Triton X-100, 2 mM EDTA- Na_2 , 10% Glycerol and protease inhibitor (Thermo Scientific)), vortexed and incubated for 10 min at 37°C. The cells were pelleted at 16,000 g for 10 min and the supernatant was transferred to a fresh tube. The supernatant was cleared with 20 μ l of protein G-agarose beads (Santa Cruz) and incubated for 30 min at 4°C, centrifuged at 1000 g for 30 sec at 4°C, and the supernatant was transferred to a fresh tube and 2 μ g mouse monoclonal Mad1 antibody or a 1/5 dilution of a hybridoma supernatant containing mouse monoclonal Nup153 antibody (SA1) were added and incubated for 2 hours on ice. Prewashed protein G-agarose slurry, 40 μ l, was added to the lysate and incubated at 4°C on a rocker platform for 1 hour. The immunoprecipitate was collected by centrifugation at 1000 g for 30 sec at 4°C and the supernatant was carefully removed and kept to analyze as unbound fraction. The pellet was washed 3x with lysis buffer, resuspended in electrophoresis sample buffer, boiled at 95°C for 5 min and subjected to electrophoresis and Western blotting.

2.5.10 Solution binding assays

The in vitro interaction between Nup153 and Mad1 was tested as described previously (Walter et al., 2006).

2.5.11 Immuno-EM

Mature (stage 6) oocytes were surgically removed from female *Xenopus laevis*, and their nuclei were isolated as described (Pante et al., 1994). Colloidal gold particles, ~8-nm in diameter, were prepared by reduction of tetrachloroauric acid with sodium citrate in the presence of tannic acid and antibodies were conjugated to colloidal gold particles as described (Baschong and Wrigley, 1990). Isolated nuclei were labeled with anti-Mad1 antibodies as described previously (Fahrenkrog et al., 2002). Labeled nuclei were fixed and processed for EM as described (Fahrenkrog et al., 2002; Paulillo et al., 2005). EM micrographs were recorded on a Phillips CM-100 transmission electron microscope equipped with a CCD camera. Elliptic location clouds were calculated as described (Fahrenkrog et al., 2002).

2.6 Acknowledgements

The authors wish to thank Katie Ullman and Brian Burke for providing us with antibodies against Nup153. Sara Paulillo is kindly acknowledged for initiating the RNA interference experiments and Markus Affolter for helpful suggestions. This work is supported by research grants from the Swiss National Science Foundation as well as the Kanton Basel Stadt and the M.E. Müller Foundation of Switzerland (to B.F).

3

Direct association of the nucleoporin Nup88 with lamin A

Yvonne C. Lussi¹, Ilona Hügi¹, Birthe Fahrenkrog^{1,2,□}

¹M.E. Müller Institute for Structural Biology, Biozentrum, University of Basel,

Klingelbergstrasse 70, 4056 Basel, Switzerland

²Laboratoire du Biologie du Noyau, Institut de Biologie & de Médecine Moléculaire,

Université Libre de Bruxelles, Rue Profs Jeener & Brachet, 12, B-6041 Charleroi,

Belgium

Running title: Nup88 interacts with lamin A

Keyword: Nup88; nuclear pore complex; lamin A; nuclear lamina; epitope masking;

3.1 Abstract

Nuclear pore complexes (NPCs) are embedded in the nuclear envelope (NE) and mediate bidirectional nucleocytoplasmic transport. Their spatial distribution in the NE is organized by the nuclear lamina, a meshwork of nuclear intermediate filament proteins. Major constituents of the nuclear lamina are A- and B-type lamins. In this work, we have identified Nup88 as novel interaction partner of lamin A in pull-down experiments. By immunoprecipitation assays, we showed that the interaction takes place *in vivo*. Further characterization of the Nup88-lamin A complex by solution-binding assays revealed that the N-terminus of Nup88 specifically binds to the Ig-fold of lamin A, but not the Ig-fold of B-type lamins. Additionally, we have localized the nucleoporin Nup88 to the cytoplasmic and nuclear face of the NPC by immunoelectron microscopy using *Xenopus laevis* oocyte nuclei. Moreover, we found that overexpression of GFP-tagged lamin A is masking the binding site of Nup88 antibodies in immunofluorescence assays, supporting the interaction of lamin A with Nup88 in a cellular context. We further demonstrated that the epitope masking phenotype is lost in cells overexpressing Ig-fold mutants of lamin A that are associated with Emery-Dreifuss muscular dystrophy (EDMD) and Dunnigan-type familial partial lipodystrophy (FPLD). Consistently, the interaction of GST-Nup88 with the *in vitro* expressed lamin A Ig-fold mutants was lost in a solution-binding assay. Together, our data suggest that a pool of Nup88 is localizing to the nuclear side of the NPC, where it provides a novel interaction with lamin A.

3.2 Introduction

In eukaryotic cells, the nuclear envelope (NE) is spatially separating the molecular events in the cytoplasm and the nuclear compartment. Nuclear pore complexes (NPCs) are embedded in the double membrane of the NE, thereby bridging the nucleus and cytoplasm in interphase cells. The vertebrate NPC consists of about 30 different proteins called nucleoporins (or Nups) (Cronshaw et al., 2002), which are organized in distinct subcomplexes to form the major building blocks of the NPC: the central framework, which exhibits octagonal rotational symmetry, and the cytoplasmic and nuclear ring moiety (Akey and Radermacher, 1993; Beck et al., 2004; Hinshaw et al., 1992; Stoffler et al., 2003). Filamentous structures decorate the cytoplasmic and nuclear face of the NPC, known as cytoplasmic filaments and nuclear basket, respectively. Nup88 is associated within a subcomplex with Nup214 and Nup358 on the cytoplasmic side of the NPC, which is implicated in CRM1-mediated nuclear protein export (Bernad et al., 2006; Bernad et al., 2004; Fornerod et al., 1997b; Roth et al., 2003). Nup88 consists of two structural domains: the N-terminal two-thirds of the protein (residues 1-584) fold into a β -propeller based on secondary structure prediction, and the C-terminal third (residues 585-742) is predicted to be largely coiled-coil in structure (Fornerod et al., 1997b; Schwartz, 2005). The coiled-coil domain is mediating the interaction with Nup214 and connects Nup88 to the NPC (Bastos et al., 1997; Bernad et al., 2004; Fornerod et al., 1997b). The N-terminal β -propeller domain of Nup88 interacts with the NPC-targeting domain of Nup98, a nucleoporin that is discussed to localize to both the nuclear and cytoplasmic side of the NPC and to interact with distinct subcomplexes, i.e. the Nup88-Nup214 subcomplex on the cytoplasmic side and the Nup107-160 complex on the nuclear side of the NPC (Griffis et al., 2003; Radu et al., 1995).

The nuclear lamina is a component of the NE, lying between the inner nuclear membrane and the peripheral chromatin and is tightly associated with the NPCs (Akey, 1989; Furukawa et al., 2009). The nuclear lamina has been suggested to be involved in maintaining the structural integrity of the NE, the organization of chromatin structure and function and the spacing of NPCs (Broers et al., 2006; Lenz-Bohme et al., 1997; Liu et al., 2000; Sullivan et al., 1999). The lamina is formed by type-V intermediate filament proteins, which are composed of A- and B-type lamins (Aebi et al., 1986; Stuurman et al.,

1998). The A-type lamins lamin A and lamin C (lamin A/C) arise through alternative splicing of a common transcript and differ only in the last 83 amino acids of their C-terminus, whereas the B-type lamins lamin B1 and B2 are encoded by separate genes (Moir et al., 1995; Stuurman et al., 1998). While B-type lamins are constitutively expressed in cells throughout development, A-type lamins are only expressed in later stages of development and in differentiated cells (Broers et al., 2006; Hutchison et al., 2001). Both types directly interact with integral proteins of the inner nuclear membrane, NPC proteins, chromosomal proteins and DNA, and play roles in nuclear activities including gene expression and DNA replication (Broers et al., 2006; Schirmer and Foisner, 2007). Several studies in *C. elegans*, *D. melanogaster* and cultured mammalian cells suggest that B-type lamins are essential for viability (Lenz-Bohme et al., 1997; Liu et al., 2003), whereas the targeted disruption of lamin A/C in mice causes muscular dystrophy, loss of adipose tissue and early cell death (Sullivan et al., 1999). Mutations in lamin A/C as well as several inner nuclear membrane proteins that bind the lamina are associated with a diverse array of human diseases, so-called laminopathies. One particular point mutation in the immunoglobulin (Ig)-fold domain of lamin A, i.e. the missense mutation of an arginine at position 453 to a tryptophan (R453W), is leading to Emery-Dreifuss muscular dystrophy (EDMD) in humans, which is characterized by muscle weakness and wasting and contractures of certain joints (Burke and Stewart, 2002; Hutchison and Worman, 2004; Mounkes et al., 2003; Wilson, 2000). R453 resides in the Ig-fold domain of lamin A, is involved in a salt bridge formation between two β -sheets and its mutation leads to abrogation of the salt bridge and to a destabilization of the C-terminal domain of lamin A (Dhe-Paganon et al., 2002; Krimm et al., 2002). The missense mutation R482W in lamin A results in Dunnigan-type familial partial lipodystrophy (FPLD), characterized by variable loss of body fat from the extremities as well as from the truncal region (Speckman et al., 2000). Residue R482 locates on the surface of the Ig-fold and its mutation destroys a positively charged interaction site of lamin A-binding proteins (Dhe-Paganon et al., 2002; Krimm et al., 2002). The most common mutation found in Hutchison-Gilford progeria syndrome (HGPS) is the mutation of C1824 to a T, a silent mutation, however, it results in the generation of an alternative splice site, leading to a truncated version of lamin A lacking 50 amino acids in its Ig-fold

neighbored C-terminus, called LA Δ 50 or progerin (Broers et al., 2006). LA Δ 50 is permanently farnesylated and anchored to NE, affecting its localization and overall function (Eriksson et al., 2003; Scaffidi and Misteli, 2005).

To fully understand lamina function as well as the implications of the lamina-NPC interaction in laminopathies, it is crucial to identify lamin-binding components. In this study, we found Nup88 as novel interaction partner of lamin A. We show that Nup88 and lamin A interact in vitro as well as in vivo. Further characterization of the interaction revealed that the N-terminal domain of Nup88 and the Ig-fold of lamin A are mediating the binding of the two proteins. Additionally, we show that Nup88 is localizing to both sides of the NPC by immunoelectron microscopy using *Xenopus laevis* oocyte nuclei. Furthermore, we show that overexpression of GFP-lamin A leads to a masking of a Nup88 antibody epitope in human cells. Moreover, we show that the EDMD-associated R453W and the FPLD-associated R482W mutant lamin A abolish the interaction between the two proteins, however the progeria mutant lamin A Δ 50 is still able to bind Nup88. Together, our data describe a new interaction between the nucleoporin Nup88 and the nuclear intermediate filament protein lamin A and its loss of interaction with disease-linked Ig-fold mutants. Understanding the details of this interaction might be essential to shed light on the underlying molecular mechanism of lamin-linked diseases.

3.3 Results

3.3.1 Lamin A is an interaction partner of Nup88

In order to identify new interaction partners of Nup88, we performed an in vitro binding assay. To do so, a lysate of isolated HeLa S3 nuclei was incubated with purified, recombinant glutathione-S-transferase (GST)-tagged Nup88 fusion protein or GST alone immobilized on glutathione sepharose beads. Proteins that bound immobilized GST-Nup88 or GST were separated on SDS-PAGE and detected using colloidal blue staining. One protein band of ~74 kDa was identified in the lane corresponding to the GST-Nup88 bound fraction but not in the GST control (Figure 3.1A). Mass spectrometry analysis of peptide fragments derived from this polypeptide revealed that the 74 kDa protein was lamin A. Other bands identified were either degradation products of GST-Nup88, linker histone H1, ribosomal protein L7a or M-phase phosphoprotein 4. Since connections between the NPC and the nuclear lamina were already described before, lamin A was a promising candidate as novel interaction partner of Nup88 (Hawryluk-Gara et al., 2005; Smythe et al., 2000). By immunoblot analysis using a polyclonal antibody against lamin A, we confirmed that lamin A copurified with GST-Nup88, but not with GST. However, a protein with slightly higher molecular weight than lamin A is recognized unspecific by the lamin A antibody in both samples (indicated with *) (Figure 3.1B).

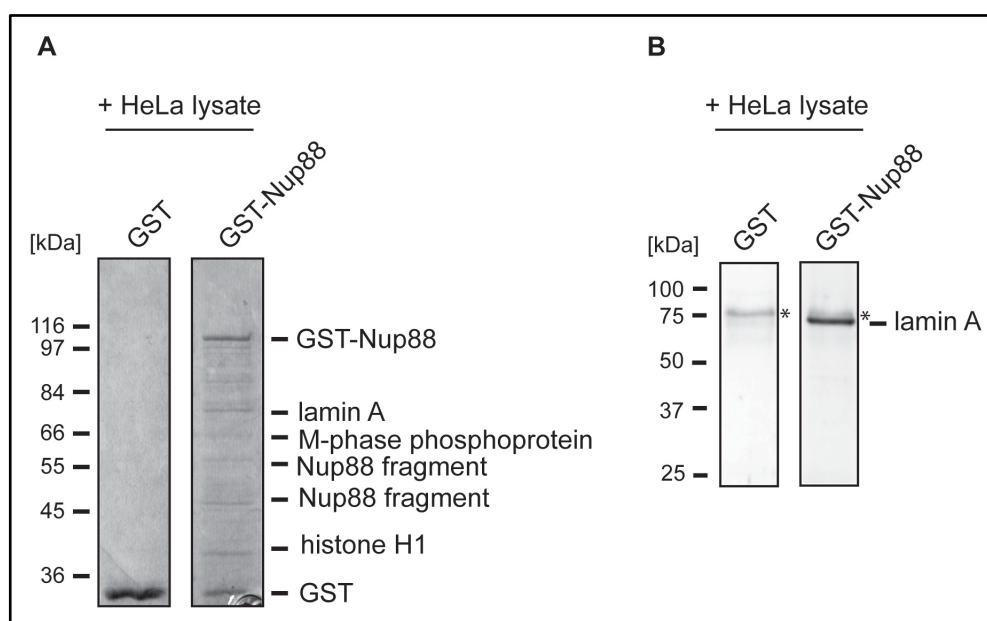


Figure 3.1: Lamin A is a novel interaction partner of Nup88.

Bacterially expressed GST-Nup88 and GST were bound to glutathione sepharose beads and incubated with HeLa cell lysate. Bound fractions were analyzed by SDS-PAGE, colloidal staining (**A**) and mass spectroscopy or by immunoblotting with lamin A antibody (**B**). Lamin A was bound to GST-Nup88, but not to GST. The locations of molecular weight (MW) markers are indicated on the left.

3.3.2 Nup88 is interacting with lamin A in vivo and in vitro

To confirm that Nup88 is interacting with lamin A in vivo, HeLa cell lysates were immunoprecipitated with antibodies directed against Nup88 (Figure 3.2A). The HeLa lysate (L), supernatant (S), and pellet (P) proteins were separated by SDS-PAGE, transferred to a PVDF (Polyvinylidene Difluoride) membrane and probed with antibodies against Nup88 and lamin A, respectively. As shown in Figure 3.2A, lamin A is co-immunoprecipitated with Nup88, indicating that Nup88 associates with lamin A in vivo (Figure 3.2A).

To test whether Nup88 and lamin A are interacting directly, we performed blot-overlay assays between Nup88 and lamin A using recombinantly expressed lamin A and in vitro transcribed/translated ^{35}S -labeled Nup88 using the rabbit reticulocyte lysate system (Figure 3.2B). Equal amounts of bacterially expressed and purified cytoplasmic intermediate filament (IF) protein vimentin as a control (Figure 3.2B, lane 1) and lamin A (Figure 3.2B, lane 2) were subjected to SDS-PAGE (Coomassie), transferred to a PVDF

membrane and overlaid with the ^{35}S -labeled Nup88. As shown in Figure 3.2B (overlay), Nup88 was binding to lamin A, but not to vimentin.

To further determine the domains of Nup88 and lamin A, respectively, that are required for the interaction between the two proteins, we performed solution binding assays with purified recombinant his-tagged lamin A bound to nickel beads and *in vitro* transcribed and translated ^{35}S -labeled Nup88 fragments, i. e. the full-length protein, the N-terminal domain (residues 1-550) or the C-terminal domain (residues 551-741) of Nup88 (Figure 3.2C). The bound (B) and unbound (U) fractions to lamin A immobilized on nickel beads were separated by SDS-PAGE, transferred to a PVDF membrane and analyzed by autoradiography. As shown in Figure 3.2C, full-length Nup88 (left panel) and the N-terminal domain (middle panel) were interacting with lamin A, but not so the C-terminus of Nup88 (right panel). Together, this data indicate that the interaction of Nup88 with lamin A is mediated by Nup88's N-terminus.

To further determine which domain of lamin A interacts with Nup88, we next performed solution-binding assays using purified recombinant GST-Nup88 and GST as control immobilized on sepharose beads and *in vitro* transcribed and translated ^{35}S -labeled domains of lamin A, lamin B1 and B2, respectively. GST-Nup88 interacted with the full-length lamin A, the tail domain of lamin A (i.e. residues 386 to 548) and the immunoglobulin (Ig)-fold domain of lamin A, but not with the Ig-folds of lamin B1 and lamin B2 (Figure 3.2D). None of our different lamin constructs was significantly interacting with GST alone. Together, these data indicate that the interaction of lamin A with Nup88 is specifically mediated by the Ig-fold of lamin A.

Nup88 has been implicated in CRM1 mediated protein export, and importin α and β appear to act as nuclear import factors for lamin A (Adam et al., 2008; Fornerod et al., 1997b; Loewinger and McKeon, 1988). To analyze if the observed Nup88-lamin A complex might be associated with nucleocytoplasmic transport, we tested if importin α , importin β or CRM1 are associated with the lamin A-Nup88 complex. To do so, we immunoblotted reticulocyte lysate used for *in vitro* expression and ^{35}S -labeling of lamin A as well as the fractions bound to GST-Nup88 and GST, respectively with monoclonal antibodies against importin α , importin β and CRM1 (Figure S7.9). While CRM1, importin α and β are detectable in the reticulocyte lysate, neither importin α , importin β

or CRM1 were found to be bound to GST-Nup88 or GST, indicating that the Nup88-lamin A complex is not part of a nuclear import or export complex.

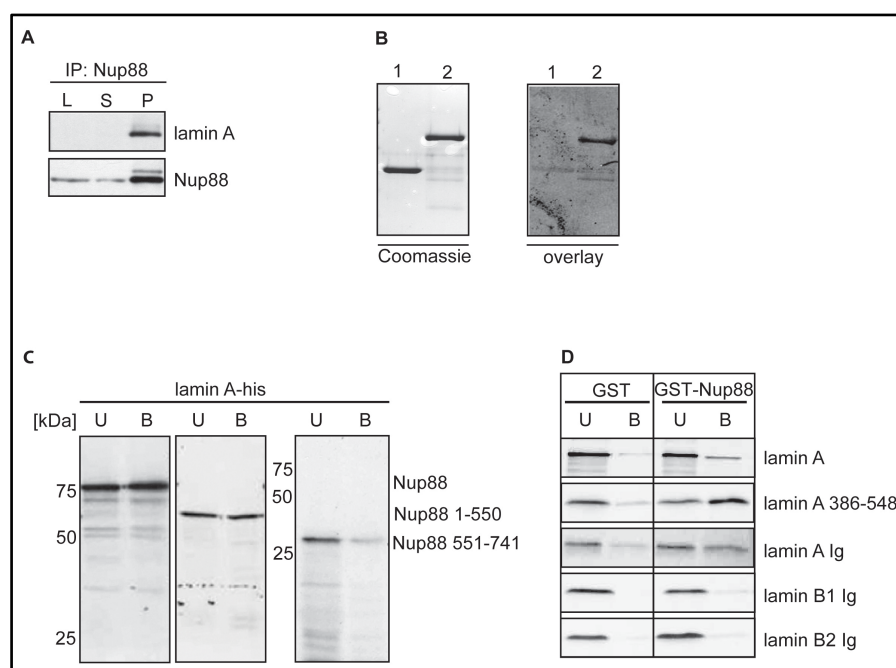


Figure 3.2: Nup88 is interacting with lamin A in vivo and in vitro.

(A) HeLa cell lysates were immunoprecipitated with Nup88 antibody. HeLa cell lysate (L), immune supernatant (S) and immune precipitate (P) proteins were analyzed by SDS-PAGE and immunoblotted with Nup88 and lamin A antibodies. Lamin A is found to be co-immunoprecipitated with Nup88. (B) Blot binding assay employing bacterially expressed and purified vimentin and lamin A and in vitro expressed and ^{35}S -labeled Nup88. Samples of purified vimentin (lane 1) and lamin A (lane 2) were separated by SDS-PAGE, stained with Coomassie blue (left panel) or transferred to a PVDF membrane and overlaid with ^{35}S -labeled Nup88 (right panel). ^{35}S -labeled Nup88 was visualized by autoradiography. (C) Bacterially expressed his-tagged lamin A was bound to nickel beads and incubated with in vitro synthesized ^{35}S -labeled full-length, N-terminal (residues 1-550) or C-terminal (residues 551-741) Nup88. Unbound and bound fractions were analyzed by SDS-PAGE and autoradiography. ^{35}S -full-length Nup88 and N-terminal ^{35}S -Nup88 were binding to lamin A-his, whereas C-terminal ^{35}S -Nup88 was not able to bind lamin A-his. (D) Bacterially expressed GST-Nup88 and GST were bound to glutathione sepharose beads and incubated with in vitro synthesized ^{35}S -labeled full-length lamin A, lamin A tail domain (residues 386-548), and the Ig-folds of lamin A, lamin B1 and B2. Unbound and bound fractions were analyzed by SDS-PAGE and autoradiography. Whereas full-length lamin A, lamin A tail and lamin A Ig-fold were able to bind GST-Nup88 but not GST, the Ig-folds of lamin B1 and B2 did not bind to GST-Nup88 or GST.

3.3.3 Nup88 is localizing partially to the nuclear face of the NPC

An epitope of Nup88 was previously localized to the cytoplasmic side of the

NPC in *Xenopus* oocyte nuclei using an antibody recognizing the C-terminus of Nup88 (Bernad et al., 2004). However, the novel interaction of Nup88 with lamin A suggests that a pool of Nup88 might also be localized on the nuclear side of the NPC. In an effort to more precisely determine the position of Nup88 within the NPC, we performed immuno-electron microscopy (EM) using *Xenopus* oocyte nuclei and domain-specific antibodies against distinct domains of human Nup88. *Xenopus* oocyte nuclei were isolated manually and incubated with distinct anti-Nup88 antibodies directly conjugated to 8-nm colloidal gold and processed for thin-sectioning EM. As illustrated in Figure 3.3A, the antibody against the N-terminus of Nup88 recognized epitopes on both the nuclear and the cytoplasmic side of the NPC. Quantification of the gold particle distribution with respect to the central plane of the NE revealed that about 40% of the gold particles were associated with the nuclear face of the NPC at a mean distance of $-31.9 \text{ nm} \pm 16.7 \text{ nm}$ from the central plane (Figure 3.3B). Together with corresponding mean radial distance of $25.7 \text{ nm} \pm 19.6 \text{ nm}$ this corresponds to an epitope near the nuclear ring moiety of the NPC. The remaining 60% of the gold particles were found on the cytoplasmic side of the NPC, with a mean distance of $16.8 \text{ nm} \pm 8.6 \text{ nm}$ from the central plane and a mean radial distance of $8.2 \text{ nm} \pm 8.7 \text{ nm}$.

Previously, we have shown that recombinant hNup153 incorporates into the NPC after microinjection of a plasmid encoding epitope-tagged hNup153 into the nuclei of *Xenopus* oocyte (Fahrenkrog et al., 2002). We therefore aimed to confirm the localization of the N-terminus using a N-terminal green fluorescent protein (GFP)-tag (GFP-Nup88). *Xenopus* oocytes were microinjected with the plasmids and the localization of the incorporated proteins was determined by using a monoclonal anti-GFP antibody directly coupled to 8 nm colloidal gold. The anti-GFP antibody recognized epitopes both on the cytoplasmic and the nuclear side of the NPC. As shown in Figure 3.3C, quantification of the labeling pattern relative to the central plane of the NPC revealed that 51% of the particles were detected at a mean distance of $38.1 \text{ nm} \pm 12.2 \text{ nm}$ and a mean radial distance of $27.3 \text{ nm} \pm 15.4 \text{ nm}$, on the cytoplasmic side and 49% of the gold particles were localized on the nucleoplasmic side with a mean distance of $-49.8 \text{ nm} \pm 26.1 \text{ nm}$ from the central plane and a mean radial distance of $24.2 \text{ nm} \pm 15.4 \text{ nm}$, consistent with the localization data of the untagged N-terminus of Nup88. The bigger vertical distance

could be explained by the fact that the GFP-tag extends the Nup88 protein. These data are suggesting that indeed a pool of Nup88 is localizing to the nucleoplasmic side of the NPC.

To revise the localization of Nup88's C-terminus by immuno EM studies, we then used an antibody against the C-terminus of Nup88, which recognized an epitope exclusively on the cytoplasmic side of the NPC (Figure 3.3D). Quantification of the labeling pattern (Figure 3.3E) relative to the central plane revealed that 87.7% of the gold particles were detected at a mean distance of 30.7 nm \pm 9.2 nm from the central plane with a radial distance of 16.5 nm \pm 12.8 nm, which is consistent with a previous ultrastructural localization study of the C-terminus of *Xenopus laevis* Nup88 (Bernad et al., 2004).

We further localized the position of recombinant Nup88 with a C-terminal myc-tag (Nup88-myc). *Xenopus* oocytes were microinjected with the plasmids and the localization of the incorporated proteins was determined by using an anti-myc antibody directly coupled to 8 nm colloidal gold. Quantification of the labeling distribution (Figure 3.3F) revealed that 76.3% (n=29) of the gold particles was associated with the cytoplasmic side of the NPC (mean distance from the central plane of the NPC 41.6 nm \pm 12.2 nm with a corresponding radial distance of 33.2 nm \pm 22 nm). This detection of the C-terminal myc-tag is similar, although further away from the central plane and the radial axis, to the labeling seen with the domain-specific antibody against the C-terminus of Nup88 (Figure 3.3E). Together, the C-terminus of Nup88 seems to be detectable almost exclusively on the cytoplasmic side of the NPC.

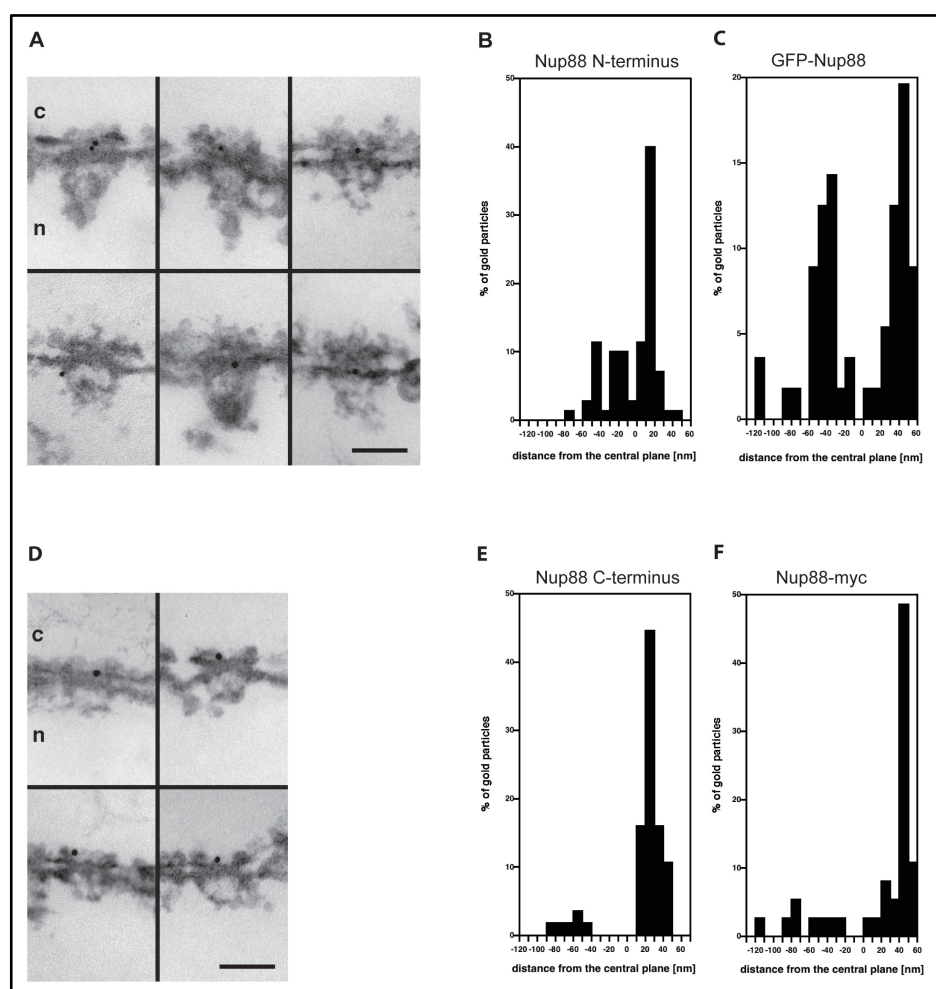


Figure 3.3: Domain topology of endogenous and ectopically expressed Nup88 within the NPC.

Nuclei were isolated manually and labeled with antibodies directly conjugated to 8nm colloidal gold. (A) Nup88 localizes to both the cytoplasmic and the nuclear side of the NPC with a monoclonal Nup88 antibody directed against the N-terminus of Nup88. Shown are selected examples of gold-labeled NPCs in cross-section. c, cytoplasm; n, nucleus. (B) Quantitative analysis of the gold particle distribution associated with the NPC using an antibody against the N-terminus of Nup88. 70 gold particles were scored. (C) Quantitative analysis of the gold particle distribution associated with the NPC using an antibody against the N-terminal GFP-tag of Nup88. 55 gold particles were scored (D) Nup88 is found mainly on the cytoplasmic side of the NPC with a monoclonal Nup88 antibody directed against an epitope in the C-terminus of Nup88. Shown are selected examples of gold-labeled NPCs in cross-section. c, cytoplasm; n, nucleus. (E) Quantitative analysis of the gold particle distribution associated with the NPC using antibodies against the Nup88 C-terminus. 57 gold particles were scored. (F) Quantitative analysis of the gold particle distribution with anti-myc antibodies. 38 gold particles were scored. Scale bars, 100 nm.

3.3.4 The apparent depletion of Nup88 in human embryonic kidney cells overexpressing GFP-lamin A is due to epitope masking

By indirect immunofluorescence, we determined that endogenous lamin A is found at the nuclear rim and distributed in the nucleoplasm and Nup88 is localizing to the nuclear rim with a partial overlap with lamin A in human embryonic kidney (HEK) interphase cells, as described before (Figure S7.10) (Fornerod et al., 1997b; Lehner et al., 1986). To examine whether ectopic expression of lamin A has any effect on Nup88 in HEK cells, we performed a co-immunostaining experiment of HEK cells transfected with green-fluorescent protein (GFP)-tagged lamin A and indirectly labeled Nup88 using an antibody recognizing an epitope in the N-terminus of Nup88 (residues 314-425). 24 hours after transfection, GFP-lamin A was readily expressed and localized to the NE and the nucleoplasm as examined by immunofluorescence and immunoblot analysis (Figure 3.4A + B). However, HEK cells transfected with GFP-lamin A showed a significant reduction of Nup88 staining upon immunolabeling with monoclonal antibody directed against the N-terminal Nup88 epitope with the residues 314-425 as compared to non-transfected cells (Figure 3.4A). We have not observed any reduction in the staining of Nup88 in cells transfected with GFP-lamin B1 nor in the staining of FG-repeat nucleoporins detected with the monoclonal antibody mAb414 in cells transfected with GFP-lamin A or GFP-lamin B1 (Figure 3.4A), indicating that GFP-lamin A overexpression specifically leads to a reduction of Nup88 signal. The transfection efficiency in cells transfected with the GFP-lamin A construct was determined to be 48%, whereof 27.6% showed a masking phenotype (57.8% of total transfected cells, 680 cells counted). The quantification of the fluorescence intensity revealed a reduction of 35% of fluorescence signal in cells transfected with GFP-lamin A compared to non-transfected cells.

Using a tetracycline inducible expression system based on HEK cells, we induced overexpression of Nup88-myc upon presence of tetracycline in the medium, whereupon the protein localizes, besides being incorporated into the NPC, to the cytoplasm of the cell (Figure S7.11A, upper panel). Expression of recombinant Nup88-myc was verified by immunoblot using an anti-myc antibody (Figure S7.11B). In this background, we studied the effects of GFP-lamin A overexpression on Nup88 by immunofluorescence microscopy. In cells transfected with GFP-lamin A, we observed a reduction of Nup88

staining at the nuclear rim and in the cytoplasm, as Nup88 was almost completely vanished from the cytoplasm and only a slight rim staining could be observed (Figure S7.11A, lower panel).

Two scenarios can be thought of to explain the observed reduction of Nup88 staining, one is that either Nup88 protein levels are decreased due to degradation of the protein, or second that Nup88 is in fact present in the cells, but the antibody epitope is masked by binding of excess GFP-lamin A. To examine whether Nup88 protein levels are decreased in cells overexpressing GFP-lamin A, we analyzed Nup88 protein levels by Western blotting. Quantification of the Western blot in Figure 3.4B revealed that the levels of Nup88 in GFP-lamin A and mock transfected cells are not significantly altered (104% versus 100%, respectively), indicating that Nup88 is not depleted in GFP-lamin A overexpressing cells and suggests that the antibody epitope in Nup88 is masked in these cells. We have then reinvestigated this problem by using a polyclonal antibody recognizing a different epitope in the N-terminus of Nup88, i.e. residues 27-45 (Figure S7.12A). Immunofluorescence analysis of GFP-lamin A overexpressing cells with this Nup88 antibody did not show a reduction of Nup88 staining as compared to control cells (Figure S7.12B). Together, these findings suggest that GFP-lamin A specifically hinders the Nup88 antibody directed against residues 314-425 to react with Nup88.

In an effort to extract the antibody epitope, we used an alternative fixation method with methanol instead of formaldehyde to precipitate the proteins. Formaldehyde fixation crosslinks the proteins with very little extraction, and possibly mutilates or sterically blocks an epitope. Methanol, in contrast, does not crosslink the proteins but precipitates the proteins what might lead to an extraction of the hidden Nup88 epitope. Indeed, in methanol-fixed HEK cells transfected with GFP-lamin A and immunostained with the Nup88 antibody recognizing the residues 314-425 epitope, no reduction of the Nup88 signal is observed anymore (Figure S7.12C), further supporting the notion that the reduction in Nup88 staining is due to epitope masking. These results demonstrate that an ectopic expression of lamin A is efficiently masking the Nup88 antibody epitope at residues 314-425 and moreover, confirming the *in vitro* solution binding data showing that the interaction site of Nup88 with lamin A lies in the central N-terminus of the

protein (Figure 3.2C), which corresponds to the predicted N-terminal β -propeller domain (Schwartz, 2005).

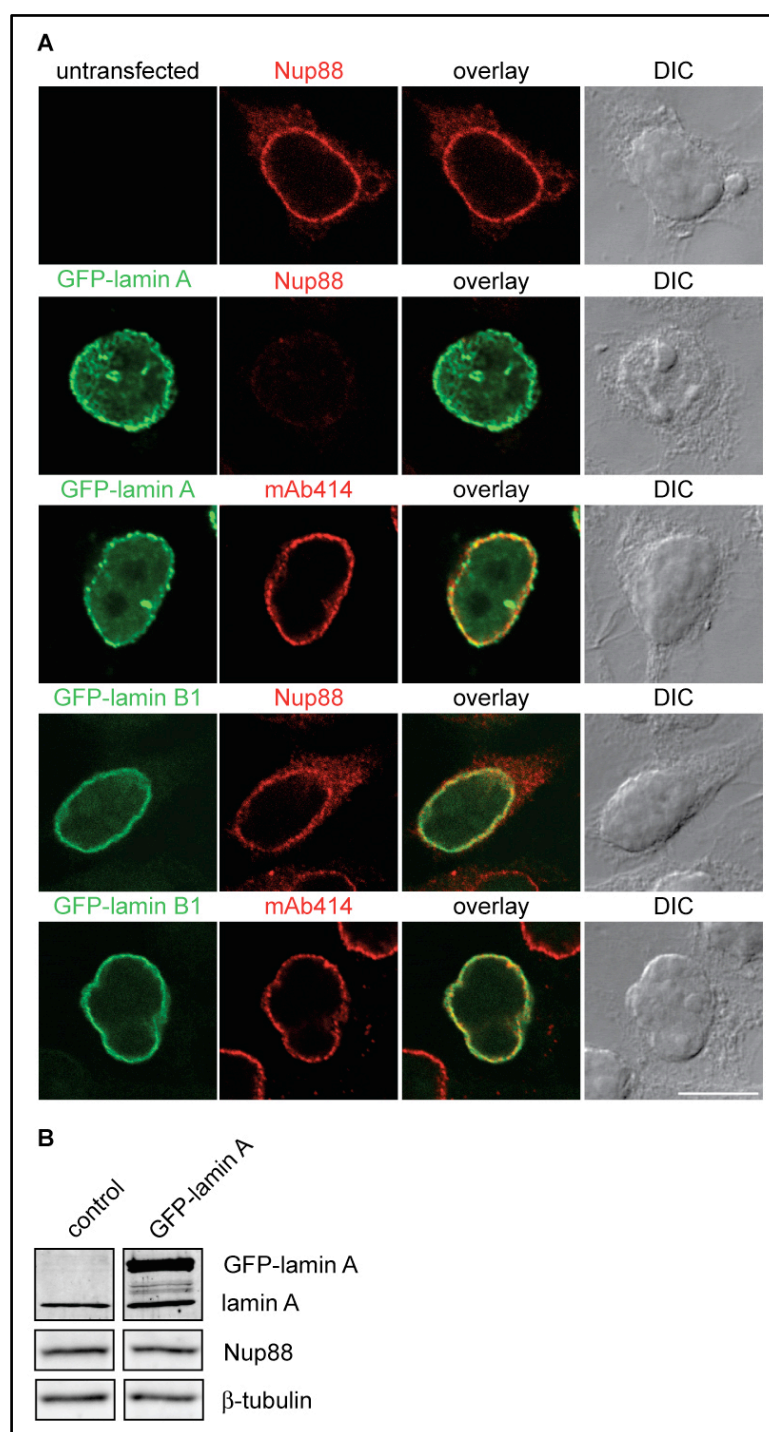


Figure 3.4: Overexpression of GFP-lamin A is masking an antibody epitope within the N-terminus of Nup88.

(A) HEK cells transfected with GFP-lamin A or GFP-lamin B1 were prepared for immunofluorescence 24 hours after transfection using monoclonal antibodies directed against residues 314-425 of Nup88 or the FXFG-repeat containing nucleoporins (mAb414). Cells

transfected with GFP-lamin A, but not with lamin B1, showed a decreased signal for Nup88 staining, but not for staining with monoclonal antibody mAb414. Scale bar, 10 μ m. **(B)** Protein levels of Nup88 were analyzed in HEK cells transfected with GFP-lamin A or mock transfected control cells. No changes in protein levels of Nup88 were observed when compared with β -tubulin.

3.3.5 Nup88 interaction with lamin A is lost in presence of the EDMD-associated R453W mutant and the FPLD-associated R482W mutant lamin A

To further characterize the interaction between Nup88 and lamin A and to assert the importance of the lamin A Ig-fold for the binding, we performed solution binding assays with recombinantly expressed GST-Nup88 and GST as control and in vitro transcribed/translated and 35 S-labeled lamin A mutants. The Emery-Dreifuss muscular dystrophy-associated lamin A Ig(R453W) mutant and the Dunnigan-type familial partial lipodystrophy (FPLD)-associated mutant lamin A Ig(R482W) were used in this study, two mutations lying in the Ig-fold domain of lamin A. Furthermore, we analyzed binding with the Hutchison-Gilford progeria syndrome-associated mutant lamin A Δ 50, where 50 residues are deleted in the Ig-fold neighbored C-terminus of lamin A. Purified recombinant Nup88 fused to GST or GST as control were attached to glutathione sepharose beads and incubated with in vitro transcribed and translated 35 S-labeled lamin A mutants (Figure 3.5A). Unbound (U) and bound (B) fractions were separated on SDS-PAGE, transferred to a PVDF membrane and analyzed by radiography (Figure 3.5A). The mutant lamin A Ig(R453W) and lamin A Ig(R482W) were not binding to GST-Nup88 or GST, whereas the HGPS-associated lamin A Δ 50 mutant was still binding to Nup88 (Figure 3.5A). The loss of interaction of Nup88 with the two Ig-fold mutants is further highlighting the importance of the Ig-fold for the interaction between Nup88 and lamin A.

To study the interaction of Nup88 with the lamin A mutants in a cellular context, we next performed co-immunostaining experiments of GFP-lamin A(R453W), GFP-lamin A(R482W), GFP-lamin A Δ 50 and wild-type GFP-lamin A with Nup88 by indirect immunolabeling Nup88 with the monoclonal antibody recognizing the residues 314-425 in the N-terminus of Nup88 (Figure 3.5B). In contrast to the effect of wild-type GFP-lamin A, we could not observe a masking phenotype in cells overexpressing GFP-lamin A(R453W) or GFP-lamin A(R482W) (Figure 3.5B), indicating that the interaction of

Nup88 with the R453W and the R482W mutation is disrupted in vivo. However, overexpression of GFP-lamin A Δ 50 had a comparable masking effect as observed for wild-type lamin A, suggesting that GFP-lamin A Δ 50 is still able to bind Nup88 in vivo (Figure 3.5B).

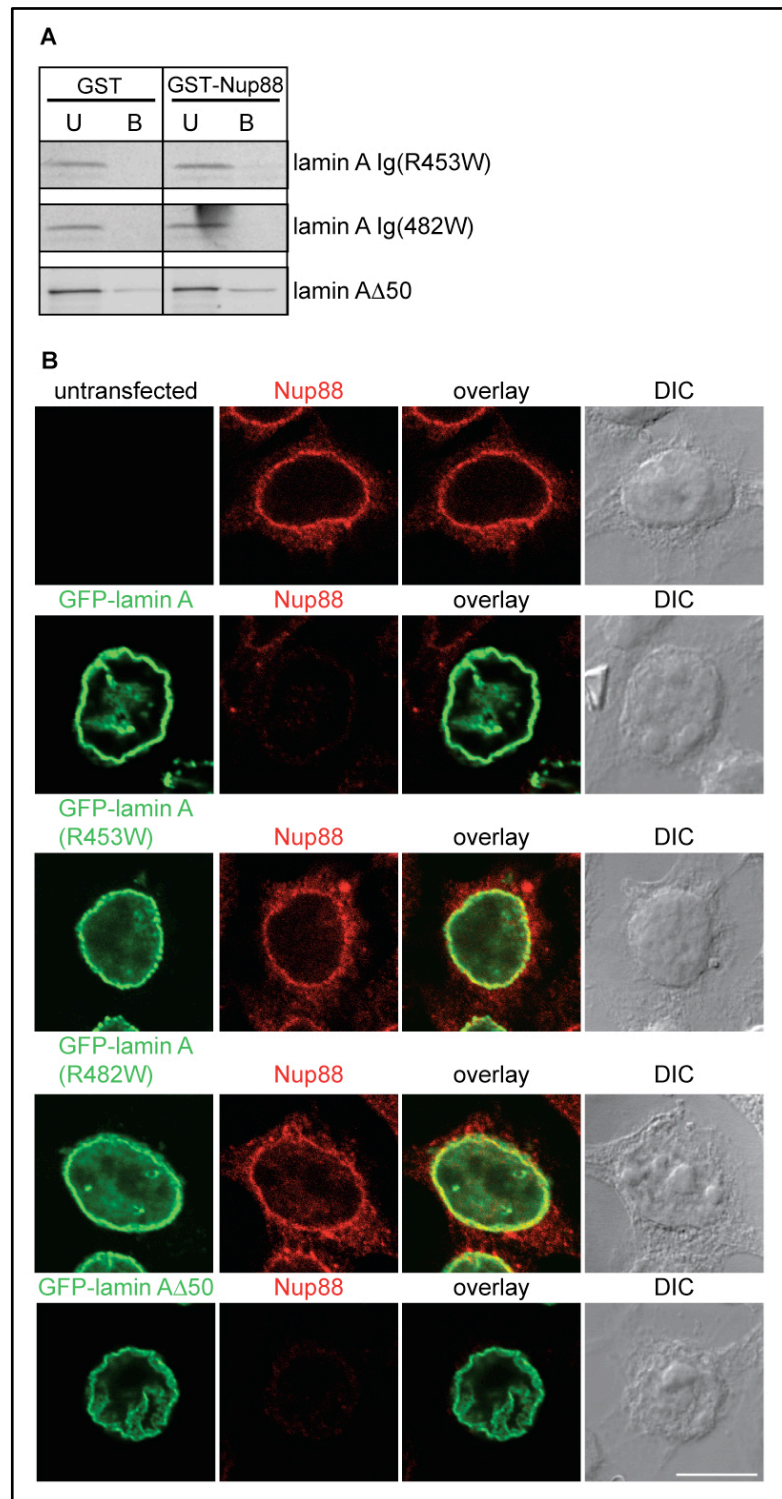


Figure 3.5: EDMD-associated lamin A(R453W) and FPLD-associated lamin A(R482W) mutants do not interact with Nup88.

(A) Bacterially expressed GST-Nup88 and GST were bound to glutathione sepharose beads and incubated with in vitro synthesized ³⁵S-labeled lamin A Ig(R453W), lamin A Ig(R482W) and lamin AΔ50. Unbound and bound fractions were analyzed by SDS-PAGE and autoradiography. The interaction of Nup88 with the lamin A (R453W) mutant as well as with the lamin A Ig(R482W) mutant was lost, whereas lamin AΔ50 was able to bind Nup88. (B) HEK cells transfected with GFP-lamin A(R453W), GFP-lamin A(R482W), GFP-lamin AΔ50 or wild-type GFP-lamin A were prepared for immunofluorescence 24 hours post transfection using monoclonal antibodies directed against residues 314-425. The epitope masking phenotype, as it is observed in cells transfected with wild-type GFP-lamin A, is lost in cells expressing the GFP-tagged lamin A(R453W) and lamin A(R482W) mutants, whereas it is still observed in cells expressing GFP-lamin AΔ50. Scale bar, 10 μm.

3.4 Discussion

In this work, we report that lamin A is a novel interaction partner of Nup88. We could show that the two proteins interact *in vitro* and *in vivo* by solution-binding, overlay and immunoprecipitation assays. We could characterize the interaction between lamin A and Nup88 insofar that it is the N-terminus of Nup88 binding to lamin A and Nup88 interaction is specifically with the lamin A Ig-fold domain, but not with the Ig-fold of lamin B1 or B2. We could show by immunogold localization studies that a pool of Nup88 is localizing to the nucleoplasmic side of the NPC. Furthermore, GFP-lamin A is masking an antibody epitope of Nup88 in immunofluorescence assays, supporting the finding that the two proteins interact *in vivo*. However, interaction of Nup88 with lamin A is lost when mutations in the Ig-fold are present, supporting the notion that the lamin A Ig-fold domain is mediating the interaction with Nup88. Taken together, our data indicate that, besides being involved in building the cytoplasmic Nup88/Nup214 subcomplex, Nup88 is localizing to the nucleoplasmic side of the NPC, where it provides a novel connection between the NPC and the nuclear lamina by interacting with lamin A.

3.4.1 Lamin A is a novel interaction partner of Nup88

By biochemical analysis, we have shown for the first time that the nucleoporin Nup88 and the nuclear intermediate filament protein lamin A interact *in vivo* and *in vitro* (Figure 3.1 and Figure 3.2A-D). The observed interaction seems to be specific for nuclear lamin A, since Nup88 is not interacting with the cytoplasmic intermediate filament protein vimentin in a blot overlay assay (Figure 3.2B). Furthermore, Nup88 interacts specifically with the lamin A Ig-fold but not with the Ig-folds of lamin B1 and B2, what makes Nup88 a novel A-type lamin binding partner (Figure 3.2D). We find that the interaction with lamin A is mediated by the N-terminal domain of Nup88, which folds into a predicted β -propeller (Figure 3.2C). It is therefore possible that the C-terminal coiled-coil domain of Nup88 mediates its interaction with an unknown partner on the nuclear side of the NPC, as it is observed for the cytoplasmic interaction with Nup214 (Bastos et al., 1997; Fornerod et al., 1997b), whereas the N-terminal β -propeller binds to lamin A.

Using RNA interference to deplete endogenous lamin A, we find that reducing the cellular levels of lamin A produced a corresponding decrease in Nup88 protein levels in an immunoblot analysis (Figure S7.13A). Nup88 protein levels were reduced for 40% percent in cells treated with siRNA against lamin A compared to Nup88 protein levels in cells treated with control siRNA (cyclophilin B) or untreated cells (Figure S7.13B). A likely explanation for this observation is that reduced lamin A protein levels lead to unstable free Nup88 that is then more rapidly degraded. Similar results have been observed for other protein complexes, where the stability of the complex is decreased by depletion of individual members (Bernad et al., 2004). However, it cannot be excluded that the observed reduction of Nup88 protein levels is due to a change in transcription caused by reduced lamin A levels, as lamin A has been implicated in transcriptional regulation (Andres and Gonzalez, 2009).

Nup88 has been implicated in CRM1-mediated export and lamin A is imported into the nucleus in an importin α/β dependent manner. However, we could rule out an nucleocytoplasmic transport-associated interaction of Nup88 with lamin A, as CRM1, importin α and β from the reticulocyte lysate did not associate with the Nup88-lamin A complex in solution binding assays, suggesting a new type of interaction apart from Nup88 transport function (Figure S7.9).

3.4.2 Nup88 is localizing to both sides of the NPC

Consistent with previous localization experiments, we localized the C-terminus of Nup88 to the cytoplasmic side of the NPC, whereas for the N-terminus, we observed a cytoplasmic and nuclear localization pattern (Figure 3.3). It is rather unlikely that Nup88 is anchored to the cytoplasmic side by its C-terminus and that the N-terminus can reach through the NPC to the nucleoplasmic side, as Nup88 does not contain any FG-repeat domain found in nucleoporins which are more flexible and can reach through the pore (Fahrenkrog et al., 2002; Paulillo et al., 2005). The difference in N- and C-terminal location lies more likely in their epitope accessibility so that the C-terminus is more readily accessible on the cytoplasmic side of the NPC, but hidden for an antibody access on the nuclear side, whereas the N-terminus seems to be similar accessible on both sides. The idea that a pool of Nup88 is cytoplasmic and a pool of Nup88 resides at the nuclear

ring moiety of the NPC is consistent with the idea that Nup88 interacts with lamin A on the nuclear side of the NPC. Notably, another lamin interacting nucleoporin, Nup153, is located at the nuclear ring moiety, and the location therefore appears to be a good prerequisite for lamin A interaction (Fahrenkrog et al., 2002; Smythe et al., 2000).

Nup153 depends on the nuclear lamina for its recruitment to the NE and the nuclear lamina itself is involved in NPC assembly and spacing within the NE (Smythe et al., 2000; Walther et al., 2001). Therefore, it is feasible that Nup88 as a novel lamin A-binding protein plays a role in maintaining nuclear architecture. However, lamin A exists in at least two forms in the cell: in a filamentous form incorporated in the nuclear lamina, and in a more soluble form distributed throughout the nucleoplasm. Hence, a possibility could be that Nup88 interacts with the soluble fraction lamin A, which is further supported by the idea that only soluble lamin A co-precipitated with the Nup88 antibodies in the immunoprecipitation experiment, as the immunoprecipitation conditions we used in our experiment seem to extract more the soluble lamins than the lamina filaments (Moir et al., 2000b; Muralikrishna et al., 2004). Further indication for this scenario provides the finding that Nup88 interacts with lamin A and LAP2 α in a trimeric complex in a GST-solution binding assay (Lussi et al., data not shown). LAP2 α is a known interaction partner of soluble nucleoplasmic lamin A. Future studies will be directed towards understanding the nature and function of the interaction between Nup88 and lamin A.

Until now, it is unclear which binding partner Nup88 possesses within the nuclear side of the NPC. A putative nuclear binding partner is Nup98, as Nup98 localizes to both sides of the NPC and furthermore, it was shown to interact with Nup88 (Griffis et al., 2003). Moreover, it was shown that overexpression of GFP-Nup98 leads to active relocation of Nup88 into the nucleus, suggesting an import mechanism similar to Nup96, where Nup98 has been described to be responsible for the import of Nup96 into the nucleus, after which Nup96 is incorporated into the nucleoplasmic side of the NPC (Fontoura et al., 1999). A similar mechanism could be imagined for Nup88.

3.4.3 Nup88 interaction is lost with disease-associated lamin A Ig-fold mutants

Characterization of the interaction between Nup88 and lamin A showed that Nup88's N-terminus is required to interact with lamin A, and that it is the Ig-fold domain of lamin A mediating the binding to Nup88 (Figure 3.2C and D). Many laminopathy-associated mutations were identified within the Ig-fold domain of lamin A (Worman and Bonne, 2007). Here, we examined the nature of interaction between Nup88 and two Ig-fold-related mutants, lamin A(R453W) and (R482W) causing Emery-Dreifuss muscular dystrophy and Dunnigan-type lipodystrophy, respectively, and a mutant affecting the very C-terminus of lamin A leading to Hutchison-Gilford progeria syndrome, lamin A Δ 50. Our results show that the interaction of Nup88 with the Ig-fold-related mutations is abrogated, whereas the lamin A Δ 50 mutant is still able to bind Nup88 in vitro and in vivo (Figure 3.5). This implicates that the overall Ig-fold structure, and more specifically the site around R482W, which has been shown to be a binding site for lamin A-binding partners, is critical for Nup88 binding as well (Dhe-Paganon et al., 2002; Krimm et al., 2002). This is in agreement with the in vivo finding that wild-type lamin A and lamin A Δ 50 are masking a Nup88 epitope through interaction with its N-terminus, whereas the masking phenotype is lost with the Ig-fold mutants, and, accordingly, in vivo interaction of Nup88 with these mutants (Figure 3.4 and Figure 3.5). However, the implications of Nup88 in laminopathies concerning the abrogated interaction with the Ig-fold lamin A mutants needs to be elucidated.

3.4.4 Overexpression of GFP-lamin A is masking the Nup88 antibody epitope

We have shown that the reduced Nup88 staining observed with antibodies against the residues 314- 425 in HEK cells transfected with GFP-lamin A is due to epitope masking, rather than an absence of the protein antigen (Figure 3.4, Figure 3.5, Figure S7.11 and Figure S7.12). Antigen masking can occur as a result of conformational changes in the antigen, post-translational modification or interaction with other macromolecules that physically block the epitope. Nup88 epitope masking takes place when GFP-lamin A is overexpressed, suggesting that the abundant lamin A is binding more Nup88 than under native conditions in these cells, leading to the observed phenomenon. We could overcome this occurrence can by the use of a different epitope of

Nup88 or a different fixation method in the immunofluorescence assay (Figure S7.12). Normally, a high affinity antibody would be capable of displacing interacting proteins from an antigen by mass action. Chemical cross-linking can prevent such displacement and might explain why the masking is observed in formaldehyde-fixed samples but not in methanol-fixed samples. Interestingly, the masking phenotype is lost with the lamin A(R453W) and the lamin A(R482W) mutant, suggesting that the interaction between the two proteins is lost *in vivo*, strengthening our *in vitro* findings that interaction between Nup88 and the lamin A Ig(R453W) and lamin A Ig(R482W) mutants is abolished in solution binding assays and confirming that the Ig-fold is crucial for Nup88 binding *in vitro* and *in vivo* (Figure 3.2 and Figure 3.5).

Altogether, with this work on the interaction of Nup88 and lamin A, we provide evidence for a novel link between the NPC and the nuclear lamina. It will be interesting to determine the functional significance of this interaction, and its pathological implications in laminopathies.

3.5 Materials and Methods

3.5.1 Preparation of nuclei from HeLa cell suspension cultures by osmotic swelling

HeLa S3 cells were grown in suspension culture and harvested by centrifugation at 600g for 5 min. The pelleted cells were washed in 5 volumes of prechilled Earle's balanced salt solution. The pelleted cells were then resuspended in 10 volumes of RSB buffer (0.01 M NaCl, 1,5 mM MgCl₂, 0.01 M Tris-HCl, pH 7.4) and incubated for 10 min on ice. Cells with swollen cytoplasm were homogenized in a prechilled glass Douncer and examined in the phase contrast microscope. The homogenized cell suspension with a free nuclei: intact cell ratio of 9 or greater was centrifuged at 1000g for 3 min to pellet the nuclei. The nuclear pellet was washed in 10 volumes of RSB.

3.5.2 Cell culture and transfections

HEK cells were grown in Dulbecco's modified Eagle's medium (DMEM) supplemented with 10% fetal bovine serum (FBS) plus penicillin and streptomycin. Cells were transfected using TransIt®-293 transfection reagent (Mirus Bio LLC, Madison, USA) following the instructions of the manufacturer.

A stable cell line based on HEK cells was generated expressing a myc-tagged Nup88 upon addition of tetracycline to the medium (Invitrogen). Nup88-myc HEK cells grown in the absence of tetracycline expressed only endogenous Nup88. Upon addition of 1 µg/ml tetracycline to the medium, the cells express Nup88-myc as analyzed by immunofluorescence microscopy and immunoblot (Figure S7.11A, upper panel and B).

3.5.3 Constructs

N-terminally tagged GST-Nup88 was cloned into NcoI/KpnI cut pGEX-CS vector (Amersham-Pharmacia, Little Chalfont, England). N-terminally tagged GFP-lamin A and GFP-lamin B1 were kindly received from Prof. Robert D. Goldman (University of Chicago). The pET-lamin A Ig was constructed with HindIII and XhoI restriction sites. The lamin A Ig(R453W) and GFP-lamin A(R453W) constructs were made by Dr. Teba Al-Haboubi by site-directed mutagenesis with primers (5'- GAG GGC AAG TTT GTC

TGG CTG CGC AAC AAC TCC) and (3'- (GGA GTT GTT GCG CAG CCA GAC AAA CTT GCC CTC) on pET-lamin A Ig and pEGFP-lamin A and the lamin A Ig(R483W) and GFP-lamin A(R482W) with primers (5'-CCC TTG CTG ACT TAC TGG TTC CCA CCA AAG TTC) and (3'-GAA CTT TGG TGG GAA CCA GTA AGT CAG CAA GGG) on pET-lamin A Ig and pEGFP-lamin A. The pET-lamin AΔ50 and pEGFP-lamin AΔ50 were kindly received from Harald Herrmann (German Research Center, DKFZ, Heidelberg).

3.5.4 Antibodies

The polyclonal antibody against the residues 27-45 of human Nup88 (1:1000 for immunofluorescence) was kindly provided by Prof. Ulrike Kutay (ETH, Zürich) and the polyclonal anti-lamin A antibody (1:500) was kindly received from Prof. Robert D. Goldman. The monoclonal antibodies against the amino acids 314-425 of human Nup88 (1:500, BD Biosciences, Pharmingen) and against the amino acids 509-741 (Novocastra Laboratories, Newcastle) were used in this study. Further primary antibodies were the monoclonal antibodies mAB414 (1:2000; Covance, Berkely, CA), anti-β tubulin (1:2000; Chemicon, Billerica, MA), anti-importin α (1:1000; Sigma Aldrich) and anti-importin β (1:1000; BD Biosciences, Pharmingen). Secondary antibodies include anti-mouse IgG-Alexa 568, anti-rabbit IgG-Alexa 488 and anti-rabbit IgG-Alexa 568 from Molecular Probes (Paisley, UK) and used 1:1000.

3.5.5 Immunofluorescence

Cells were grown on poly-lysine coated glass coverslips and fixed either in 2% formaldehyde for 15 min or - 20°C methanol for 5 min, washed three times for 10 min with PBS, and permeabilized with PBS containing 1% bovine serum albumin (BSA) and 0.2% Triton X-100 for 5 min on ice. Next, the cells were washed three times for 10 min in PBS containing 1% BSA and incubated with the appropriate primary antibodies for 1 hour, washed three times in PBS containing 1% BSA and incubated with the appropriate secondary antibodies for 1 hour, washed 4x 10 min with PBS, mounted with a drop of Mowiol and stored at 4°C until viewed. Cells were viewed using a confocal laser-scanning microscope (Leica TCS NT/SP5, Leica, Vienna, Austria). Images were recorded

using the microscope system software and processed using Adobe Photoshop (Adobe Systems, Mountain View, CA, USA).

3.5.6 Gel electrophoresis and immunoblotting

Cells were resuspended in lysis buffer containing 50 mM Tris-HCl pH 7.8, 150 mM NaCl, 1% Nonidet P-40, and protease inhibitor cocktail tablets (Roche, Basel, Switzerland). Sample aliquots were resolved by sodium dodecyl sulfate-polyacrylamide gel electrophoresis (SDS-PAGE; 10%). The proteins were transferred onto a PVDF membrane and the membrane was incubated in I-Block solution (Tropix, Bedford, MA) containing 0.1% Tween- 20 (blocking solution) over night at 4°C, then incubated in blocking solution containing a primary antibody directed against either Nup88 (1:800) or anti- β -tubulin (1:1000) for 1 hour followed by washing 3x with PBS containing 0.1% Tween-20. The membrane was then incubated in the dark with anti-mouse IRDye 800 (1:10000; LI-COR, Biosciences, NE, USA) in blocking solution. Images were recorded using the Odyssey infrared imaging system and analyzed by the systems software program (LI-COR, Biosciences, NE, USA).

3.5.7 Colloidal blue staining

Colloidal blue staining (Invitrogen, Pailsey, UK) was performed according to manufacturer's instructions.

3.5.8 Immunoprecipitation

Subconfluent HeLa cells (3×10^6) were trypsinized, washed with PBS and resuspended in 160 μ l lysis buffer (50 mM Tris-HCl, pH 7.4, 250 mM NaCl, 0.1 % Triton X-100, 2 mM EDTA- Na_2 , 10% glycerol and protease inhibitor (Thermo Scientific)), vortexed and incubated for 10 min at 37°C. The cells were pelleted at 16,000 g for 10 min and the supernatant was transferred to a fresh tube. The supernatant was cleared with 20 μ l of protein G-agarose beads (Santa Cruz) and incubated for 30 min at 4°C, centrifuged at 1000 g for 30 sec at 4°C, and the supernatant was transferred to a fresh tube and 1 μ g mouse monoclonal anti-Nup88 antibody was added and incubated for 2 hours on ice. 40 μ l prewashed protein G- agarose slurry was added to the lysate and

incubated at 4°C on a rocker platform for 1 hour. The immunoprecipitate was collected by centrifugation at 1000 g for 30 sec at 4°C and the supernatant was carefully removed and kept to analyze as unbound fraction. The pellet was washed 3x with lysis buffer, resuspended in electrophoresis sample buffer, boiled at 95°C for 5 min and subjected to electrophoresis and Western blotting.

3.5.9 In vitro transcription and translation

Nup88, Nup88 (1-550) and Nup88 (551-741), lamin A, lamin A (386-548), lamin A Ig, lamin A Ig (R453W), lamin A Ig (R482W), lamin AΔ50, lamin B1 Ig and lamin B2 Ig were obtained by in vitro transcription and translation with the TNT-coupled reticulocyte lysate system (Promega, Madison, USA) in the presence of residue L-[³⁵S]methionine-cysteine (Amersham Bioscience, Uppsala, Sweden) following the instructions of the manufacturer.

3.5.10 Expression of recombinant Nup88 and lamin A

GST, GST-Nup88 and lamin A-his were expressed in *E. coli* BL21 (DE3) cells. Protein expression was induced with 0.5 mM isopropyl-beta-D-thiogalactopyranoside (IPTG) for 5 hours at 25°C. Cells were lysed by sonication (Branson Digital Sonifier, Branson Ultrasonics Corporation, Danbury, CT, USA) in 2xPBS containing 1% Triton X-100 and protease inhibitor (Thermo Scientific). Lysed cells were spun at 60,000 g for 1 hour, and the cleared lysates were stored at -80°C.

3.5.11 In vitro binding assays

The in vitro interaction between Nup88 and lamin A was tested by binding GST and GST-Nup88 to glutathione-sepharose beads (Amersham Bioscience, Uppsala, Sweden) or lamin A-his to Ni-sepharose 6 fast flow beads (GE Healthcare, formerly Amersham Biosciences, Sweden) for 1 hour at 4°C. Beads were washed twice with 2xPBS containing 1% Triton X-100 and protease inhibitor (Thermo Scientific). In vitro translated Nup88, Nup88 (1-550) and Nup88 (551-741), lamin A, lamin A (386-548), lamin A Ig, lamin A Ig (R453W), lamin B1 Ig and lamin B2 Ig were allowed to bind for 16 to 20 hours at 4°C. After binding, the beads were washed twice in 2xPBS containing

1% Triton X-100 and protease inhibitor (Thermo Scientific) followed by two washes in 2xPBS. Samples were eluted in 50 μ l SDS sample buffer, analyzed on a 10% SDS polyacrylamide gel and detected by autoradiography.

3.5.12 Expression and purification of lamin A and vimentin

Purified human vimentin in urea was a kind gift of Prof. Harald Herrmann (German Cancer Research Center (DKFZ), Heidelberg, Germany). Purified human lamin A in urea was a kind gift of Prof. Robert D. Goldman (Northwestern University, Chicago, IL).

3.5.13 Blot-overlay assay

Purified vimentin and lamin A were separated on SDS-PAGE, transferred to a PVDF membrane, blocked with I-block o/n at 4°C and then incubated with in vitro transcribed/translated ³⁵S-labeled Nup88. After washing, binding of Nup88 was visualized by autoradiography.

3.5.14 Immuno-EM

Mature (stage 6) oocytes were surgically removed from female *Xenopus laevis*, and their nuclei were isolated as described (Pante et al., 1994). Colloidal gold particles, ~8-nm in diameter, were prepared by reduction of tetrachloroauric acid with sodium citrate in the presence of tannic acid and antibodies were conjugated to colloidal gold particles as described (Baschong and Wrigley, 1990). Isolated nuclei were labeled with monoclonal Nup88 antibodies (BD Biosciences, Pharmingen; Novocastra Laboratories, Newcastle) as described previously and labeled nuclei were fixed and processed for EM as described (Fahrenkrog et al., 2002; Paulillo et al., 2005). EM micrographs were recorded on a Phillips CM-100 transmission electron microscope equipped with a CCD camera.

4

The nucleoporin Nup88 is a regulator of the lamin A-LAP2 α complex

Yvonne C. Lussi¹ and Birthe Fahrenkrog^{1,2,□}

¹M.E. Müller Institute for Structural Biology, Biozentrum, University of Basel, Klingelbergstrasse 70, 4056 Basel, Switzerland

²Laboratoire du Biologie du Noyau, Institut de Biologie & de Médecine Moléculaire, Université Libre de Bruxelles, Rue Profs Jeener & Brachet, 12, B-6041 Charleroi, Belgium

Running title: Nup88 regulates lamin A-LAP2 α complex

Keyword: Nup88; nuclear pore complex; lamin A; LAP2 α ; pRb; G1 checkpoint

4.1 Abstract

Nuclear pore complexes (NPCs) are embedded in the nuclear envelope (NE) and mediate bidirectional nucleocytoplasmic transport. Besides the control of macromolecule transport, it became evident that individual nucleoporins play important roles in other cellular processes, including cell cycle regulation. In this work, we identified the nucleoporin Nup88 as putative regulator of cell cycle progression. By pull-down experiments, we identified lamin A and LAP2 α to be in a complex with Nup88. The lamin A- LAP2 α complex was previously shown to control cell proliferation by binding to the retinoblastoma protein (pRb), and repressing the expression of pRb/E2F-dependent cell cycle regulatory genes important for G1-S phase transition. Misregulation of the lamin A- LAP2 α complex is leading to impaired pRb repressor activity and hyperproliferation of mice fibroblasts. Here, we found that Nup88 overexpression interferes with the normal distribution of lamin A and LAP2 α in G1, furthermore disrupting the lamin A- LAP2 α complex. Consistently, we show that Nup88 overexpression leads to an inefficient cell cycle arrest in G0 by serum starvation and slightly accelerates cell cycle progression from G1 to S. In contrast, stable downregulation of Nup88 by RNA interference does not affect the association of the lamin A- LAP2 α complex, but delays progression from G1 to S phase in a synchronized cell culture. The effects of Nup88 on cell cycle progression might be relevant for the Nup88 overexpression phenotype observed in many human tumors.

4.2 Introduction

Nuclear pore complexes (NPCs) are macromolecular structures that are embedded in the double membrane of the nuclear envelope (NE) and mediate bidirectional nucleocytoplasmic transport. The vertebrate NPC consist of about 30 nucleoporins (Nups), one of which is Nup88. In a previous study, we have shown that Nup88 is localized to both the cytoplasmic and nuclear side of the NPC, where it interacts with distinct subcomplexes; the Nup214 subcomplex on the cytoplasmic side and lamin A on the nuclear side (Bernad et al., 2004) (Lussi et al., submitted). Nup88 was found to be overexpressed in a wide range of human tumors and Nup88 levels have been correlated to tumor development and aggressiveness (Agudo et al., 2004; Emterling et al., 2003; Gould et al., 2000; Gould et al., 2002; Martinez et al., 1999; Zhang et al., 2002; Zhang et al., 2007). Although the exact function of Nup88 in tumorigenesis remained elusive, it was suggested that Nup88 might play a role in proliferation, as it is not only expressed during tumorigenesis but also in fetal tissue of the lung and during embryological differentiation in chicken embryos (Gould et al., 2000; Schneider et al., 2004).

The nuclear lamina is a major structural element of the NE and is closely associated with the inner nuclear membrane (INM) and attached to the periphery of NPCs and to chromatin (Aaronson and Blobel, 1975; Fawcett, 1966; Patrizi and Poger, 1967). The nuclear lamina is involved in nuclear architecture, NPC spacing and was found to be involved in many cellular processes, including gene regulation (Hutchison, 2002). The major constituents are type V intermediate filament (IF) proteins, the nuclear lamins, which can be classified in A- and B-type lamins, according to their homology. A-type lamins are also found distributed throughout the nucleoplasm and have been implicated in chromatin organization (Gruenbaum et al., 2005), DNA replication (Moir et al., 2000a), RNA Pol II-dependent transcription (Spann et al., 2002) and gene regulation (Bridger et al., 1993; Hozak et al., 1995).

The organization of lamins at the nuclear periphery as well as within the nucleoplasm is influenced by numerous lamin-binding proteins (Dorner et al., 2007; Schirmer and Foisner, 2007; Wagner and Krohne, 2007). One of those is the lamina-associated polypeptide 2 α , LAP2 α , which is found in a stable complex with lamin A/C in the nucleoplasm (Dechat et al., 2000a). LAP2 α is a splice variant of the *LAP2* gene, from

which up to six isoforms exist in humans (α , β , γ , δ , ϵ and ζ) (Berger et al., 1996; Foisner and Gerace, 1993; Harris et al., 1994). LAP2 proteins have a closely related N-terminus, but the C-terminus in LAP2 α is structurally and functionally unique: it lacks a membrane-spanning domain found in the other LAP2 proteins, and is, as a result, distributed diffusely throughout the interphase nucleus (Dechat et al., 1998). LAP2 α is targeting a pool of lamin A to the nucleoplasm, where the two proteins form a stable complex (Dechat et al., 2004; Dechat et al., 2000a; Markiewicz et al., 2002).

The lamin A- LAP2 α complex was previously shown to control cell proliferation by binding to the hypophosphorylated form of the retinoblastoma protein (pRb) (Dorner et al., 2006; Mancini et al., 1994; Markiewicz et al., 2002; Mittnacht and Weinberg, 1991; Ozaki et al., 1994), which is the predominant form of pRb in G1 phase of proliferating cells or in G0 of resting cells. Hypophosphorylated Rb is tethered in the nucleus and blocks transition into S phase by inhibiting the activity of E2F transcription factors that are essential for the expression of S phase-specific genes (Bracken et al., 2004; Classon and Harlow, 2002; Dyson, 1998; Kaelin, 1999). Hyperphosphorylation of Rb during late G1 phase releases it from nuclear tethers, which in turn releases and derepresses E2F and leads to transition through S phase. Misregulation of the lamin A- LAP2 α complex impairs pRb repressor activity and leads to hyperproliferation of mice fibroblasts, failure in efficient cell cycle arrest or impaired myoblast differentiation (Frock et al., 2006; Nitta et al., 2006; Van Berlo et al., 2005).

We have recently identified the nucleoporin Nup88 as novel lamin A interacting partner. In this study, we further identified the lamin A-binding protein LAP2 α to be associated with Nup88. The lamin A-LAP2 α complex is known to repress pRb and to regulate G1-S transition. We then investigated whether Nup88 affects the lamin A- LAP2 α complex and cell cycle progression. We can show that overexpression of Nup88 leads to a disruption of the lamin A-LAP2 α complex, leading to an inefficient G0/1 arrest and accelerated progression through G1-S transition in a human cell culture. Knockdown of Nup88 leaves the lamin A- LAP2 α complex intact, but, however, slows down S-phase progression significantly, indicating a hyperrepression of pRb. This data suggest that Nup88 regulates lamin A- LAP2 α repressor activity by influencing the stability of the

lamin A-LAP2 α complex. Together, we identified the nucleoporin Nup88 as a novel regulator of the lamin A- LAP2 α complex and of cell cycle progression.

4.3 Results

4.3.1 Nup88 associates with lamin A and LAP2 α

In a previous study, we have localized Nup88 on the cytoplasmic and nuclear side of the NPC and identified lamin A as novel interaction partner of Nup88 on the nuclear face of the NPC (Lussi et al., submitted). In order to elucidate the functionality of this interaction, we aimed to identify other proteins in this complex. For this experiment, recombinant glutathione-S-transferase (GST)-tagged Nup88 fusion protein or GST alone was expressed in *E. coli*, purified, immobilized on glutathione sepharose beads and incubated with a lysate of isolated HeLa S3 nuclei. Proteins that bound GST-Nup88 or GST were separated on SDS-PAGE and detected by immunoblot analysis (Figure 4.1). We confirmed that lamin A co-purified with GST-Nup88, but not with GST (Figure 4.1) (Lussi et al., submitted). Furthermore, we found that the lamina associated protein 2 alpha, LAP2 α , an interaction partner of lamin A, coprecipitated with GST-Nup88, but not with GST alone (Figure 4.1). Therefore, the three proteins Nup88, lamin A and LAP2 α can build a complex in vitro.

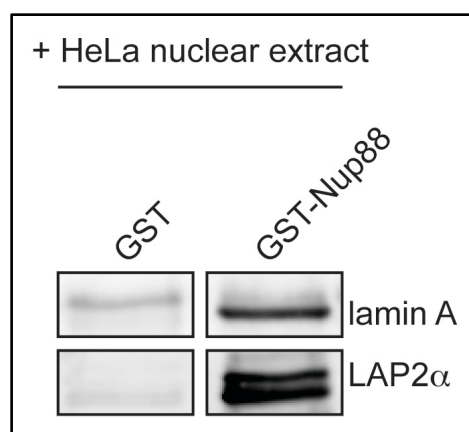


Figure 4.1: Nup88 associates with lamin A and Lap2 α .

HeLa S3 nuclei lysate was incubated with purified, recombinant glutathione-S-transferase (GST)-tagged Nup88 fusion protein or GST alone immobilized on glutathione sepharose beads. Proteins bound to GST-Nup88 or GST were separated on SDS-PAGE and detected by immunoblot analysis with polyclonal lamin A antibody or polyclonal LAP2 α antibody.

4.3.2 Nup88 overexpression disrupts the lamin A-LAP2 α complex and accelerates G1 to S transition

The lamin A-LAP2 α complex binds hypophosphorylated pRb in the nucleus and it is suggested that nucleoplasmic lamin A-LAP2 α complexes may regulate its repression activity on the E2F family transcription factors during G1 phase of the cell cycle by either increase pRb's repressor function or delay its deactivation (Dorner et al., 2006; Dyson, 1998; Markiewicz et al., 2002; Nitta et al., 2006). To analyze if the overexpression of Nup88 influences the stability of the lamin A- LAP2 α complex, we performed co-immunoprecipitation experiments with lysates of HEK cells overexpressing Nup88-myc in a tetracycline inducible manner or of control cells (Figure 4.2A). Overexpression of Nup88-myc was assessed by immunoblotting of cell lysates using an anti-myc antibody (Figure 4.2A). We immunoprecipitated lamin A/C from lysates of HEK cells that were treated with tetracycline (tet) to overexpress Nup88-myc (+ tet) or from control cells (- tet) using a monoclonal lamin A/C antibody. Co-immunoprecipitation of LAP2 α was assessed by immunoblotting using a polyclonal LAP2 α antibody. As shown in Figure 4.2A, LAP2 α could be co-immunoprecipitated with LA/C in control cells, whereas it was not detectable in the co-immunoprecipitate of Nup88-myc overexpressing cells. Neither lamin A nor LAP2 α were found to bind unspecifically to the protein G-agarose beads alone (Figure 4.2A). Together, our data indicate that Nup88 overexpression abrogates the association of the lamin A-LAP2 α complex.

The lamin A-LAP2 α complex localizes to the nucleoplasm in a cell cycle dependent manner, and highest concentrations of the complex in the nucleoplasm can be found in early G1 (Naetar and Foisner, 2009). To examine the effect of ectopic Nup88 expression on the distribution of lamin A and LAP2 α during G0/1 phase of the cell cycle, we performed a co-immunostaining experiment with human telomerase immortalized primary fibroblast cells (BJ1-hTERT) transiently transfected with green-fluorescent protein (GFP)-tagged Nup88 or GFP as control. Expression of the proteins was verified by immunoblot analysis using a GFP antibody (Figure S7.14). 24 hours after transfection, the cells were arrested in G0 phase of the cell cycle by serum starvation and were indirectly labeled with antibodies against lamin A and LAP2 α (Figure 4.2B). Cell transfected with GFP showed the typical rim staining for lamin A and a diffuse lamin A

distribution within the nucleoplasm and LAP2 α was localized in patches at the nuclear periphery and in the nucleoplasm (Figure 4.2B, upper panel). Cells expressing GFP-Nup88 showed a less uniformly distribution of lamin A in the nucleoplasm and the nucleoplasmic patches of LAP2 α were significantly reduced (Figure 4.2B, lower panel). These data suggest that excess Nup88 is delocalizing lamin A and LAP2 α and possibly affecting the stability of the lamin A- LAP2 α complex *in vivo*.

To further investigate if the disrupted interaction of lamin A and LAP2 α had any impact on pRb repression and E2F-dependent cell cycle gene transcription, we performed flow cytometric analysis to determine the cell cycle distribution of cells overexpressing GFP-Nup88 or GFP. For this analysis, we utilized BJ1-hTERT cells that were transiently transfected to express GFP or GFP-Nup88 and that were arrested in G0 by serum starvation. After labeling with propidium iodide, cell cycle distribution was analyzed by flow cytometry. Interestingly, cells overexpressing GFP-Nup88 were not as efficiently arrested in G0 phase as control cells after 3 days of serum starvation. DNA flow cytometry analysis revealed that GFP-Nup88 expressing cells showed a decrease in the relative number of cells in G1 phase (61.4 to 74.5%) and an increase of cells in S phase (31.1 to 18.6%) compared to GFP expressing cells at time point 0 hours after serum addition to the growth medium (Figure 4.2C and D). Moreover, cells expressing GFP-Nup88 showed a slight but reproducible acceleration of the cell cycle, i.e. more cells in S and G2 compared to the control cells after 24 hours of serum addition (41.2% in S phase and 12.5% in G2 phase compared to 33.4% (S) and 9.2% (G2), respectively (Figure 4.2C and D). Cells were growing asynchronous after 48 h and no significant difference between GFP-Nup88 and GFP overexpressing cells was detectable (Figure 4.2C and D). Taken together, we concluded that increased GFP-Nup88 levels negatively affect the G0/1 arrest and positively affect the G1 to S phase transition. These data suggest that the disruption of the lamin A-LAP2 α complex by overexpression of Nup88 leads to an impairment of pRb repression and to an inefficient arrest in G0.

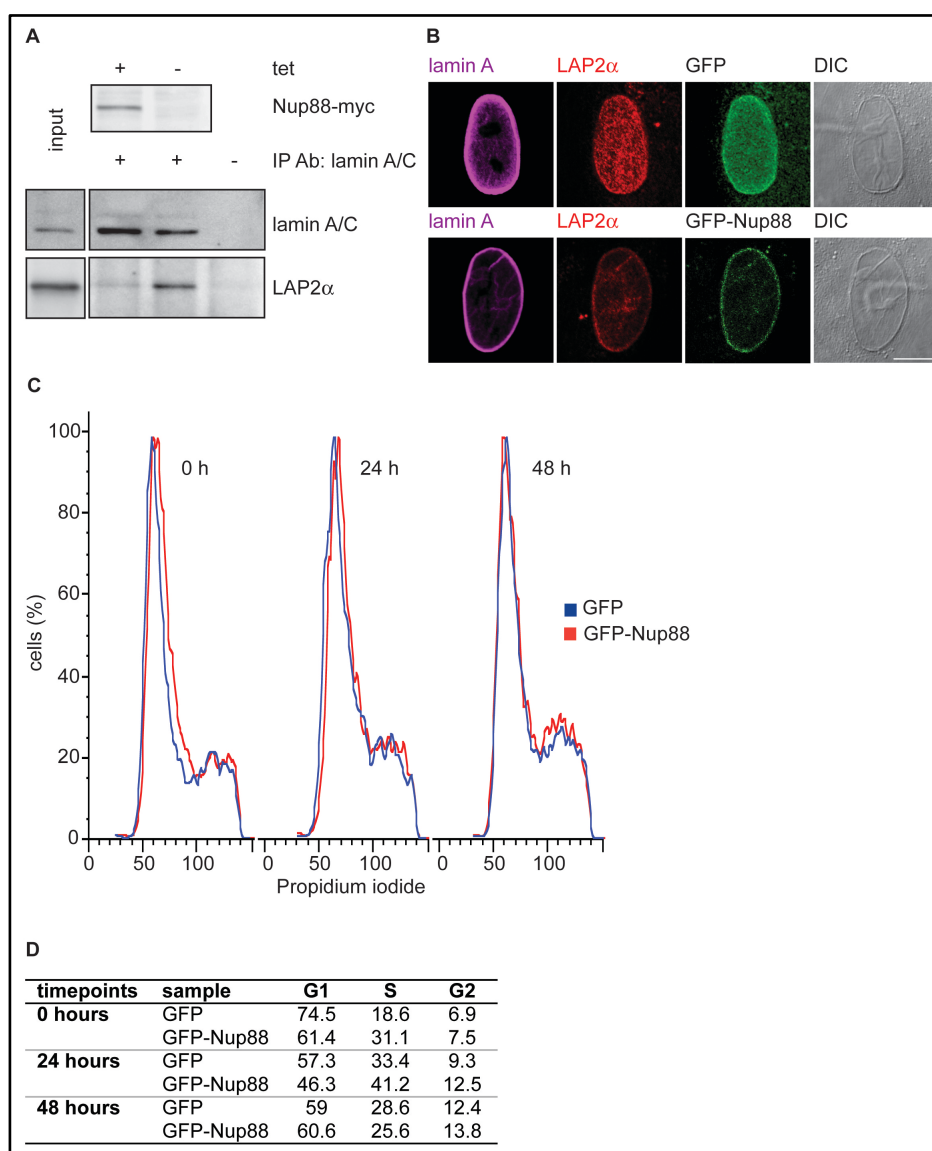


Figure 4.2: Overexpression of Nup88 disrupts the lamin A-LAP2 α complex and accelerates cell cycle progression.

(A) Lysates of HEK cells overexpressing Nup88-*myc* (I) or control cells (NI) were immunoprecipitated with monoclonal lamin A/C antibody. Lysate, unbound and precipitate fractions were analyzed by immunoblotting using monoclonal lamin A/C antibody or polyclonal LAP2 α antibody. Lysates of HEK cells overexpressing Nup88-*myc* (I) and control cells (NI) were analyzed by immunoblotting using monoclonal myc antibodies. (B) BJ1-hTERT fibroblasts were transfected with GFP-Nup88 or GFP, arrested in G0 by serum starvation and visualized by indirect fluorescence microscopy with antibodies against lamin A and LAP2 α . DNA was stained with DAPI. Scale bar, 10 μ m. (C) BJ1-hTERT cells overexpressing GFP-Nup88 or GFP were arrested in G0, labeled with propidium iodide and analyzed by flow cytometry at the indicated time points. (D) Table of cell cycle distribution of GFP-Nup88 and GFP transfected cells at indicated time points.

4.3.3 Depletion of Nup88 slows down S-phase, leaving the lamin A-LAP2 α complex intact

We next investigated the effect of depleting Nup88 on the lamin A-LAP2 α complex as well as on cell cycle progression. To do so, we depleted Nup88 from HEK 293 cells using RNA interference (RNAi) and synchronized the cells at the G1/S border by applying a double thymidine block. Transfection of HEK cells with siRNA against Nup88 resulted in a significant reduction in Nup88 protein levels as determined by immunoblotting and compared to control cells transfected with an unrelated control siRNA (cyclophilin B) at indicated time points (80% reduction of Nup88 protein levels at time point 0h, 73% at 9 and 24h, and 70% at 48 h after double thymidine block release, respectively, compared to Nup88 levels in cyclophilin B siRNA treated cells) (Figure 4.3A). Flow cytometric analysis of synchronized cells that were depleted of Nup88 or cyclophilin B and labeled with propidium iodide revealed that Nup88 depleted cells progressed significantly slower through cell cycle than the control cells (Figure 4.3B and C). At timepoint 0 hours after double thymidine block release, 84% of cells treated with cyclophilin B and 84.7% of Nup88 siRNA treated cells were arrested in G1, respectively. After 9 hours of release, cyclophilin B treated cells processed through S and G2 phase (42.7% in G1, 21.9% in S and 35.4% in G2), whereas Nup88 depleted cells progressed through S phase with a delay as compared to control cells (44% in G1, 38.7% in S and 17.3% in G2). The delay in cell cycle progression was persistent 24 and 48 hours after double thymidine block release (Figure 4.3B and C).

To analyze if Nup88 depletion had any effect on lamin A-LAP2 α complex stability, we next performed co-immunoprecipitation experiments. We immunoprecipitated lamin A/C from lysates of HEK cells transfected with siRNA against Nup88 or cyclophilin B using a monoclonal lamin A/C antibody (Figure 4.3D). Co-immunoprecipitation of LAP2 α was assessed by immunoblotting using a polyclonal LAP2 α antibody. LAP2 α was co-immunoprecipitated in control as well as in Nup88 depleted cells, indicating that Nup88 depletion had no significant influence on the stability of the lamin A-LAP2 α complex (Figure 4.3D). Neither lamin A nor Lap2 α were found to bind the protein G-agarose beads alone (Figure 4.3D).

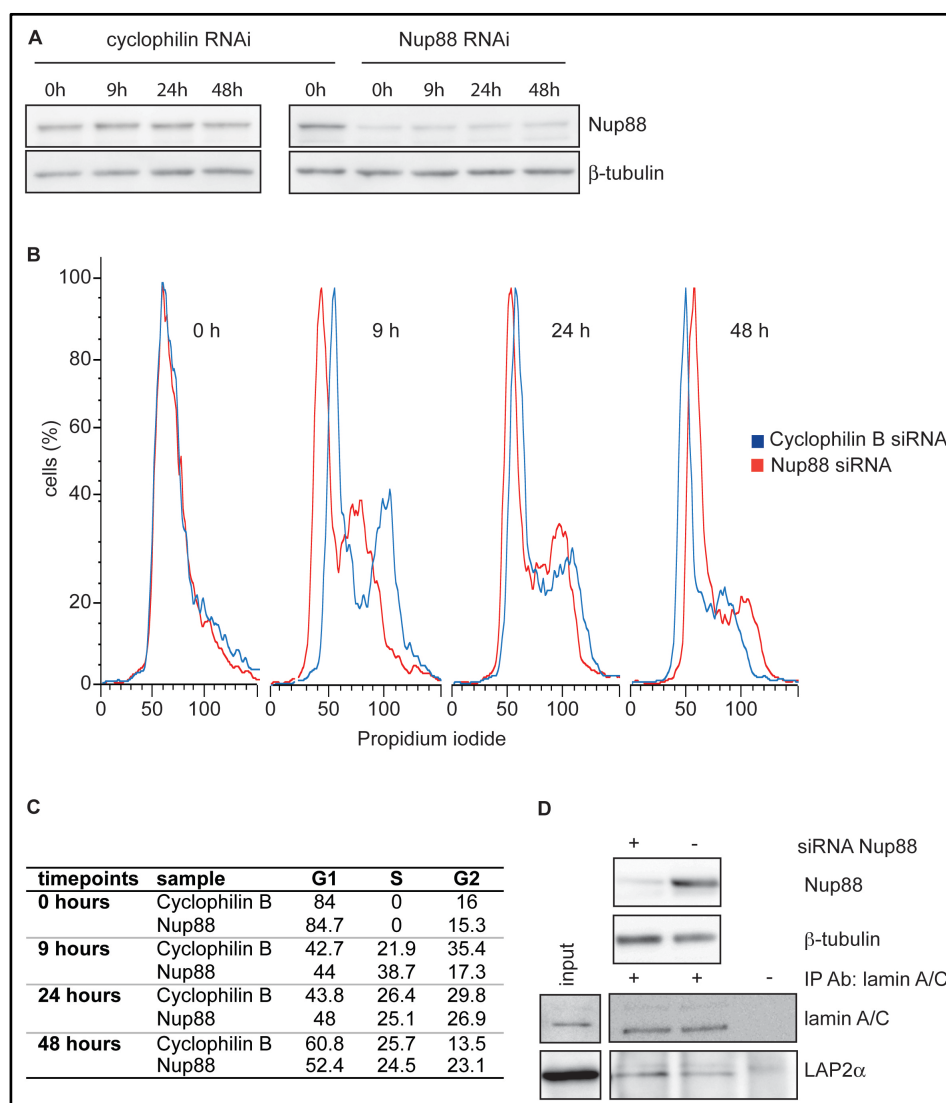


Figure 4.3: Depletion of Nup88 slows down S-phase, leaving the lamin A- LAP2 α complex intact.

(A) HEK cells were transfected with Nup88-specific siRNA or with siRNA targeting cyclophilin B and arrested in G1 by a double thymidine block. Nup88 protein levels were assessed by immunoblotting with monoclonal Nup88 and β -tubulin antibodies at the indicated time points. (B) HEK cells were transfected with siRNA against Nup88 or cyclophilin B, arrested in G1 by a double thymidine block, labeled with propidium iodide and analyzed by flow cytometry at the indicated time points. (C) Table of cell cycle distribution of siRNA treated cells at indicated time points. (D) Lysates of HEK cells transfected with siRNA against Nup88 or cyclophilin B were immunoprecipitated with monoclonal lamin A/C antibody. Lysate, unbound and precipitated fractions were analyzed by immunoblotting using monoclonal lamin A/C antibody or polyclonal LAP2 α antibody. Lysates of HEK cells transfected with Nup88 or cyclophilin B siRNA were analyzed by immunoblotting with monoclonal Nup88 and β -tubulin antibodies.

4.4 Discussion

The nucleoporin Nup88 was found to be overexpressed in a wide variety of human cancers and Nup88 protein levels were correlated with aggressiveness and tumor development, implicating Nup88 in cell proliferation. However, the exact mechanism of how Nup88 might influence proliferation was not known so far. We have shown here that Nup88 influences cell cycle progression through interaction with the lamin A-LAP2 α complex.

4.4.1 Nup88 associates with the lamin A- LAP2 α complex

In a previous study, we have shown that Nup88 is interacting with the nuclear intermediate filament protein lamin A (Lussi et al., submitted). In vitro, we have mapped the interaction domains of the two proteins in the N-terminus of Nup88 and in the Ig-fold domain of lamin A, respectively. The two proteins are interacting in vivo as well, as lamin A is co-precipitating with Nup88 antibodies and an excess of lamin A hinders the accessibility of Nup88 in human cells. However, it had remained unclear whether Nup88 interacts with filamentous lamin A or the more soluble nucleoplasmic lamin A.

To gain more insight into the nature and functional significance of the Nup88 interaction with lamin A, we have performed a GST-pull down assay with purified GST-Nup88 and HeLa S3 nuclear lysate and found that lamin A as well as LAP2 α bind to GST-Nup88, suggesting that the three proteins associate in a complex in vitro (Figure 4.1A+B). LAP2 α is a binding partner of soluble lamin A and lamin A-LAP2 α complexes can be found distributed throughout the nucleoplasm. Our finding therefore suggests that Nup88 interacts with the soluble nucleoplasmic lamin A together in a complex with LAP2 α . Whether the interaction between Nup88 and LAP2 α also takes place in vivo and whether the two proteins interact directly or indirectly needs to be further elucidated. As we localized a pool of Nup88 to the nuclear side of the NPC (Lussi et al., submitted), we speculate that the interaction of the lamin A-LAP2 α complex with Nup88 takes place at the nuclear periphery. However, it cannot be excluded that the trimeric complex exists in the nucleoplasm, since Nup88 has been observed in the nucleoplasm as well (Capelson et al.; Kodiha et al., 2008b).

4.4.2 Overexpression of Nup88 is associated with the disruption of the lamin A-LAP2 α complex and impaired G1 cell cycle arrest

To gain further insight into the cellular significance of Nup88 association with the lamin A-LAP2 α complex, we overexpressed Nup88 in HEK cells and precipitated the lamin A-LAP2 α complex with monoclonal lamin A/C antibodies. In control cells, LAP2 α was co-precipitated with lamin A/C. However, we found that overexpression of Nup88 disrupts the lamin A-LAP2 α complex, as co-immunoprecipitation of LAP2 α with lamin A was lost in these cells (Figure 4.2A). Consistently, overexpression of Nup88 in BJ1-hTERT fibroblasts leads to a reduction of nucleoplasmic lamin A and LAP2 α , indicating that the nucleoplasmic lamin A-LAP2 α complex is disrupted *in vivo* as well (Figure 4.2). Furthermore, overexpression of Nup88 weakens the serum starvation induced G0/1 arrest in BJ1-hTERT fibroblasts, consistent with the loss of the lamin A-LAP2 α complex and decreased pRb/E2F repression (Dorner et al., 2006) (Figure 4.2C and D). Taken together, our data suggest that overexpression of Nup88 leads to destabilization of the lamin A-LAP2 α complex, possibly by recruiting lamin A to the nuclear periphery, and a weakening of its repressor function at pRb/E2F gene loci, leading to advanced G1 to S progression (Figure 4.4).

4.4.3 Depletion of Nup88 slows down G1-S transition

To test whether depletion of Nup88 had opposing effects on the lamin A-LAP2 complex stability and cell cycle regulation, we performed siRNA experiments targeting Nup88. Indeed, we found that Nup88 depleted cells progressed significantly slower through S phase than control cells (Figure 4.3A+B). However, the delay in G1-S progression was not associated with a change in lamin A-LAP2 α association (Figure 4.3C). Nevertheless, the experiment performed shows a static moment of lamin A-LAP2 α association. Therefore, we hypothesize that loss of Nup88 might positively affect lamin A-LAP2 α association over time, thereby leading to a more stable complex and prolonged repression of pRb/E2F-dependent genes (Figure 4.4). It will be interesting to test if the stability of the lamin A-LAP2 α complex is changed over time in Nup88 depleted cells and if the phenotype is associated with a stronger inhibition of pRb/E2F dependent cell cycle genes.

Although the depletion experiments were performed in HEK cells, where pRb is partially inactivated through adenoviral proteins (Graham et al., 1977; Jackson et al., 2005) (Baus et al., 2003; Moran, 1993), it seems that depletion of Nup88 had a very strong negative effect on cell cycle progression, especially on G1-S transition. Whether this phenotype is linked to a stronger pRb repression on E2F-dependent cell cycle genes needs to be further elucidated by quantification of appropriate E2F target gene products, e.g. cyclin D1.

In summary, we have shown that the mislocalization of lamin A and LAP2 α caused by Nup88 overexpression is associated with a disruption of the lamin A-LAP2 α complex and accompanied by an increase in cell cycle progression in BJ1-hTERT fibroblasts. On the other hand, depletion of Nup88 from HEK cells results in delayed cell cycle progression. Altogether, we found a novel role of Nup88 in cell cycle checkpoint regulation and G1 to S transition. Here, we propose that Nup88 is a regulator of the pRb/E2F repressor complex lamin A-LAP2 α by influencing its stability and the localization of lamin A and LAP2 α . Recent literature indicates Nup88 as putative oncogene, since its overexpression in a wide variety of human tumors is correlated with tumor development and aggressiveness. In Rb-deficient cells, a decrease in differentiation potential, in addition to an increase in proliferation rates is observed (Kaelin, 1999). Therefore, it might be feasible that Nup88 overexpression in those tumors interferes with lamin A-LAP2 α -dependent E2F repression and might lead to hyperproliferation in those cancer cells.

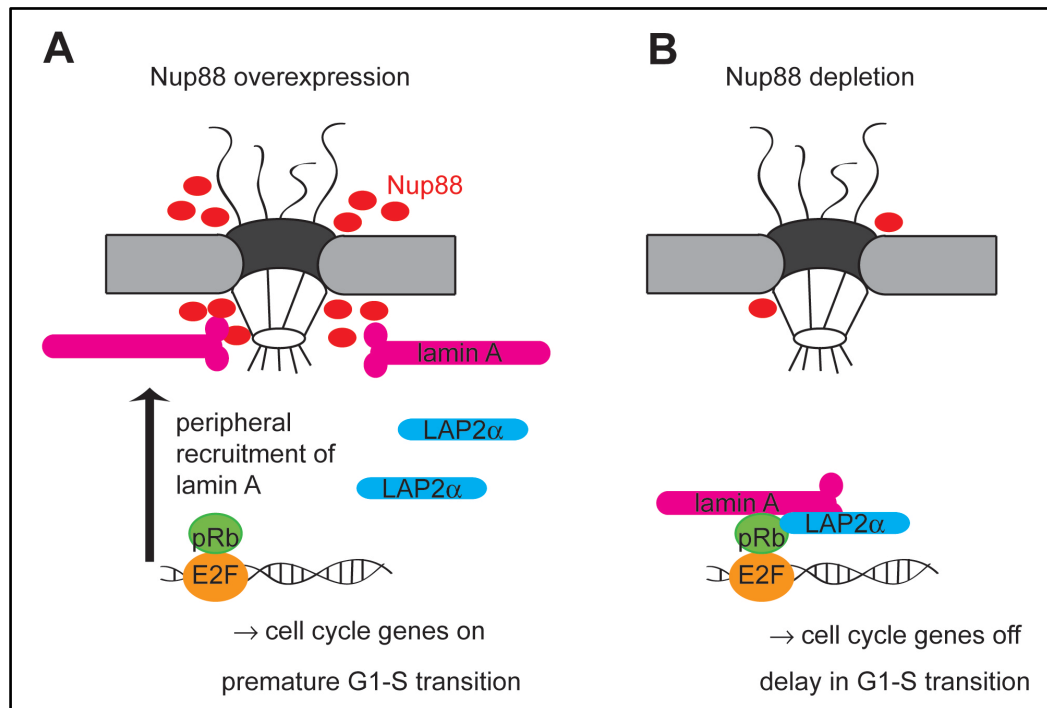


Figure 4.4: Model depicting the potential function of Nup88 in the regulation of the lamin A-LAP2 α complex in pRb-mediated cell cycle progression

While in S phase cells A-type lamins are found exclusively at the nuclear periphery, LAP2 α stabilizes a pool of A-type lamins in the nuclear interior during G1 phase. The nucleoplasmic lamin A- LAP2 α complex binds to pRb at E2F-dependent promoters in G1 phase and helps to inhibit E2F-dependent transcription. In S phase, pRb is phosphorylated, causing dissociation of the complex, loss of nucleoplasmic lamin A and C and activation of E2F-dependent transcription. **(A)** In Nup88 overexpressing cells, lamin A is more strongly recruited to the nuclear periphery by increased Nup88, the lamin A- LAP2 α complex is dissociated, and E2F-dependent promoters are derepressed, causing progression from G1 to S phase of the cell cycle. **(B)** In Nup88-depleted cells, lamin A does not get recruited to the nuclear periphery, and the lamin A- LAP2 α complex is longer associated with pRb and E2F-dependent genes stay repressed, causing cells to progress much slower through G1-S transition.

4.5 Materials and Methods

4.5.1 Cell culture and transfections

A stable cell line based on HEK 293 cells was generated expressing a myc-tagged Nup88 upon addition of tetracycline to the medium (Invitrogen) as described before (Lussi et al., submitted, Chapter 3). BJ-hTERT cells were kindly received from Prof. Dr. Roland Foisner (Max F. Perutz Labor, Vienna).

HEK 293 and BJ1-hTERT cells were grown in Dulbecco's modified Eagle's medium (DMEM) supplemented with 10% fetal bovine serum (FBS) plus penicillin and streptomycin. Cells were transfected using Solution R and Program 024 with the Amaxa Nucleofector (Lonza Group Ltd, Switzerland). For a G0/1 block by serum starvation, cells were serum starved for 3 days and released by adding 10% fetal bovine serum to the medium. For the double thymidine block, cells were synchronized by thymidine block (2mM) for 19 h, released for 9 h, blocked a second time with thymidine and released after 16 h.

4.5.2 Constructs and Antibodies

N-terminally GFP-tagged Nup88 was produced using the Kpn1-Xba1 restriction sites in pEGFP-C1 (Clontech, Palo Alto, CA). The monoclonal antibody against lamin A/C (1/200) as well as the polyclonal antibody against LAP2a (1/250) were both purchased from Abcam, the monoclonal GFP-antibody is bought from Roche Applied Science, the polyclonal lamin A (1/200) antibody was kindly received from Professor RD Goldman (University of Chicago). Monoclonal Nup88 antibody was from BD Bioscience (1:500, BD Biosciences, Pharmingen). Secondary antibodies include anti-mouse Alexa 647 and anti-rabbit Alexa 568 from Invitrogen and used 1:350 (Alexa 647) and 1:1000 (Alexa 568). 4',6-Diamidino-2-phenylindol (DAPI) was acquired from Sigma.

4.5.3 Immunofluorescence microscopy

Cells were grown on coverslips and fixed in 2% formaldehyde for 15 min, washed three times for 10 min with PBS, and permeabilized with PBS containing 1% bovine serum albumin (BSA) and 0.2% Triton X-100 for 5 min on ice. Next the cells

were washed three times for 5-10 min in PBS containing 1% BSA and incubated with the appropriate primary antibodies for 1 hour, washed three times in PBS containing 1% BSA and incubated with the appropriate secondary antibodies for 1 hour, washed 5x with PBS then mounted with Mowiol and stored at 4°C until viewed. Cells were viewed using a confocal laser-scanning microscope (Leica TCS SP5, Leica, Vienna, Austria). Some images were taken with the Zeiss Observer using AxioVision 4.6 with Multichannel Fluorescence. Images were recorded using the microscope system software and processed using Adobe Photoshop (Adobe Systems, Mountain View, CA, USA).

4.5.4 RNA interference

HEK cells were depleted of Nup88 using On-target smart pool duplex siRNA to human Nup88 (Dharmacon, Lafayette, CO). Cells were grown on 12 mm diameter coverslips and exposed to the Nup88 siRNA in the presence of Lipofectamine RNAiMax (Invitrogen, Paisley, UK) following the instructions of the manufacturer. As a control cells were exposed to Lipofectamine RNAiMax alone or to siRNA against cyclophilin B (Dharmacon, Lafayette, CO). Knock down efficiency was determined by immunoblotting 48 h post transfection.

4.5.5 Quantitative immunoblotting and gel electrophoresis

Cells were resuspended in lysis buffer containing 50 mM Tris-HCl pH 7.8, 150 mM NaCl, 1% Nonidet P-40 and protease inhibitor (Thermo Scientific). Sample aliquots were resolved by sodium dodecyl sulfate-polyacrylamide (10%) gel electrophoresis (SDS-PAGE). The proteins were transferred onto a PVDF membrane and the membrane was incubated in I-Block solution (Tropix, Bedford, MA) containing 0.1% Tween-20 (blocking solution) over night at 4°C, then incubated in blocking solution containing a primary antibody directed against either lamin A (1:2000), LAP2 α (1:250), Nup88 (1:500) or anti- β -tubulin (1:1000) for 1 hour followed by washing 3x with PBS containing 0.1% Tween-20. The membrane was then incubated with secondary antibodies in blocking solution, mouse-IgG-alkaline phosphatase (AP) (1/20000) or rabbit IgG-AP (1/20000), respectively. After washing twice with assay buffer (200 mM Tris pH 9.8, 10 mM MgCl₂), alkaline phosphatase substrate (CDP-Star solution, Tropic, Applied

Biosystems) was added for 5 min on the immunoblot. Images were recorded using the Las-4000 imaging system from Bucher Biotec and analyzed by the systems software program and Multigauge.

4.5.6 Flow cytometry

Cells were fixed in ice-cold 70% ethanol for 30 minutes, washed 2x in PBS by vortexing and pelleting at 1000 g for 5 minutes, and suspended at 10^6 cells/ml with PI stain (50 μ g/ml propidium iodide, 100 μ g/ml RNase A, 0.1% Triton-X 100) for 40 minutes at 37°C. The cell preparation was stored at 4°C in the dark until flow cytometric acquisition and analysis.

4.5.7 Immunoprecipitation

Subconfluent HEK cells (3×10^6) were trypsinized, washed with PBS and resuspended in 160 μ l lysis buffer (50 mM Tris-HCl, pH 7.4, 250 mM NaCl, 0.1 % Triton X-100, 2 mM EDTA- Na_2 , 10% glycerol and protease inhibitor (Thermo Scientific)), vortexed and incubated for 10 min at 37°C. The cells were pelleted at 16000 g for 10 min and the supernatant was transferred to a fresh tube. The supernatant was cleared with 20 μ l of prewashed protein G agarose beads (Santa Cruz) and incubated for 30 min at 4°C, centrifuged at 1000 g for 30 sec at 4°C, and the supernatant was transferred to a fresh tube and 2 μ g mouse monoclonal lamin A/C antibody was added and incubated for 2 hours on ice. 40 μ l prewashed protein G agarose slurry was added to the lysate and incubated at 4°C on a rocker platform for 1 hour. The immunoprecipitate was collected by centrifugation at 1000 g for 30 sec at 4°C and the supernatant was carefully removed and kept to analyze as unbound fraction. The pellet was washed 3x with lysis buffer, resuspended in electrophoresis sample buffer, boiled at 95°C for 5 min and subjected to electrophoresis and immunoblotting.

5

Conclusions and Perspectives

In recent years, it has become more and more evident that nucleoporins and NPC-associated proteins, such as Nup98 and the Nup107-160 complex, required for nucleocytoplasmic transport have important cellular functions independent of their role in mediating transport through the NPC (Capelson et al.; Liodice et al., 2004; Orjalo et al., 2006). Nucleoporins have been implicated in mitotic events, gene expression and nuclear organization. Here, we give insight into novel functions for the two nucleoporins Nup153 and Nup88, in mitosis and cell cycle regulation, respectively, which appear to be independent of their nucleocytoplasmic transport function.

5.1 Nup153 as a novel regulator of the spindle assembly checkpoint protein Mad1

Although Nup153 has been associated with NE breakdown by recruiting the coatmer coat protein I (COPI) complex to the NE (Liu et al., 2003), it became only recently clear that Nup153 also plays a direct role in mitosis (Liu et al., 2003; Lussi et al., 2010; Mackay et al., 2009). Recent work by Mackay and coworkers showed that depletion of Nup153 in human cells led to defects in both early and late stages of mitosis in a concentration-dependent manner and to an accumulation of cells with multilobed nuclei (Mackay et al., 2009). The multilobed nuclei phenotype was independent of the FG-domain, whereas the FG-domain of Nup153 was required to rescue the late defects, indicating two distinct mitotic functions for Nup153 (Mackay et al., 2009).

Our study employing overexpression and depletion experiments of Nup153 in human cell cultures revealed furthermore that overexpression of Nup153 leads to the appearance of multinucleated cells and induces the formation of multipolar spindles (Figure 2.1, Figure 2.2 and Figure 2.3). Importantly, the observed phenotype was linked to residues 39 to 339

of Nup153 corresponding to the NPC assembly region (NPAR) (Enarson et al., 1998), as overexpression of a GFP-Nup153-39-339 fusion protein caused a similar phenotype as observed with full-length Nup153 (Figure 2.3). Residues 39-339 of Nup153 are not known to interact with any of the nuclear transport factors, indicating that the observed phenotype is independent of its role in nucleocytoplasmic transport.

Furthermore, we could show that Nup153 and the SAC protein Mad1 are directly interacting both in asynchronous and mitotic cell cultures and that the interaction between the two proteins is mediated by Nup153's N-terminus containing the NPAR domain, suggesting that the observed mitotic defects induced by Nup153 overexpression is mediated through the interaction with Mad1 (Figure 2.4). In addition, Nup153 overexpression affected Mad1 phosphorylation during mitosis, which is critical for mitotic function, indicating that Nup153 overexpression affects SAC by impeding Mad1 phosphorylation (Chen et al., 1999) (Figure 2.5). We could observe a co-localization of Mad1 with Nup153 at the NE and in intranuclear foci when Nup153 was overexpressed (Figure 2.6). Therefore, we speculate that Nup153 perturbs Mad1 localization in mitosis, what might lead to the decreased phosphorylation of Mad1. Together, we show that overexpression of Nup153 causes hypophosphorylation of Mad1, leading to an impaired SAC and consequently chromosome missegregation and failures in cytokinesis. Interestingly, loss of Mad1 function in human cells mimics the phenotype observed upon Nup153 overexpression, suggesting that the by Nup153 overexpression mediated decrease in Mad1 phosphorylation causes decreased Mad1 activity leading to a weakened SAC (Jin et al., 1998).

During interphase, the SAC proteins Mad1 and Mad2 localize to NPCs (Campbell et al., 2001; Iouk et al., 2002) and it has been suggested that NPCs are implicated in correct timing of the SAC during mitosis (Kastenmayer et al., 2005; Scott et al., 2005). In mitosis, Mad1 and Mad2 localize to kinetochores, where they regulate SAC function (Campbell et al., 2001; Musacchio and Salmon, 2007; Suijkerbuijk and Kops, 2008). In our work we could show that depletion of Nup153 using RNA interference not only affects the association of Mad1 at the NPC during interphase, but also causes a delayed dissociation of Mad1 from kinetochores in metaphase (Figure 2.6). Depletion of Nup153 did not affect phosphorylation of Mad1. However, depletion of Nup153 was

associated with increased number of unresolved midbodies, indicating defects in cytokinesis (Figure 2.7). Reduced levels of Nup153 might therefore lead to persistently activated SAC due to prolonged localization of Mad1 to the kinetochores, consistent with the observed delay or aborted cytokinesis.

Taken together, both overexpression and depletion of Nup153 affect the SAC mediated by its interaction with Mad1. A model of the effects of Nup153 overexpression and depletion on mitosis is depicted in Figure 5.1. Overexpression of Nup153 affects Mad1 phosphorylation, possibly by affecting its localization in mitosis, leading to an impaired SAC. However, Nup153 depletion affects localization at the kinetochores without affecting Mad1 phosphorylation, suggesting that the SAC is functionally intact, yet, persistent in time, leading to the observed defects in mitosis.

It will be interesting to address the question in future as to how exactly Nup153 affects Mad1 phosphorylation and SAC activity. It is known that the polo-like kinase I (PLKI) is involved in the phosphorylation of Mad1 in mitosis and it will be a challenging task to examine how Nup153 influences Mad1 phosphorylation by PLK1 (Chi et al., 2008).

Weakening of the mitotic checkpoint can promote aneuploidy and a weakened checkpoint is prevalent among tumor cells (Kops et al., 2005; Weaver and Cleveland, 2006). Given that Nup153 expression is increased urothelial and retinoblastoma cancer, the here-described findings might give insight in how Nup153 contributes to cancer development (Heidenblad et al., 2008; Orlic et al., 2006). Furthermore, the importance of Nup153 is highlighted by the fact that it is essential for the viability of *C. elegans* embryos and growth of tissue culture cells, which is not likely explained by its sole nucleocytoplasmic transport function, as FG-containing nucleoporins are thought to have redundant functions concerning nucleocytoplasmic transport and cells can compensate the loss of about 50% of the FG-domains (Galy et al., 2003; Harborth et al., 2001; Strawn et al., 2004; Zeitler and Weis, 2004). Therefore, Nup153 is most likely essential for viability due to its crucial mitotic function.

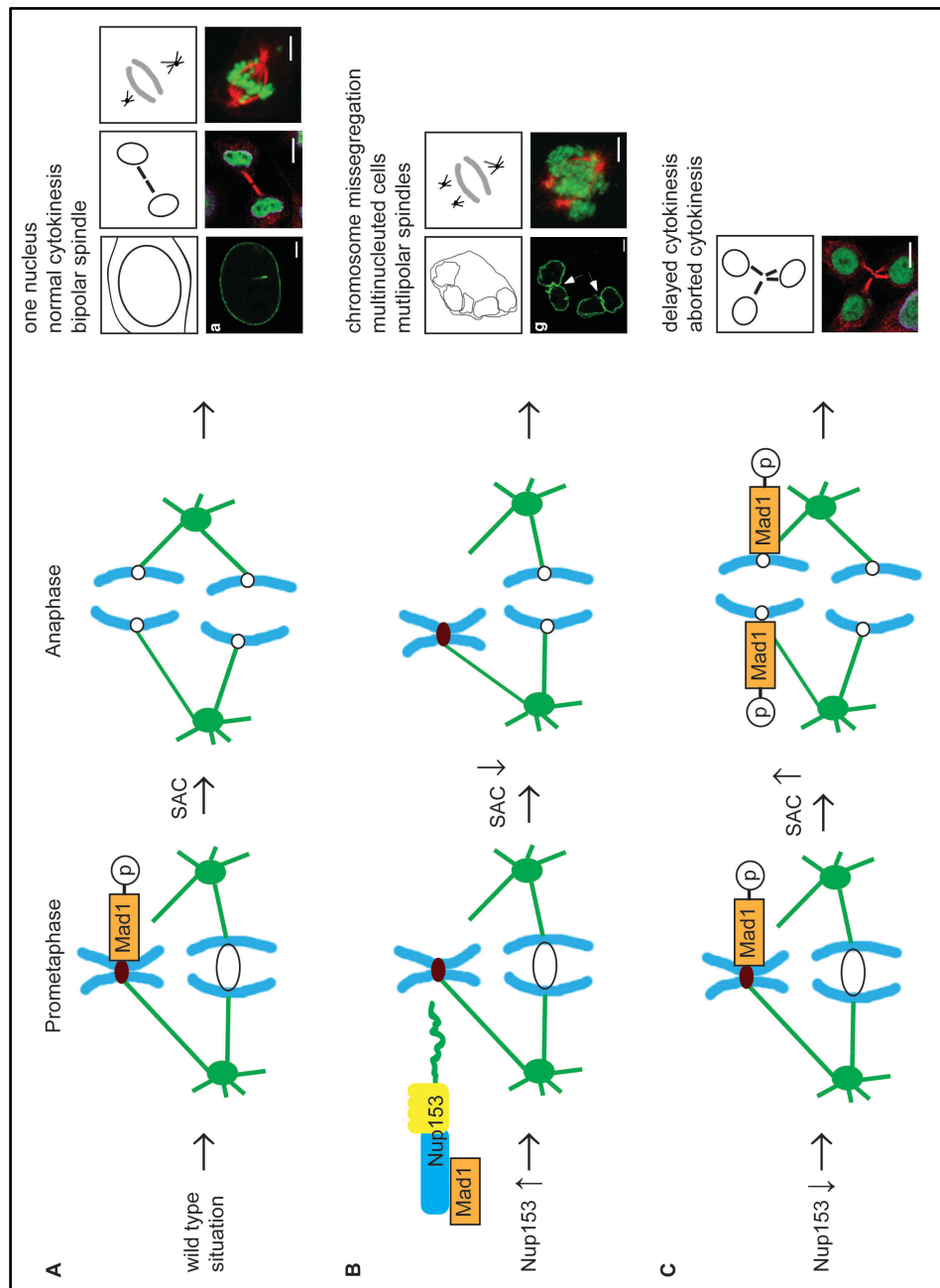


Figure 5.1: Schematic model depicting the effect of Nup153 overexpression and depletion on Mad1, the SAC and mitosis.

(A) Mitosis in the wild type situation. In prometaphase, Mad1 is recruited to unattached kinetochores (brown) and phosphorylated (p). The spindle assembly checkpoint (SAC) is active until all chromosomes (blue) are attached to the spindle apparatus (green). Sister chromatids are separated in anaphase, resulting in mononucleated cells, normal midbodies and bipolar spindles. (B) Overexpression of Nup153 leads to mislocalization of Mad1, subsequent Mad1 hypophosphorylation, impairment of the SAC, followed by chromosome missegregation, aneuploidy and failures in cytokinesis (i.e. multinucleated cells followed by multipolar spindles).

(C) Depletion of Nup153 does not affect Mad1 phosphorylation, however to a prolonged localization of Mad1 at the kinetochores, leading to a persistently active SAC and delayed and aborted cytokinesis (i.e. abnormal midbodies). Adapted from (Musacchio and Salmon, 2007) and (Suijkerbuijk and Kops, 2008).

5.2 **Nup88 interacts with the lamin A Ig-fold: implications in laminopathies?**

An association between the NPC and the nuclear lamina has already been documented in 1976 by Dwyer and Blobel (Dwyer and Blobel, 1976). The nucleoporins Nup153 and Nup53 have been reported to interact with lamin B, and only recently, it has been shown that Nup153 interacts with lamin A as well (Al-Haboubi et al., submitted)(Hawryluk-Gara et al., 2005; Smythe et al., 2000). The nucleoporin-lamin interactions have been implicated in proper assembly of the NPCs into the nuclear envelope, since depletion of lamins lead to NPC clustering and incorporation of certain nucleoporins, like Nup153, into the NPC depends on lamina assembly (Furukawa et al., 2009; Hawryluk-Gara et al., 2005; Smythe et al., 2000).

Here, we provide a novel molecular link between the nucleoporin Nup88 and lamin A (Lussi et al., submitted). By solution-binding, overlay and immunoprecipitation assays and by immunofluorescence microscopy, we show that Nup88 and lamin A interact in vitro as well as in vivo (Figure 3.1, Figure 3.2 and Figure 3.4). Our studies showed that the N-terminus of Nup88 is binding to lamin A in vitro, and that it is the Ig-fold domain of lamin A which is mediating the binding to Nup88 (Figure 3.2). In solution binding assays, the presence of lamin A-associated mutants abrogated the interaction with Nup88 and supported the notion that the Ig-fold of lamin A is necessary for Nup88 binding (Figure 3.5). Our studies showed that the EDMD-associated lamin A mutant (R453W), which causes destabilization of the Ig-fold domain, loses its ability to bind Nup88 in vitro and in vivo. Another mutation in the Ig-fold domain of lamin A, the mutation of R482 to a W, which is responsible for FPLD, also impairs Nup88 binding. Interestingly, this mutation lies on the surface of the lamin A Ig-fold and is suggested to be a polar interaction site for lamin A-associated proteins (Dhe-Paganon et al., 2002; Krimm et al., 2002). In contrast, a lamin A truncation found in HGPS, lamin A Δ 50, does

not affect binding to Nup88, further indicating the importance of the Ig-fold domain for the Nup88 interaction.

Interestingly, a study with cells from progeria patients showed that Nup88 mRNA levels decreased in cells derived from progeria patients or from old people compared to Nup88 levels in cells from healthy people (Ly et al., 2000). Similarly, we could observe a reduction of Nup88 protein levels in lamin A-deficient cells, indicating that lamin A might influence Nup88 expression levels (Figure S7.13). How lamin A regulates Nup88 expression levels and if Nup88 has a physiological role in aging needs to be further elaborated. On the other hand, altered interactions of Nup88 with the above mentioned laminopathy-associated mutants might affect Nup88 function in vivo and contribute to disease development.

5.3 Implications of Nup88 in nuclear assembly?

The nuclear lamina has been implicated in proper assembly of the NE and NPCs after mitosis (Furukawa et al., 2009; Holaska et al., 2002). Therefore, the interaction of Nup88 with lamin A might have a structural role in nuclear architecture and nuclear assembly. To study the effects of increased Nup88 levels on nuclear assembly, we used the cell-free system based on *Xenopus laevis* egg extract and demembrated sperm chromatin to reconstitute nuclei (Figure 5.2A). Crude extract, sperm chromatin and an ATP-regenerating system were incubated for 120 minutes with an excess of either purified GST-Nup88 or GST as negative control and assembled nuclei were visualized by fluorescence microscopy and DAPI staining. We could observe an abnormal nuclear shape in nuclei incubated with an excess of Nup88 compared to control nuclei, suggesting that the excess Nup88 interferes with proper nuclear assembly (Figure 5.2A). Furthermore, when Nup88-myc is overexpressed in a tetracycline-inducible HEK cell line, large nuclear invaginations are observed as compared to control cells, similar to the phenotype observed in reconstituted nuclei (Figure 5.2B). These observations indicate that Nup88 might play a role in nuclear assembly, but whether the observed phenotypes are indeed dependent on lamin A needs to be further elaborated.

However, lamin A exists in at least two different populations in the cell, as filamentous structure near the nuclear envelope and as more soluble fraction in association with LAP2 α (see Chapter 4). Our findings that Nup88 interacts with lamin A together with LAP2 α and that Nup88 protein levels influence the lamin A-LAP α complex stability and cell cycle progression supports the idea that Nup88 interacts with the more soluble lamin A (Figure 4.1, Figure 4.2 and Figure 4.3). Whether the interaction takes place at the NPC or in the nucleoplasm has to be further investigated, as Nup88 has been observed, beside its peripheral nuclear localization at the NPC, within the nucleoplasm, where Nup88 was implicated in gene regulation and cellular stress response (Capelson et al.; Chen et al., 2007; Kodiha et al., 2008b)(Lussi et al, submitted).

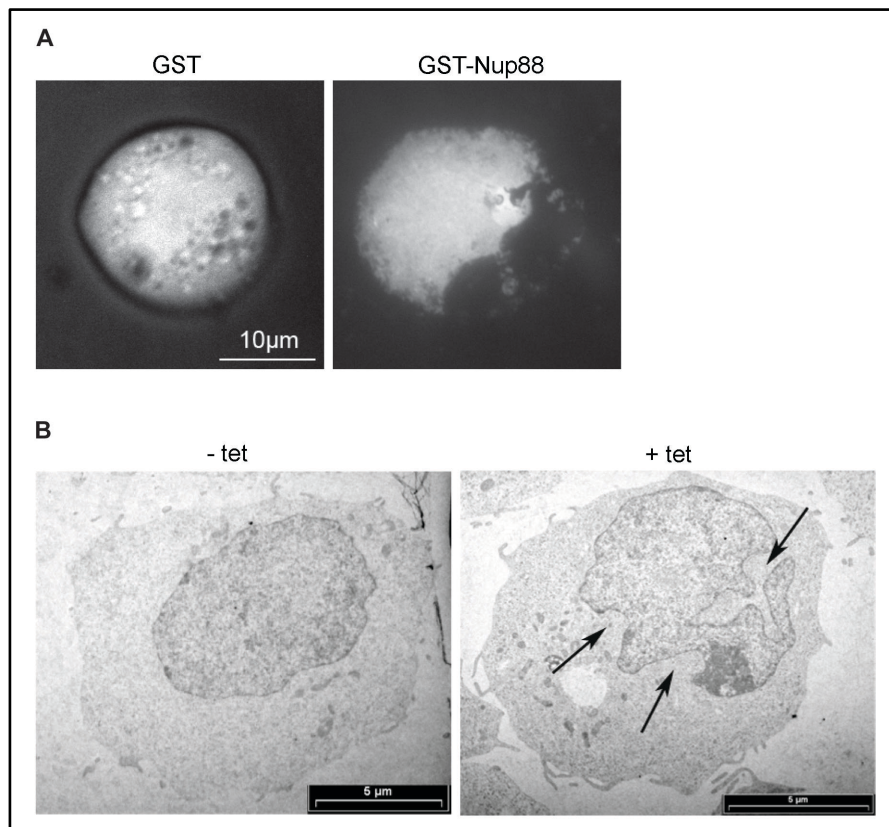


Figure 5.2: Excess Nup88 leads to aberrant nuclear morphology.

(A) Reconstituted nuclei from *Xenopus* oocyte extract display abnormal nuclear shape when purified GST-Nup88 is added to the assembly reaction (right panel), compared to nuclei where purified GST as control was added (left panel). Nuclei were visualized by Dapi staining and immunofluorescence microscopy (B) Stable HEK cells induced with tetracycline to express Nup88-myc show large nuclear invaginations (right panel, arrows) compared to non-induced control cells (left panel).

5.4 Nup88 localizes on both the cytoplasmic and nuclear side of the NPC

Here, we could demonstrate by immuno-EM studies in *Xenopus* oocyte nuclei that Nup88 is localized on both the cytoplasmic and nuclear side of the NPC, complementing recent data where Nup88 was shown to be cytoplasmically localized (Figure 3.3)(Bernad et al., 2004). Rout and coworkers suggest that the abundance of nucleoporins and their localization within the NPC correlates insofar that low abundance, i.e. one copy per spoke, correlates with asymmetric distribution within the NPC, and higher abundance (several copies per spoke) with a more symmetric distribution within the NPC (Rout et al., 2000). This notion supports the idea that Nup88 might be symmetrically distributed within the NPC, since Nup88 was found to be a highly abundant nucleoporin with 32 copies per NPC, i.e. 4 copies per spoke (Rout et al., 2000). Furthermore, the finding that Nup88 is also localized on the nuclear side of the NPC is consistent with the novel interaction of Nup88 with lamin A (Lussi et al, submitted).

5.5 Nup88 in proliferation

Nup88 was implicated in cell proliferation and differentiation, as it was found to be overexpressed in developing tissue as well as in different cancer cell lines and tumors (Agudo et al., 2004; Emterling et al., 2003; Gould et al., 2000; Gould et al., 2002; Martinez et al., 1999; Schneider et al., 2004; Zhang et al., 2002; Zhang et al., 2007). The exact mechanism, however, as to how Nup88 influences proliferation was not clear.

Here, we show that Nup88 associates with the lamin A-LAP2 α complex and that Nup88 overexpression leads to a destabilization of the lamin A-LAP2 α complex, followed by a weakened G0/G1 arrest and accelerated cell cycle progression (Figure 4.1 and Figure 4.2). On the other hand, depletion of Nup88 leaves the lamin A-LAP2 α complex intact, but significantly decelerates G1-S transition in human cells (Figure 4.3). However, the immunoprecipitation experiments give us only a static view of the interaction of the two proteins, and it would be possible that LAP2 α binding to lamin A is not stronger, but longer during the cell cycle. So, loss of Nup88 might lead to a more stable lamin A-LAP2 α association over time and to a longer repression of E2F-dependent

cell cycle genes. To gain more insight into Nup88's effect on cell cycle progression, it will be necessary to analyze expression of endogenous E2F target genes, e.g. cyclin D1, thymidine kinase or cyclin E, and an unrelated gene product like actin, by quantitative PCR to correlate Nup88 overexpression and depletion defects in cell cycle to pRb/E2F gene regulation. E2F genes are differentially expressed during the cell cycle, and gene expression needs to be analyzed in a synchronized cell culture in the G1 to S transition and during S phase. Additionally to the propidium iodide based cell cycle analysis, it will be helpful to analyze the quantity of transcribed DNA by BrdU pulse labeling of actively transcribed DNA to make conclusions about the amount of cells in S phase.

Although the depletion experiments were performed in HEK cells, which is a virus-transformed cell line and where pRb is partially inactivated through adenoviral proteins (Graham et al., 1977), Nup88 depletion had a very strong effect on cell cycle progression. However, to verify the observed phenotype of Nup88 depletion in a non-transformed cell line, it will be necessary to perform the experiment in BJ1-hTERT fibroblasts or a similar non-transformed cell line.

A possible mechanism of how Nup88 regulates cell cycle progression might be by recruiting the lamin A-LAP2 α complex away from its inhibitory site of action, and as a consequence, decreases pRb's repressor function or accelerates its deactivation during G1-S transition (Figure 4.4). However, we cannot fully exclude the possibility that Nup88 impacts cell cycle progression via a lamin A or LAP2 α independent mechanism. To address this question, cell cycle studies in lamin A and LAP2 α knockout cells need to be performed. These cells should not be responsive to Nup88 overexpression or depletion concerning cell cycle progression, and these findings would indicate a common pathway of Nup88 and the lamin A-LAP2 α complex in cell cycle regulation.

For the future, it will be interesting to analyze the question how Nup88 can regulate the lamin A-LAP2 α complex in a cell cycle-dependent manner. It is known that Nup88 is phosphorylated (Kodiha et al., 2008a), and other modifications can be thought of to regulate Nup88's localization or binding with its interaction partners, e.g. ubiquitination.

Alternatively, it has been shown that protein levels of members of the Nup107-160 complex are regulated during the cell cycle, mainly via the ubiquitin-proteasome

pathway, which subsequently regulates cell cycle progression and phase-specific gene expression (Chakraborty et al., 2008). Therefore, another scenario might be that protein levels of Nup88 itself are regulated in a cell cycle-dependent manner, which further regulates the lamin A-LAP2 α complexes.

5.6 Implications of nucleoporins in gene regulation

Only recently, it has been shown for the first time that nucleoporins are involved in gene regulatory functions in multicellular organisms (Capelson et al.; Kalverda et al.). These findings reveal the nucleoporins as new class of transcription factors, as several nucleoporins, such as Nup88, Nup98, Sec13 and FG-containing nucleoporins, have been shown to be present in the nuclear interior, where they bind certain genes and regulate their expression, including developmentally regulated genes needed for cell differentiation and tissue development. These findings support strongly our results that Nup88 is implicated in gene expression and cell cycle regulation (Lussi et al., in preparation).

We started to focus on the cellular functions of yet another nucleoporin, Nup98. Nup98 is found in leukemia fused to proteins important for gene expression. The best-studied Nup98 fusion is Nup98/HoxA, where Nup98 is fused to the homeodomain of HoxA (Borrow et al., 1996; Nakamura et al., 1996). Nup98/HoxA provides aberrant self-renewal capacity, blocks myeloid differentiation in vitro and induces AML-like disease in vivo (Kroon et al., 2001). *NUP98* can also be fused to the hematopoietic homeobox gene *HHEX* also known as proline-rich homeobox (*PRH*) (Manfioletti et al., 1995; Morgutti et al., 2001). The resulting Nup98/HHEX fusion has transforming activity in vitro and in vivo, which is dependent on the GLFG repeats of Nup98 and the integrity of the HHEX homeodomain. Comparative gene expression analysis revealed a partially overlapping target profile of Nup98/HHEX and Nup98/HoxA (Chung et al., 2006; Jankovic et al., 2008; Palmqvist et al., 2007; Takeda et al., 2006). It is possible that several Nup98 fusions (and other leukemogenic fusions containing transcriptional regulators) have common critical targets that would be interesting as potential targets for therapeutic intervention.

To illuminate the role of the nucleoporin Nup98 in leukemogenic transformations, particularly the fusion of Nup98 to HoxA and HHEX, we analyzed interactions partners of Nup98 and its fusion proteins Nup98/HoxA and Nup98/HHEX by immunoprecipitation assays with GFP-tagged wild-type Nup98 and Nup98/HoxA and Nup98/HHEX fusion proteins using a monoclonal GFP-antibody (Figure 5.3). Interestingly, we found that Nup88 is interacting with wild-type Nup98, as it has been shown previously (Griffis et al., 2003). However, the interaction was lost with the leukemogenic fusion proteins Nup98/HoxA and Nup98/HHEX (Figure 5.3). To understand the importance of the loss of interaction between Nup98 and Nup88, it is crucial to first understand the physiological function of this interaction in a cellular context. Furthermore, we found that lamin A and lamin B1 are binding to Nup98 as well as its fusion proteins with HoxA and HHEX. It will be interesting to analyze in future whether Nup98 is implicated in gene regulation in a lamin A-dependent manner, similarly to Nup88. Insight into Nup98's involvement in lamin A-mediated gene regulation might be important to understand its leukemogenic potential.

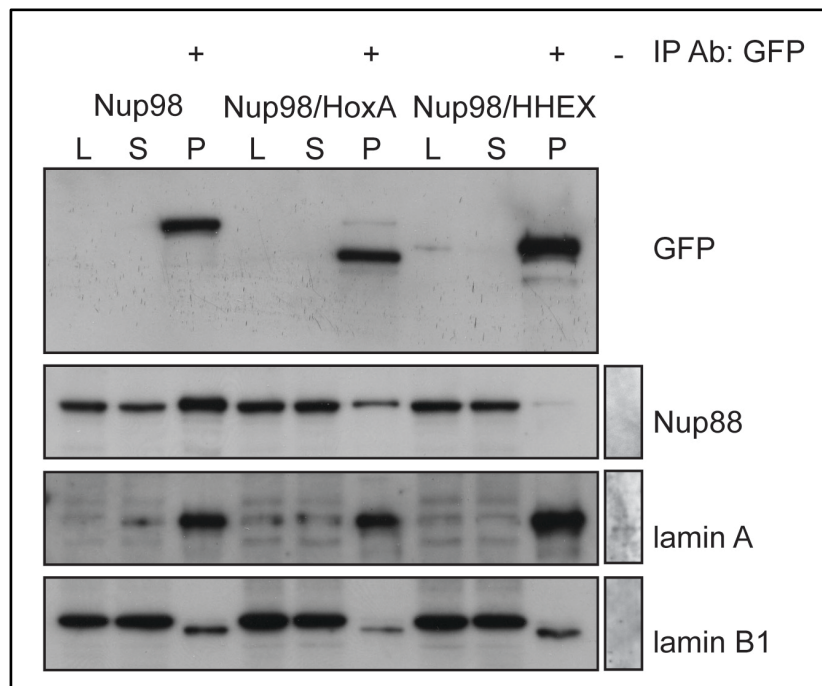


Figure 5.3: Immunoprecipitation assays with HEK cells transfected with GFP-Nup98, GFP-Nup98/HoxA and GFP-Nup98/HHEX fusion proteins using monoclonal GFP-antibodies. Nup88 is co-precipitating with GFP-Nup98, whereas the interaction with Nup88 is reduced with GFP-Nup98/HoxA fusion protein and almost completely interrupted with the Nup98/HHEX fusion

protein. Lamin A and lamin B1 are precipitating with GFP-Nup98, GFP-Nup98/HoxA and GFP-Nup98/HHEX.

6

References

- Aaronson, R.P., and G. Blobel. 1975. Isolation of nuclear pore complexes in association with a lamina. *Proc Natl Acad Sci U S A.* 72:1007-11.
- Adam, S.A., K. Sengupta, and R.D. Goldman. 2008. Regulation of nuclear lamin polymerization by importin alpha. *J Biol Chem.* 283:8462-8.
- Aebi, U., J. Cohn, L. Buhle, and L. Gerace. 1986. The nuclear lamina is a meshwork of intermediate-type filaments. *Nature.* 323:560-4.
- Agudo, D., F. Gomez-Esquer, F. Martinez-Arribas, M.J. Nunez-Villar, M. Pollan, and J. Schneider. 2004. Nup88 mRNA overexpression is associated with high aggressiveness of breast cancer. *Int J Cancer.* 109:717-20.
- Aitchison, J.D., M.P. Rout, M. Marelli, G. Blobel, and R.W. Wozniak. 1995. Two novel related yeast nucleoporins Nup170p and Nup157p: complementation with the vertebrate homologue Nup155p and functional interactions with the yeast nuclear pore-membrane protein Pom152p. *J Cell Biol.* 131:1133-48.
- Akey, C.W. 1989. Interactions and structure of the nuclear pore complex revealed by cryo-electron microscopy. *J Cell Biol.* 109:955-70.
- Akey, C.W., and M. Radermacher. 1993. Architecture of the *Xenopus* nuclear pore complex revealed by three-dimensional cryo-electron microscopy. *J Cell Biol.* 122:1-19.
- Alber, F., S. Dokudovskaya, L.M. Veenhoff, W. Zhang, J. Kipper, D. Devos, A. Suprpto, O. Karni-Schmidt, R. Williams, B.T. Chait, M.P. Rout, and A. Sali. 2007a. Determining the architectures of macromolecular assemblies. *Nature.* 450:683-94.
- Alber, F., S. Dokudovskaya, L.M. Veenhoff, W. Zhang, J. Kipper, D. Devos, A. Suprpto, O. Karni-Schmidt, R. Williams, B.T. Chait, A. Sali, and M.P. Rout. 2007b. The molecular architecture of the nuclear pore complex. *Nature.* 450:695-701.
- Allen, N.P., S.S. Patel, L. Huang, R.J. Chalkley, A. Burlingame, M. Lutzmann, E.C. Hurt, and M. Rexach. 2002. Deciphering networks of protein interactions at the nuclear pore complex. *Mol Cell Proteomics.* 1:930-46.
- Allen, T.D., G.R. Bennion, S.A. Rutherford, S. Reipert, A. Ramalho, E. Kiseleva, and M.W. Goldberg. 1996. Accessing nuclear structure for field emission, in lens, scanning electron microscopy (FEISEM). *Scanning Microsc Suppl.* 10:149-63; discussion 163-4.
- Allgrove, J., G.S. Clayden, D.B. Grant, and J.C. Macaulay. 1978. Familial glucocorticoid deficiency with achalasia of the cardia and deficient tear production. *Lancet.* 1:1284-6.
- Andres, V., and J.M. Gonzalez. 2009. Role of A-type lamins in signaling, transcription, and chromatin organization. *J Cell Biol.* 187:945-57.
- Andres-Hernando, A., M.A. Lanaspá, C.J. Rivard, and T. Berl. 2008. Nucleoporin 88 (Nup88) is regulated by hypertonic stress in kidney cells to retain the transcription factor tonicity enhancer-binding protein (TonEBP) in the nucleus. *J Biol Chem.* 283:25082-90.
- Antonin, W., C. Franz, U. Haselmann, C. Antony, and I.W. Mattaj. 2005. The integral membrane nucleoporin pom121 functionally links nuclear pore complex assembly and nuclear envelope formation. *Mol Cell.* 17:83-92.

- Arnautov, A., Y. Azuma, K. Ribbeck, J. Joseph, Y. Boyarchuk, T. Karpova, J. McNally, and M. Dasso. 2005. Crm1 is a mitotic effector of Ran-GTP in somatic cells. *Nat Cell Biol.* 7:626-32.
- Askjaer, P., A. Bachi, M. Wilm, F.R. Bischoff, D.L. Weeks, V. Ogniewski, M. Ohno, C. Niehrs, J. Kjems, I.W. Mattaj, and M. Fornerod. 1999. RanGTP-regulated interactions of CRM1 with nucleoporins and a shuttling DEAD-box helicase. *Mol Cell Biol.* 19:6276-85.
- Askjaer, P., V. Galy, E. Hannak, and I.W. Mattaj. 2002. Ran GTPase cycle and importins alpha and beta are essential for spindle formation and nuclear envelope assembly in living *Caenorhabditis elegans* embryos. *Mol Biol Cell.* 13:4355-70.
- Babu, J.R., K.B. Jeganathan, D.J. Baker, X. Wu, N. Kang-Decker, and J.M. van Deursen. 2003. Rael is an essential mitotic checkpoint regulator that cooperates with Bub3 to prevent chromosome missegregation. *J Cell Biol.* 160:341-53.
- Bagley, S., M.W. Goldberg, J.M. Cronshaw, S. Rutherford, and T.D. Allen. 2000. The nuclear pore complex. *J Cell Sci.* 113 (Pt 22):3885-6.
- Bakay, M., Z. Wang, G. Melcon, L. Schiltz, J. Xuan, P. Zhao, V. Sartorelli, J. Seo, E. Pegoraro, C. Angelini, B. Shneiderman, D. Escolar, Y.W. Chen, S.T. Winokur, L.M. Pachman, C. Fan, R. Mandler, Y. Nevo, E. Gordon, Y. Zhu, Y. Dong, Y. Wang, and E.P. Hoffman. 2006. Nuclear envelope dystrophies show a transcriptional fingerprint suggesting disruption of Rb-MyoD pathways in muscle regeneration. *Brain.* 129:996-1013.
- Ball, J.R., and K.S. Ullman. 2005. Versatility at the nuclear pore complex: lessons learned from the nucleoporin Nup153. *Chromosoma.* 114:319-30.
- Barrowman, J., C. Hamblet, C.M. George, and S. Michaelis. 2008. Analysis of prelamin A biogenesis reveals the nucleus to be a CaaX processing compartment. *Mol Biol Cell.* 19:5398-408.
- Baschong, W., and N.G. Wrigley. 1990. Small colloidal gold conjugated to Fab fragments or to immunoglobulin G as high-resolution labels for electron microscopy: a technical overview. *J Electron Microsc Tech.* 14:313-23.
- Bastos, R., A. Lin, M. Enarson, and B. Burke. 1996. Targeting and function in mRNA export of nuclear pore complex protein Nup153. *J Cell Biol.* 134:1141-56.
- Bastos, R., L. Ribas de Pouplana, M. Enarson, K. Bodoor, and B. Burke. 1997. Nup84, a novel nucleoporin that is associated with CAN/Nup214 on the cytoplasmic face of the nuclear pore complex. *J Cell Biol.* 137:989-1000.
- Baus, F., V. Gire, D. Fisher, J. Piette, and V. Dulic. 2003. Permanent cell cycle exit in G2 phase after DNA damage in normal human fibroblasts. *EMBO J.* 22:3992-4002.
- Bayliss, R., T. Littlewood, and M. Stewart. 2000. Structural basis for the interaction between FxFG nucleoporin repeats and importin-beta in nuclear trafficking. *Cell.* 102:99-108.
- Beck, M., F. Forster, M. Ecke, J.M. Plitzko, F. Melchior, G. Gerisch, W. Baumeister, and O. Medalia. 2004. Nuclear pore complex structure and dynamics revealed by cryoelectron tomography. *Science.* 306:1387-90.
- Beck, M., V. Lucic, F. Forster, W. Baumeister, and O. Medalia. 2007. Snapshots of nuclear pore complexes in action captured by cryo-electron tomography. *Nature.* 449:611-5.
- Beer, D.G., S.L. Kardia, C.C. Huang, T.J. Giordano, A.M. Levin, D.E. Misek, L. Lin, G. Chen, T.G. Gharib, D.G. Thomas, M.L. Lizyness, R. Kuick, S. Hayasaka, J.M. Taylor, M.D. Iannettoni, M.B. Orringer, and S. Hanash. 2002. Gene-expression profiles predict survival of patients with lung adenocarcinoma. *Nat Med.* 8:816-24.
- Belgareh, N., G. Rabut, S.W. Bai, M. van Overbeek, J. Beaudouin, N. Daigle, O.V. Zatssepina, F. Pasteau, V. Labas, M. Fromont-Racine, J. Ellenberg, and V. Doye. 2001. An evolutionarily conserved NPC subcomplex, which redistributes in part to kinetochores in mammalian cells. *J Cell Biol.* 154:1147-60.
- Belgareh, N., C. Snay-Hodge, F. Pasteau, S. Dagher, C.N. Cole, and V. Doye. 1998. Functional characterization of a Nup159p-containing nuclear pore subcomplex. *Mol Biol Cell.* 9:3475-92.

- Berger, R., L. Theodor, J. Shoham, E. Gokkel, F. Brok-Simoni, K.B. Avraham, N.G. Copeland, N.A. Jenkins, G. Rechavi, and A.J. Simon. 1996. The characterization and localization of the mouse thymopoietin/lamina-associated polypeptide 2 gene and its alternatively spliced products. *Genome Res.* 6:361-70.
- Berke, I.C., T. Boehmer, G. Blobel, and T.U. Schwartz. 2004. Structural and functional analysis of Nup133 domains reveals modular building blocks of the nuclear pore complex. *J Cell Biol.* 167:591-7.
- Bernad, R., D. Engelsma, H. Sanderson, H. Pickersgill, and M. Fornerod. 2006. Nup214-Nup88 nucleoporin subcomplex is required for CRM1-mediated 60 S preribosomal nuclear export. *J Biol Chem.* 281:19378-86.
- Bernad, R., H. van der Velde, M. Fornerod, and H. Pickersgill. 2004. Nup358/RanBP2 attaches to the nuclear pore complex via association with Nup88 and Nup214/CAN and plays a supporting role in CRM1-mediated nuclear protein export. *Mol Cell Biol.* 24:2373-84.
- Blobel, G. 1985. Gene gating: a hypothesis. *Proc Natl Acad Sci U S A.* 82:8527-9.
- Blower, M.D., M. Nachury, R. Heald, and K. Weis. 2005. A Rae1-containing ribonucleoprotein complex is required for mitotic spindle assembly. *Cell.* 121:223-34.
- Boehmer, T., J. Enninga, S. Dales, G. Blobel, and H. Zhong. 2003. Depletion of a single nucleoporin, Nup107, prevents the assembly of a subset of nucleoporins into the nuclear pore complex. *Proc Natl Acad Sci U S A.* 100:981-5.
- Boehmer, T., S. Jeudy, I.C. Berke, and T.U. Schwartz. 2008. Structural and functional studies of Nup107/Nup133 interaction and its implications for the architecture of the nuclear pore complex. *Mol Cell.* 30:721-31.
- Bogerd, A.M., J.A. Hoffman, D.C. Amberg, G.R. Fink, and L.I. Davis. 1994. nup1 mutants exhibit pleiotropic defects in nuclear pore complex function. *J Cell Biol.* 127:319-32.
- Boguslavsky, R.L., C.L. Stewart, and H.J. Worman. 2006. Nuclear lamin A inhibits adipocyte differentiation: implications for Dunnigan-type familial partial lipodystrophy. *Hum Mol Genet.* 15:653-63.
- Bonifacino, J.S., and B.S. Glick. 2004. The mechanisms of vesicle budding and fusion. *Cell.* 116:153-66.
- Bonne, G., M.R. Di Barletta, S. Varnous, H.M. Becane, E.H. Hammouda, L. Merlini, F. Muntoni, C.R. Greenberg, F. Gary, J.A. Urtizberea, D. Duboc, M. Fardeau, D. Toniolo, and K. Schwartz. 1999. Mutations in the gene encoding lamin A/C cause autosomal dominant Emery-Dreifuss muscular dystrophy. *Nat Genet.* 21:285-8.
- Borrow, J., A.M. Shearman, V.P. Stanton, Jr., R. Becher, T. Collins, A.J. Williams, I. Dube, F. Katz, Y.L. Kwong, C. Morris, K. Ohyashiki, K. Toyama, J. Rowley, and D.E. Housman. 1996. The t(7;11)(p15;p15) translocation in acute myeloid leukaemia fuses the genes for nucleoporin NUP98 and class I homeoprotein HOXA9. *Nat Genet.* 12:159-67.
- Bracken, A.P., M. Ciro, A. Cocito, and K. Helin. 2004. E2F target genes: unraveling the biology. *Trends Biochem Sci.* 29:409-17.
- Brickner, D.G., I. Cajigas, Y. Fondufe-Mittendorf, S. Ahmed, P.C. Lee, J. Widom, and J.H. Brickner. 2007. H2A.Z-mediated localization of genes at the nuclear periphery confers epigenetic memory of previous transcriptional state. *PLoS Biol.* 5:e81.
- Bridger, J.M., I.R. Kill, M. O'Farrell, and C.J. Hutchison. 1993. Internal lamin structures within G1 nuclei of human dermal fibroblasts. *J Cell Sci.* 104 (Pt 2):297-306.
- Brito, D.A., and C.L. Rieder. 2006. Mitotic checkpoint slippage in humans occurs via cyclin B destruction in the presence of an active checkpoint. *Curr Biol.* 16:1194-200.
- Broers, J.L., B.M. Machiels, G.J. van Eys, H.J. Kuijpers, E.M. Manders, R. van Driel, and F.C. Ramaekers. 1999. Dynamics of the nuclear lamina as monitored by GFP-tagged A-type lamins. *J Cell Sci.* 112 (Pt 20):3463-75.
- Broers, J.L., F.C. Ramaekers, G. Bonne, R.B. Yaou, and C.J. Hutchison. 2006. Nuclear lamins: laminopathies and their role in premature ageing. *Physiol Rev.* 86:967-1008.

- Brown, C.R., C.J. Kennedy, V.A. Delmar, D.J. Forbes, and P.A. Silver. 2008. Global histone acetylation induces functional genomic reorganization at mammalian nuclear pore complexes. *Genes Dev.* 22:627-39.
- Brown, C.R., and P.A. Silver. 2007. Transcriptional regulation at the nuclear pore complex. *Curr Opin Genet Dev.* 17:100-6.
- Bruzzoni-Giovanelli, H., A. Faille, G. Linares-Cruz, M. Nemani, F. Le Deist, A. Germani, D. Chassoux, G. Millot, J.P. Roperch, R. Amson, A. Telerman, and F. Calvo. 1999. SIAH-1 inhibits cell growth by altering the mitotic process. *Oncogene.* 18:7101-9.
- Burke, B., and J. Ellenberg. 2002. Remodelling the walls of the nucleus. *Nat Rev Mol Cell Biol.* 3:487-97.
- Burke, B., and C.L. Stewart. 2002. Life at the edge: the nuclear envelope and human disease. *Nat Rev Mol Cell Biol.* 3:575-85.
- Cabal, G.G., A. Genovesio, S. Rodriguez-Navarro, C. Zimmer, O. Gadal, A. Lesne, H. Buc, F. Feuerbach-Fournier, J.C. Olivo-Marin, E.C. Hurt, and U. Nehrbass. 2006. SAGA interacting factors confine sub-diffusion of transcribed genes to the nuclear envelope. *Nature.* 441:770-3.
- Cai, M., Y. Huang, R. Ghirlando, K.L. Wilson, R. Craigie, and G.M. Clore. 2001. Solution structure of the constant region of nuclear envelope protein LAP2 reveals two LEM-domain structures: one binds BAF and the other binds DNA. *EMBO J.* 20:4399-407.
- Campbell, M.S., G.K. Chan, and T.J. Yen. 2001. Mitotic checkpoint proteins HsMAD1 and HsMAD2 are associated with nuclear pore complexes in interphase. *J Cell Sci.* 114:953-63.
- Capelson, M., Y. Liang, R. Schulte, W. Mair, U. Wagner, and M.W. Hetzer. Chromatin-Bound Nuclear Pore Components Regulate Gene Expression in Higher Eukaryotes. *Cell.* 140:372-383.
- Casolari, J.M., C.R. Brown, D.A. Drubin, O.J. Rando, and P.A. Silver. 2005. Developmentally induced changes in transcriptional program alter spatial organization across chromosomes. *Genes Dev.* 19:1188-98.
- Chakraborty, P., Y. Wang, J.H. Wei, J. van Deursen, H. Yu, L. Malureanu, M. Dasso, D.J. Forbes, D.E. Levy, J. Seemann, and B.M. Fontoura. 2008. Nucleoporin levels regulate cell cycle progression and phase-specific gene expression. *Dev Cell.* 15:657-67.
- Chen, R.H., D.M. Brady, D. Smith, A.W. Murray, and K.G. Hardwick. 1999. The spindle checkpoint of budding yeast depends on a tight complex between the Mad1 and Mad2 proteins. *Mol Biol Cell.* 10:2607-18.
- Chen, R.H., A. Shevchenko, M. Mann, and A.W. Murray. 1998. Spindle checkpoint protein Xmad1 recruits Xmad2 to unattached kinetochores. *J Cell Biol.* 143:283-95.
- Chen, Y., H.L. Liu, G.H. Cui, Q.L. Wu, J. He, and W.H. Chen. 2007. [Deguelin regulates cell cycle and nuclear pore complex protein Nup98 and Nup88 in U937 cells in vitro]. *Zhonghua Xue Ye Xue Za Zhi.* 28:115-8.
- Chi, Y.H., K. Haller, M.D. Ward, O.J. Semmes, Y. Li, and K.T. Jeang. 2008. Requirements for protein phosphorylation and the kinase activity of polo-like kinase 1 (Plk1) for the kinetochore function of mitotic arrest deficiency protein 1 (Mad1). *J Biol Chem.* 283:35834-44.
- Chial, H.J., M.P. Rout, T.H. Giddings, and M. Winey. 1998. *Saccharomyces cerevisiae* Ndc1p is a shared component of nuclear pore complexes and spindle pole bodies. *J Cell Biol.* 143:1789-800.
- Chung, K.Y., G. Morrone, J.J. Schuringa, M. Plasilova, J.H. Shieh, Y. Zhang, P. Zhou, and M.A. Moore. 2006. Enforced expression of NUP98-HOXA9 in human CD34(+) cells enhances stem cell proliferation. *Cancer Res.* 66:11781-91.
- Clark, A.J., and A. Weber. 1998. Adrenocorticotropin insensitivity syndromes. *Endocr Rev.* 19:828-43.

- Classon, M., and E. Harlow. 2002. The retinoblastoma tumour suppressor in development and cancer. *Nat Rev Cancer*. 2:910-7.
- Collin, L., K. Schlessinger, and A. Hall. 2008. APC nuclear membrane association and microtubule polarity. *Biol Cell*. 100:243-52.
- Cordes, V.C., S. Reidenbach, H.R. Rackwitz, and W.W. Franke. 1997. Identification of protein p270/Tpr as a constitutive component of the nuclear pore complex-attached intranuclear filaments. *J Cell Biol*. 136:515-29.
- Cronshaw, J.M., A.N. Krutchinsky, W. Zhang, B.T. Chait, and M.J. Matunis. 2002. Proteomic analysis of the mammalian nuclear pore complex. *J Cell Biol*. 158:915-27.
- Cronshaw, J.M., and M.J. Matunis. 2003. The nuclear pore complex protein ALADIN is mislocalized in triple A syndrome. *Proc Natl Acad Sci U S A*. 100:5823-7.
- Cronshaw, J.M., and M.J. Matunis. 2004. The nuclear pore complex: disease associations and functional correlations. *Trends Endocrinol Metab*. 15:34-9.
- D'Angelo, M.A., and M.W. Hetzer. 2008. Structure, dynamics and function of nuclear pore complexes. *Trends Cell Biol*. 18:456-66.
- Dawlaty, M.M., L. Malureanu, K.B. Jeganathan, E. Kao, C. Sustmann, S. Tahk, K. Shuai, R. Grosschedl, and J.M. van Deursen. 2008. Resolution of sister centromeres requires RanBP2-mediated SUMOylation of topoisomerase IIalpha. *Cell*. 133:103-15.
- Dechat, T., S.A. Adam, and R.D. Goldman. 2009. Nuclear lamins and chromatin: when structure meets function. *Adv Enzyme Regul*. 49:157-66.
- Dechat, T., A. Gajewski, B. Korbei, D. Gerlich, N. Daigle, T. Haraguchi, K. Furukawa, J. Ellenberg, and R. Foisner. 2004. LAP2alpha and BAF transiently localize to telomeres and specific regions on chromatin during nuclear assembly. *J Cell Sci*. 117:6117-28.
- Dechat, T., J. Gotzmann, A. Stockinger, C.A. Harris, M.A. Talle, J.J. Siekierka, and R. Foisner. 1998. Detergent-salt resistance of LAP2alpha in interphase nuclei and phosphorylation-dependent association with chromosomes early in nuclear assembly implies functions in nuclear structure dynamics. *EMBO J*. 17:4887-902.
- Dechat, T., B. Korbei, O.A. Vaughan, S. Vlcek, C.J. Hutchison, and R. Foisner. 2000a. Lamina-associated polypeptide 2alpha binds intranuclear A-type lamins. *J Cell Sci*. 113 Pt 19:3473-84.
- Dechat, T., K. Pflieger, K. Sengupta, T. Shimi, D.K. Shumaker, L. Solimando, and R.D. Goldman. 2008. Nuclear lamins: major factors in the structural organization and function of the nucleus and chromatin. *Genes Dev*. 22:832-53.
- Dechat, T., S. Vlcek, and R. Foisner. 2000b. Review: lamina-associated polypeptide 2 isoforms and related proteins in cell cycle-dependent nuclear structure dynamics. *J Struct Biol*. 129:335-45.
- Delphin, C., T. Guan, F. Melchior, and L. Gerace. 1997. RanGTP targets p97 to RanBP2, a filamentous protein localized at the cytoplasmic periphery of the nuclear pore complex. *Mol Biol Cell*. 8:2379-90.
- Denning, D.P., S.S. Patel, V. Uversky, A.L. Fink, and M. Rexach. 2003. Disorder in the nuclear pore complex: the FG repeat regions of nucleoporins are natively unfolded. *Proc Natl Acad Sci U S A*. 100:2450-5.
- Denning, D.P., V. Uversky, S.S. Patel, A.L. Fink, and M. Rexach. 2002. The *Saccharomyces cerevisiae* nucleoporin Nup2p is a natively unfolded protein. *J Biol Chem*. 277:33447-55.
- Devos, D., S. Dokudovskaya, F. Alber, R. Williams, B.T. Chait, A. Sali, and M.P. Rout. 2004. Components of coated vesicles and nuclear pore complexes share a common molecular architecture. *PLoS Biol*. 2:e380.
- Devos, D., S. Dokudovskaya, R. Williams, F. Alber, N. Eswar, B.T. Chait, M.P. Rout, and A. Sali. 2006. Simple fold composition and modular architecture of the nuclear pore complex. *Proc Natl Acad Sci U S A*. 103:2172-7.
- Dhe-Paganon, S., E.D. Werner, Y.I. Chi, and S.E. Shoelson. 2002. Structure of the globular tail of nuclear lamin. *J Biol Chem*. 277:17381-4.

- Dilworth, D.J., A.J. Tackett, R.S. Rogers, E.C. Yi, R.H. Christmas, J.J. Smith, A.F. Siegel, B.T. Chait, R.W. Wozniak, and J.D. Aitchison. 2005. The mobile nucleoporin Nup2p and chromatin-bound Prp20p function in endogenous NPC-mediated transcriptional control. *J Cell Biol.* 171:955-65.
- Dorner, D., J. Gotzmann, and R. Foisner. 2007. Nucleoplasmic lamins and their interaction partners, LAP2alpha, Rb, and BAF, in transcriptional regulation. *FEBS J.* 274:1362-73.
- Dorner, D., S. Vlcek, N. Foeger, A. Gajewski, C. Makolm, J. Gotzmann, C.J. Hutchison, and R. Foisner. 2006. Lamina-associated polypeptide 2alpha regulates cell cycle progression and differentiation via the retinoblastoma-E2F pathway. *J Cell Biol.* 173:83-93.
- Dwyer, N., and G. Blobel. 1976. A modified procedure for the isolation of a pore complex-lamina fraction from rat liver nuclei. *J Cell Biol.* 70:581-91.
- Dyson, N. 1998. The regulation of E2F by pRB-family proteins. *Genes Dev.* 12:2245-62.
- Eggert, U.S., T.J. Mitchison, and C.M. Field. 2006. Animal cytokinesis: from parts list to mechanisms. *Annu Rev Biochem.* 75:543-66.
- Emterling, A., J. Skoglund, G. Arbman, J. Schneider, S. Evertsson, J. Carstensen, H. Zhang, and X.F. Sun. 2003. Clinicopathological significance of Nup88 expression in patients with colorectal cancer. *Oncology.* 64:361-9.
- Enarson, P., M. Enarson, R. Bastos, and B. Burke. 1998. Amino-terminal sequences that direct nucleoporin nup153 to the inner surface of the nuclear envelope. *Chromosoma.* 107:228-36.
- Eriksson, C., C. Rustum, and E. Hallberg. 2004. Dynamic properties of nuclear pore complex proteins in gp210 deficient cells. *FEBS Lett.* 572:261-5.
- Eriksson, M., W.T. Brown, L.B. Gordon, M.W. Glynn, J. Singer, L. Scott, M.R. Erdos, C.M. Robbins, T.Y. Moses, P. Berglund, A. Dutra, E. Pak, S. Durkin, A.B. Csoka, M. Boehnke, T.W. Glover, and F.S. Collins. 2003. Recurrent de novo point mutations in lamin A cause Hutchinson-Gilford progeria syndrome. *Nature.* 423:293-8.
- Fahrenkrog, B., and U. Aebi. 2003. The nuclear pore complex: nucleocytoplasmic transport and beyond. *Nat Rev Mol Cell Biol.* 4:757-66.
- Fahrenkrog, B., E.C. Hurt, U. Aebi, and N. Pante. 1998. Molecular architecture of the yeast nuclear pore complex: localization of Nsp1p subcomplexes. *J Cell Biol.* 143:577-88.
- Fahrenkrog, B., B. Maco, A.M. Fager, J. Koser, U. Sauder, K.S. Ullman, and U. Aebi. 2002. Domain-specific antibodies reveal multiple-site topology of Nup153 within the nuclear pore complex. *J Struct Biol.* 140:254-67.
- Fang, G., H. Yu, and M.W. Kirschner. 1998. The checkpoint protein MAD2 and the mitotic regulator CDC20 form a ternary complex with the anaphase-promoting complex to control anaphase initiation. *Genes Dev.* 12:1871-83.
- Favreau, C., H.J. Worman, R.W. Wozniak, T. Frappier, and J.C. Courvalin. 1996. Cell cycle-dependent phosphorylation of nucleoporins and nuclear pore membrane protein Gp210. *Biochemistry.* 35:8035-44.
- Fawcett, D.W. 1966. On the occurrence of a fibrous lamina on the inner aspect of the nuclear envelope in certain cells of vertebrates. *Am J Anat.* 119:129-45.
- Feldherr, C., D. Akin, T. Littlewood, and M. Stewart. 2002. The molecular mechanism of translocation through the nuclear pore complex is highly conserved. *J Cell Sci.* 115:2997-3005.
- Fernandez, A.G., and F. Piano. 2006. MEL-28 is downstream of the Ran cycle and is required for nuclear-envelope function and chromatin maintenance. *Curr Biol.* 16:1757-63.
- Feuerbach, F., V. Galy, E. Trelles-Sticken, M. Fromont-Racine, A. Jacquier, E. Gilson, J.C. Olivo-Marin, H. Scherthan, and U. Nehrbass. 2002. Nuclear architecture and spatial positioning help establish transcriptional states of telomeres in yeast. *Nat Cell Biol.* 4:214-21.
- Fischer, T., K. Strasser, A. Racz, S. Rodriguez-Navarro, M. Oppizzi, P. Ihrig, J. Lechner, and E. Hurt. 2002. The mRNA export machinery requires the novel Sac3p-Thp1p complex to dock at the nucleoplasmic entrance of the nuclear pores. *Embo J.* 21:5843-52.

- Foisner, R., and L. Gerace. 1993. Integral membrane proteins of the nuclear envelope interact with lamins and chromosomes, and binding is modulated by mitotic phosphorylation. *Cell*. 73:1267-79.
- Fontoura, B.M., G. Blobel, and M.J. Matunis. 1999. A conserved biogenesis pathway for nucleoporins: proteolytic processing of a 186-kilodalton precursor generates Nup98 and the novel nucleoporin, Nup96. *J Cell Biol*. 144:1097-112.
- Fornerod, M., J. Boer, S. van Baal, M. Jaegle, M. von Lindern, K.G. Murti, D. Davis, J. Bonten, A. Buijs, and G. Grosveld. 1995. Relocation of the carboxyterminal part of CAN from the nuclear envelope to the nucleus as a result of leukemia-specific chromosome rearrangements. *Oncogene*. 10:1739-48.
- Fornerod, M., S. van Baal, V. Valentine, D.N. Shapiro, and G. Grosveld. 1997a. Chromosomal localization of genes encoding CAN/Nup214-interacting proteins--human CRM1 localizes to 2p16, whereas Nup88 localizes to 17p13 and is physically linked to SF2p32. *Genomics*. 42:538-40.
- Fornerod, M., J. van Deursen, S. van Baal, A. Reynolds, D. Davis, K.G. Murti, J. Fransen, and G. Grosveld. 1997b. The human homologue of yeast CRM1 is in a dynamic subcomplex with CAN/Nup214 and a novel nuclear pore component Nup88. *EMBO J*. 16:807-16.
- Fribourg, S., I.C. Braun, E. Izaurralde, and E. Conti. 2001. Structural basis for the recognition of a nucleoporin FG repeat by the NTF2-like domain of the TAP/p15 mRNA nuclear export factor. *Mol Cell*. 8:645-56.
- Frock, R.L., B.A. Kudlow, A.M. Evans, S.A. Jameson, S.D. Hauschka, and B.K. Kennedy. 2006. Lamin A/C and emerin are critical for skeletal muscle satellite cell differentiation. *Genes Dev*. 20:486-500.
- Furukawa, K. 1999. LAP2 binding protein 1 (L2BP1/BAF) is a candidate mediator of LAP2-chromatin interaction. *J Cell Sci*. 112 (Pt 15):2485-92.
- Furukawa, K., K. Ishida, T.A. Tsunoyama, S. Toda, S. Osoda, T. Horigome, P.A. Fisher, and S. Sugiyama. 2009. A-type and B-type lamins initiate layer assembly at distinct areas of the nuclear envelope in living cells. *Exp Cell Res*. 315:1181-9.
- Galy, V., P. Askjaer, C. Franz, C. Lopez-Iglesias, and I.W. Mattaj. 2006. MEL-28, a novel nuclear-envelope and kinetochore protein essential for zygotic nuclear-envelope assembly in *C. elegans*. *Curr Biol*. 16:1748-56.
- Galy, V., I.W. Mattaj, and P. Askjaer. 2003. *Caenorhabditis elegans* nucleoporins Nup93 and Nup205 determine the limit of nuclear pore complex size exclusion in vivo. *Mol Biol Cell*. 14:5104-15.
- Galy, V., J.C. Olivo-Marin, H. Scherthan, V. Doye, N. Rascalou, and U. Nehrbass. 2000. Nuclear pore complexes in the organization of silent telomeric chromatin. *Nature*. 403:108-12.
- Garber, M.E., O.G. Troyanskaya, K. Schluens, S. Petersen, Z. Thaesler, M. Pacyna-Gengelbach, M. van de Rijn, G.D. Rosen, C.M. Perou, R.I. Whyte, R.B. Altman, P.O. Brown, D. Botstein, and I. Petersen. 2001. Diversity of gene expression in adenocarcinoma of the lung. *Proc Natl Acad Sci U S A*. 98:13784-9.
- Gazarian, M., C.T. Cowell, M. Bonney, and W.G. Grigor. 1995. The "4A" syndrome: adrenocortical insufficiency associated with achalasia, alacrima, autonomic and other neurological abnormalities. *Eur J Pediatr*. 154:18-23.
- Ghannam, G., A. Takeda, T. Camarata, M.A. Moore, A. Viale, and N.R. Yaseen. 2004. The oncogene Nup98-HOXA9 induces gene transcription in myeloid cells. *J Biol Chem*. 279:866-75.
- Goizet, C., B. Catargi, F. Tison, A. Tullio-Pelet, S. Hadj-Rabia, F. Pujol, A. Lagueny, S. Lyonnet, and D. Lacombe. 2002. Progressive bulbospinal amyotrophy in triple A syndrome with AAAS gene mutation. *Neurology*. 58:962-5.
- Gould, V.E., N. Martinez, A. Orucevic, J. Schneider, and A. Alonso. 2000. A novel, nuclear pore-associated, widely distributed molecule overexpressed in oncogenesis and development. *Am J Pathol*. 157:1605-13.

- Gould, V.E., A. Orucevic, H. Zentgraf, P. Gattuso, N. Martinez, and A. Alonso. 2002. Nup88 (karyoporin) in human malignant neoplasms and dysplasias: correlations of immunostaining of tissue sections, cytologic smears, and immunoblot analysis. *Hum Pathol.* 33:536-44.
- Graham, F.L., J. Smiley, W.C. Russell, and R. Nairn. 1977. Characteristics of a human cell line transformed by DNA from human adenovirus type 5. *J Gen Virol.* 36:59-74.
- Grandi, P., T. Dang, N. Pane, A. Shevchenko, M. Mann, D. Forbes, and E. Hurt. 1997. Nup93, a vertebrate homologue of yeast Nic96p, forms a complex with a novel 205-kDa protein and is required for correct nuclear pore assembly. *Mol Biol Cell.* 8:2017-38.
- Grandi, P., N. Schlaich, H. Tekotte, and E.C. Hurt. 1995. Functional interaction of Nic96p with a core nucleoporin complex consisting of Nsp1p, Nup49p and a novel protein Nup57p. *Embo J.* 14:76-87.
- Graux, C., J. Cools, C. Melotte, H. Quentmeier, A. Ferrando, R. Levine, J.R. Vermeesch, M. Stul, B. Dutta, N. Boeckx, A. Bosly, P. Heimann, A. Uyttebroeck, N. Mentens, R. Somers, R.A. MacLeod, H.G. Drexler, A.T. Look, D.G. Gilliland, L. Michaux, P. Vandenberghe, I. Wlodarska, P. Marynen, and A. Hagemeijer. 2004. Fusion of NUP214 to ABL1 on amplified episomes in T-cell acute lymphoblastic leukemia. *Nat Genet.* 36:1084-9.
- Greber, U.F., A. Senior, and L. Gerace. 1990. A major glycoprotein of the nuclear pore complex is a membrane-spanning polypeptide with a large luminal domain and a small cytoplasmic tail. *Embo J.* 9:1495-502.
- Greco, A., M.A. Pierotti, I. Bongarzone, S. Pagliardini, C. Lanzi, and G. Della Porta. 1992. TRK-T1 is a novel oncogene formed by the fusion of TPR and TRK genes in human papillary thyroid carcinomas. *Oncogene.* 7:237-42.
- Gregorio, G.V., K. Choudhuri, Y. Ma, A. Vegnente, G. Mieli-Vergani, and D. Vergani. 1999. Mimicry between the hepatitis B virus DNA polymerase and the antigenic targets of nuclear and smooth muscle antibodies in chronic hepatitis B virus infection. *J Immunol.* 162:1802-10.
- Griffis, E.R., N. Altan, J. Lippincott-Schwartz, and M.A. Powers. 2002. Nup98 is a mobile nucleoporin with transcription-dependent dynamics. *Mol Biol Cell.* 13:1282-97.
- Griffis, E.R., B. Craige, C. Dimaano, K.S. Ullman, and M.A. Powers. 2004. Distinct functional domains within nucleoporins Nup153 and Nup98 mediate transcription-dependent mobility. *Mol Biol Cell.* 15:1991-2002.
- Griffis, E.R., S. Xu, and M.A. Powers. 2003. Nup98 localizes to both nuclear and cytoplasmic sides of the nuclear pore and binds to two distinct nucleoporin subcomplexes. *Mol Biol Cell.* 14:600-10.
- Gruenbaum, Y., R.D. Goldman, R. Meyuhas, E. Mills, A. Margalit, A. Fridkin, Y. Dayani, M. Prokocimer, and A. Enosh. 2003. The nuclear lamina and its functions in the nucleus. *Int Rev Cytol.* 226:1-62.
- Gruenbaum, Y., A. Margalit, R.D. Goldman, D.K. Shumaker, and K.L. Wilson. 2005. The nuclear lamina comes of age. *Nat Rev Mol Cell Biol.* 6:21-31.
- Haigis, K., J. Sage, J. Glickman, S. Shafer, and T. Jacks. 2006. The related retinoblastoma (pRb) and p130 proteins cooperate to regulate homeostasis in the intestinal epithelium. *J Biol Chem.* 281:638-47.
- Handa, N., M. Kukimoto-Niino, R. Akasaka, S. Kishishita, K. Murayama, T. Terada, M. Inoue, T. Kigawa, S. Kose, N. Imamoto, A. Tanaka, Y. Hayashizaki, M. Shirouzu, and S. Yokoyama. 2006. The crystal structure of mouse Nup35 reveals atypical RNP motifs and novel homodimerization of the RRM domain. *J Mol Biol.* 363:114-24.
- Handschug, K., S. Sperling, S.J. Yoon, S. Hennig, A.J. Clark, and A. Huebner. 2001. Triple A syndrome is caused by mutations in AAAS, a new WD-repeat protein gene. *Hum Mol Genet.* 10:283-90.
- Hansen, J.B., C. Jorgensen, R.K. Petersen, P. Hallenborg, R. De Matteis, H.A. Boye, N. Petrovic, S. Enerback, J. Nedergaard, S. Cinti, H. te Riele, and K. Kristiansen. 2004.

- Retinoblastoma protein functions as a molecular switch determining white versus brown adipocyte differentiation. *Proc Natl Acad Sci U S A.* 101:4112-7.
- Harborth, J., S.M. Elbashir, K. Bechert, T. Tuschl, and K. Weber. 2001. Identification of essential genes in cultured mammalian cells using small interfering RNAs. *J Cell Sci.* 114:4557-65.
- Harel, A., A.V. Orjalo, T. Vincent, A. Lachish-Zalait, S. Vasu, S. Shah, E. Zimmerman, M. Elbaum, and D.J. Forbes. 2003. Removal of a single pore subcomplex results in vertebrate nuclei devoid of nuclear pores. *Mol Cell.* 11:853-64.
- Harper, N.C., N.T. Al-Greene, M.A. Basrai, and K.D. Belanger. 2008. Mutations affecting spindle pole body and mitotic exit network function are synthetically lethal with a deletion of the nucleoporin NUP1 in *S. cerevisiae*. *Curr Genet.* 53:95-105.
- Harris, C.A., P.J. Andryuk, S. Cline, H.K. Chan, A. Natarajan, J.J. Siekierka, and G. Goldstein. 1994. Three distinct human thymopoietins are derived from alternatively spliced mRNAs. *Proc Natl Acad Sci U S A.* 91:6283-7.
- Hase, M.E., and V.C. Cordes. 2003. Direct interaction with nup153 mediates binding of Tpr to the periphery of the nuclear pore complex. *Mol Biol Cell.* 14:1923-40.
- Hawryluk-Gara, L.A., E.K. Shibuya, and R.W. Wozniak. 2005. Vertebrate Nup53 interacts with the nuclear lamina and is required for the assembly of a Nup93-containing complex. *Mol Biol Cell.* 16:2382-94.
- Hays, J.L., and S.J. Watowich. 2003. Oligomerization-induced modulation of TPR-MET tyrosine kinase activity. *J Biol Chem.* 278:27456-63.
- Heidenblad, M., D. Lindgren, T. Jonson, F. Liedberg, S. Veerla, G. Chebil, S. Gudjonsson, A. Borg, W. Mansson, and M. Hoglund. 2008. Tiling resolution array CGH and high density expression profiling of urothelial carcinomas delineate genomic amplicons and candidate target genes specific for advanced tumors. *BMC Med Genomics.* 1:3.
- Hernando, E., Z. Nahle, G. Juan, E. Diaz-Rodriguez, M. Alaminos, M. Hemann, L. Michel, V. Mittal, W. Gerald, R. Benezra, S.W. Lowe, and C. Cordon-Cardo. 2004. Rb inactivation promotes genomic instability by uncoupling cell cycle progression from mitotic control. *Nature.* 430:797-802.
- Herrmann, H., and U. Aebi. 2004. Intermediate filaments: molecular structure, assembly mechanism, and integration into functionally distinct intracellular Scaffolds. *Annu Rev Biochem.* 73:749-89.
- Herrmann, H., H. Bar, L. Kreplak, S.V. Strelkov, and U. Aebi. 2007. Intermediate filaments: from cell architecture to nanomechanics. *Nat Rev Mol Cell Biol.* 8:562-73.
- Higa, M.M., S.L. Alam, W.I. Sundquist, and K.S. Ullman. 2007. Molecular characterization of the Ran-binding zinc finger domain of Nup153. *J Biol Chem.* 282:17090-100.
- Hinshaw, J.E., B.O. Carragher, and R.A. Milligan. 1992. Architecture and design of the nuclear pore complex. *Cell.* 69:1133-41.
- Hodel, A.E., M.R. Hodel, E.R. Griffis, K.A. Hennig, G.A. Ratner, S. Xu, and M.A. Powers. 2002. The three-dimensional structure of the autoproteolytic, nuclear pore-targeting domain of the human nucleoporin Nup98. *Mol Cell.* 10:347-58.
- Holaska, J.M., K.L. Wilson, and M. Mansharamani. 2002. The nuclear envelope, lamins and nuclear assembly. *Curr Opin Cell Biol.* 14:357-64.
- Houlden, H., S. Smith, M. De Carvalho, J. Blake, C. Mathias, N.W. Wood, and M.M. Reilly. 2002. Clinical and genetic characterization of families with triple A (Allgrove) syndrome. *Brain.* 125:2681-90.
- Hozak, P., A.M. Sasseville, Y. Raymond, and P.R. Cook. 1995. Lamin proteins form an internal nucleoskeleton as well as a peripheral lamina in human cells. *J Cell Sci.* 108 (Pt 2):635-44.
- Hsia, K.C., P. Stavropoulos, G. Blobel, and A. Hoelz. 2007. Architecture of a coat for the nuclear pore membrane. *Cell.* 131:1313-26.

- Huh, M.S., M.H. Parker, A. Scime, R. Parks, and M.A. Rudnicki. 2004. Rb is required for progression through myogenic differentiation but not maintenance of terminal differentiation. *J Cell Biol.* 166:865-76.
- Hutchison, C.J. 2002. Lamins: building blocks or regulators of gene expression? *Nat Rev Mol Cell Biol.* 3:848-58.
- Hutchison, C.J., M. Alvarez-Reyes, and O.A. Vaughan. 2001. Lamins in disease: why do ubiquitously expressed nuclear envelope proteins give rise to tissue-specific disease phenotypes? *J Cell Sci.* 114:9-19.
- Hutchison, C.J., and H.J. Worman. 2004. A-type lamins: guardians of the soma? *Nat Cell Biol.* 6:1062-7.
- Hutten, S., and R.H. Kehlenbach. 2006. Nup214 is required for CRM1-dependent nuclear protein export in vivo. *Mol Cell Biol.* 26:6772-85.
- Hwang, L.H., L.F. Lau, D.L. Smith, C.A. Mistrot, K.G. Hardwick, E.S. Hwang, A. Amon, and A.W. Murray. 1998. Budding yeast Cdc20: a target of the spindle checkpoint. *Science.* 279:1041-4.
- Invernizzi, P., M. Podda, P.M. Battezzati, A. Crosignani, M. Zuin, E. Hitchman, M. Maggioni, P.L. Meroni, E. Penner, and J. Wesierska-Gadek. 2001. Autoantibodies against nuclear pore complexes are associated with more active and severe liver disease in primary biliary cirrhosis. *J Hepatol.* 34:366-72.
- Iouk, T., O. Kerscher, R.J. Scott, M.A. Basrai, and R.W. Wozniak. 2002. The yeast nuclear pore complex functionally interacts with components of the spindle assembly checkpoint. *J Cell Biol.* 159:807-19.
- Ishii, K., G. Arib, C. Lin, G. Van Houwe, and U.K. Laemmli. 2002. Chromatin boundaries in budding yeast: the nuclear pore connection. *Cell.* 109:551-62.
- Itoh, S., T. Ichida, T. Yoshida, A. Hayakawa, M. Uchida, T. Tashiro-Itoh, Y. Matsuda, K. Ishihara, and H. Asakura. 1998. Autoantibodies against a 210 kDa glycoprotein of the nuclear pore complex as a prognostic marker in patients with primary biliary cirrhosis. *J Gastroenterol Hepatol.* 13:257-65.
- Jackson, M.W., M.K. Agarwal, J. Yang, P. Bruss, T. Uchiumi, M.L. Agarwal, G.R. Stark, and W.R. Taylor. 2005. p130/p107/p105Rb-dependent transcriptional repression during DNA-damage-induced cell-cycle exit at G2. *J Cell Sci.* 118:1821-32.
- Jankovic, D., P. Gorello, T. Liu, S. Ehret, R. La Starza, C. Desjobert, F. Baty, M. Brutsche, P.S. Jayaraman, A. Santoro, C. Mecucci, and J. Schwaller. 2008. Leukemogenic mechanisms and targets of a NUP98/HHEX fusion in acute myeloid leukemia. *Blood.* 111:5672-82.
- Jeganathan, K.B., D.J. Baker, and J.M. van Deursen. 2006. Securin associates with APCCdh1 in prometaphase but its destruction is delayed by Rae1 and Nup98 until the metaphase/anaphase transition. *Cell Cycle.* 5:366-70.
- Jeganathan, K.B., L. Malureanu, and J.M. van Deursen. 2005. The Rae1-Nup98 complex prevents aneuploidy by inhibiting securin degradation. *Nature.* 438:1036-9.
- Jeady, S., and T.U. Schwartz. 2007. Crystal structure of nucleoporin Nic96 reveals a novel, intricate helical domain architecture. *J Biol Chem.* 282:34904-12.
- Jin, D.Y., F. Spencer, and K.T. Jeang. 1998. Human T cell leukemia virus type 1 oncoprotein Tax targets the human mitotic checkpoint protein MAD1. *Cell.* 93:81-91.
- Johnson, B.R., R.T. Nitta, R.L. Frock, L. Mounkes, D.A. Barbie, C.L. Stewart, E. Harlow, and B.K. Kennedy. 2004. A-type lamins regulate retinoblastoma protein function by promoting subnuclear localization and preventing proteasomal degradation. *Proc Natl Acad Sci U S A.* 101:9677-82.
- Joseph, J., S.T. Liu, S.A. Jablonski, T.J. Yen, and M. Dasso. 2004. The RanGAP1-RanBP2 complex is essential for microtubule-kinetochore interactions in vivo. *Curr Biol.* 14:611-7.
- Joseph, J., S.H. Tan, T.S. Karpova, J.G. McNally, and M. Dasso. 2002. SUMO-1 targets RanGAP1 to kinetochores and mitotic spindles. *J Cell Biol.* 156:595-602.

- Kaelin, W.G., Jr. 1999. Functions of the retinoblastoma protein. *Bioessays*. 21:950-8.
- Kalverda, B., H. Pickersgill, V.V. Shloma, and M. Fornerod. Nucleoporins Directly Stimulate Expression of Developmental and Cell-Cycle Genes Inside the Nucleoplasm. *Cell*. 140:360-371.
- Kasper, L.H., P.K. Brindle, C.A. Schnabel, C.E. Pritchard, M.L. Cleary, and J.M. van Deursen. 1999. CREB binding protein interacts with nucleoporin-specific FG repeats that activate transcription and mediate NUP98-HOXA9 oncogenicity. *Mol Cell Biol*. 19:764-76.
- Kastenmayer, J.P., M.S. Lee, A.L. Hong, F.A. Spencer, and M.A. Basrai. 2005. The C-terminal half of *Saccharomyces cerevisiae* Mad1p mediates spindle checkpoint function, chromosome transmission fidelity and CEN association. *Genetics*. 170:509-17.
- Kau, T.R., J.C. Way, and P.A. Silver. 2004. Nuclear transport and cancer: from mechanism to intervention. *Nat Rev Cancer*. 4:106-17.
- Kehlenbach, R.H., A. Dickmanns, A. Kehlenbach, T. Guan, and L. Gerace. 1999. A role for RanBP1 in the release of CRM1 from the nuclear pore complex in a terminal step of nuclear export. *J Cell Biol*. 145:645-57.
- Khelif, K., M.H. De Laet, B. Chaouachi, V. Segers, and J.M. Vanderwinden. 2003. Achalasia of the cardia in Allgrove's (triple A) syndrome: histopathologic study of 10 cases. *Am J Surg Pathol*. 27:667-72.
- Kim, S.H., D.P. Lin, S. Matsumoto, A. Kitazono, and T. Matsumoto. 1998. Fission yeast Slp1: an effector of the Mad2-dependent spindle checkpoint. *Science*. 279:1045-7.
- Kimber, J., B.N. McLean, M. Prevett, and S.R. Hammans. 2003. Allgrove or 4 "A" syndrome: an autosomal recessive syndrome causing multisystem neurological disease. *J Neurol Neurosurg Psychiatry*. 74:654-7.
- King, H.W., P.R. Tempest, K.R. Merrifield, and A.J. Rance. 1988. tpr homologues activate met and raf. *Oncogene*. 2:617-9.
- King, R.W. 2008. When 2+2=5: the origins and fates of aneuploid and tetraploid cells. *Biochim Biophys Acta*. 1786:4-14.
- Kiseleva, E., T.D. Allen, S. Rutherford, M. Bucci, S.R. Wentz, and M.W. Goldberg. 2004. Yeast nuclear pore complexes have a cytoplasmic ring and internal filaments. *J Struct Biol*. 145:272-88.
- Kiseleva, E., M.W. Goldberg, T.D. Allen, and C.W. Akey. 1998. Active nuclear pore complexes in *Chironomus*: visualization of transporter configurations related to mRNP export. *J Cell Sci*. 111 (Pt 2):223-36.
- Kitagawa, M., H. Higashi, I.S. Takahashi, T. Okabe, H. Ogino, Y. Taya, S. Hishimura, and A. Okuyama. 1994. A cyclin-dependent kinase inhibitor, butyrolactone I, inhibits phosphorylation of RB protein and cell cycle progression. *Oncogene*. 9:2549-57.
- Kitano, H. 2004. Biological robustness. *Nat Rev Genet*. 5:826-37.
- Klemm, J.D., C.R. Beals, and G.R. Crabtree. 1997. Rapid targeting of nuclear proteins to the cytoplasm. *Curr Biol*. 7:638-44.
- Knoess, M., A.K. Kurz, O. Goreva, N. Bektas, K. Breuhahn, M. Odenthal, P. Schirmacher, H.P. Dienes, C.T. Bock, H. Zentgraf, and A. zur Hausen. 2006. Nucleoporin 88 expression in hepatitis B and C virus-related liver diseases. *World J Gastroenterol*. 12:5870-4.
- Kodiha, M., P. Banski, D. Ho-Wo-Cheong, and U. Stochaj. 2008a. Dissection of the molecular mechanisms that control the nuclear accumulation of transport factors importin-alpha and CAS in stressed cells. *Cell Mol Life Sci*. 65:1756-67.
- Kodiha, M., D. Tran, C. Qian, A. Morogan, J.F. Presley, C.M. Brown, and U. Stochaj. 2008b. Oxidative stress mislocalizes and retains transport factor importin-alpha and nucleoporins Nup153 and Nup88 in nuclei where they generate high molecular mass complexes. *Biochim Biophys Acta*. 1783:405-18.
- Kops, G.J., B.A. Weaver, and D.W. Cleveland. 2005. On the road to cancer: aneuploidy and the mitotic checkpoint. *Nat Rev Cancer*. 5:773-85.

- Korenjak, M., and A. Brehm. 2005. E2F-Rb complexes regulating transcription of genes important for differentiation and development. *Curr Opin Genet Dev.* 15:520-7.
- Kosova, B., N. Pante, C. Rollenhagen, and E. Hurt. 1999. Nup192p is a conserved nucleoporin with a preferential location at the inner site of the nuclear membrane. *J Biol Chem.* 274:22646-51.
- Kraemer, D., R.W. Wozniak, G. Blobel, and A. Radu. 1994. The human CAN protein, a putative oncogene product associated with myeloid leukemogenesis, is a nuclear pore complex protein that faces the cytoplasm. *Proc Natl Acad Sci U S A.* 91:1519-23.
- Krimm, I., C. Ostlund, B. Gilquin, J. Couprie, P. Hossenlopp, J.P. Mornon, G. Bonne, J.C. Courvalin, H.J. Worman, and S. Zinn-Justin. 2002. The Ig-like structure of the C-terminal domain of lamin A/C, mutated in muscular dystrophies, cardiomyopathy, and partial lipodystrophy. *Structure.* 10:811-23.
- Kroon, E., U. Thorsteinsdottir, N. Mayotte, T. Nakamura, and G. Sauvageau. 2001. NUP98-HOXA9 expression in hemopoietic stem cells induces chronic and acute myeloid leukemias in mice. *EMBO J.* 20:350-61.
- Krull, S., J. Thyberg, B. Bjorkroth, H.R. Rackwitz, and V.C. Cordes. 2004. Nucleoporins as components of the nuclear pore complex core structure and Tpr as the architectural element of the nuclear basket. *Mol Biol Cell.* 15:4261-77.
- Lam, D.H., and P.D. Aplan. 2001. NUP98 gene fusions in hematologic malignancies. *Leukemia.* 15:1689-95.
- Lau, C.K., T.H. Giddings, Jr., and M. Winey. 2004. A novel allele of *Saccharomyces cerevisiae* NDC1 reveals a potential role for the spindle pole body component Ndc1p in nuclear pore assembly. *Eukaryot Cell.* 3:447-58.
- Lee, S.H., H. Sterling, A. Burlingame, and F. McCormick. 2008. Tpr directly binds to Mad1 and Mad2 and is important for the Mad1-Mad2-mediated mitotic spindle checkpoint. *Genes Dev.* 22:2926-31.
- Lehner, C.F., V. Kurer, H.M. Eppenberger, and E.A. Nigg. 1986. The nuclear lamin protein family in higher vertebrates. Identification of quantitatively minor lamin proteins by monoclonal antibodies. *J Biol Chem.* 261:13293-301.
- Lenz-Bohme, B., J. Wismar, S. Fuchs, R. Reifegerste, E. Buchner, H. Betz, and B. Schmitt. 1997. Insertional mutation of the *Drosophila* nuclear lamin Dm0 gene results in defective nuclear envelopes, clustering of nuclear pore complexes, and accumulation of annulate lamellae. *J Cell Biol.* 137:1001-16.
- Li, M., A. Makkinje, and Z. Damuni. 1996. The myeloid leukemia-associated protein SET is a potent inhibitor of protein phosphatase 2A. *J Biol Chem.* 271:11059-62.
- Li, R. 2007. Cytokinesis in development and disease: variations on a common theme. *Cell Mol Life Sci.* 64:3044-58.
- Li, Y., C. Gorbea, D. Mahaffey, M. Rechsteiner, and R. Benzra. 1997. MAD2 associates with the cyclosome/anaphase-promoting complex and inhibits its activity. *Proc Natl Acad Sci U S A.* 94:12431-6.
- Lim, R.Y., U. Aebi, and B. Fahrenkrog. 2008. Towards reconciling structure and function in the nuclear pore complex. *Histochem Cell Biol.* 129:105-16.
- Lim, R.Y., U. Aebi, and D. Stoffler. 2006. From the trap to the basket: getting to the bottom of the nuclear pore complex. *Chromosoma.* 115:15-26.
- Lim, R.Y., and B. Fahrenkrog. 2006. The nuclear pore complex up close. *Curr Opin Cell Biol.* 18:342-7.
- Lin, F., D.L. Blake, I. Callebaut, I.S. Skerjanc, L. Holmer, M.W. McBurney, M. Paulin-Levasseur, and H.J. Worman. 2000. MAN1, an inner nuclear membrane protein that shares the LEM domain with lamina-associated polypeptide 2 and emerin. *J Biol Chem.* 275:4840-7.
- Lipinski, M.M., and T. Jacks. 1999. The retinoblastoma gene family in differentiation and development. *Oncogene.* 18:7873-82.

- Liu, J., A.J. Prunuske, A.M. Fager, and K.S. Ullman. 2003. The COPI complex functions in nuclear envelope breakdown and is recruited by the nucleoporin Nup153. *Dev Cell*. 5:487-98.
- Liu, J., T. Rolef Ben-Shahar, D. Riemer, M. Treinin, P. Spann, K. Weber, A. Fire, and Y. Gruenbaum. 2000. Essential roles for *Caenorhabditis elegans* lamin gene in nuclear organization, cell cycle progression, and spatial organization of nuclear pore complexes. *Mol Biol Cell*. 11:3937-47.
- Liu, S.M., and M. Stewart. 2005. Structural basis for the high-affinity binding of nucleoporin Nup1p to the *Saccharomyces cerevisiae* importin-beta homologue, Kap95p. *J Mol Biol*. 349:515-25.
- Lloyd, D.J., R.C. Trembath, and S. Shackleton. 2002. A novel interaction between lamin A and SREBP1: implications for partial lipodystrophy and other laminopathies. *Hum Mol Genet*. 11:769-77.
- Loewinger, L., and F. McKeon. 1988. Mutations in the nuclear lamin proteins resulting in their aberrant assembly in the cytoplasm. *EMBO J*. 7:2301-9.
- Loidice, I., A. Alves, G. Rabut, M. Van Overbeek, J. Ellenberg, J.B. Sibarita, and V. Doye. 2004. The entire Nup107-160 complex, including three new members, is targeted as one entity to kinetochores in mitosis. *Mol Biol Cell*. 15:3333-44.
- Lucchesi, J.C., W.G. Kelly, and B. Panning. 2005. Chromatin remodeling in dosage compensation. *Annu Rev Genet*. 39:615-51.
- Lupu, F., A. Alves, K. Anderson, V. Doye, and E. Lacy. 2008. Nuclear pore composition regulates neural stem/progenitor cell differentiation in the mouse embryo. *Dev Cell*. 14:831-42.
- Lussi, Y.C., D.K. Shumaker, T. Shimi, and B. Fahrenkrog. 2010. The nucleoporin Nup153 affects spindle checkpoint activity due to an association with Mad1. *Nucleus*. 1.
- Luthra, R., S.C. Kerr, M.T. Harreman, L.H. Apponi, M.B. Fasken, S. Ramineni, S. Chaurasia, S.R. Valentini, and A.H. Corbett. 2007. Actively transcribed GAL genes can be physically linked to the nuclear pore by the SAGA chromatin modifying complex. *J Biol Chem*. 282:3042-9.
- Lutzmann, M., R. Kunze, A. Buerer, U. Aebi, and E. Hurt. 2002. Modular self-assembly of a Y-shaped multiprotein complex from seven nucleoporins. *Embo J*. 21:387-97.
- Ly, D.H., D.J. Lockhart, R.A. Lerner, and P.G. Schultz. 2000. Mitotic misregulation and human aging. *Science*. 287:2486-92.
- Ma, Z., D.A. Hill, M.H. Collins, S.W. Morris, J. Sumegi, M. Zhou, C. Zuppan, and J.A. Bridge. 2003. Fusion of ALK to the Ran-binding protein 2 (RANBP2) gene in inflammatory myofibroblastic tumor. *Genes Chromosomes Cancer*. 37:98-105.
- Mackay, D.R., S.W. Elgort, and K.S. Ullman. 2009. The nucleoporin Nup153 has separable roles in both early mitotic progression and the resolution of mitosis. *Mol Biol Cell*. 20:1652-60.
- Madrid, A.S., J. Mancuso, W.Z. Cande, and K. Weis. 2006. The role of the integral membrane nucleoporins Ndc1p and Pom152p in nuclear pore complex assembly and function. *J Cell Biol*. 173:361-71.
- Maeshima, K., K. Yahata, Y. Sasaki, R. Nakatomi, T. Tachibana, T. Hashikawa, F. Imamoto, and N. Imamoto. 2006. Cell-cycle-dependent dynamics of nuclear pores: pore-free islands and lamins. *J Cell Sci*. 119:4442-51.
- Mancini, M.A., B. Shan, J.A. Nickerson, S. Penman, and W.H. Lee. 1994. The retinoblastoma gene product is a cell cycle-dependent, nuclear matrix-associated protein. *Proc Natl Acad Sci U S A*. 91:418-22.
- Manfioletti, G., V. Gattei, E. Buratti, A. Rustighi, A. De Iuliis, D. Aldinucci, G.H. Goodwin, and A. Pinto. 1995. Differential expression of a novel proline-rich homeobox gene (Prh) in human hematolymphopoietic cells. *Blood*. 85:1237-45.
- Mansfeld, J., S. Guttinger, L.A. Hawryluk-Gara, N. Pante, M. Mall, V. Galy, U. Haselmann, P. Muhlhauser, R.W. Wozniak, I.W. Mattaj, U. Kutay, and W. Antonin. 2006. The

- conserved transmembrane nucleoporin NDC1 is required for nuclear pore complex assembly in vertebrate cells. *Mol Cell*. 22:93-103.
- Marelli, M., C.P. Lusk, H. Chan, J.D. Aitchison, and R.W. Wozniak. 2001. A link between the synthesis of nucleoporins and the biogenesis of the nuclear envelope. *J Cell Biol*. 153:709-24.
- Markiewicz, E., T. Dechat, R. Foisner, R.A. Quinlan, and C.J. Hutchison. 2002. Lamin A/C binding protein LAP2alpha is required for nuclear anchorage of retinoblastoma protein. *Mol Biol Cell*. 13:4401-13.
- Markiewicz, E., M. Ledran, and C.J. Hutchison. 2005. Remodelling of the nuclear lamina and nucleoskeleton is required for skeletal muscle differentiation in vitro. *J Cell Sci*. 118:409-20.
- Martinez, N., A. Alonso, M.D. Moragues, J. Ponton, and J. Schneider. 1999. The nuclear pore complex protein Nup88 is overexpressed in tumor cells. *Cancer Res*. 59:5408-11.
- Matunis, M.J., E. Coutavas, and G. Blobel. 1996. A novel ubiquitin-like modification modulates the partitioning of the Ran-GTPase-activating protein RanGAP1 between the cytosol and the nuclear pore complex. *J Cell Biol*. 135:1457-70.
- Melcak, I., A. Hoelz, and G. Blobel. 2007. Structure of Nup58/45 suggests flexible nuclear pore diameter by intermolecular sliding. *Science*. 315:1729-32.
- Mendjan, S., and A. Akhtar. 2007. The right dose for every sex. *Chromosoma*. 116:95-106.
- Mendjan, S., M. Taipale, J. Kind, H. Holz, P. Gebhardt, M. Schelder, M. Vermeulen, A. Buscaino, K. Duncan, J. Mueller, M. Wilm, H.G. Stunnenberg, H. Saumweber, and A. Akhtar. 2006. Nuclear pore components are involved in the transcriptional regulation of dosage compensation in *Drosophila*. *Mol Cell*. 21:811-23.
- Menon, B.B., N.J. Sarma, S. Pasula, S.J. Deminoff, K.A. Willis, K.E. Barbara, B. Andrews, and G.M. Santangelo. 2005. Reverse recruitment: the Nup84 nuclear pore subcomplex mediates Rap1/Gcr1/Gcr2 transcriptional activation. *Proc Natl Acad Sci U S A*. 102:5749-54.
- Michel, L.S., V. Liberal, A. Chatterjee, R. Kirchwegger, B. Pasche, W. Gerald, M. Dobles, P.K. Sorger, V.V. Murty, and R. Benezra. 2001. MAD2 haplo-insufficiency causes premature anaphase and chromosome instability in mammalian cells. *Nature*. 409:355-9.
- Miller, B.R., M. Powers, M. Park, W. Fischer, and D.J. Forbes. 2000. Identification of a new vertebrate nucleoporin, Nup188, with the use of a novel organelle trap assay. *Mol Biol Cell*. 11:3381-96.
- Mittnacht, S., and R.A. Weinberg. 1991. G1/S phosphorylation of the retinoblastoma protein is associated with an altered affinity for the nuclear compartment. *Cell*. 65:381-93.
- Moir, R.D., T.P. Spann, and R.D. Goldman. 1995. The dynamic properties and possible functions of nuclear lamins. *Int Rev Cytol*. 162B:141-82.
- Moir, R.D., T.P. Spann, H. Herrmann, and R.D. Goldman. 2000a. Disruption of nuclear lamin organization blocks the elongation phase of DNA replication. *J Cell Biol*. 149:1179-92.
- Moir, R.D., M. Yoon, S. Khuon, and R.D. Goldman. 2000b. Nuclear lamins A and B1: different pathways of assembly during nuclear envelope formation in living cells. *J Cell Biol*. 151:1155-68.
- Moore, P.S., R.M. Couch, Y.S. Perry, E.P. Shuckett, and J.S. Winter. 1991. Allgrove syndrome: an autosomal recessive syndrome of ACTH insensitivity, achalasia and alacrima. *Clin Endocrinol (Oxf)*. 34:107-14.
- Moran, E. 1993. Interaction of adenoviral proteins with pRB and p53. *FASEB J*. 7:880-5.
- Morgutti, M., E. Demori, V. Pecile, A. Amoroso, A. Rustighi, and G. Manfioletti. 2001. Genomic organization and chromosome mapping of the human homeobox gene HHEX. *Cytogenet Cell Genet*. 94:30-2.
- Mounkes, L., S. Kozlov, B. Burke, and C.L. Stewart. 2003. The laminopathies: nuclear structure meets disease. *Curr Opin Genet Dev*. 13:223-30.

- Mounkes, L.C., and C.L. Stewart. 2004. Aging and nuclear organization: lamins and progeria. *Curr Opin Cell Biol.* 16:322-7.
- Muralikrishna, B., S. Thanumalayan, G. Jagatheesan, N. Rangaraj, A.A. Karande, and V.K. Parnaik. 2004. Immunolocalization of detergent-susceptible nucleoplasmic lamin A/C foci by a novel monoclonal antibody. *J Cell Biochem.* 91:730-9.
- Musacchio, A., and E.D. Salmon. 2007. The spindle-assembly checkpoint in space and time. *Nat Rev Mol Cell Biol.* 8:379-93.
- Naetar, N., and R. Foisner. 2009. Lamin complexes in the nuclear interior control progenitor cell proliferation and tissue homeostasis. *Cell Cycle.* 8:1488-93.
- Naetar, N., B. Korbei, S. Kozlov, M.A. Kerényi, D. Dorner, R. Kral, I. Gotic, P. Fuchs, T.V. Cohen, R. Bittner, C.L. Stewart, and R. Foisner. 2008. Loss of nucleoplasmic LAP2alpha-lamin A complexes causes erythroid and epidermal progenitor hyperproliferation. *Nat Cell Biol.* 10:1341-8.
- Nakamura, T., D.A. Largaespada, M.P. Lee, L.A. Johnson, K. Ohyashiki, K. Toyama, S.J. Chen, C.L. Willman, I.M. Chen, A.P. Feinberg, N.A. Jenkins, N.G. Copeland, and J.D. Shaughnessy, Jr. 1996. Fusion of the nucleoporin gene NUP98 to HOXA9 by the chromosome translocation t(7;11)(p15;p15) in human myeloid leukaemia. *Nat Genet.* 12:154-8.
- Nakielny, S., S. Shaikh, B. Burke, and G. Dreyfuss. 1999. Nup153 is an M9-containing mobile nucleoporin with a novel Ran-binding domain. *Embo J.* 18:1982-95.
- Napetschnig, J., G. Blobel, and A. Hoelz. 2007. Crystal structure of the N-terminal domain of the human protooncogene Nup214/CAN. *Proc Natl Acad Sci U S A.* 104:1783-8.
- Nehrbass, U., M.P. Rout, S. Maguire, G. Blobel, and R.W. Wozniak. 1996. The yeast nucleoporin Nup188p interacts genetically and physically with the core structures of the nuclear pore complex. *J Cell Biol.* 133:1153-62.
- Nitta, R.T., S.A. Jameson, B.A. Kudlow, L.A. Conlan, and B.K. Kennedy. 2006. Stabilization of the retinoblastoma protein by A-type nuclear lamins is required for INK4A-mediated cell cycle arrest. *Mol Cell Biol.* 26:5360-72.
- Nybakken, K., S.A. Vokes, T.Y. Lin, A.P. McMahon, and N. Perrimon. 2005. A genome-wide RNA interference screen in *Drosophila melanogaster* cells for new components of the Hh signaling pathway. *Nat Genet.* 37:1323-32.
- Orjalo, A.V., A. Arnaoutov, Z. Shen, Y. Boyarchuk, S.G. Zeitlin, B. Fontoura, S. Briggs, M. Dasso, and D.J. Forbes. 2006. The Nup107-160 nucleoporin complex is required for correct bipolar spindle assembly. *Mol Biol Cell.* 17:3806-18.
- Orlic, M., C.E. Spencer, L. Wang, and B.L. Gallie. 2006. Expression analysis of 6p22 genomic gain in retinoblastoma. *Genes Chromosomes Cancer.* 45:72-82.
- Osouda, S., Y. Nakamura, B. de Saint Phalle, M. McConnell, T. Horigome, S. Sugiyama, P.A. Fisher, and K. Furukawa. 2005. Null mutants of *Drosophila* B-type lamin Dm(0) show aberrant tissue differentiation rather than obvious nuclear shape distortion or specific defects during cell proliferation. *Dev Biol.* 284:219-32.
- Ou, Y., P. Enarson, J.B. Rattner, S.G. Barr, and M.J. Fritzler. 2004. The nuclear pore complex protein Tpr is a common autoantigen in sera that demonstrate nuclear envelope staining by indirect immunofluorescence. *Clin Exp Immunol.* 136:379-87.
- Ozaki, T., M. Saijo, K. Murakami, H. Enomoto, Y. Taya, and S. Sakiyama. 1994. Complex formation between lamin A and the retinoblastoma gene product: identification of the domain on lamin A required for its interaction. *Oncogene.* 9:2649-53.
- Palmqvist, L., N. Pineault, C. Wasslavik, and R.K. Humphries. 2007. Candidate genes for expansion and transformation of hematopoietic stem cells by NUP98-HOX fusion genes. *PLoS One.* 2:e768.
- Panagopoulos, I., M. Isaksson, R. Billstrom, B. Strombeck, F. Mitelman, and B. Johansson. 2003. Fusion of the NUP98 gene and the homeobox gene HOXC13 in acute myeloid leukemia with t(11;12)(p15;q13). *Genes Chromosomes Cancer.* 36:107-12.

- Pante, N., R. Bastos, I. McMorrow, B. Burke, and U. Aebi. 1994. Interactions and three-dimensional localization of a group of nuclear pore complex proteins. *J Cell Biol.* 126:603-17.
- Pante, N., and M. Kann. 2002. Nuclear pore complex is able to transport macromolecules with diameters of about 39 nm. *Mol Biol Cell.* 13:425-34.
- Park, M., M. Dean, C.S. Cooper, M. Schmidt, S.J. O'Brien, D.G. Blair, and G.F. Vande Woude. 1986. Mechanism of met oncogene activation. *Cell.* 45:895-904.
- Patel, A.S., K.M. Murphy, A.L. Hawkins, J.S. Cohen, P.P. Long, E.J. Perlman, and C.A. Griffin. 2007. RANBP2 and CLTC are involved in ALK rearrangements in inflammatory myofibroblastic tumors. *Cancer Genet Cytogenet.* 176:107-14.
- Patrizi, G., and M. Poger. 1967. The ultrastructure of the nuclear periphery. The zonula nucleum limitans. *J Ultrastruct Res.* 17:127-36.
- Paulillo, S.M., E.M. Phillips, J. Koser, U. Sauder, K.S. Ullman, M.A. Powers, and B. Fahrenkrog. 2005. Nucleoporin domain topology is linked to the transport status of the nuclear pore complex. *J Mol Biol.* 351:784-98.
- Pekovic, V., J. Harborth, J.L. Broers, F.C. Ramaekers, B. van Engelen, M. Lammens, T. von Zglinicki, R. Foisner, C. Hutchison, and E. Markiewicz. 2007. Nucleoplasmic LAP2alpha-lamin A complexes are required to maintain a proliferative state in human fibroblasts. *J Cell Biol.* 176:163-72.
- Pendas, A.M., Z. Zhou, J. Cadiganos, J.M. Freije, J. Wang, K. Hultenby, A. Astudillo, A. Wernerson, F. Rodriguez, K. Tryggvason, and C. Lopez-Otin. 2002. Defective prelamin A processing and muscular and adipocyte alterations in Zmpste24 metalloproteinase-deficient mice. *Nat Genet.* 31:94-9.
- Persic, M., I. Prpic, A. Huebner, and S. Severinski. 2001. Achalasia, alacrima, adrenal insufficiency, and autonomic dysfunction: double A, triple A, or quaternary A syndrome? *J Pediatr Gastroenterol Nutr.* 33:503-4.
- Plans, V., M. Guerra-Rebollo, and T.M. Thomson. 2008. Regulation of mitotic exit by the RNF8 ubiquitin ligase. *Oncogene.* 27:1355-65.
- Powers, M.A., C. Macaulay, F.R. Masiarz, and D.J. Forbes. 1995. Reconstituted nuclei depleted of a vertebrate GLFG nuclear pore protein, p97, import but are defective in nuclear growth and replication. *J Cell Biol.* 128:721-36.
- Pritchard, C.E., M. Fornerod, L.H. Kasper, and J.M. van Deursen. 1999. RAE1 is a shuttling mRNA export factor that binds to a GLEBS-like NUP98 motif at the nuclear pore complex through multiple domains. *J Cell Biol.* 145:237-54.
- Prpic, I., A. Huebner, M. Persic, K. Handschug, and M. Pavletic. 2003. Triple A syndrome: genotype-phenotype assessment. *Clin Genet.* 63:415-7.
- Prufert, K., A. Vogel, and G. Krohne. 2004. The lamin CxxM motif promotes nuclear membrane growth. *J Cell Sci.* 117:6105-16.
- Prunuske, A.J., J. Liu, S. Elgort, J. Joseph, M. Dasso, and K.S. Ullman. 2006. Nuclear envelope breakdown is coordinated by both Nup358/RanBP2 and Nup153, two nucleoporins with zinc finger modules. *Mol Biol Cell.* 17:760-9.
- Radu, A., M.S. Moore, and G. Blobel. 1995. The peptide repeat domain of nucleoporin Nup98 functions as a docking site in transport across the nuclear pore complex. *Cell.* 81:215-22.
- Ralle, T., C. Grund, W.W. Franke, and R. Stick. 2004. Intranuclear membrane structure formations by CaaX-containing nuclear proteins. *J Cell Sci.* 117:6095-104.
- Rasala, B.A., A.V. Orjalo, Z. Shen, S. Briggs, and D.J. Forbes. 2006. ELYS is a dual nucleoporin/kinetochore protein required for nuclear pore assembly and proper cell division. *Proc Natl Acad Sci U S A.* 103:17801-6.
- Rieder, C.L., R.W. Cole, A. Khodjakov, and G. Sluder. 1995. The checkpoint delaying anaphase in response to chromosome monoorientation is mediated by an inhibitory signal produced by unattached kinetochores. *J Cell Biol.* 130:941-8.

- Rieder, C.L., and H. Maiato. 2004. Stuck in division or passing through: what happens when cells cannot satisfy the spindle assembly checkpoint. *Dev Cell*. 7:637-51.
- Rieder, C.L., A. Schultz, R. Cole, and G. Sluder. 1994. Anaphase onset in vertebrate somatic cells is controlled by a checkpoint that monitors sister kinetochore attachment to the spindle. *J Cell Biol*. 127:1301-10.
- Robinson, M.A., S. Park, Z.Y. Sun, P.A. Silver, G. Wagner, and J.M. Hogle. 2005. Multiple conformations in the ligand-binding site of the yeast nuclear pore-targeting domain of Nup116p. *J Biol Chem*. 280:35723-32.
- Rodrigues, G.A., and M. Park. 1993. Dimerization mediated through a leucine zipper activates the oncogenic potential of the met receptor tyrosine kinase. *Mol Cell Biol*. 13:6711-22.
- Rodriguez-Navarro, S., T. Fischer, M.J. Luo, O. Antunez, S. Brettschneider, J. Lechner, J.E. Perez-Ortin, R. Reed, and E. Hurt. 2004. Sus1, a functional component of the SAGA histone acetylase complex and the nuclear pore-associated mRNA export machinery. *Cell*. 116:75-86.
- Rosati, R., R. La Starza, A. Veronese, A. Aventin, C. Schwienbacher, T. Vallespi, M. Negrini, M.F. Martelli, and C. Mecucci. 2002. NUP98 is fused to the NSD3 gene in acute myeloid leukemia associated with t(8;11)(p11.2;p15). *Blood*. 99:3857-60.
- Roth, P., N. Xylourgidis, N. Sabri, A. Uv, M. Fornerod, and C. Samakovlis. 2003. The Drosophila nucleoporin DNup88 localizes DNup214 and CRM1 on the nuclear envelope and attenuates NES-mediated nuclear export. *J Cell Biol*. 163:701-6.
- Rout, M.P., J.D. Aitchison, A. Suprpto, K. Hjertaas, Y. Zhao, and B.T. Chait. 2000. The yeast nuclear pore complex: composition, architecture, and transport mechanism. *J Cell Biol*. 148:635-51.
- Royce-Tolland, M., and B. Panning. 2008. X-inactivation: it takes two to count. *Curr Biol*. 18:R255-6.
- Ruiz, S., M. Santos, C. Segrelles, H. Leis, J.L. Jorcano, A. Berns, J.M. Paramio, and M. Vooijs. 2004. Unique and overlapping functions of pRb and p107 in the control of proliferation and differentiation in epidermis. *Development*. 131:2737-48.
- Salina, D., P. Enarson, J.B. Rattner, and B. Burke. 2003. Nup358 integrates nuclear envelope breakdown with kinetochore assembly. *J Cell Biol*. 162:991-1001.
- Sandrini, F., C. Farmakidis, L.S. Kirschner, S.M. Wu, A. Tullio-Pelet, S. Lyonnet, D.L. Metzger, C.J. Bourdony, D. Tiosano, W.Y. Chan, and C.A. Stratakis. 2001. Spectrum of mutations of the AAAS gene in Allgrove syndrome: lack of mutations in six kindreds with isolated resistance to corticotropin. *J Clin Endocrinol Metab*. 86:5433-7.
- Scaffidi, P., and T. Misteli. 2005. Reversal of the cellular phenotype in the premature aging disease Hutchinson-Gilford progeria syndrome. *Nat Med*. 11:440-5.
- Schirmer, E.C., and R. Foisner. 2007. Proteins that associate with lamins: many faces, many functions. *Exp Cell Res*. 313:2167-79.
- Schirmer, E.C., T. Guan, and L. Gerace. 2001. Involvement of the lamin rod domain in heterotypic lamin interactions important for nuclear organization. *J Cell Biol*. 153:479-89.
- Schmid, M., G. Arib, C. Laemmli, J. Nishikawa, T. Durussel, and U.K. Laemmli. 2006. Nup-PI: the nucleopore-promoter interaction of genes in yeast. *Mol Cell*. 21:379-91.
- Schmittmann-Ohters, K., A. Huebner, A. Richter-Unruh, and B.P. Hauffa. 2001. Clinical and novel molecular findings in a 6.8-year-old Turkish boy with triple A syndrome. *Horm Res*. 56:67-72.
- Schneider, J., R. Linares, F. Martinez-Arribas, M.D. Moragues, M.J. Nunez-Villar, M.A. Palomar, and J. Ponton. 2004. Developing chick embryos express a protein which shares homology with the nuclear pore complex protein Nup88 present in human tumors. *Int J Dev Biol*. 48:339-42.
- Schrader, N., P. Stelter, D. Flemming, R. Kunze, E. Hurt, and I.R. Vetter. 2008. Structural basis of the nic96 subcomplex organization in the nuclear pore channel. *Mol Cell*. 29:46-55.

- Schwartz, T.U. 2005. Modularity within the architecture of the nuclear pore complex. *Curr Opin Struct Biol.* 15:221-6.
- Schwarz-Herion, K., B. Maco, U. Sauder, and B. Fahrenkrog. 2007. Domain topology of the p62 complex within the 3-D architecture of the nuclear pore complex. *J Mol Biol.* 370:796-806.
- Scott, R.J., C.P. Lusk, D.J. Dilworth, J.D. Aitchison, and R.W. Wozniak. 2005. Interactions between Mad1p and the nuclear transport machinery in the yeast *Saccharomyces cerevisiae*. *Mol Biol Cell.* 16:4362-74.
- Shah, J.V., and D.W. Cleveland. 2000. Waiting for anaphase: Mad2 and the spindle assembly checkpoint. *Cell.* 103:997-1000.
- Shah, S., S. Tugendreich, and D. Forbes. 1998. Major binding sites for the nuclear import receptor are the internal nucleoporin Nup153 and the adjacent nuclear filament protein Tpr. *J Cell Biol.* 141:31-49.
- Sharp-Baker, H., and R.H. Chen. 2001. Spindle checkpoint protein Bub1 is required for kinetochore localization of Mad1, Mad2, Bub3, and CENP-E, independently of its kinase activity. *J Cell Biol.* 153:1239-50.
- Shumaker, D.K., K.K. Lee, Y.C. Tanhehco, R. Craigie, and K.L. Wilson. 2001. LAP2 binds to BAF.DNA complexes: requirement for the LEM domain and modulation by variable regions. *EMBO J.* 20:1754-64.
- Siniosoglou, S., C. Wimmer, M. Rieger, V. Doye, H. Tekotte, C. Weise, S. Emig, A. Segref, and E.C. Hurt. 1996. A novel complex of nucleoporins, which includes Sec13p and a Sec13p homolog, is essential for normal nuclear pores. *Cell.* 84:265-75.
- Smith, E.D., B.A. Kudlow, R.L. Frock, and B.K. Kennedy. 2005. A-type nuclear lamins, progerias and other degenerative disorders. *Mech Ageing Dev.* 126:447-60.
- Smith, T.F., C. Gaitatzes, K. Saxena, and E.J. Neer. 1999. The WD repeat: a common architecture for diverse functions. *Trends Biochem Sci.* 24:181-5.
- Smythe, C., H.E. Jenkins, and C.J. Hutchison. 2000. Incorporation of the nuclear pore basket protein nup153 into nuclear pore structures is dependent upon lamina assembly: evidence from cell-free extracts of *Xenopus* eggs. *EMBO J.* 19:3918-31.
- Spann, T.P., A.E. Goldman, C. Wang, S. Huang, and R.D. Goldman. 2002. Alteration of nuclear lamin organization inhibits RNA polymerase II-dependent transcription. *J Cell Biol.* 156:603-8.
- Speckman, R.A., A. Garg, F. Du, L. Bennett, R. Veile, E. Arioglu, S.I. Taylor, M. Lovett, and A.M. Bowcock. 2000. Mutational and haplotype analyses of families with familial partial lipodystrophy (Dunnigan variety) reveal recurrent missense mutations in the globular C-terminal domain of lamin A/C. *Am J Hum Genet.* 66:1192-8.
- Stagg, S.M., P. LaPointe, A. Razvi, C. Gurkan, C.S. Potter, B. Carragher, and W.E. Balch. 2008. Structural basis for cargo regulation of COPII coat assembly. *Cell.* 134:474-84.
- Stavru, F., B.B. Hulsmann, A. Spang, E. Hartmann, V.C. Cordes, and D. Gorlich. 2006a. NDC1: a crucial membrane-integral nucleoporin of metazoan nuclear pore complexes. *J Cell Biol.* 173:509-19.
- Stavru, F., G. Nautrup-Pedersen, V.C. Cordes, and D. Gorlich. 2006b. Nuclear pore complex assembly and maintenance in POM121- and gp210-deficient cells. *J Cell Biol.* 173:477-83.
- Stoffler, D., B. Feja, B. Fahrenkrog, J. Walz, D. Typke, and U. Aebi. 2003. Cryo-electron tomography provides novel insights into nuclear pore architecture: implications for nucleocytoplasmic transport. *J Mol Biol.* 328:119-30.
- Strawn, L.A., T. Shen, N. Shulga, D.S. Goldfarb, and S.R. Wentz. 2004. Minimal nuclear pore complexes define FG repeat domains essential for transport. *Nat Cell Biol.* 6:197-206.
- Stuurman, N., S. Heins, and U. Aebi. 1998. Nuclear lamins: their structure, assembly, and interactions. *J Struct Biol.* 122:42-66.

- Sudakin, V., G.K. Chan, and T.J. Yen. 2001. Checkpoint inhibition of the APC/C in HeLa cells is mediated by a complex of BUBR1, BUB3, CDC20, and MAD2. *J Cell Biol.* 154:925-36.
- Suijkerbuijk, S.J., and G.J. Kops. 2008. Preventing aneuploidy: the contribution of mitotic checkpoint proteins. *Biochim Biophys Acta.* 1786:24-31.
- Sukegawa, J., and G. Blobel. 1993. A nuclear pore complex protein that contains zinc finger motifs, binds DNA, and faces the nucleoplasm. *Cell.* 72:29-38.
- Sullivan, T., D. Escalante-Alcalde, H. Bhatt, M. Anver, N. Bhat, K. Nagashima, C.L. Stewart, and B. Burke. 1999. Loss of A-type lamin expression compromises nuclear envelope integrity leading to muscular dystrophy. *J Cell Biol.* 147:913-20.
- Sun, Y., and H.C. Guo. 2008. Structural constraints on autoprocessing of the human nucleoporin Nup98. *Protein Sci.* 17:494-505.
- Suntharalingam, M., and S.R. Wentz. 2003. Peering through the pore: nuclear pore complex structure, assembly, and function. *Dev Cell.* 4:775-89.
- Suzuki, A., Y. Ito, G. Sashida, S. Honda, T. Katagiri, T. Fujino, T. Nakamura, and K. Ohyashiki. 2002. t(7;11)(p15;p15) Chronic myeloid leukaemia developed into blastic transformation showing a novel NUP98/HOXA11 fusion. *Br J Haematol.* 116:170-2.
- Suzuki-Takahashi, I., M. Kitagawa, M. Saijo, H. Higashi, H. Ogino, H. Matsumoto, Y. Taya, S. Nishimura, and A. Okuyama. 1995. The interactions of E2F with pRB and with p107 are regulated via the phosphorylation of pRB and p107 by a cyclin-dependent kinase. *Oncogene.* 10:1691-8.
- Taddei, A., G. Van Houwe, F. Hediger, V. Kalck, F. Cubizolles, H. Schober, and S.M. Gasser. 2006. Nuclear pore association confers optimal expression levels for an inducible yeast gene. *Nature.* 441:774-8.
- Takahashi, N., J.W. van Kilsdonk, B. Ostendorf, R. Smeets, S.W. Bruggeman, A. Alonso, F. van de Loo, M. Schneider, W.B. van den Berg, and G.W. Swart. 2008. Tumor marker nucleoporin 88 kDa regulates nucleocytoplasmic transport of NF-kappaB. *Biochem Biophys Res Commun.* 374:424-30.
- Takano, H., and J.F. Gusella. 2002. The predominantly HEAT-like motif structure of huntingtin and its association and coincident nuclear entry with dorsal, an NF-kB/Rel/dorsal family transcription factor. *BMC Neurosci.* 3:15.
- Takeda, A., C. Goolsby, and N.R. Yaseen. 2006. NUP98-HOXA9 induces long-term proliferation and blocks differentiation of primary human CD34+ hematopoietic cells. *Cancer Res.* 66:6628-37.
- Taketani, T., T. Taki, R. Ono, Y. Kobayashi, K. Ida, and Y. Hayashi. 2002a. The chromosome translocation t(7;11)(p15;p15) in acute myeloid leukemia results in fusion of the NUP98 gene with a HOXA cluster gene, HOXA13, but not HOXA9. *Genes Chromosomes Cancer.* 34:437-43.
- Taketani, T., T. Taki, N. Shibuya, E. Ito, J. Kitazawa, K. Terui, and Y. Hayashi. 2002b. The HOXD11 gene is fused to the NUP98 gene in acute myeloid leukemia with t(2;11)(q31;p15). *Cancer Res.* 62:33-7.
- Taketani, T., T. Taki, N. Shibuya, A. Kikuchi, R. Hanada, and Y. Hayashi. 2002c. Novel NUP98-HOXC11 fusion gene resulted from a chromosomal break within exon 1 of HOXC11 in acute myeloid leukemia with t(11;12)(p15;q13). *Cancer Res.* 62:4571-4.
- Taylor, S.S., D. Hussein, Y. Wang, S. Elderkin, and C.J. Morrow. 2001. Kinetochores localisation and phosphorylation of the mitotic checkpoint components Bub1 and BubR1 are differentially regulated by spindle events in human cells. *J Cell Sci.* 114:4385-95.
- Therizols, P., C. Fairhead, G.G. Cabal, A. Genovesio, J.C. Olivo-Marin, B. Dujon, and E. Fabre. 2006. Telomere tethering at the nuclear periphery is essential for efficient DNA double strand break repair in subtelomeric region. *J Cell Biol.* 172:189-99.
- To-Ho, K.W., H.W. Cheung, M.T. Ling, Y.C. Wong, and X. Wang. 2008. MAD2DeltaC induces aneuploidy and promotes anchorage-independent growth in human prostate epithelial cells. *Oncogene.* 27:347-57.

- Tran, E.J., and S.R. Wentz. 2006. Dynamic nuclear pore complexes: life on the edge. *Cell*. 125:1041-53.
- Tsao, C.Y., C.A. Romshe, W.D. Lo, F.S. Wright, and A. Sommer. 1994. Familial adrenal insufficiency, achalasia, alacrima, peripheral neuropathy, microcephaly, normal plasma very long chain fatty acids, and normal muscle mitochondrial respiratory chain enzymes. *J Child Neurol*. 9:135-8.
- Tullio-Pelet, A., R. Salomon, S. Hadj-Rabia, C. Mugnier, M.H. de Laet, B. Chaouachi, F. Bakiri, P. Brottier, L. Cattolico, C. Penet, M. Begeot, D. Naville, M. Nicolino, J.L. Chaussain, J. Weissenbach, A. Munnich, and S. Lyonnet. 2000. Mutant WD-repeat protein in triple-A syndrome. *Nat Genet*. 26:332-5.
- Ullman, K.S., S. Shah, M.A. Powers, and D.J. Forbes. 1999. The nucleoporin nup153 plays a critical role in multiple types of nuclear export. *Mol Biol Cell*. 10:649-64.
- Uv, A.E., P. Roth, N. Xylourgidis, A. Wickberg, R. Cantera, and C. Samakovlis. 2000. members only encodes a Drosophila nucleoporin required for rel protein import and immune response activation. *Genes Dev*. 14:1945-57.
- Van Berlo, J.H., J.W. Voncken, N. Kubben, J.L. Broers, R. Duisters, R.E. van Leeuwen, H.J. Crijns, F.C. Ramaekers, C.J. Hutchison, and Y.M. Pinto. 2005. A-type lamins are essential for TGF-beta1 induced PP2A to dephosphorylate transcription factors. *Hum Mol Genet*. 14:2839-49.
- van Deursen, J., J. Boer, L. Kasper, and G. Grosveld. 1996. G2 arrest and impaired nucleocytoplasmic transport in mouse embryos lacking the proto-oncogene CAN/Nup214. *Embo J*. 15:5574-83.
- Vasu, S., S. Shah, A. Orjalo, M. Park, W.H. Fischer, and D.J. Forbes. 2001. Novel vertebrate nucleoporins Nup133 and Nup160 play a role in mRNA export. *J Cell Biol*. 155:339-54.
- Vasu, S.K., and D.J. Forbes. 2001. Nuclear pores and nuclear assembly. *Curr Opin Cell Biol*. 13:363-75.
- Vergnes, L., M. Peterfy, M.O. Bergo, S.G. Young, and K. Reue. 2004. Lamin B1 is required for mouse development and nuclear integrity. *Proc Natl Acad Sci U S A*. 101:10428-33.
- Vetter, I.R., C. Nowak, T. Nishimoto, J. Kuhlmann, and A. Wittinghofer. 1999. Structure of a Ran-binding domain complexed with Ran bound to a GTP analogue: implications for nuclear transport. *Nature*. 398:39-46.
- Vinciguerra, P., N. Iglesias, J. Camblong, D. Zenklusen, and F. Stutz. 2005. Perinuclear Mlp proteins downregulate gene expression in response to a defect in mRNA export. *Embo J*. 24:813-23.
- Vlcek, S., B. Korbei, and R. Foisner. 2002. Distinct functions of the unique C terminus of LAP2alpha in cell proliferation and nuclear assembly. *J Biol Chem*. 277:18898-907.
- von Lindern, M., S. van Baal, J. Wiegant, A. Raap, A. Hagemeyer, and G. Grosveld. 1992. Can, a putative oncogene associated with myeloid leukemogenesis, may be activated by fusion of its 3' half to different genes: characterization of the set gene. *Mol Cell Biol*. 12:3346-55.
- Wagner, N., and G. Krohne. 2007. LEM-Domain proteins: new insights into lamin-interacting proteins. *Int Rev Cytol*. 261:1-46.
- Walter, D., S. Wissing, F. Madeo, and B. Fahrenkrog. 2006. The inhibitor-of-apoptosis protein Bir1p protects against apoptosis in *S. cerevisiae* and is a substrate for the yeast homologue of Omi/HtrA2. *J Cell Sci*. 119:1843-51.
- Walther, T.C., A. Alves, H. Pickersgill, I. Liodice, M. Hetzer, V. Galy, B.B. Hulsmann, T. Kocher, M. Wilm, T. Allen, I.W. Mattaj, and V. Doye. 2003. The conserved Nup107-160 complex is critical for nuclear pore complex assembly. *Cell*. 113:195-206.
- Walther, T.C., M. Fornerod, H. Pickersgill, M. Goldberg, T.D. Allen, and I.W. Mattaj. 2001. The nucleoporin Nup153 is required for nuclear pore basket formation, nuclear pore complex anchoring and import of a subset of nuclear proteins. *EMBO J*. 20:5703-14.

- Walther, T.C., H.S. Pickersgill, V.C. Cordes, M.W. Goldberg, T.D. Allen, I.W. Mattaj, and M. Fornerod. 2002. The cytoplasmic filaments of the nuclear pore complex are dispensable for selective nuclear protein import. *J Cell Biol.* 158:63-77.
- Weaver, B.A., and D.W. Cleveland. 2006. Does aneuploidy cause cancer? *Curr Opin Cell Biol.* 18:658-67.
- Weirich, C.S., J.P. Erzberger, J.M. Berger, and K. Weis. 2004. The N-terminal domain of Nup159 forms a beta-propeller that functions in mRNA export by tethering the helicase Dbp5 to the nuclear pore. *Mol Cell.* 16:749-60.
- Wilken, N., U. Kossner, J.L. Senecal, U. Scheer, and M.C. Dabauvalle. 1993. Nup180, a novel nuclear pore complex protein localizing to the cytoplasmic ring and associated fibrils. *J Cell Biol.* 123:1345-54.
- Wilson, K.L. 2000. The nuclear envelope, muscular dystrophy and gene expression. *Trends Cell Biol.* 10:125-9.
- Worman, H.J., and G. Bonne. 2007. "Laminopathies": a wide spectrum of human diseases. *Exp Cell Res.* 313:2121-33.
- Worman, H.J., and J.C. Courvalin. 2003. Antinuclear antibodies specific for primary biliary cirrhosis. *Autoimmun Rev.* 2:211-7.
- Wozniak, R.W., and G. Blobel. 1992. The single transmembrane segment of gp210 is sufficient for sorting to the pore membrane domain of the nuclear envelope. *J Cell Biol.* 119:1441-9.
- Wozniak, R.W., G. Blobel, and M.P. Rout. 1994. POM152 is an integral protein of the pore membrane domain of the yeast nuclear envelope. *J Cell Biol.* 125:31-42.
- Wu, X., L.H. Kasper, R.T. Mantcheva, G.T. Mantchev, M.J. Springett, and J.M. van Deursen. 2001. Disruption of the FG nucleoporin NUP98 causes selective changes in nuclear pore complex stoichiometry and function. *Proc Natl Acad Sci U S A.* 98:3191-6.
- Xylourgidis, N., P. Roth, N. Sabri, V. Tsarouhas, and C. Samakovlis. 2006. The nucleoporin Nup214 sequesters CRM1 at the nuclear rim and modulates NFkappaB activation in *Drosophila*. *J Cell Sci.* 119:4409-19.
- Yang, Q., M.P. Rout, and C.W. Akey. 1998. Three-dimensional architecture of the isolated yeast nuclear pore complex: functional and evolutionary implications. *Mol Cell.* 1:223-34.
- Yu, H. 2002. Regulation of APC-Cdc20 by the spindle checkpoint. *Curr Opin Cell Biol.* 14:706-14.
- Zabel, U., V. Doye, H. Tekotte, R. Wepf, P. Grandi, and E.C. Hurt. 1996. Nic96p is required for nuclear pore formation and functionally interacts with a novel nucleoporin, Nup188p. *J Cell Biol.* 133:1141-52.
- Zeitler, B., and K. Weis. 2004. The FG-repeat asymmetry of the nuclear pore complex is dispensable for bulk nucleocytoplasmic transport in vivo. *J Cell Biol.* 167:583-90.
- Zhang, H., and I. Rosdahl. 2003. Ultraviolet A and B differently induce intracellular protein expression in human skin melanocytes--a speculation of separate pathways in initiation of melanoma. *Carcinogenesis.* 24:1929-34.
- Zhang, H., J. Schneider, and I. Rosdahl. 2002. Expression of p16, p27, p53, p73 and Nup88 proteins in matched primary and metastatic melanoma cells. *Int J Oncol.* 21:43-8.
- Zhang, Y.Q., and K.D. Sarge. 2008. Sumoylation regulates lamin A function and is lost in lamin A mutants associated with familial cardiomyopathies. *J Cell Biol.* 182:35-9.
- Zhang, Z.Y., Z.R. Zhao, L. Jiang, J.C. Li, Y.M. Gao, D.S. Cui, C.J. Wang, J. Schneider, M.W. Wang, and X.F. Sun. 2007. Nup88 expression in normal mucosa, adenoma, primary adenocarcinoma and lymph node metastasis in the colorectum. *Tumour Biol.* 28:93-9.
- Zuccolo, M., A. Alves, V. Galy, S. Bolhy, E. Formstecher, V. Racine, J.B. Sibarita, T. Fukagawa, R. Shiekhata, T. Yen, and V. Doye. 2007. The human Nup107-160 nuclear pore subcomplex contributes to proper kinetochore functions. *EMBO J.* 26:1853-64.

7

Appendix

7.1 Supplementary Figures

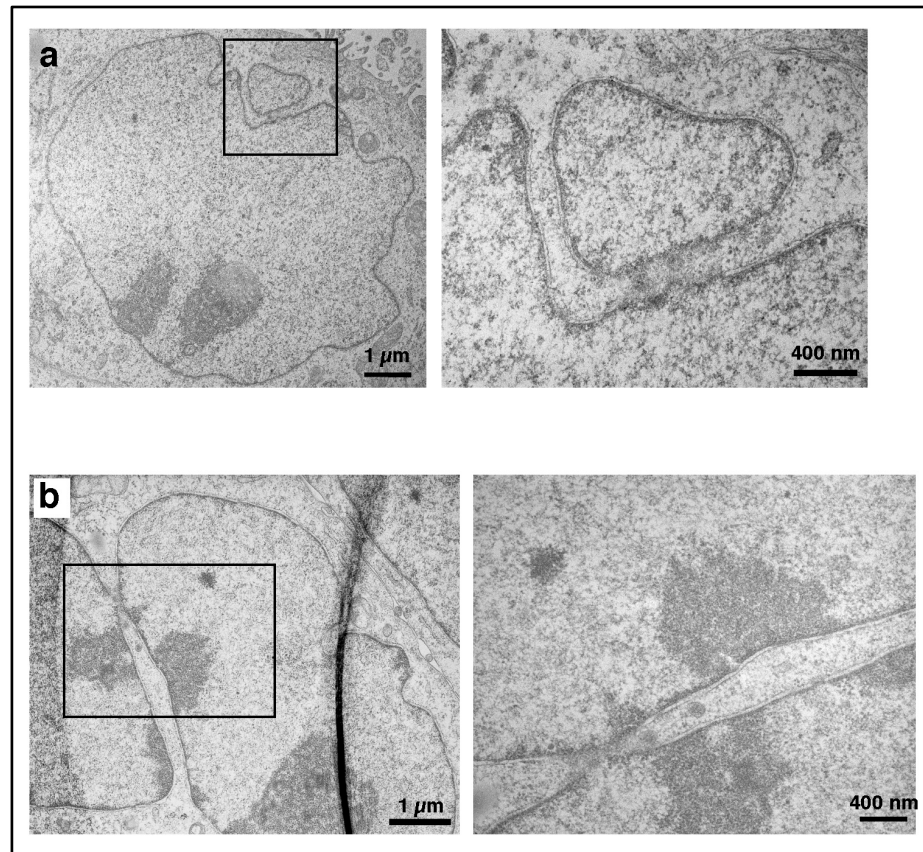


Figure S7.1: Electron micrographs of GFP-Nup153 overexpressing cells.

HeLa cells were transiently transfected with GFP-Nup153 and prepared for thin-sectioning EM 48 hours after transfection. Cells were fixed in glutaraldehyde, postfixed in osmium tetroxide, dehydrated in a series of ethanol and embedded in Epon resin. Electron micrographs were recorded on a Philipps CM 100 electron microscope equipped with a CCD camera. Images were processed using Adobe Photoshop. Shown are two examples of a multinucleated cell at low magnification and a higher magnification of the marked area, highlighting the fusion between the two nuclei.

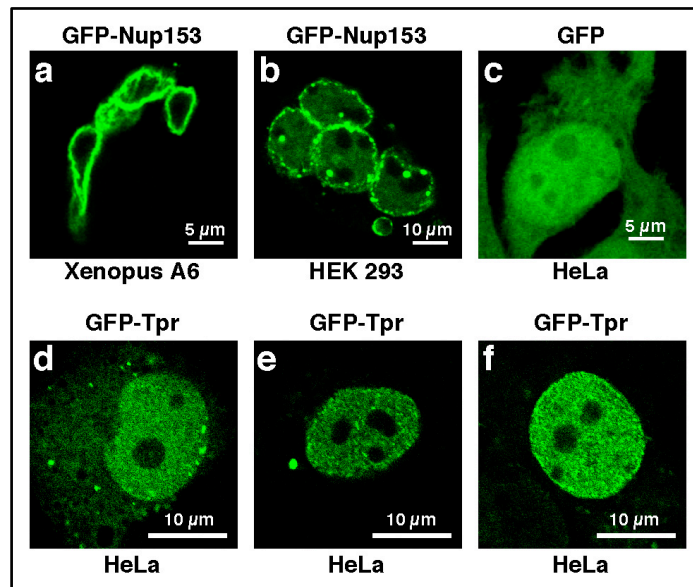


Figure S7.2: Over-expression of Nup153 induces cellular multinucleation.

(a) *Xenopus* A6 cells and (b) human HEK 293 cells were transiently transfected with GFP-Nup153 and analyzed by direct epifluorescence 48 hours after transfection. Expression of GFP-Nup153 resulted in multinucleated cells. (c) HeLa cells transiently expressing GFP do not accumulate GFP at the nuclear envelope but is distributed throughout the nucleoplasm. No multinucleation of the cells was observed. (d, e, f) GFP-Tpr localizes to the nuclear envelope and the nucleoplasm in transiently transfected HeLa cells. No multinucleation of the cells was observed.

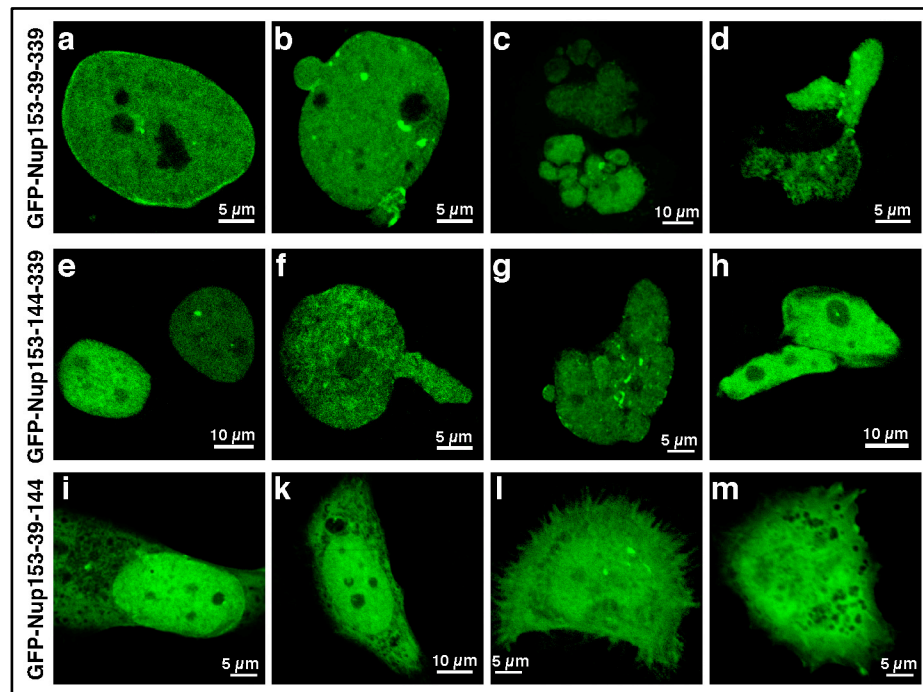


Figure S7.3: HeLa cells expressing truncations of the N-terminal domain of human Nup153 cause nuclear lobulations and multinucleation.

HeLa cells were transiently transfected and analyzed 48 hours later by epifluorescence microscopy. GFP-Nup153-39-339 was localized to the nuclear envelope. High levels of expression caused nuclear lobulation and multinucleation. Expression of GFP-Nup153-144-339 displayed nuclear localization mainly in internal nuclear foci and caused nuclear lobulation. Expression of GFP-Nup153-39-144 was localized throughout the cell.

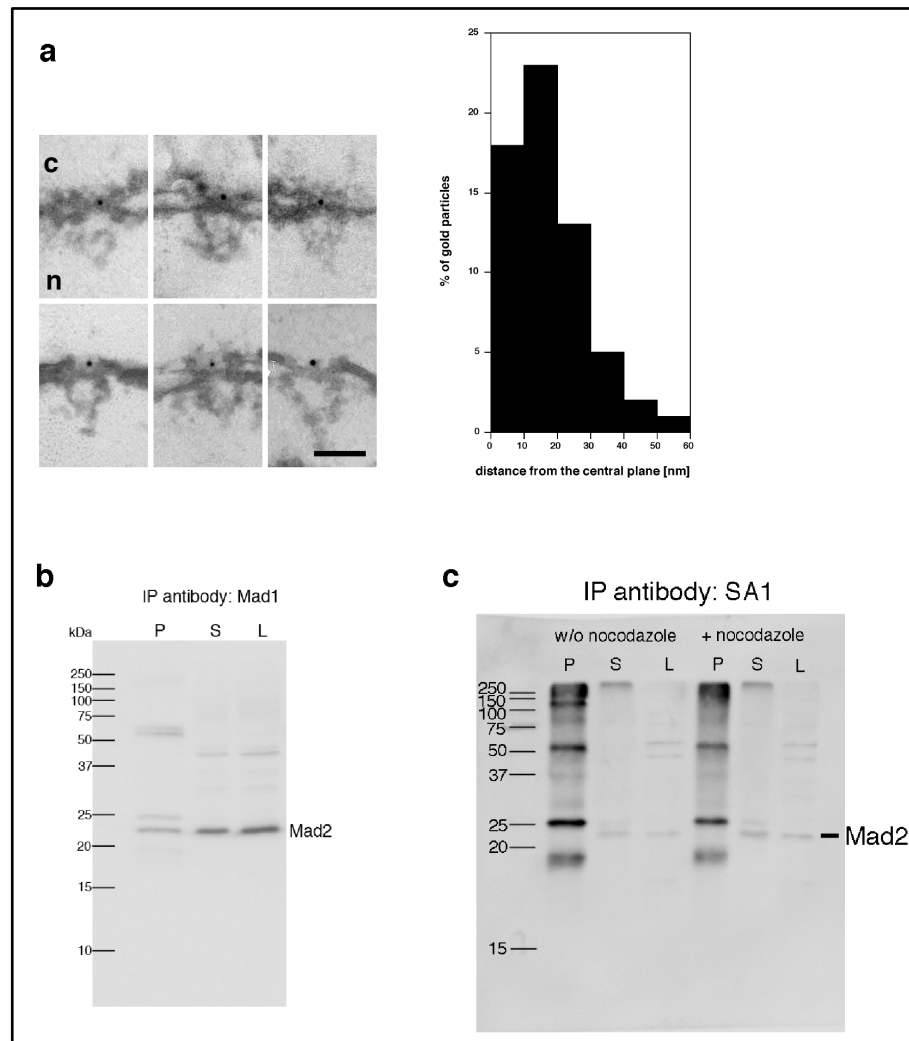


Figure S7.4: Mad2 localization and co-precipitation with Mad1

(a) Immuno-electron microscopy localization of Mad2 in *Xenopus* oocyte nuclei. Nuclei were isolated manually and labelled with a monoclonal Mad2 antibody directly conjugated to 8nm colloidal gold. Mad2 localises to the centre of the NPC with additional epitopes on the cytoplasmic face of the NPC (left). Quantification of the gold particle distribution from particles that were associated with the NPC (right).

Total HeLa extracts from unsynchronised or nocodazole arrested cells were immunoprecipitated using either (b) anti-Mad1 or (c) anti-Nup153 antibodies. Equivalent amounts of HeLa extracts (L), immune supernatants (S) and immune precipitate (P) were separated by SDS-PAGE and analyzed by immunoblotting using Mad2 antibodies. Mad2 is co-precipitated with Mad1, but not with Nup153.

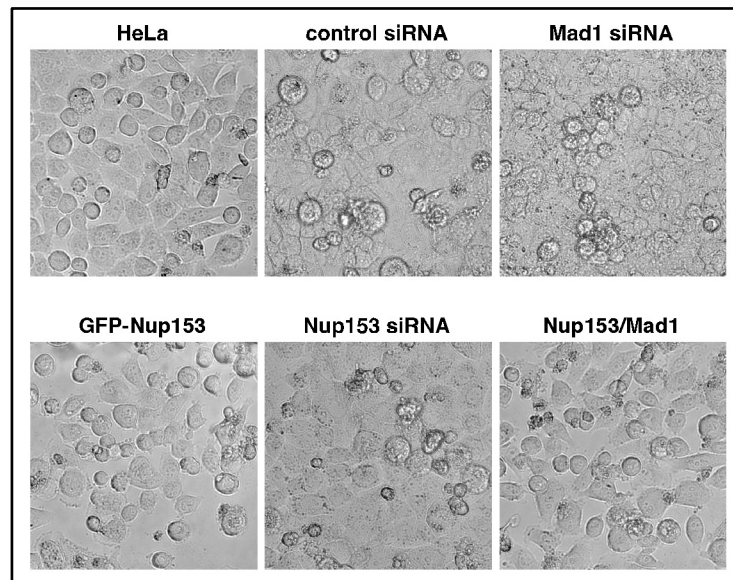


Figure S7.5: Enhanced levels of Nup153 do not cause G1 or G2 arrest.

Phase contrast images of untransfected HeLa cells or cells that were transfected with control siRNA, Mad1 siRNA, Nup153 siRNA, GFP-Nup153 or GFP-Nup153 and GFP-Mad1, respectively, and treated with thymidine for 16 hours to arrest cells in G1. Cells were released from thymidine block by incubation in fresh medium, prior to a second block with thymidine for another 16 hours. Cells were released into fresh medium and images 9 hours after release. No G1 or G2 arrest was observed for any condition.

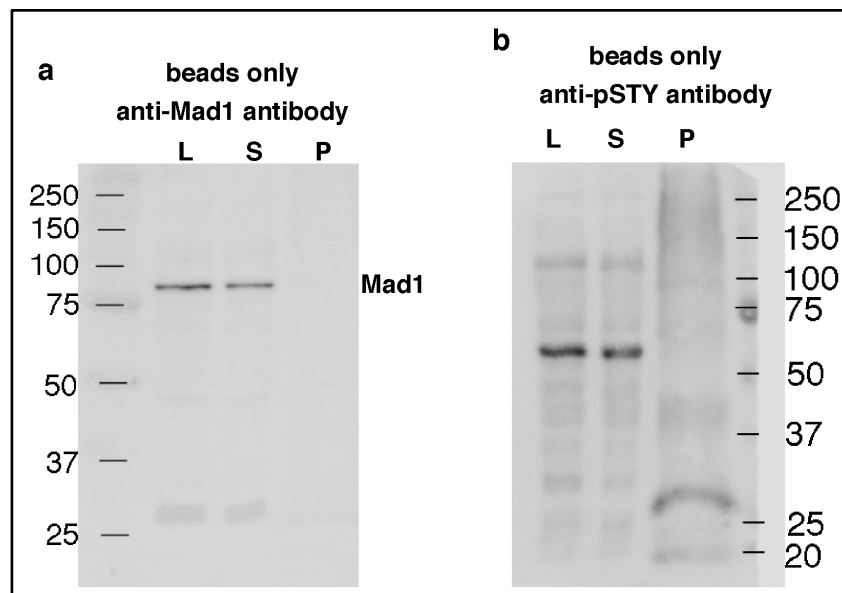


Figure S7.6: Mad1 does not precipitate with protein G agarose beads.

Protein G agarose beads were incubated with total HeLa extracts from unsynchronised cells were analyzed using either (a) anti-Mad1 or (b) anti-pSTY antibodies. Mad1 is detectable in the HeLa

extracts (L) and the supernatant (S), but did not bind to the beads (P). The pSTY antibody recognised some proteins in the extract, the supernatant, but did not react with the beads.

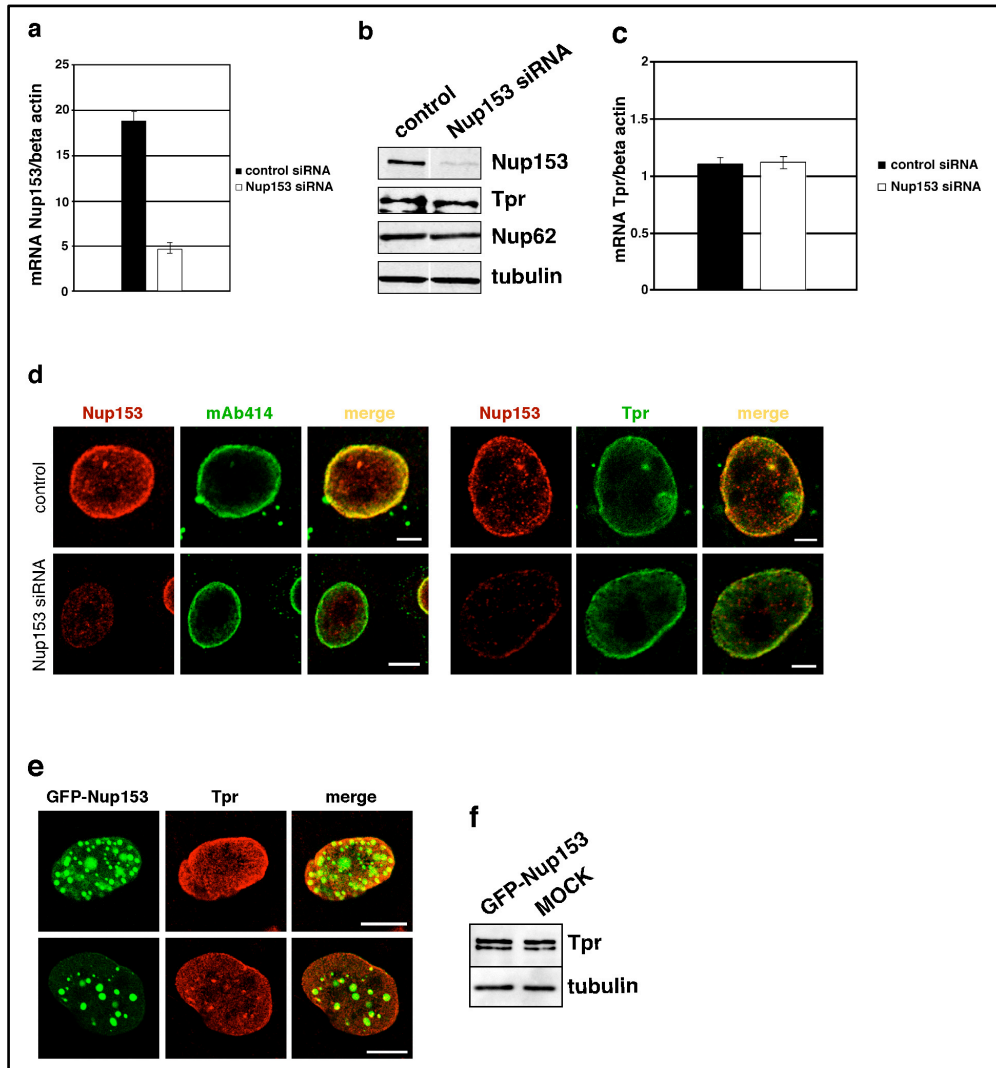


Figure S7.7: HeLa cells expressing histone H2B-GFP were transfected either with Nup153 siRNA or siRNA directed against cyclophilin B as a control.

Knockdown of Nup153 was verified 48 hours after transfection by (a) real-time PCR with the Nup153 signal normalised to the concentration of actin mRNA. (b) In addition, the corresponding decrease in Nup153 protein was examined by quantitative Western blotting using cell extracts from cells treated with control or Nup153 siRNAs using antibodies directed against Nup153, Tpr, Nup62, and tubulin. (d) No changes in Tpr mRNA levels occur upon depletion of Nup153 with the Tpr signal normalised to the concentration of actin mRNA. The decrease in the protein level of Nup153 was also examined by (c) dual immunofluorescence microscopy after fixation and staining for Nup153 and either FG-repeat proteins with mAb414 or Tpr. In the absence of Nup153 Tpr and the FG-repeat proteins appeared to be associated with nuclear pore complexes. Expression of GFP-Nup153 does not affect (e) Tpr localisation or (f) expression levels in transiently transfected HeLa cells.

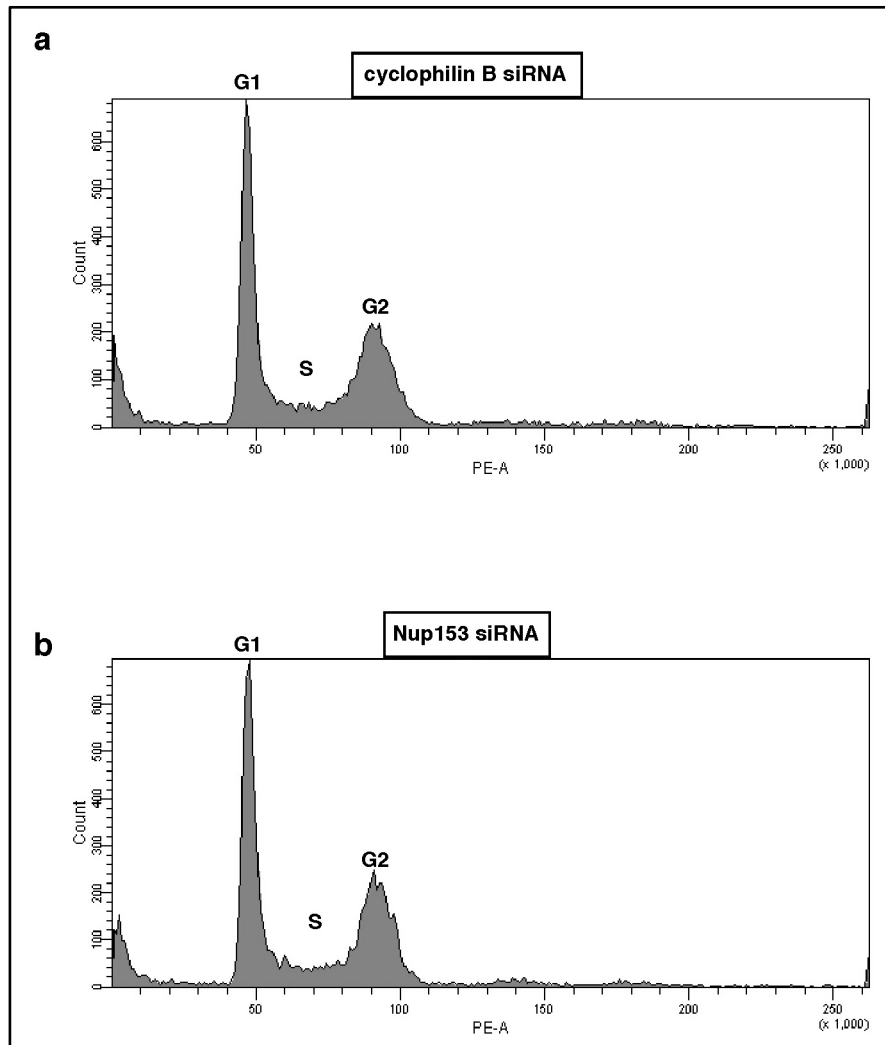


Figure S7.8: Flow cytometric analysis of siRNA treated HeLa cells expressing histone H2B-GFP.

Cells were transfected with (a) control siRNA against cyclophilin B and (b) Nup153 siRNAs, fixed 48 hours post transfection and stained with propidium iodide to analyze their DNA content. Knocking down Nup153 had no effect on cell cycle compared with control treatment.

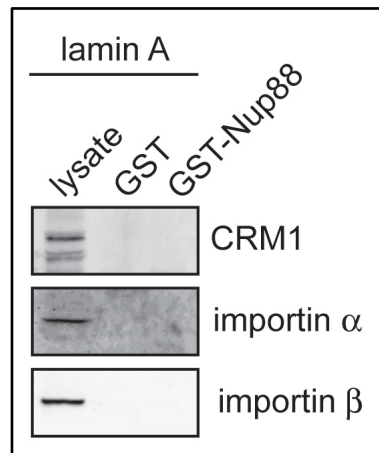


Figure S7.9: Nup88-lamin A complex is not associated with transport.

Bacterially expressed GST-Nup88 and GST were bound to glutathione sepharose beads and incubated with in vitro synthesized ^{35}S -labeled full-length lamin A. The reticulocyte lysate used for in vitro expression and ^{35}S -labeling of lamin A and the bound fractions to GST-Nup88 and GST were then analyzed by SDS-PAGE and immunoblotting with antibodies against CRM1, importin α and importin β . Neither CRM1, importin α nor importin β were found to be associated with the Nup88-lamin A complex.

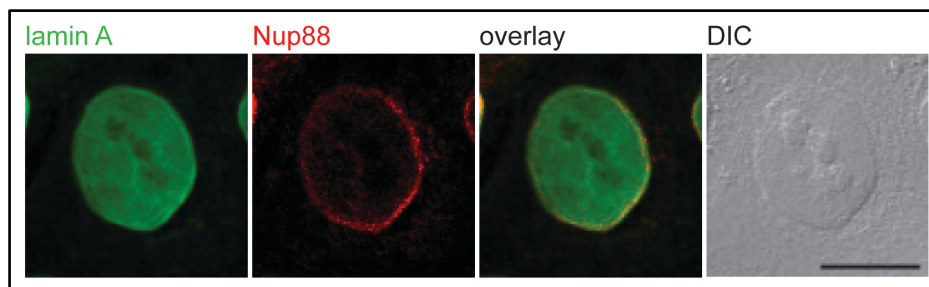


Figure S7.10: Localization of endogenous lamin A and Nup88 in HEK cells.

HEK cells were indirectly immunolabeled with antibodies against Nup88 and lamin A. Scale bar, 10 μm .

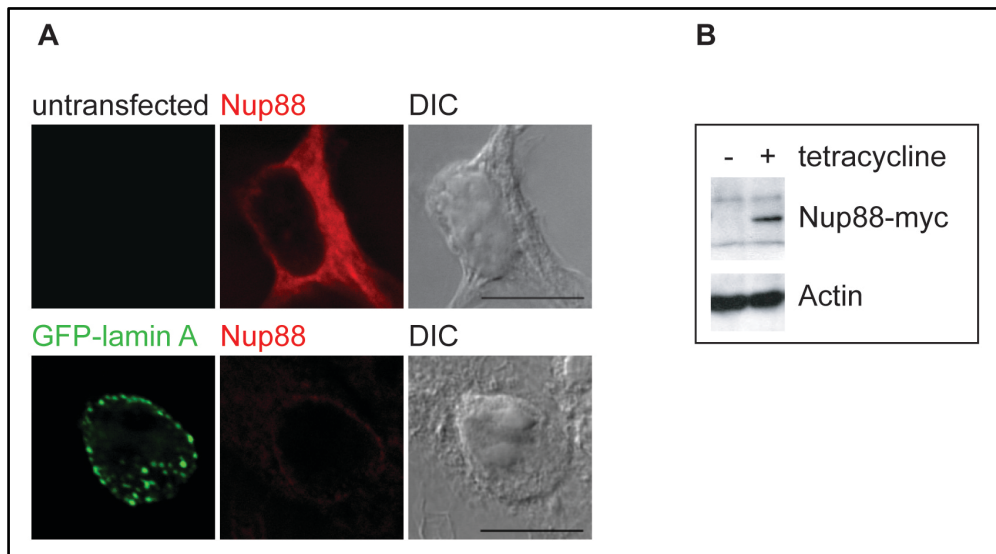


Figure S7.11: Expression of GFP-lamin A in Nup88-myc overexpressing HEK cells.

(A) Stable HEK-hNup88 cells were induced to express Nup88-myc upon tetracycline in the medium, transiently transfected with GFP-lamin A, indirectly immunolabeled with a Nup88 antibody recognizing residues 314-425 and analyzed by fluorescence microscopy. Scale bars, 10 μm (B) HEK cells were induced to express Nup88-myc upon tetracycline in the medium and analyzed by immunoblot analysis using myc-antibodies. Actin antibodies were used as loading control.

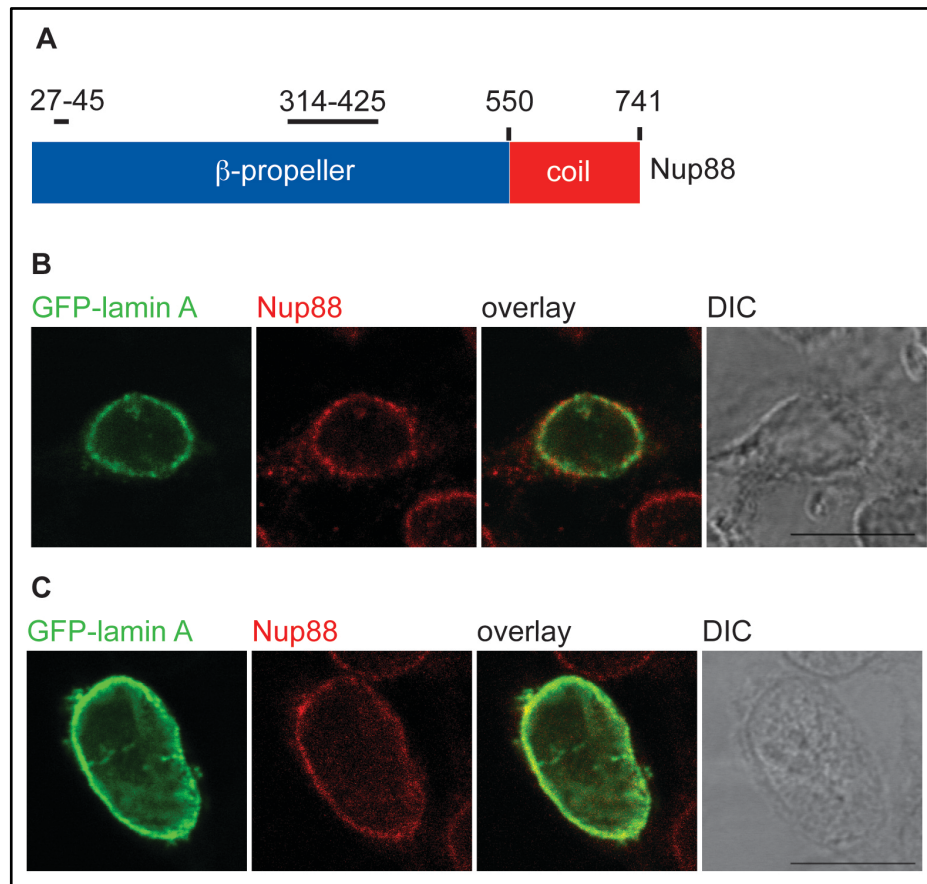


Figure S7.12: Masking can be circumvented by the use of a different antibody epitope or a different fixation method.

(A) Schematic representation of the antibody epitopes in Nup88. (B) HEK cells transfected with GFP-lamin A were prepared for immunofluorescence 24 hours post transfection using a polyclonal antibody directed against residues 27-45 in the N-terminus of Nup88. (C) HEK cells transfected with GFP-lamin A were fixed with 100% ice-cold methanol 24 hours post transfection and prepared for immunofluorescence using monoclonal Nup88 antibody against the N-terminal residues 314-425. Scale bars, 10 μm .

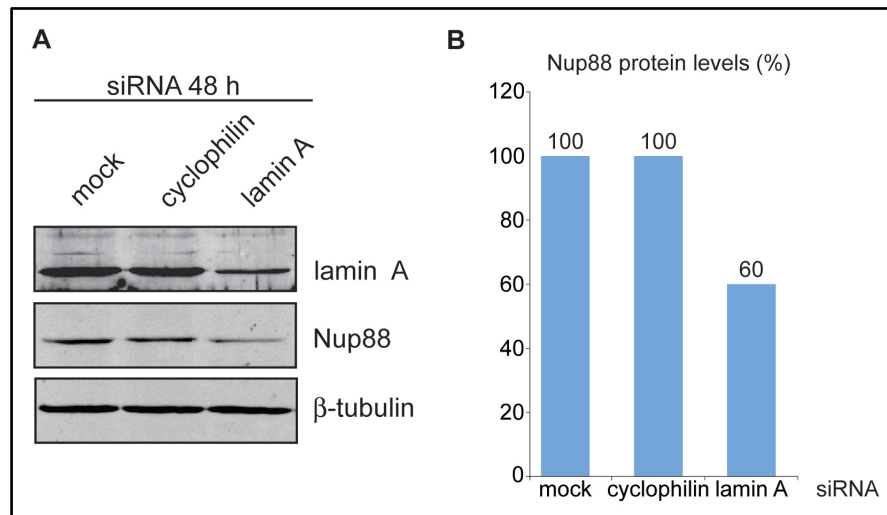


Figure S7.13: Nup88 protein levels are dependent on lamin A.

(A) HeLa cells were transfected with cyclophilin or lamin A siRNA respectively, or mock transfected. Protein levels were analyzed by immunoblot 48 hours after transfection with antibodies against lamin A, Nup88 or β -tubulin as loading control. (B) Protein levels of Nup88 were quantified using MultiGauge (FujiFilm) and normalized with β -tubulin protein levels. Nup88 protein levels of mock-transfected cells are set to 100%.

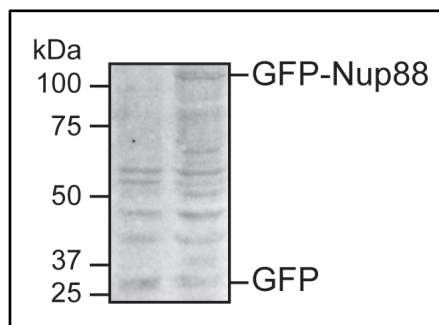


Figure S7.14: Immunoblot analysis of BJ1 fibroblasts transfected with GFP-Nup88 or GFP, respectively.

BJ1 fibroblast cells were transiently transfected with plasmids encoding GFP-Nup88 or GFP and the cells were analyzed for protein expression by immunoblot analysis 24 hours after transfection using a monoclonal GFP antibody.

7.2 Curriculum Vitae

Surname Yvonne
 Name Lussi
 Address M.E. Müller Institute for Structural Biology
 Biozentrum, University of Basel
 Klingelbergstrasse 70
 4056 Basel
 Switzerland
 E-mail yvonne.lussi@unibas.ch
 Telephone +41 61 267 2255

Education	<ul style="list-style-type: none"> • April 2006-March 2010: Dissertation in Cell Biology M.E. Müller Institute for Structural Biology, Biozentrum, University of Basel, Switzerland Prof. Ueli Aebi Advisor: Prof. Dr. Birthe Fahrenkrog Thesis Topic: Characterization of the cellular functions of the nucleoporins Nup153 and Nup88 • November 15, 2005: Master in Molecular Biology at the University of Basel • Oktober 2004-November 2005: Master student in the laboratory of Prof. Dr. Guy Cornelis, Biozentrum Advisor: Dr. Céline Agrain Thesis topic: YscU and the substrate specificity switch in the <i>Yersinia enterocolitica</i> injectisome • July 2004: Bachelor in Molecular Biology consisting of: Structural Biology, Biochemistry, Cell Biology, Microbiology • 2003: Intermediate Exam in Molecular Biology • 2001: Matriculation at the University Basel • 2000: High School Diploma with main subject Latin • 1993-2000: High School at Kollegium St. Fidelis in Stans (Switzerland) • 1987-1993: Primary School in Stans (Switzerland)
Professional Experience	<ul style="list-style-type: none"> • 2002-2006: Working student at SOLVIAS AG in Basel in the laboratory of Dr. Andreas Pospiech

	<p>Experience in Microbiology, Cloning and Sequencing</p> <ul style="list-style-type: none"> February 2001-October 2001: Sales Woman at Bucherer AG in Lucerne
Talks	<ul style="list-style-type: none"> 2008, Basel, Switzerland Core Symposium Structural Biology and Biophysics ‘The nucleoporin Nup88 interacts with the nuclear intermediate filament protein lamin A: implications in human aging?’ 2007, St.Andrews, Scotland 20th Wilhelm Bernhard Workshop on the Cell Nucleus ‘Elucidating the functional role of the nucleoporin Nup88’
Posters	<ul style="list-style-type: none"> 2009, Jerusalem, Israel 17th School in Life Science ‘The nucleoporin Nup88: a novel connection between the nuclear pore complex and the nuclear intermediate filament protein lamin A’ 2009, Vienna, Austria EMBO Workshop: The Multiple Faces of Lamins in Aging and Disease ‘Direct association of lamin A with the nuclear pore protein Nup88’ 2007, Vienna, Austria 32nd FEBS Congress: Molecular Machines ‘Elucidating the effects of nucleoporin Nup88 overexpression’ 2006, Heidelberg, Germany 8th Young Scientist meeting of the DGZ: Cell Biology of Cancer ‘Elucidating the functional role of the nucleoporin Nup88 overexpression in tumor cells’
Awards	<ul style="list-style-type: none"> 2009, Vienna, Austria EMBO Workshop: The Multiple Faces of Lamins in Aging and Disease Poster Prize
Teaching	<ul style="list-style-type: none"> 2006-2009, Biozentrum Basel Introduction in Immunofluorescence Microscopy, 1 week course within the Blockkurs ‘Biophysics and Structural Biology’ for Bachelor students in Molecular Biology
Supervision	<ul style="list-style-type: none"> 2008-2009 Kai Schleicher, Master student, Biozentrum, University

	<p>of Basel, Switzerland</p> <ul style="list-style-type: none">• 2007-2008 Ilona Hügi, Master student, Biozentrum, University of Basel, Switzerland
--	---

7.3 List of Publications

Research papers	<ul style="list-style-type: none"> • Yvonne C. Lussi, Dale K. Shumaker, Takeshi Shimi and Birthe Fahrenkrog ‘The nucleoporin Nup153 affects spindle checkpoint activity due to an association with Mad1’ Nucleus 1:1 (2010) 71-84 • Isabel Sorg, Stefanie Wagner, Marlise Amstutz, Shirley A. Müller, Petr Broz, Yvonne Lussi, Andreas Engel and Guy R. Cornelis ‘YscU recognizes translocators as export substrates of the <i>Yersinia</i> injectisome’ EMBO J 26 (2007) 3015-24 • Yvonne C. Lussi, Ilona Hügi and Birthe Fahrenkrog ‘Direct association of the nucleoporin Nup88 with lamin A’ Molecular Biology of the Cell, submitted • Yvonne C. Lussi and Birthe Fahrenkrog ‘The nucleoporin Nup88 is a regulator of the lamin A-LAP2α complex’ manuscript in preparation
Review	<ul style="list-style-type: none"> • Yvonne Lussi and Birthe Fahrenkrog ‘Nuclear pore complex organization and nucleoporin function’ Landes Bioscience, 2009, Chapter 2 in ‘Nuclear Transport’

7.4 Acknowledgements

I am very grateful to Prof. Dr. Birthe Fahrenkrog for giving me the opportunity to work on this project, the chance to learn new skills, her encouragement and motivation during my PhD time and the beautiful lab hikes we experienced together, I sincerely thank Prof. Dr. Ueli Aebi for his support throughout my time at the M.E Müller Institute, Prof. Dr. Roland Foisner who readily agreed to be my co-referee for my dissertation and for the good discussion we had when we met at the Biozentrum and at meetings and Prof. Dr. Martin Spiess for being chairman at my PhD exam. I would like to remember Ilona Hügi and the joy she brought in our lab, I will never forget her. Special thanks to Kai Schleicher for the time he was working on the Nup88 project, Dr. Cora-Ann Schönenberger for her interest, input and discussions, Dr. Cristian Mittelholzer for the inspirations, Dr. Sara Paulillo for introducing me into the project and cell biology in general and the time we spent together, Dr. Teiba Al-Haboubi for providing me the lamin mutants and the fruitful scientific exchange, Dr. Larisa Kapinos for the purified lamin constructs and the many discussions on lamins and others, Dr. Sofia Georgakopoulou for the purified vimentin protein and the lovely climbing evenings, Marija Plodinec for a lot of fun, Dr. Kyrill Schwarz-Herion, Dr. Joachim Köser, Prof. Dr. Laurent Kreplak, Prof. Dr. Roderick Lim, Dr. Bohumil Maco, Dr. Ulrich Schröder, Therese Tschon, Dr. Esther Owsianowski, Anja Matter, Josephine Jüttner and Claudia Michael for all the help and the good times, Ursula Sauder and Vesna Olivieri for the technical contribution to the EM studies, Gianni Morson for the help with the electron microscopy, Markus Dörenberger for the assistance in light microscopy, Beat Schumacher for all the administrative work, Bea Müller for the support with the FACS and special thanks for the help of Barbara Merz, Robert Wyss, Liselotte Walti, Rosmarie Sütterlin, Debbie Neyer, Roland Bürki, Margrit Jenni, all the former and present lab members of the Birthe Fahrenkrog group, the Ueli Aebi group and the Rod Lim group for the nice times we had at the Biozentrum and out of work, Dr. Marko Loparic, Dr. Unai Silvan, Janne Hyötylä, Rafael Schoch Raphael Wagner, Meret Hornstein and Orit Peleg, all the people on the third floor and in the Biozentrum who I met and who helped me during my PhD time, and David Walter, my friends and family for support and being there. I would like to thank the M.E. Müller Institute and the Swiss National Foundation for financial support of the project.